INFORMATION TO USERS

This manuscript has been reproduced from the microfilm master. UMI films the text directly from the original or copy submitted. Thus, some thesis and dissertation copies are in typewriter face, while others may be from any type of computer printer.

The quality of this reproduction is dependent upon the quality of the copy submitted. Broken or indistinct print, colored or poor quality illustrations and photographs, print bleedthrough, substandard margins, and improper alignment can adversely affect reproduction..

In the unlikely event that the author did not send UMI a complete manuscript and there are missing pages, these will be noted. Also, if unauthorized copyright material had to be removed, a note will indicate the deletion.

Oversize materials (e.g., maps, drawings, charts) are reproduced by sectioning the original, beginning at the upper left-hand corner and continuing from left to right in equal sections with small overlaps.

Photographs included in the original manuscript have been reproduced xerographically in this copy. Higher quality 6" x 9" black and white photographic prints are available for any photographs or illustrations appearing in this copy for an additional charge. Contact UMI directly to order.

UMI®

UNIVERSITY OF ALBERTA

STRUCTURAL STUDIES OF

ACTIVE PLASMINOGEN ACTIVATOR INHIBITOR-1

AND SHIGA-LIKE TOXIN-1

By

ALLAN MURRAY SHARP   ©

A THESIS

SUBMITTED TO THE FACULTY OF GRADUATE STUDIES AND RESEARCH

IN PARTIAL FULFILLMENT OF THE REQUIREMENTS FOR THE

DEGREE OF DOCTOR OF PHILOSOPHY

DEPARTMENT OF BIOCHEMISTRY

EDMONTON, ALBERTA

SPRING 2000

The author has granted a non-exclusive licence allowing the National Library of Canada to reproduce, loan, distribute or sell copies of this thesis in microform, paper or electronic formats.

The author retains ownership of the copyright in this thesis. Neither the thesis nor substantial extracts from it may be printed or otherwise reproduced without the author's permission.

L'auteur a accordé une licence non exclusive permettant à la Bibliothèque nationale du Canada de reproduire, prêter, distribuer ou vendre des copies de cette thèse sous la forme de microfiche/film, de reproduction sur papier ou sur format électronique.

L'auteur conserve la propriété du droit d'auteur qui protège cette thèse. Ni la thèse ni des extraits substantiels de celle-ci ne doivent être imprimés ou autrement reproduits sans son autorisation.

0-612-60020-3

Canadä

University of Alberta

Library Release Form

Name of Author: Allan Murray Sharp

Title of Thesis: Structural Studies of Active Plasminogen Activator
Inhibitor-1 and Shiga-Like Toxin-1

Degree: Doctor of Philosophy

Year this Degree Granted: 2000

Permission is hereby granted to the University of Alberta Library to reproduce single copies of this thesis and to lend or sell such copies for private, scholarly, or scientific purpose only.

The author reserves all other publication and other rights in association with the copyright in the thesis, and except as hereinbefore provided, neither the thesis nor any substantial portion thereof may be printed or otherwise reproduced in any material form whatever without the author's prior written permission.

Allan Murray Sharp
Department of Biochemistry,
University of Alberta,
Edmonton, Alberta,
T6G 2H7

Date: January 28 2000

University of Alberta

Faculty of Graduate Studies and Research

The undersigned certify that they have read and recommend to the Faculty of Graduate Studies and Research for acceptance, a thesis entitled "Structural Studies of Active Plasminogen Activator Inhibitor-1 and Shiga-Like Toxin-1" submitted by Allan Murray Sharp in partial fulfillment of the requirements for the degree of Doctor of Philosophy.
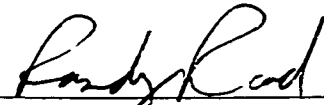
Dr. Randy J. Read

Dr. Michael N. G. James

Dr. Paul Scott

Dr. Laura Frost

Dr. H. Tonie Wright

Date: January 28 2000

ABSTRACT

The first part of this thesis deals with plasminogen activator inhibitor-1 (PAI-1). PAI-1 is the primary physiological inhibitor of the serine proteinase plasminogen activator, and serves a primary role in control of fibrinolysis in plasma and the extracellular matrix. It is involved in several disorders, including cardiovascular disease and cancer, and is a drug design target. PAI-1 is a member of the serpin family of inhibitors, whose inhibitory mechanism involves a conformational change in a surface loop. This reactive centre loop (RCL) is cleaved by the inhibited proteinase but is inserted into a central β-sheet without deacylation. PAI-1 is uniquely able to make this transformation, into the 'latent' form, without being cleaved. PAI-1 plays an important role in regulating the activity of the matrix protein vitronectin, which only binds the uninserted, non-latent, active form of PAI-1.

The X-ray crystallographic structure of a quadruple mutant of active PAI-1 has been solved at 3.0 Å. The RCL is disordered in two of four molecules in the asymmetric unit, and in the others forms a polymerization interaction with the edge of the central β-sheet of symmetry related molecules. Three of the mutations change the conformation of a loop segment, probably affecting the ease of PAI-1's latency transition. Unlike the latent form of the molecule, the 'gate' loop is ordered. The vitronectin binding face is rearranged.

The refinement of the PAI-1 structure with a 2.2 Å dataset has revealed signs of flexibility in two loops that may influence the latency transition. Several theories of latency have been assessed. Two inhibitors of PAI-1 have been docked against the active structure, obtaining plausible docking conformations.

The second part of the thesis deals with Shiga-like toxin-1 (SLT-1). The B-pentamer of SLT-1 is responsible, via interactions with globotrisaccharide receptors, for the holotoxin's cell binding and penetration activity. The structures of the wild type B-pentamer, and of a sugar-binding deficient mutant have been refined. The effects of zinc ions on crystal morphology, and the crystal contacts that induce distortions in the pentamer are explored. The mutation affects only the mutated residue's conformation, confirming its importance in sugar binding.

Acknowledgements

The Read lab has been a productive and supportive working environment, and I greatly appreciate the efforts of its members to make it so. Bart Hazes has been an important teacher and troubleshooter in matters concerning crystallography and computation; he also did preliminary data collection trials on PAI-1 and assisted in collecting the high-resolution data set. Dr. Penelope Stein participated in collecting the wild-type and F30A mutant Shiga-like toxins, and has been an invaluable collaborator on all of my research projects. Dr. Trevor Hart has advised me in the use of the DockVision program, and given a great deal of general assistance with computers. Dr. Norma Duke was unflaggingly helpful and made outstanding contributions to the infrastructure of the Read lab. Dr. Anita Sielecki and Dr. Catherine McPhalen have given considerable advice in the completion of research projects and in composition. Anita has also given me considerable advice in the field of stress management. Dr. Hong Ling has been very helpful in sharing her knowledge in the field of Shiga-like toxins and their structure. Mr. Navraj Pannu shared his expertise in maximum likelihood refinement, and the results of his tests on the low-resolution PAI-1 structure. In addition to Ami, Koto, Bart, Penny, Trevor, Norma, Anita, Cathy, Hong, and Raj, I would like to thank Dr. Maxwell Cummings, and Mr. Stephen Ness, for being wonderful people to work with.

It has been very helpful to be able to draw upon the resources of the Departments of Biochemistry and of Medical Microbiology and Immunology. The structural biology group has been particularly helpful. The members of the James lab have been of great assistance. In addition to Kathy and Maia, I would like to particularly thank Dr. Helen Blanchard, Dr. Bret Church, Dr. Marie Fraser, Dr. Kui Huang, Mr. Ron Meleshko, Dr. Stanley Moore, and Dr. Steve Mosimann for advice and support.

I appreciate the great efforts that Dr. Michael James and Dr. Zygmunt Derewenda have taken in my education in matters of crystallography and the culture of science.

And above all, I owe a great deal of thanks, and a debt of gratitude, to my supervisor, Dr. Randy Read, for data collections, the production of an excellent research laboratory, considerable efforts to make sure that my research was as complete and well executed as possible, for assistance in research, for crystallographic education, for general advice, and for extraordinary patience.

Table of Contents

List of Tables

List of Figures

List of Symbols and Abbreviations

Å	Angstrom
A335E	A site-directed mutant of PAI-1 with Alanine 335 mutated to Glutamate
A335P	A site-directed mutant of PAI-1 with Alanine 335 mutated to Proline
Ala	Alanine
Arg	Arginine
ARH0	Compound AR-H029953XX
Asn	Asparagine
Asp	Aspartate
B	Crystallographic temperature factor
C	Degree Celsius
cDNA	Complementary DNA
D17E/W34A	A site-directed double mutant of SLT-1 with Aspartate 17 mutated to Glutamate and Tryptophan 62 mutated to Alanine
E. coli	*Escherichia coli*
EDTA	Ethylenediaminetetraacetic acid
ER	Endoplasmic Reticulum
F30A/W34A	A site-directed double mutant of SLT-1 with Phenylalanine mutated to Alanine and Tryptophan 62 mutated to Alanine
F30A	A site-directed mutant of SLT-1 with Phenylalanine mutated to Alanine
$|F|$	Structure factor amplitude
F_c	Calculated structure factor
F_{mut}	Measured structure factor for mutant protein

F_{nat}	Measured structure factor for native (wild-type) protein
F_o	Observed structure factor
G62T	A site-directed mutant of SLT-1 with Glycine 62 mutated to Threonine
Gb3	Globotriaosyl ceramide
Gb4	Globotetraosyl ceramide
Glu	Glutamate
Gln	Glutamine
Gly	Glycine
His	Histidine
HTG-VLDL	High triglyceride very low density lipoprotein
HUS	Hemolytic-uremic syndrome
IgG	Immunoglobulin-G
Ile	Isoleucine
INF-γ	Interferon-gamma
K	Degree Kelvin
K	Potassium
K154T	A site-directed mutation site in PAI-1 with Lysine 154 mutated to Threonine
Leu	Leucine
Lp(a)	Lipoprotein (a)
LRP	Low density lipoprotein receptor related protein
Lys	Lysine
M	Molar

M354I	A site-directed mutation site in PAI-1 with Methionine 354 mutated to Isoleucine
Met	Methionine
mM	Millimolar
mRNA	Messenger RNA
N150H	A site-directed mutation site in PAI-1 with Asparagine 150 mutated to Histidine
Na	Sodium
NCS	Non-crystallographic symmetry
NMR	Nuclear magnetic resonance
P	Gb_4 blood group antigen
PA	Plasminogen activator
PAI	Plasminogen activator inhibitor
PAI-1	Plasminogen activator inhibitor-1
PAI-2	Plasminogen activator inhibitor-2
P. aruginosa	*Pseudomonas aruginosa*
PDB	Protein Data Bank
Phe	Phenylalanine
pI	Isoelectric point
P^k	Gb_3 blood group antigen
P^k-MCO	Gb_3-methoxycarbonyloctyl
Pro	Proline
Q319L	A site-directed mutation site in PAI-1 with Glutamate 319 mutated to

	Leucine
R271C	A site-directed mutant of PAI-1 with Arginine 271 mutated to Cysteine
RCL	Reactive centre loop
R-factor	Standard crystallographic residual
R_{free}	Free R-factor
RGD	Arg-Gly-Asp binding sequence
R_{merge}	Merging R-factor
r.m.s.	Root-mean square
r.m.s.d.	Root-mean square deviation
σ	Standard deviation
Ser	Serine
SLT	Shiga-like-toxin
SLTB	Shiga-like-toxin B subunit
SLT-1	Shiga-like-toxin-1
SLT-2	Shiga-like-toxin-2
SLT-2c	Shiga-like-toxin-2 variant c
SLT-2e	Shiga-like-toxin-2 variant e
SMB	Somatomedin binding domain
$t_{1/2}$	Half-life
TGFβ	Transforming growth factor-beta
Thr	Threonine
TNFα	Tumor necrosis factor-alpha

tPA	Tissue-plasminogen activator
Trp	Tryptophan
Tyr	Tyrosine
uPA	Urokinase plasminogen activator
VLDL	Very low density lipoprotein
VT	verotoxin
VTB	Verotoxin B-subunit
VT-1	Verotoxin-1
VT-2	Verotoxin-2
W34A	A site-directed mutant of SLT-1 with Tryptophan 62 mutated to Alanine
Wat	Crystallographic water
XR51	Compound XR5118
Zn	Crystallographic zinc atom
14-B	A site-directed quadruple mutant of PAI-1 with Asparagine 150 mutated to Histadine, Lysine 154 mutated to Threonine, Glutamine 319 mutated to Leucine, and Alanine 335 mutated to Glutamate

1.0 Introduction

1.1   Overview

It is common for structural biologists to view a macromolecule in relatively homogeneous conditions; inside a crystal capillary or an NMR tube containing one or a small number of proteins. The protein sample will be in an aqueous salt and buffer solution, with possibly a cofactor or inhibitor present. It is important, however, to remember that such conditions are non-biological. In a living organism, a molecule comes in contact with thousands of proteins, polysaccharides, nucleic acids, ions, and small organic molecules. A macromolecule is likely to encounter lipid membranes, extracellular or intracellular structures of polysaccharides, and multi-protein complexes, which form discontinuities or even separate phases in its environment. The molecule must carry out specific interactions with some of these elements, allow others to influence its activity, and coexist with blind indifference to the majority of them. The molecules with which it interacts, and the general nature of its environment, have an influence on its own structure and function.

While the above points are sufficiently general to be obvious, they are often neglected, and they do pertain to several of the points that are raised in this thesis. Both projects discussed - the structure of the active form of a quadruple mutant of human Plasminogen Activator Inhibitor-1 (PAI-1), and the refined structures of a native and a

mutant verotoxin B-pentamer (VTB) - contain examples of the structure being influenced

by contacts with its neighbors in the crystal state. In the case of PAI-1 these changes

yield potentially useful information on the mobility of functionally important regions of

the molecule. Both projects are concerned to a large extent with explaining the nature of

the interactions the molecules have with other proteins, complex polysaccharides, or

small molecule inhibitors. The interactions holding together the subunits of the verotoxin

B pentamer, and the distortions that can be induced in that structure are considered, while

their relevance to the pentamer's function, binding cell surface globotriaosylceramides, is

touched upon. In the case of PAI-1, the effects of the structural rearrangements brought

about by interactions with its target proteinases, and the effects these have on its

interactions with activating and inhibiting molecules are addressed.

1.2   Plasminogen Activator Inhibitor-1 Background

1.2.1 PAI-1 Basic Information

Plasminogen activator inhibitor-1 (PAI-1) is an inhibitor of the serine proteinases

tissue plasminogen activator (tPA) and urokinase plasminogen activator (uPA). It serves

as a major controller of the plasmin system of extracellular proteolysis, which plays

important roles in vascular fibrinolysis and tissue remodelling (Figure 1.1). It also serves

to regulate the interactions of the structural glycoprotein vitronectin (Figure 1.2). (These

interactions and functions are described in detail in section 1.2.3.)

PAI-1 is a 379 amino acid glycoprotein (Andreasen et al., 1986; Ginsburg et al.,

1986; Ny et al., 1986; Pannekoek et al., 1986), with a molecular weight of approximately

43 kDa unglycosylated, or 52 kDa with glycosylation (Figure 1.3). cDNA studies show

ActivePAI-1   Latent PAI-1

Plasminogen Activator   Plasminogen Activator
PAI-1 covalent
complex

Clearance by
LRP receptor

Plasminogen   Plasmin

Fibrin Clot   Fibrin Fragments
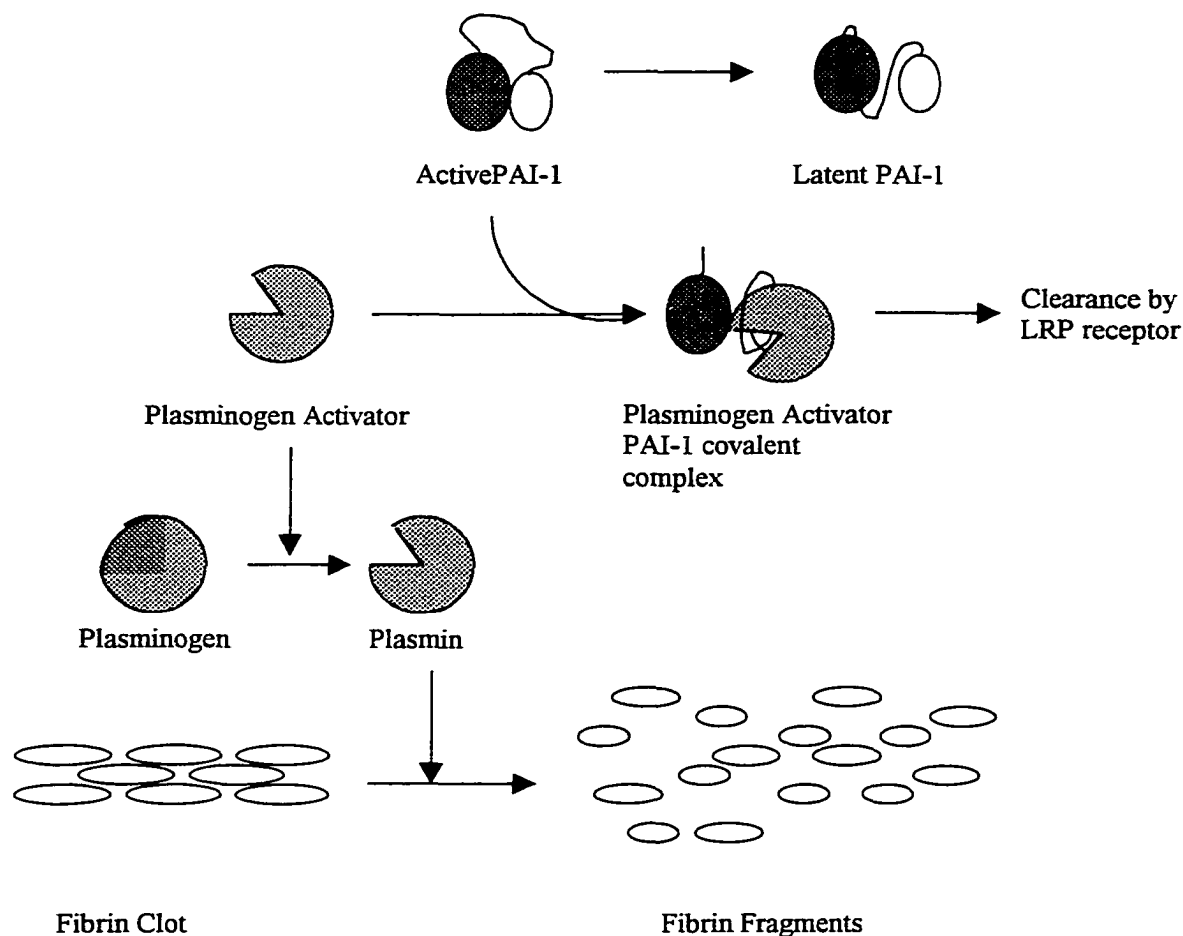
Figure 1.1: Biological functions of PAI-1: control of fibrinolysis: PAI-1 inhibits plasminogen activators (tPA and uPA), which otherwise initiate the fibrinolysis cascade. PAI-1 is itself regulated by its expression levels, and by the latency transition. Other proteins that regulate PA activity to a lesser degree include PAI-2, protein C inhibitor, and proteinase nexin I. Plasmin is inhibited by α_2-antiplasmin. Fragment 1 of PAI-1 (Stein & Chothia, 1991) is represented by a dark grey ellipse, while fragment 2 is in white. The reactive centre loop/strand 4A is represented as a line between the fragments. PAI-1-proteinase complexes are cleared by the low-density lipoprotein-like (LRP) receptor.

Figure 1.2: Biological functions of PAI-1:regulation of vitronectin activity: PAI-1

stimulates the transition of vitronectin from the closed form found in serum to the open

form found in extracellular matrix. It binds at or near the RGD sequence by which

vitronectin binds integrin. Binding of vitronectin stabilizes PAI-1 and increases its

activity against thrombin. The latency transition over time, or reaction with plasminogen

activators, releases PAI-1 from vitronectin, allowing access to the RGD sequence. Hence

PAI-1 serves as a molecular switch, regulating the functions of vitronectin.

RGD

Active PAI-1

Closed Vitronectin

Cell

X
No interaction

Integrin

Extracellular
Matrix

X
No interaction

Plasminogen
Activator or
time

Thrombin

RGD

Covalent PA-PAI-1
complex
or

Extracellular Matrix with
open vitronectin bound and
bound PAI-1 blocking
RGD sequence

Latent PAI-1

RGD

Extracellular Matrix with
open vitronectin bound and
integrin binding RGD site

Figure 1.3: Sequence of the N150H, K154T, Q319L, M354I quadruple mutant of PAI-1. Mutation sites are underlined and in bold italicized characters. The reactive centre (underlined and in bold type) is indicated with a ↓ symbol. α-helices are shown by ‿ symbols and β-sheets by ==>, as identified in molecule A of the active PAI-1 structure by the DSSP algorithm. The Huber-Carrell nomenclature for the secondary structure is shown above the sequence, while some trivial names of specific regions are shown in italics (Huber & Carrell, 1989). *ph* = proximal hinge, *dh* = distal hinge s = strand, t = turn h = helix. The Stein and Chothia structural fragments are also indicated (Stein & Chothia, 1991). Numbering is from the beginning of the mature PAI-1 structure.

```
|--------------------Fragment 1----------------------------------
              hA            thAs6B s6B        hB      thBhC       hC
  1 VHHPPSYVAH LASDFGVRVF QQVAQASKDR NVVFSPYGVA SVLAMLQLTT GGETQQQIQA
    ~~~~~~~~~~~~~~~~~~~~~               ==> ~~~~~~~~~~~~~~~   ~~~~~~~~~


      --|------Flexible joint--------| fragment 2 |---Flexible joint---
         thChD          hD        thDs2A    s2A    ts2AhE      hE   thEs1A
 61 AMGFKIDDKG MAPALRHLYK ELMGPWNKDE ISTTDAIFVQ RDLKLVQGFM PHFFRLFRST
    ~~            ~~~~~~~~~~~~     ========>              ~~~~~~~


      -|------------------------ Fragment 2 ----------------------|----
       s1A   ts1AhF      hF             thFs3A           s3A      ts3AhF1
121 VKQVDFSEVE RARFIINDWV KTHTKGMISH LLGTGAVDQL TRLVLVNALY FNGQWKTPFP
    ==>         ~~~~~~~~~~~~~~                         ========>


      ------------------------ Fragment 1 --------------------------
      'Gate Loop' or 'Loop 1'
      hF1 s4C ts4Cs3C     s3C   ts3Cs1B s1B ts1Bs2B s2B    ts2Bs3B s3B
181 DSSTHRRLFH KSDGSTVSVP MMAQTNKFNY TEFTTPDGHY YDILELPYHG DTLSMFIAAP
    ~~~ =====>        ==============>======>      ========>      =======>


      ------------------------ Fragment 1 --------------------------
      'loop 2'
      ts3BhG   hG        hH     thHs2C    s2C       s6A        hI      hI1
241 YEKEVPLSAL TNILSAQLIS HWKGNMTRLP RLLVLPKFSL ETEVDLRKPL ENLGMTDMFR
      ~~~~~      ~~~~~~~~~~~ ===========> ========> ~~~~~~~~   ~~~


      -------------------------Fragment 1--------------------------
                              ph Reactive Centre Loop dh
         thIls5A            s5A       ts5As4A (s4A)   ↓   s1C       s4B
301 QFQADFTSLS DQEPLHVALA LQKVKIEVNE SGTVASSSTA VIVSARMAPE EIIIDRPFLF
              ==========>                        ====>    ==>


      --Fragment 1--------|

      ts4Bs5B s5B ts5Bc-ter
361 VVRHNPTGTV LFMGQVMEP
    ===>     ========>
```

that a 23 amino acid endoplasmic reticulum signal sequence is removed to form the mature protein (Pannekoek *et al.*, 1986). The mature protein has a calculated pI of 6.97, and an amino acid composition whose most interesting feature is the complete lack of cysteine (Ny *et al.*, 1986; Pannekoek *et al.*, 1986). Its structure is therefore not stabilized by disulphide bridges like many extracellular proteins. The sequence contains three possible N-linked glycosylation sites, at Asn 209, Asn 265, and Asn 329. The crystal structure of the peptide-inhibited form of PAI-1, the only form solved with protein expressed in a mammalian system, shows evidence of glycosylation at residues 209 and 265 (Xue *et al.*, 1998).

The human PAI-1 gene contains nine exons, which are contained within 12.3 kilobases of the DNA of chromosome 7 (Ginsburg *et al.*, 1986; Klinger *et al.*, 1987; Loskutoff *et al.*, 1987; Strandberg *et al.*, 1988). There is no evidence of alternative splicing, and, while the exon boundaries roughly correspond to ends of secondary structural elements, they are not conserved among other members of the serpin family (Loskutoff *et al.*, 1987; Strandberg *et al.*, 1988). The mRNA is found with two different molecular weights, apparently due to alternate degrees of polyadenylation (Loskutoff *et al.*, 1987). The 5' untranslated region has also been sequenced (Riccio *et al.*, 1988; Strandberg *et al.*, 1988). Several studies have discovered variations in this region that may be significant to gene expression (Dawson *et al.*, 1991; Dawson *et al.*, 1993; Henry *et al.*, 1997; Klinger *et al.*, 1987). One in particular, involving a 4G/5G polymorphism at nucleotide -675 has been suggested to have a major effect on plasma PAI-1 activity, with 4G homozygotes having much higher activity (Dawson *et al.*, 1991; Ye *et al.*, 1995). However, the clinical significance of this variation has not been clearly established

(Juhan-Vague & Alessi, 1997). Several cytokines and hormones have been identified which are involved in the modulation of PAI-1 expression and secretion. Unfortunately, the relative importance of these different factors, and the mechanisms by which they modulate PAI-1 are not entirely clear, and in some cases are matters of considerable controversy. Some factors, with demonstrated roles *in vivo*, are discussed in section 1.2.3.

The sequence of PAI-1 indicates that it is a member of the serpin family of serine proteinase inhibitors (Andreasen *et al.*, 1986; Ginsburg *et al.*, 1986; Ny *et al.*, 1986; Pannekoek *et al.*, 1986). This is a family of large proteins (> 400 amino acids), most of whose members serve as inhibitors of serine proteinases. Non-inhibitory members of the serpin structural family are known to function as storage proteins (ovalbumin), hormone precursors (angiotensinogen), carrier proteins (Cortisol-binding globulin, Thyroxin-binding globulin), and as heat-shock proteins (HSP70) (Reviewed in Whisstock *et al.*, 1998). Serpins are known to function as suicide inhibitors (Engh *et al.*, 1995). Suicide inhibitors (also called suicide substrates or mechanism-based inhibitors) are substrate mimics that can form stable, often covalent complexes with their targets, making them highly effective inhibitors (Waley, 1980; Waley, 1985). However, when a suicide inhibitor is dissociated from its target, it never functions again, behaving as a processed substrate. Often the rate of substrate formation is significant, so that the suicide inhibitor mechanism can be seen as a competion between an inhibition pathway in which the stable complex is formed, and a substrate reaction forming inactived inhibitor. In the case of the serpins, proteinase-inhibitor complexes have been shown to be covalent and to have half-lives measurable in days or weeks (Kruithof *et al.*, 1986a; Lawrence *et al.*, 1995;

Lobermann *et al.*, 1982; Olson *et al.*, 1995a; Olson *et al.*, 1995b; Stromqvist *et al.*, 1996).

The nature of the covalent modification and the nature of the serpin-proteinase complex

are two of the most interesting features of serpins.

Several crystal structures have been determined for serpins. The common fold of the

family consists of a complex, single domain, mixed α/β structure (Figure 1.4). The fold

is built around a central five or six-stranded mixed β-sheet known as the A sheet (the

number of strands is dependent on the functional stage of the inhibition mechanism, as

explained below). This is backed by a six-stranded antiparallel β-sheet, the B sheet. The

strands of the B-sheet run roughly perpendicular to those in the A sheet. A third mixed

four-stranded β-sheet, the C sheet, lies on one edge of the A and B sheets. The A and B

sheets are also surrounded by nine α-helices (commonly labeled A to I), as well as some

helical turns $(hF_1, hI_1)^*$, and some large surface loops.

Crystal structures of different serpins have revealed an interesting variation in the

structure of the A sheet. As noted above, it may contain either five or six strands. In the

case of the five stranded, or active, serpin, the segment that would otherwise form strand

4A is exposed on the surface in a long loop (Figure 1.4 a). The prototype for six-stranded

serpins is the cleaved serpin, in which strand 4A is inserted into sheet A; space for this

insertion is provided by the translation of strands 1A, 2A, and 3A and helix F away from

the remainder of the molecule (Figure 1.4 b). Helices D and E serve as joints between

the major and minor fragment of the molecule (Stein & Chothia, 1991). In a cleaved

---

* A nomenclature for labeling the secondary structural features of serpins has been developed by Huber and Carrell (1989) and will be employed in this thesis. Strands (abbreviated as s) are described by sheet letter (A,B,C) and strand number, running from one edge of the sheet to the other. Hence s1A and s6A are the outer edges of sheet A. Helices (abbreviated as h) are described by letter (with subscript letter for minor helical turns). Hence hA is the first helix while hF_1 is a minor helical segment between hF and hG. Turns
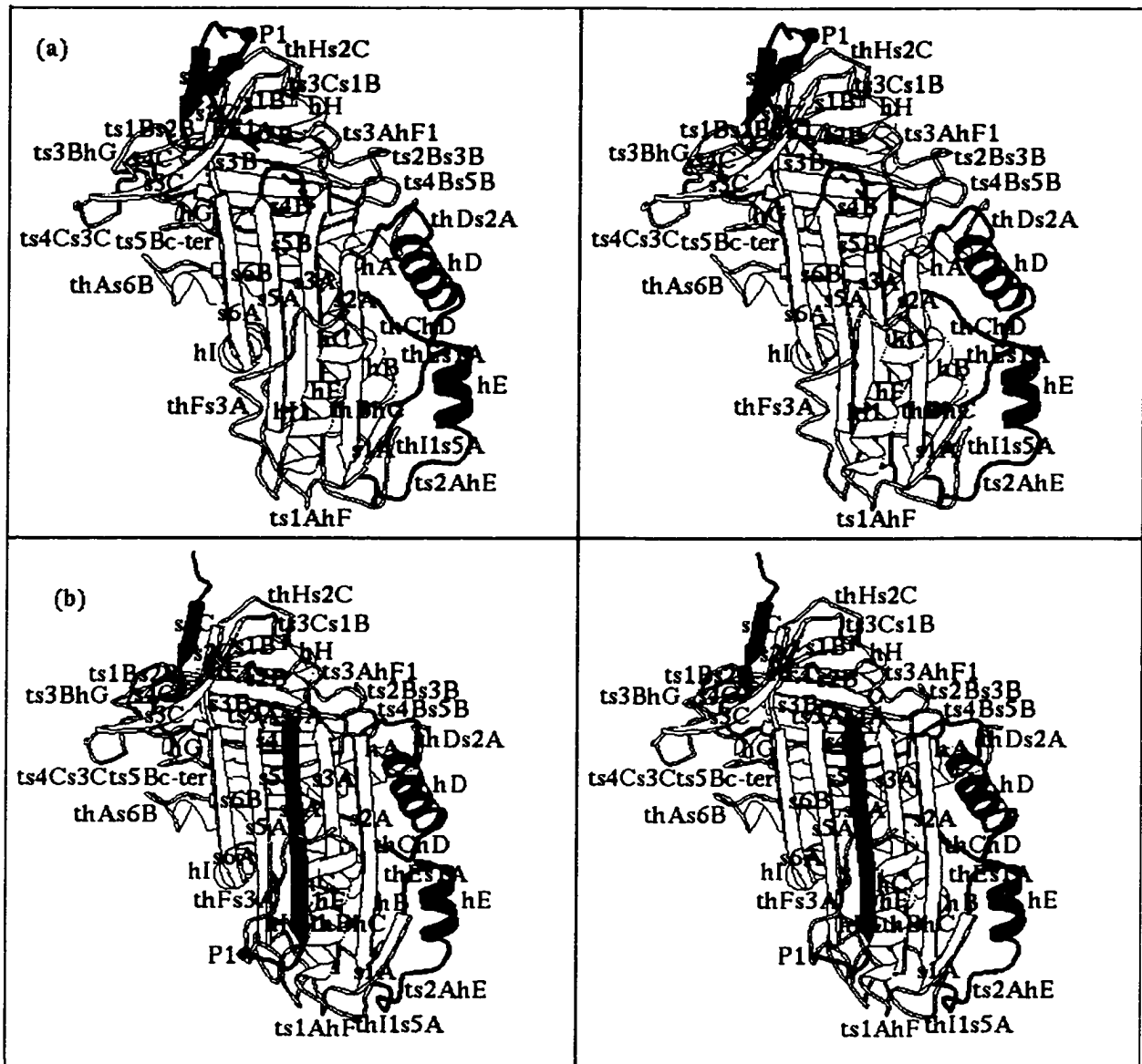
Figure 1.4: Serpin secondary structure. The Huber-Carrell nomenclature (Huber & Carrell, 1989) is indicated on active and cleaved serpins a) active PAI-1 (molecule A) (Sharp *et al.*, 1999) b) cleaved PAI-1 (Aertgeerts *et al.*, 1995). The P1 residue of the reactive centre is indicated. Stein and Chothia's 'fragment 1' is coloured white, 'fragment 2' in yellow, the reactive centre loop is shown in red, 'flexible joint 1' in green, and 'flexible joint 2' in magenta. This figure was produced using the Molscript program (Kraulis, 1991).

(abbreviated as t) are described by the ordered structures they join. Hence thHs2C is the turn joining helix

serpin, the C-terminus of strand 4A and the N-terminus of strand 1C, which are contiguous in the sequence, are found at opposite ends of the structure separated by >70.0 Å. The break in the chain occurs at a sequence with the character of a substrate for the target proteinase, so that it appears to be the result of a proteolytic cleavage and a structural reorganization (Aertgeerts *et al.*, 1995b; Baumann *et al.*, 1992; Baumann *et al.*, 1991; Loebermann *et al.*, 1984; Mourey *et al.*, 1993). It has been demonstrated that cleaved serpins are inactive as inhibitors (Gettins *et al.*, 1993; Lobermann *et al.*, 1982; Nielsen *et al.*, 1986), so this modification is believed to play a role in the suicide mechanism. The cleavage site is called the 'reactive centre', hence the loop that strand 4A forms in active serpins is often called the 'reactive centre loop' (RCL).

The mechanism of serpin action has been postulated to be thus (Figure1.5) (Patston *et al.*, 1994; Wright & Scarsdale, 1995): the serine proteinase forms a normal Michaelis complex with the reactive site loop, and carries out the first half of its catalytic cycle. A covalent tetrahedral intermediate is formed between the catalytic serine of the enzyme and the carbonyl carbon of the reactive site peptide bond. The inhibitor's backbone is cleaved as the tetrahedral intermediate breaks down to an acyl-enzyme complex. Before the remainder of the catalytic cycle (hydrolysis of the acyl-enzyme) can occur, the serpin undergoes a structural rearrangement that stabilizes the acyl-enzyme. This rearrangement is generally believed to be the insertion of the cleaved reactive site loop into the A sheet as strand 4A. Some protein crosslinking and fluorescence studies suggest that the insertion of the reactive site loop is partial, with the serine proteinase interacting with the protein in the vicinity of helix F (Stratikos & Gettins, 1997; Wilczynska *et al.*, 1997). Other fluorescence and antibody studies favor a complex with the loop completely

---

H to strand 2 of the C sheet.
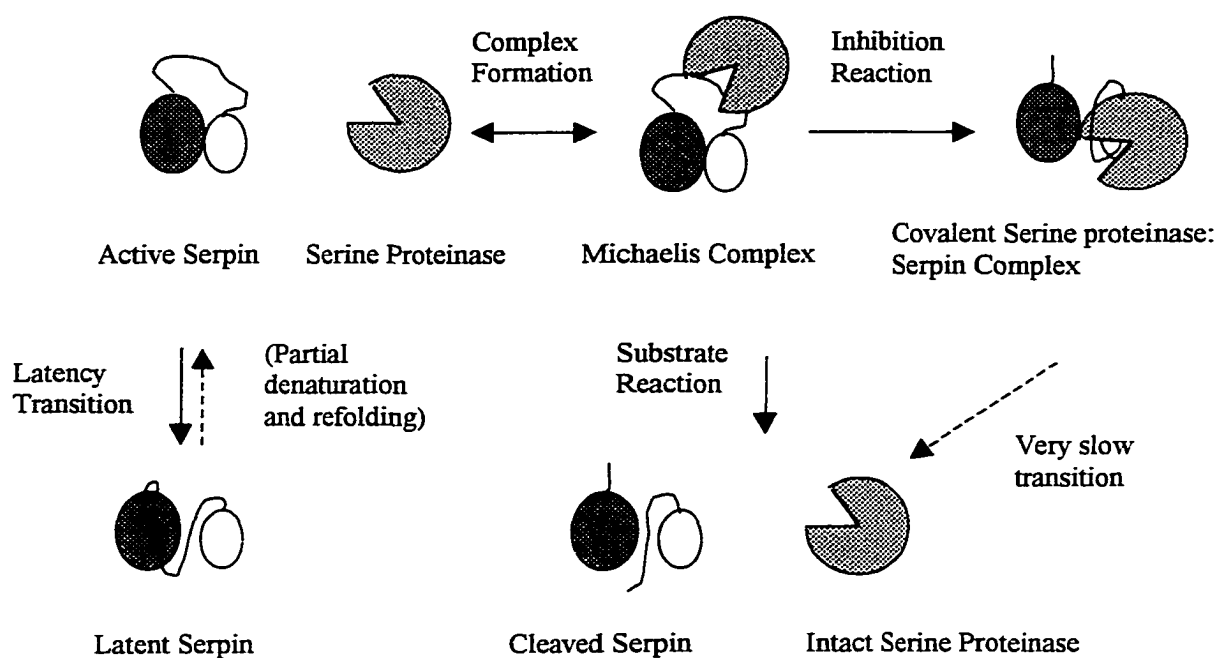
Figure 1.5: Structural rearrangements of serpins and their role in the reaction mechanism with serine proteinases. Fragment 1 of the serpin is represented by the dark grey ellipse, while fragment 2 is in white. The reactive centre loop/strand 4A is represented as a line between the fragments. A generic serine proteinase is shown in light grey.

inserted, and the serine proteinase interacting with the opposite end of the serpin from that where the Michaelis complex formed (Björquist *et al.*, 1999; Stratikos & Gettins, 1997; Stratikos & Gettins, 1999). The precise nature of the complex is not well defined, but the serine proteinase reactive site is presumably distorted and unable to complete the catalytic cycle.

The labile nature of strand 4A has some interesting implications relating to disease conditions. Strand 4A has a considerable propensity for forming β-sheet interactions promiscuously, which may explain how the serpin α_1-antichymotrypsin provides nucleation sites for β-sheet amyloid fibrils (Janciauskiene *et al.*, 1996). In addition, several serpins, principally antitrypsin (Lomas, 1996), antithrombin (Bruce *et al.*, 1994) and C1-inhibitor (Aulak *et al.*, 1993; Eldering *et al.*, 1995; Levy *et al.*, 1990; Verpy *et al.*, 1995), are known to form polymers. These polymers are sometimes major health concerns: not only do the polymerized proteins fail to carry out their functions, they can accumulate and cause tissue damage as well (Stein & Carrell, 1995). The most likely explanation for this phenomenon is the insertion of the reactive centre loop from one serpin molecule into the A sheet of another, thus achieving the 6-stranded form without the need for strand cleavage (Elliott *et al.*, 1996). An alternative possibility for dimerization of serpins has been suggested by the crystal structure of antithrombin III (Carrell *et al.*, 1994; Schreuder *et al.*, 1994). One of the two antithrombin molecules in the asymmetric unit is in the latent form (see below). The molecule in the active form makes a β-sheet interaction between its reactive centre loop and the exposed edge of sheet C in the latent molecule.

1.2.2 PAI-1 as a serpin

PAI-1 has been reported to form inhibitory complexes with several plasma serine proteinases, including tPA, uPA (Sprengers & Kluft, 1987), thrombin (Ehrlich *et al.*, 1990), and protein C (de Fouw *et al.*, 1987). The second-order rate association constant with tPA and uPA is around 10^7 $M^{-1}s^{-1}$ (Berkenpas *et al.*, 1995; Ehrlich *et al.*, 1990). The second order rate association constant for thrombin is around 10^3 $M^{-1}s^{-1}$, except in the presence of vitronectin (10^6 $M^{-1}s^{-1}$)(Ehrlich *et al.*, 1990), or heparin (10^4 $M^{-1}s^{-1}$) (Meijer *et al.*, 1997). PAI-1 interacts with its serine proteinase targets through its reactive centre Arg-Met sequence (residues 346 and 347). This presumably mimics the Arg-Val target of the plasminogen activators (Lijnen *et al.*, 1994). The residues in the positively charged '37 loop' region of tPA (so-called from the central residue of the equivalent loop in the sequence of chymotrypsinogen – in tPA these are actually residues 296 to 304) have been proposed to interact with PAI-1 (Madison *et al.*, 1989). Deletion of segments of the 37 loop, or the substitution of negatively charged residues for positive ones, have been shown to reduce the inhibitory rate of PAI-1 to around 10^4 $M^{-1}s^{-1}$ (Madison *et al.*, 1989; Madison *et al.*, 1990). Substitution of this region in thrombin with the sequence from tPA increases the inhibition rate constant of PAI-1 for thrombin to around 10^4 $M^{-1}s^{-1}$ (Horrevoets *et al.*, 1993). The '60 loop' region (again named from chymotrypsinogen, residues 324 to 332 in tPA) has also been proposed to be involved in PAI-1 binding (Lamba *et al.*, 1996; Spraggon *et al.*, 1995). Interactions of PAI-1 with the second kringle domain of tPA have been suggested (Kaneko *et al.*, 1991; Wilhelm *et al.*, 1990); however other studies have contradicted these findings (Bennett *et al.*, 1991; Bergum & Erickson, 1988) and the deletion of these domains makes no difference to the rate of the

reaction between tPA and PAI-1 (Björquist *et al.*, 1994). Studies using the antibody

CLB-2C8 have suggested that its epitope, the region of PAI-1 from residues 128 to 145

(helix F), may be a secondary binding site for tPA (Keijer *et al.*, 1991a; van Zonneveld *et

al.*, 1995). However, further studies have suggested that this may be an interaction in the

covalent complex, not the initial Michaelis complex (Björquist *et al.*, 1997).

The precise structure of the covalent PAI-1-tPA complex is unclear, as it is for all

serpins. Björquist *et al.* (1997) have characterized antibodies whose binding is affected

by the formation of the complex. Some of these have an epitope known to lie between

residues 319 and 379 of PAI-1 (probably between 346 to 356), and are suspected to bind

to the reactive centre loop. Others bind the 128 to 145 epitope described above, and there

are several with poorly defined epitopes. Wilczynska *et al.* (1997) have developed a

model, based on crosslinking and fluorescence studies on PAI-1 and on α_1-antitrypsin, in

which the cleaved reactive centre loop is partially inserted into the A sheet, while tPA

interacts with a surface region around helix F. This was initially supported by the

fluorescence work of Stratikos and Gettins (1997) on α_1-antitrypsin, who proposed it as

one of two likely models for the serpin-proteinase complex. However, further work has

led them to favor their other model (Stratikos & Gettins, 1999), in which the reactive site

loop is fully inserted. In the case of PAI-1, Wilczynska *et al.* (1997) have also been

criticized on the basis of studies that indicate the PAI-1-tPA complex can still bind

antibodies interacting with the 128 to 145 epitope (Björquist *et al.*, 1999). A model of

PAI-1 interacting with thrombin has also been published; it has strand 4A partially

inserted but no interaction of thrombin with helix F (Aertgeerts *et al.*, 1997).

PAI-1 is unique among serpins for its ability to convert relatively rapidly into a 'latent' form, where the inhibitory capacity of the protein is lost, but can be restored *in vitro* by refolding the protein (Erickson *et al.*, 1986; Hekman & Loskutoff, 1985; Hekman & Loskutoff, 1988). PAI-1 assumes the latent form under physiological conditions with a half-life of about two hours (Berkenpas *et al.*, 1995). Latency may serve as a natural method for regulating the activity of PAI-1. Since, however, active PAI-1 is cleared from plasma by an unknown hepatic receptor with a half-life of about 15 minutes (latent PAI-1 being cleared in 5) (reviewed in Lijnen *et al.*, 1994), latency may be of more significance in tissue than in circulation. Other serpins can be induced into latency with mild thermal denaturation (Carrell *et al.*, 1991), but only in the case of antithrombin III has it been suggested to occur spontaneously and to have possible biomedical relevance (Carrell *et al.*, 1994; Lomas *et al.*, 1997). The latent forms of serpins have been shown to be considerably more stable thermally than their active forms, although not as stable as their cleaved forms. (PAI-1, in its active state, is thus one of only a few truly metastable proteins, and it is a question of considerable interest how it folds into the metastable state.) Crystal structures of latent PAI-1 and antithrombin III show that the reactive site loop has inserted into the A sheet to produce a six-stranded form without being cleaved (Figure 1.6 c)(Carrell *et al.*, 1994; Mottonen *et al.*, 1992). This is achieved by disrupting the structure at the C-terminus of the reactive site loop (the distal hinge): strand 1C is pulled off the C-sheet to provide an extended loop running across the surface of the molecule.

Various theories have been proposed to explain why PAI-1 is much more likely to assume the latent state than other serpins. These include: a model for active PAI-1 where
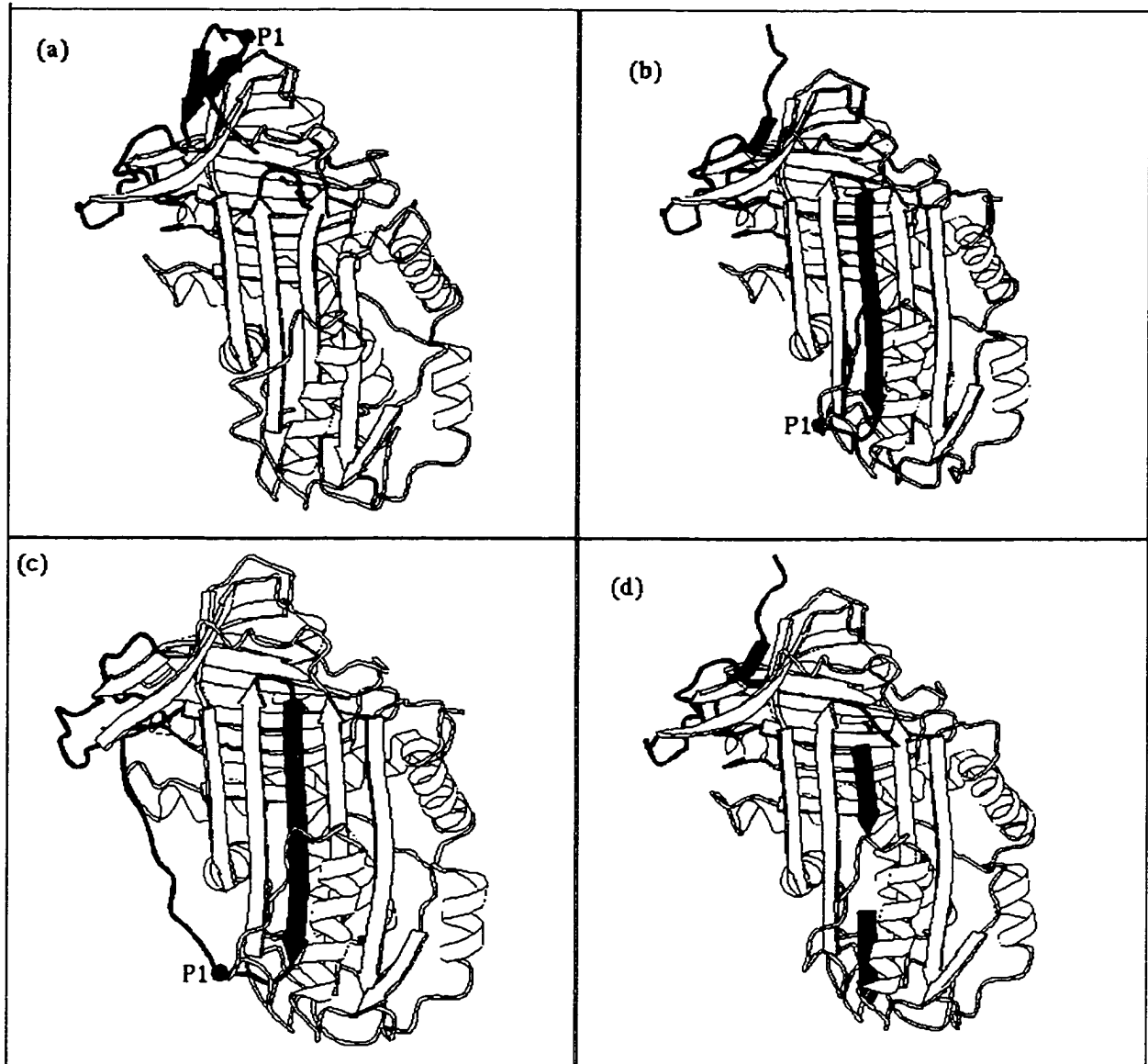
Figure 1.6: PAI-1 structures. a) active PAI-1 (molecule A) (Sharp *et al.*, 1999) b) cleaved PAI-1 (Aertgeerts *et al.*, 1995) c) latent PAI-1 (Mottonen *et al.*, 1992) d) peptide-inhibited cleaved PAI-1 (Xue *et al.*, 1998). The P1 residue of the reactive centre is indicated, except in d) where it was not observed. Strands of the A sheet are coloured yellow, the reactive centre loop is shown in red, the C-terminus in magenta, the "gate loop" or "loop 1" in blue, and "loop 2" in green. This figure was produced using the Molscript program (Kraulis, 1991).

the A sheet is already completely open (Aertgeerts *et al.*, 1994), a disordered loop

ts3Cs4C (Tucker *et al.*, 1995), an unusually strong positive charge on ts3Cs4C coupled

with charges in the distal hinge (Aertgeerts *et al.*, 1995b), a destabilizing amino acid

charge in strand 2C (Harrop *et al.*, 1999), and an intramolecular deamidation between an

Asparagine and a neighboring amide group in strand 3A (Wright, 1996; Wright &

Scarsdale, 1995). Little consensus has been reached about the relative merits of these

theories. In any event, the difference between a serpin that becomes latent in hours and

one that is stable for months could be very small, amounting to a difference of as little as

4 to 5 kcal/mole in the activation energy barrier to latency.

PAI-1 in complex with proteinases is cleared from circulation by the low density

lipoprotein receptor related protein (Nykjaer *et al.*, 1992; Kounnas *et al.*, 1993). Some

closely related receptors may also contribute to the clearance from circulation (Argraves

et al., 1995; Moestrup *et al.*, 1993). The interaction with the receptor has been shown to

involve a specific binding site on PAI-1, which overlaps with the heparin binding site

(discussed below) (Stefansson *et al.*, 1998b). It is a cryptic site, that is, one which is only

functional in PAI-1-proteinase complexes (Stefansson *et al.*, 1998b).

Considerable structural work has been done on PAI-1 (Table 1.1). The protein

structure was originally solved in the latent form, becoming the first serpin to be solved

in that form, and was an important tool in the elucidation of the nature of the latency

transition (Mottonen *et al.*, 1992) (Fig. 1.6 c). Apart from the uncleaved but inserted

reactive centre loop, and the disruption of strand 1C, latent PAI-1 differed little in

structure from other known serpins, particularly those in the cleaved conformation. The

structure of a cleaved form of an A335P mutant PAI-1 was subsequently reported, in

Table 1.1: Reported Crystal Structures of PAI-1. Data compiled from references or the PDB depositions.

Structure	Number of molecules in asymmetric unit	Resolution	Residues reported to be observed	Mutations	References
Latent	1	2.6 Å	1-379	none	(Mottonen *et al.*, 1992)
Cleaved	1	2.7 Å	1-379	A335P	(Aertgeerts *et al.*, 1995a) (Aertgeerts *et al.*, 1995b)
Peptide Inhibited	1	1.95 Å	2-333, 348-379	A335E	(Xue *et al.*, 1998)
Active	4	2.98 Å and 2.2 Å	A/C = 7-379 B/D = 7-332, 348-379	N150H, K154T, Q319L, M354I	(Sharp *et al.*, 1999) (Chapter 3 of this thesis)

In the active structure four molecules are seen. Molecules A and C are observed to different extents than are molecules B and D.

essentially the same crystal form as latent PAI-1 and at similar resolution (Aertgeerts *et al.*, 1995b) (Fig. 1.6 b). This structure differed from latent PAI-1 only in the configuration of some surface loops and at strand 1C, which was in the normal position for a cleaved serpin. Recently, the structure of a cleaved A35E mutant PAI-1 with two inhibitory pentapeptides bound has been reported (Xue *et al.*, 1998) (Figure 1.6 d). This has provided useful information on the nature of peptide inhibition with possible applications for drug design. This structure was solved at 1.95 Å resolution, a significantly higher resolution than those of previous structures of PAI-1 (≥ 2.6 Å). While the rapid transition of the active form of PAI-1 into the latent form appeared to preclude its crystallization, the discovery of a considerably more stable mutant ($t_{1/2}$=145 hours at 37C) paved the way for structural work (Berkenpas *et al.*, 1995). The structure of this quadruple mutant (N150H, K154T, Q319L, M354I) of PAI-1 is reported in this document, first at 3.0 Å and then at 2.2 Å resolution. The structure shows the non-inserted, uncleaved conformation of PAI-1 (Figure 1.6 a). The completion of this structure makes PAI-1 one of two serpins, along with antithrombin III, for which structures are available in active, cleaved, latent, and peptide-inhibited forms.

1.2.3 Physiological roles of PAI-1

PAI-1 expression occurs in many tissues, and responds to a number of physiological stimuli and conditions. It plays an important controlling role in maintaining fibrinolytic homeostasis in plasma, and also plays a role in the extracellular matrix proteolysis that is involved in many, if not all, tissue remodeling processes. Dysfunction of PAI-1 in either of these roles has been related to disease conditions. For these diseases, treatments that target the activity of PAI-1 are being developed. Interactions with several proteins or

other cofactors are important in modulating these functions, as summarized in Table 1.2.

1.2.3.1 Expression of PAI-1

PAI-1 expression has been reported in many tissues. It is not entirely clear, however, which tissue sources are relevant to its known biological roles (de Bono, 1994). Endothelial cells are probably the most significant producers of plasma PAI-1 (Erickson *et al.*, 1985; Loskutoff & Schleef, 1988). Hepatic cells (Loskutoff *et al.*, 1986; Sprengers *et al.*, 1985) and muscle tissue (Lupu *et al.*, 1993) may also produce significant amounts, under the right circumstances. Non-subcutaneous, upper body, adipose tissues have also been shown to secrete PAI-1 and may contribute significantly to PAI-1 levels in obese individuals, possibly playing a role in cardiovascular disease (Lundgren *et al.*, 1996; Morange *et al.*, 1999a; Samad & Loskutoff, 1997). Platelets release PAI-1 that is stored internally in granules (Erickson *et al.*, 1984; Kruithof *et al.*, 1986b). While platelets may not contribute much to ambient circulating PAI-1, they are probably significant sources of tPA inhibition when the granules are released during clot formation (Loskutoff *et al.*, 1993). While expression of PAI-1 in kidney cells is usually low, its expression there in some disease conditions, such as endotoxemia, may cause kidney damage (Keeton *et al.*, 1995). In general, it seems likely that many or most cells can produce PAI-1 under certain circumstances, but the tissues most likely to contribute to plasma PAI-1 are the endothelium and adipose tissue.

Many hormones and expression factors have been reported to have an effect on the expression of PAI-1, but little consensus has been reached on their relative importance. Some factors, whose importance has been established and that have relevance to a change

Table 1.2: Physiological interactions of PAI-1

Molecule	Interaction with PAI-1
Tissue plasminogen activator (tPA)	Main inhibition target
Urokinase plasminogen activator (uPA)	Important inhibition target
Thrombin	Alternative inhibition target when PAI-1 binds heparin or vitronectin. Tends to inactivate PAI-1, as the efficiency of inhibition is low.
Vitronectin	Binds active PAI-1, stabilizes its active form and adds specificity for thrombin. The interaction activates vitronectin for cell binding, but inhibits its interactions with integrins
Heparin	Binds PAI-1, adding specificity for thrombin
Fibrin	Binds active PAI-1, localizing it to fibrin clots
Low density lipoprotein receptor related protein (LRP receptor)	Binds PAI-1 complexed with proteinases, clears it from circulation

in an important PAI-1 biological function, include insulin, very low density lipoprotein

(VLDL), tumor necrosis factor-α (TNFα), transforming growth factor-β (TGFβ),

glucocorticoids, and interferon-γ (INF-γ).

Insulin, as well as insulin-like growth factor 1, stimulates PAI-1 secretion from

hepatic cell lines (Alessi *et al.*, 1988, Fattal *et al.*, 1992, Anfosso *et al.*, 1995), human

adipose cell lines (Morange *et al.*, 1999b), human endothelial cell lines (Grenett *et al.*,

1998), and *in vivo* in mouse adipose tissue (Samad & Loskutoff, 1997). Insulin, which

regulates glucose uptake and cell growth, has been linked to the elevated levels of PAI-1

found in the hyperinsulinemic conditions of insulin resistance syndrome (discussed

below) (Juhan-Vague & Alessi, 1993; Wiman, 1995).

VLDL and its component lipoprotein a (Lp(a)) have been shown to increase the

transcription and secretion of PAI-1 in human umbilical vein endothelial cells (Li *et al.*,

1997; Stiko-Rahm *et al.*, 1990). High triglyceride VLDL (HTG-VLDL) is particularly

effective (Li *et al.*, 1997; Stiko-Rahm *et al.*, 1990). As elevated HTG-VLDL levels are

associated with insulin resistance, this could be another mechanism relating this condition

to high PAI-1 levels (Asplund-Carlson *et al.*, 1993). The effect seems to be mediated by

the VLDL receptor (Nilsson *et al.*, 1999). A VLDL response element has been identified

in the 5' region of the PAI-1 gene, and has been shown to contain the site of the 4G/5G

gene variation, which might explain this variation's medical significance (Eriksson *et al.*,

1998).

Tumor necrosis factor-α (TNFα) is a cytokine produced by macrophages and other

cell types and is involved in angiogenesis and other cell wall processes. PAI-1 release by

endothelial cells is increased by TNFα, while tPA release is decreased (Medcalf *et al.*,

1988; Schleef *et al.*, 1988; van Hinsbergh *et al.*, 1988). These effects have also been observed in omental (upper body) fat tissue (Cigolini *et al.*, 1999; Morange *et al.*, 1999a; van Hinsbergh *et al.*, 1990a). While these effects of TNFα should reduce fibrinolysis in plasma, the release of uPA is stimulated basolaterally in endothelial and other cell lines, so that tissue remodelling may be stimulated (Georg *et al.*, 1989; van Hinsbergh *et al.*, 1990b). TNFα has been suggested to play a role in the upregulation of PAI-1 in insulin resistance syndrome, as TNFα is expressed by adipose tissue, and the tissue's expression of PAI-1 is increased by TNFα (Cigolini *et al.*, 1999). The exact mechanism for TNFα upregulation of PAI-1 secretion has not been determined, but increased expression and/or protection of the longer mRNA seem to play a role (Georg *et al.*, 1989; Schleef *et al.*, 1988; van Hinsbergh *et al.*, 1988).

TGFβ, a cytokine with cell proliferation and extracellular matrix stimulating effects, upregulates expression of PAI-1, while it downregulates the expression of tPA in most tissues (Laiho *et al.*, 1986; Laiho *et al.*, 1987; Lund *et al.*, 1987; Saksela *et al.*, 1987). TGFβ release by platelets may accentuate their clotting effect by stimulating PAI-1 secretion by neighboring tissues (Slivka *et al.*, 1991, Hopkins *et al.*, 1991).

Interferon-γ from activated T-cells may downregulate the secretion of PAI-1, offsetting the effects of endotoxin, and facilitating tissue invasion by cells of the immune system (Gallicchio *et al.*, 1996).

Glucocorticoids, such as hydroxycortisone, and their analogue dexamethasone, have been shown to downregulate PA's in most tissues (Rifkin, 1978; Rifkin & Crowe, 1980), while stimulating expression of PAI-1 (Andreasen *et al.*, 1987; Loskutoff *et al.*, 1986), thus restricting extracellular matrix degradation. These effects have been observed in

tissue types important for PAI-1 expression, including endothelial cell lines (Loskutoff *et al.*, 1986), adipose cell lines (Morange *et al.*, 1999b), and hepatic cell lines (Knittel *et al.*, 1996; Uno *et al.*, 1998). They have also been demonstrated in keratinocyte cell lines, possibly helping to explain the effects glucocorticoids have on epithelial wound healing (Bator *et al.*, 1998). Locations for glucocorticoid responsive elements have been proposed in the human (van Zonneveld *et al.*, 1988) and rat (Bruzdzinski *et al.*, 1990) PAI-1 genes.

Several general physiological factors have been suggested to play a role in PAI-1 expression and activity. The activity and concentration of PAI-1 is known to vary on a diurnal cycle, with the zenith of inhibitory activity occurring in the early morning. As myocardial infarction rates follow a similar pattern, this may indicate an important relationship (Juhan-Vague *et al.*, 1992; Kluft *et al.*, 1988). Exercise is known to increase fibrinolysis transiently; however, a rebound anti-fibrinolytic effect, believed to be due to increased expression of PAI's, soon sets in. The degree of rebound can be reduced by regular exercise (Boman *et al.*, 1994; de Bono, 1994). PAI-1, as well as PAI-2, is elevated during pregnancy, contributing to the hypofibrinolytic nature of that state (Declerck *et al.*, 1988a; Kruithof *et al.*, 1987; Wiman *et al.*, 1984).

A well-studied physiological influence on PAI-1 expression and activity is insulin resistance syndrome. This syndrome consists of a cluster of physiological abnormalities that can be traced to a poor cellular response to insulin. The response appears to be related to obesity, with increased obesity leading to a decrease in the number of cellular insulin receptors. Insulin resistance syndrome seems to be a pre-diabetic state, with obese sufferers tending to develop non-insulin dependent diabetes. In the absence of

obesity, most persons with the syndrome are apparently healthy. The major

abnormalities include android (upper body) obesity, hyperinsulinemia, glucose

intolerance, hypertension, elevated triglycerides and very low density lipoprotein

(VLDL), and decreased high density lipoproteins. The syndrome is considered to be a

good indicator of potential arteriosclerosis and heart disease. It has been observed that

persons with the syndrome have elevated levels of PAI-1. Various reasons have been

proposed for this, including the stimulatory effects of insulin, VLDL, and Tumor necrosis

factor-α on PAI-1 expression (Juhan-Vague, 1996; Juhan-Vague & Alessi, 1993; Juhan-

Vague & Alessi, 1997; Samad & Loskutoff, 1997; Wiman, 1995). Recent studies have

downplayed the importance of insulin on *in vivo* PAI-1 levels (Morange *et al.*, 1999a).

PAI-1 and VLDL levels have a better correlation than PAI-1 and insulin levels (Asplund-

Carlson *et al.*, 1993). However the best supported cause is simply the tendency of

omental adipose tissue to express PAI-1, possibly with the involvement of TNFα (Juhan-

Vague & Alessi, 1997; Samad & Loskutoff, 1997).

1.2.3.2 PAI-1 in plasma fibrinolytic homeostasis

PAI-1 serves as the main overall regulator of fibrin clot dissolution in blood vessels.

It is strategically located at the top level of the fibrinolysis cascade, so that, by halting the

effect of plasminogen activator, it can stop the generation of many plasmin molecules and

protect large amounts of fibrin from being cleaved (Figure 1.1). Genetic deficiency in

functional PAI-1 causes a mild bleeding disorder, presumably due to premature and

excessive fibrinolysis (Dieval *et al.*, 1991; Fay *et al.*, 1997; Fay *et al.*, 1992). The

relationship between insulin resistance syndrome, where PAI-1 activity in plasma is

increased, and heart disease, may also show the importance of PAI-1 in fibrinolysis.

Several properties of PAI-1 assist it in the control of fibrinolysis. PAI-1's tendency to take the latent form should help regulate the degradation of thrombi. In the absence of continued PAI-1 secretion in the vicinity, the latency transition would tend to accelerate the deprotection of fibrin from cleavage. Release from platelet granules helps concentrate PAI-1 at thrombi, while platelets also release transforming growth factor β-1(TGFβ) , which stimulates PAI-1 release in neighboring endothelium (Fujii *et al.*, 1989; Hopkins *et al.*, 1991; Slivka & Loskutoff, 1991a). Platelet granules also release the matrix glycoprotein vitronectin, which is involved in accentuating and modulating the activity of PAI-1 in a particularly interesting fashion.

Active, but not cleaved or latent, PAI-1 binds vitronectin (Figure 1.2)(Declerck *et al.*, 1988b; Lawrence *et al.*, 1997; Mimuro & Loskutoff, 1989). This interaction stabilizes the active form of PAI-1 (Declerck *et al.*, 1988b; Mimuro *et al.*, 1987), enhances activity against the serine proteinase thrombin (Ehrlich *et al.*, 1990; Naski *et al.*, 1993), and moderately increases the activity against uPA, but not tPA (Keijer *et al.*, 1991b). Deletion studies of vitronectin show that the interaction apparently involves residues 1-40 of the N-terminus, a somatomedin B (SMB) domain (Deng *et al.*, 1995). Mutational studies of PAI-1 have identified a region, including strand 1A and helices C and E, that serves as the vitronectin binding domain (Lawrence *et al.*, 1994). The interaction of vitronectin and PAI-1 has been proposed to be significant in the regulation of vitronectin activity (Preissner *et al.*, 1997; Stefansson *et al.*, 1998a). PAI-1 causes vitronectin to adopt an open, surface binding conformation, but blocks the RGD site it uses to bind integrins, the cell surface proteins that serve as its target (Deng *et al.*, 1996; Stefansson & Lawrence, 1996). Thus active PAI-1 can modulate or inhibit the activity of

vitronectin in various matrix interactions. As the 6-stranded forms of PAI-1 lose the ability to bind vitronectin (Lawrence *et al.*, 1997), the inhibition can be eliminated by reaction with plasminogen activators or by the latency transition. Hence PAI-1 serves as a molecular switch that can turn various interactions on or off, depending on its state. The interaction of PAI-1 with vitronectin released by platelets may help it to localize to and protect exposed extracellular matrix at the site of vascular wounds. The interaction between these two molecules may also be very significant in modulating tissue remodelling effects, as will be discussed below.

Active PAI-1 is also activated against thrombin by binding the anticoagulant glycosaminoglycan heparin (Ehrlich *et al.*, 1991). Heparin has also been reported to activate PAI-1 against tPA (Edelberg *et al.*, 1991), and heparin and heparan sulphate have been reported to activate PAI-1 against uPA (Urano *et al.*, 1994); however, other reports indicate the activity is only modulated against thrombin (Keijer *et al.*, 1991b). The binding site for heparin is a positive patch centred on helix D, close to the site for vitronectin, and similar to the sites seen in antithrombin III and other serpins (Ehrlich *et al.*, 1992). Heparin has been shown to activate thrombin in a template based fashion, that is, by binding both PAI-1 and thrombin and aligning them for their interaction (Ehrlich *et al.*, 1991; Meijer *et al.*, 1997). While heparin and vitronectin increase the rate of the inhibition reaction, they increase the rate of the substrate reaction even more. Thus, in their absence, 3 moles of PAI-1 are required to inhibit 1 mole of thrombin, while in their presence, 6 moles of PAI-1 are required (Meijer *et al.*, 1997). The interaction of heparin, heparan sulphate, or vitronectin with PAI-1 has also been suggested to induce slight structural changes, based on fluorescent probe and intrinsic fluorescence studies (Fa *et*

al., 1995; Urano *et al.*, 1994). These have been suggested to play a role in activation, by analogy to antithrombin III, where binding heparin activates the serpin not only by the template mechanism, but by expelling the reactive centre loop from an inhibitory 'pre-inserted' conformation (Huntington *et al.*, 1996; Jin *et al.*, 1997; van Boeckel *et al.*, 1994). The significance of structural changes in PAI-1 caused by heparin binding to PAI-1's activation has, however, not been demonstrated, and heparin is generally believed to induce the activation by the template mechanism.

The interaction with vitronectin or heparin (an anticoagulant) allows PAI-1 to inhibit thrombin, causing it to play a (minor) role in the termination of thrombosis. Thrombin has been reported to stimulate the secretion of both tPA and PAI-1 (Gelehrter & Sznycer-Laszuk, 1986; Hanss & Collen, 1987; Van Hinsberg *et al.*, 1987). The thrombin receptor and a variety of intracellular signal transduction elements have been shown to play a role in the stimulation (Shen *et al.*, 1998). This may form part of a feedback mechanism controlling thrombosis, due to PAI-1's (limited) activity against thrombin. Induction of tPA and PAI-1 together in response to thrombin would serve to modulate thrombosis without inducing full-scale fibrinolysis (Schleef & Loskutoff, 1988). Thrombin-mediated inactivation of PAI-1, through the substrate reaction that predominates in the presence of heparin, may also have an anticoagulant effect; more tPA would be protected to activate plasmin and increase fibrinolysis.

Active PAI-1 can also bind fibrin, which may aid in localizing it to blood clots (Keijer *et al.*, 1991a; Stringer & Pannekoek, 1995). Antibody mapping suggests that there are two fibrin binding domains, one including helices E and F, and the other including helix I (Keijer *et al.*, 1991a). The former domain is adjacent to the vitronectin

binding domain (Keijer *et al.*, 1991a). Latency or reaction with uPA eliminate the interaction of PAI-1 with fibrin; the interaction is probably also eliminated by interaction with tPA, but PAI-1-tPA complexes retain an affinity for fibrin due to tPA's interactions via its finger and kringle 2 domains (Wagner *et al.*, 1989). Fibrinogen has been reported to augment the reaction between PAI-1 and tPA; however, this may involve interactions between tPA and fibrinogen, not interactions directly involving PAI-1 (Edelberg *et al.*, 1991).

There is obviously a potential for the fibrinolytic system and for PAI-1 to be involved in diseases involving blood clots, such as myocardial infarctions, stroke and angina. The relationship has been long suspected (Declerck *et al.*, 1994), and an increasing number of studies do show a correlation. A strong correlation between PAI-1 levels and mortality from myocardial infarctions in young males has been observed (Hamsten *et al.*, 1985). Progression of coronary artery disease in young males has been shown to have strong links with fibrinolytic function, as well as disturbances in carbohydrate and lipoprotein metabolism (Bavenholm *et al.*, 1998; Meade *et al.*, 1993). In general the correlation seems stronger in younger patients (Nilsson & Johnson, 1987). Hypofibrinolysis has been shown to be a risk factor in the recurrence of venous thromboembolism (Schulman & Wiman, 1996). Deficient fibrinolysis has been associated with angina (Zalewski *et al.*, 1991) and stroke (Kristensen *et al.*, 1999; Kristensen *et al.*, 1998). The upregulation of PAI-1 activity in the insulin resistance syndrome is widely considered to be the connecting factor between the syndrome and cardiovascular disease (Juhan-Vague & Alessi, 1997; Wiman, 1995). The hypofibrinolytic state induced by elevated levels of PAI-1 and PAI-2 during pregnancy is

believed to be behind the occurence of preeclampsia and eclampsia, conditions that apparently involve the formation of clots in the placenta (Estelles *et al.*, 1989; Estelles *et al.*, 1998; Wiman *et al.*, 1984). Overexpression of PAI-1 in kidney cells seems to contribute to kidney damage in nephritis and lupus, possibly by the formation of microthrombi (Yamamoto & Loskutoff, 1997; Yamamoto & Saito, 1998).

The circulatory plasmin system has also been demonstrated to play a role in bacterial sepsis; however there are contradictory reports of the involvement of different members of the system and of the overall effect that sepsis has on fibrinolysis (Duboscq *et al.*, 1997; Philippe *et al.*, 1991; Pralong *et al.*, 1989). Bacterial endotoxin (lipopolysaccharide) has been shown to induce the expression of PAI-1 (Colucci *et al.*, 1985; Crutchley & Conanan, 1986; Emeis & Kooistra, 1986; Sawdey *et al.*, 1986). This has been suggested to play a role in bacterial septicemia and endotoxemia, by aiding the formation of tissue-damaging microthrombi, particularly in kidney tissue (Schleef & Loskutoff, 1988; Yamamoto *et al.*, 1998; Yamamoto & Saito, 1998). Studies in mice have suggested that stimulation of PAI-1 by endotoxin may occur via the induction of TNFα (Sawdey & Loskutoff, 1991).

1.2.3.3 PAI-1 in extracellular matrix proteolytic homeostasis

PAI-1 is also believed to play a role in tissue remodeling and maintenance. In addition to cleaving fibrin, plasmin can also cleave laminin, vitronectin, fibronectin, proteoglycans, and other extracellular matrix proteins, hence the members of the fibrinolytic cascade are considered to be important in the regulation of the extracellular matrix. (Scully, 1991). In addition, plasmin can activate some matrix metalloproteinases, which are involved in the degradation of collagen and other matrix components

(Goldberg *et al.*, 1990; Grant *et al.*, 1992). uPA is considered to be the primary plasminogen activator in the matrix. PAI-1 shares the regulation of uPA with PAI-2. In addition, PAI-1's interaction with vitronectin is believed to play an important role in the extracellular matrix (Figure 1.2). Vitronectin's ability to bind integrins makes it important to cell-matrix interactions. Since PAI-1 can cause vitronectin to take the open conformation, it can cause it to bind to cells. At the same time PAI-1 protects vitronectin from proteolysis and prevents it from facilitating cell-matrix binding via integrins.

Several tissue remodeling processes have been shown to be affected by the plasmin system. The ovulation process has been shown to involve the induction of the plasmin system, with PAI-1 playing a role in its control (Liu *et al.*, 1997; Ohlsson *et al.*, 1991; Shen *et al.*, 1997). The plasmin system and PAI-1 have also been shown to be activated in inflammation, including joint inflammation in rheumatoid arthritis and osteoarthritis (Cerinic *et al.*, 1998; Podor *et al.*, 1992; Seiffert *et al.*, 1990; Wallberg-Jonsson *et al.*, 1993).

PAI-1 has been shown to play an extensive role in processes involving the extracellular matrix of the vascular endothelium. Angiogenesis, the process by which new blood vessels are formed, involves the invocation of the plasmin system by invading vascular epithelial cells (Moscatelli & Rifkin, 1988). PAI-1 production is stimulated in neighboring cells, presumably to limit the damage to the extracellular matrix (Bacharach *et al.*, 1998). PAI-1 is also involved in limiting the migration of cells, especially smooth muscle and keratinocytes, into the sites of vascular wounds or remodelling (Kjoller *et al.*, 1997; Stefansson & Lawrence, 1996). This function operates via its interaction with vitronectin (Kjoller *et al.*, 1997; Stefansson & Lawrence, 1996). These cells use the

vitronectin sites blocked by PAI-1 as anchoring sites for the integrin molecules, which

are required for them to bind and move through extracellular matrix (Lauffenburger,

1996). Release of vitronectin and PAI-1 at wound sites limits the ability of motile cells

to invade the wounded area initially, then allows controlled migration as PAI-1 levels

drop because of the latency transition or reaction with tPA (Preissner *et al.*, 1997;

Stefansson *et al.*, 1998a). Local deficiency of PAI-1 activity has been suggested to be

involved in the formation of aneurysms (Shen, 1998).

There are a number of examples where PAI-1's role in tissue remodeling and

maintenance may be relevant to disease conditions. Increased expression of members of

the fibrinolysis system, including PAI-1, has been reported to play a role in the tissue

remodeling processes that characterize the chronic form of kidney transplant rejection

(Tang *et al.*, 1998). The plasmin system has also been suggested to be involved in

epithelial proliferative disorders and wound healing, with the regulation of PAI-1 and

PAI-2 playing a major role both in the disorders, and in their treatment by glucocorticoids

(Bator *et al.*, 1998; Brown & Chambers, 1984; Brown *et al.*, 1995).

The major disease where PAI-1's role in tissue remodeling comes into play is

cancer, at the stages of tissue invasion and of metastasis (Schmitt *et al.*, 1997). High

levels of PAI-1 have been correlated with poor prognoses for breast (Foekens *et al.*,

1994; Janicke *et al.*, 1991; Janicke *et al.*, 1993), ovarian (Kuhn *et al.*, 1994; Kuhn *et al.*,

1999), endometrial (Gleeson *et al.*, 1993), cervical (Kobayashi *et al.*, 1994), kidney

(Hofmann *et al.*, 1996a; Hofmann *et al.*, 1996b), gastric (Nekarda *et al.*, 1994), colorectal

(Ganesh *et al.*, 1994; Ganesh *et al.*, 1996; Ganesh *et al.*, 1997; Verspaget *et al.*, 1995),

lung (Pedersen *et al.*, 1994a; Pedersen *et al.*, 1994b), squamous cell (Zeillinger *et al.*,

1996), and chondrosarcoma (Hackel *et al.*, 1997) cancers. In order for cancer cells to spread they must be able to penetrate the extracellular matrix, hence the activation of plasmin and other proteinase systems is a requirement (Schmitt *et al.*, 1997). While this explains the observed positive correlation of tumor uPA concentration and the negative correlation of PAI-2 tumor concentration with cancer spread and metastasis, the positive correlation of PAI-1 tumor concentration with these phenomena is somewhat surprising (Schmitt *et al.*, 1997). Like PAI-2, PAI-1 would be expected to suppress the activation of the plasmin system, and prevent tissue invasion and metastasis. Several possibilities have been suggested. As PA and PAI-1 expression often increase in tandem to carefully regulate fibrinolysis, the increased PAI-1 activity may be a side effect of increased tissue degradation. Poorly regulated extracellular matrix degradation might be disadvantageous to a migrating tumor, as it might destroy suitable anchorage points. It may also be a response by neighboring tissues to overexpression of PA's by the tumor. One interesting suggestion is that PAI-1's interaction with vitronectin helps block interactions with integrins that bind cancer cells to neighboring tissues and retard tissue invasion and metastasis (Schmitt *et al.*, 1997). However vitronectin provides points of attachment for migrating cells in systems where the interaction with PAI-1 is well characterized, unlike what this theory would require. It has also been shown that PAI-1is necessary for the vascularization of tumors, although its precise role has not been clarified (Bajou *et al.*, 1998). There are also some studies which show a reduced rate of metastasis with higher PAI-1 expression, which may indicate that the effects are tissue dependant (Bell, 1996).

1.2.3.4 Potential treatments for PAI-1 dysfunction.

As the majority of the disease conditions associated with PAI-1 are associated with an excess of its inhibitory activity, various mechanisms to inhibit inhibition by PAI-1 have been proposed (Pawlowska *et al.*, 1998; Schmitt *et al.*, 1997). These include inhibition with reactive centre loop mimicking peptides which insert in the A sheet, turning PAI-1 into a substrate (Eitzman *et al.*, 1995; Xue *et al.*, 1998), inhibition with small molecule inhibitors working by unknown mechanisms (Björquist *et al.*, 1998; Friederich *et al.*, 1997), neutralization with monoclonal antibodies (Abrahamsson *et al.*, 1996; Biemond *et al.*, 1995; Levi *et al.*, 1992), and inhibiting translation with anti-PAI-1 mRNA phosphothiorate mimetics (Buczko *et al.*, 1997; Misiura *et al.*, 1998; Pawlowska *et al.*, 1998; Stec *et al.*, 1997). For the first two techniques, a structural understanding of PAI-1 provides a definite advantage.

1.2.4 Insights to be gained from the structure of active PAI-1

The active form of a serpin is of particular interest, as it is the form that interacts with the proteinase. In the case of PAI-1, while several structures have been solved (Figure 1.6), allowing the elucidation of the nature of the latent transition (Mottonen *et al.*, 1992), the cleaved form of the molecule (Aertgeerts *et al.*, 1995b), and the mechanism of inhibition by peptides (Xue *et al.*, 1998), the lack of an active form for comparison has remained a limitation. The active model would provide a form to compare the six-stranded forms to, and would allow more detailed comparisons than would be possible using models based on the structures of other active serpins.

The active form of PAI-1 is not only the form which interacts with plasminogen activators, it is also the form which interacts with vitronectin and heparin. As these

interactions are considered to be biologically significant, an active structure is not only essential for modelling the interaction face, but is also paramount for explaining the abolition of binding by the transition to other forms of PAI-1. The active form is also the form bound by small molecule inhibitors of its activity (Björquist *et al.*, 1998; Friederich *et al.*, 1997), and should facilitate understanding their function by modelling and other means. The structure of a quadruple mutant with a relatively stable active form, should help to explain the effects the mutations have on latency. It should also clarify the conformation of the reactive centre loop in the active form of the molecule. The solution of an active structure would give researchers as complete a set of important forms for PAI-1 as is available for any serpin.

1.3 Shiga-like toxin-1

1.3.1 A-B type toxin

Many pathogenic organisms produce proteins with the capacity to enter a cell and produce cell death. These proteins, which in many cases are a primary source of the organism's ability to produce disease, are known as cytotoxins, or toxins.

An interesting feature of many toxins is the division of the activities of the toxin among different subunits, with one or more subunits responsible for cell entry, and another subunit or subunits responsible for cell death. This arrangement has been observed in the plant toxins ricin and abrin, and bacterial toxins from *Shigella dysenteriae*, *Vibrio cholerae*, *Pseudomonas aruginosa*, *Corynebacterium diptheriae*, *Bordetella pertussis*, several strains of *Escherichia coli*, and many other bacteria (Brunton, 1990; Gill, 1978; Locht & Keith, 1986; Nicosia *et al.*, 1986). Cytotoxins with this structure have been referred to as A-B toxins, the toxic subunit being A, and the cell-

entry subunit being B (Brunton, 1990). The A-B pairing is believed to allow the

combination of different toxic and cell entry mechanisms. Several different types of A

subunit toxicity and many different forms of B subunit cell entry have been observed. In

effect, the pathogenic organisms have been able to tailor specific toxicities by assembling

toxins from different combinations of subunits.

1.3.2 AB$_5$ toxins

A classic example of the A-B type toxins are the subgroup known as the AB$_5$ toxins

(Merritt & Hol, 1995; Murzin, 1992; Murzin, 1993). In these, a toxic A subunit of

variable nature is connected to a homopentamer (heteropentamer in pertussis toxin) of B

subunits. Hence, in cholera toxin, *E. coli* heat labile enterotoxin, and pertussis toxin, the

A subunit is an ADP-ribosylase of regulatory G-proteins (Moss & Vaughan, 1988;

Spangler, 1992), while in Shiga toxin, and the *E. coli* Shiga-like toxins (verotoxins), the

A subunit is a ricin-like N-glycosidase, targeting an adenine in the 28S ribosomal RNA

(Endo *et al.*, 1988; Saxena *et al.*, 1989). While the B-subunits in many cases lack any

sequence identity, they share a common fold (Murzin, 1992; Murzin, 1993; Sixma *et al.*,

1993; Stein *et al.*, 1992). The individual B-monomers have a mixed α–β structure, with

6 antiparallel β-strands, and one α-helix (Figure 1.7). The monomers are arranged in the

pentamer so that the helices line a central pore, whereas the β-strands form the outer

perimeter of the pentamer. The strands are arranged so that each β-sheet is composed of

three strands from each of two adjacent monomers. The B-pentamers facilitate entry of

their toxins by acting as lectins, binding cell surface glycolipids or glycoproteins (Dalziel
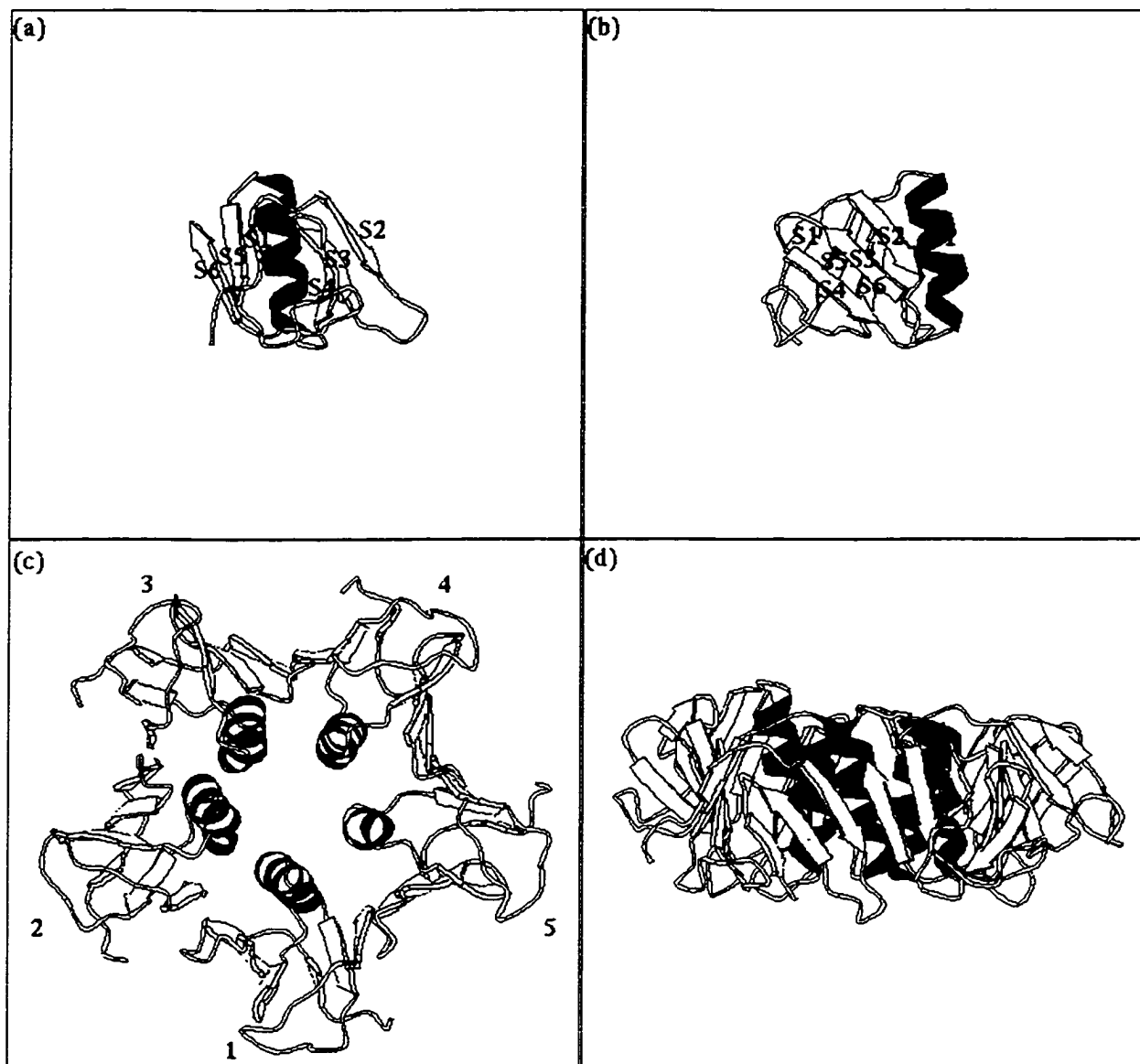
Figure 1.7: SLT-1 monomer and pentamer structure (Stein *et al.*, 1992). A typical monomer (3) is shown in 2 orientations, differing by 90°, in (a) and (b). Beta strands are shown in yellow, and the helix in red. The complete pentamer is shown in 2 orientations, differing by 90°, in (c) and (d). The monomers are numbered in C. The interface disrupted by the lockwasher distortion lies between monomers 1 and 2. The degree to which monomer 2 is pushed out of the plane can be seen in (d). This figure was made using Molscript (Kraulis, 1991).

et al., 1984; Fishman *et al.*, 1980; Heerze *et al.*, 1992; Jacewicz *et al.*, 1986; King &

Van Heyningen, 1973; Lindberg *et al.*, 1987; Lingwood *et al.*, 1987; Saukkonen *et al.*,

1992; van't Wout *et al.*, 1992). AB$_5$ toxins enter the cell via clathrin-mediated or

clathrin-independent endocytosis (Montesano *et al.*, 1982; Sandvig *et al.*, 1989; Sandvig

et al., 1991). While a large fraction of the internalized toxin travels to the lysosomes

(Sandvig *et al.*, 1989; Sandvig *et al.*, 1991), a small fraction, apparently responsible for

the toxic effects, is sent to the Golgi apparatus (Sandvig *et al.*, 1993; Sandvig *et al.*,

1991). The intracellular routes travelled by the AB$_5$ toxins are not completely

understood, and may vary from toxin to toxin, but they appear to involve retrograde

transport to the endoplasmic reticulum (ER) (Lencer *et al.*, 1993; Sandvig *et al.*, 1992;

Spangler, 1992),

presumably followed by translocation to the site of action in the cytoplasm (reviewed by

Hazes & Read, 1997).

The A subunits are believed to be released from the B-pentamer prior to carrying out

their catalytic activity in the cytoplasm. This release is generally believed to occur in the

ER, where it has been shown to occur for *P. aeruginosa* exotoxin A (Ogata *et al.*, 1990).

1.3.3 Shiga toxins

The Shiga toxin from *Shigella dysenteriae* and the Shiga-like toxins from

enterohemorrhagic strains of *E. coli* form a closely related family of AB$_5$ toxins (Merritt

& Hol, 1995). Both the A subunits and the B subunits show clear sequence similarity to

each other (Figure 1.8). The Shiga toxins can be divided into two groups, based on the

sequence of the B-pentamer, and immune cross-reactivity (Brunton, 1990). Shiga toxin

```
Secondary Structural Element      β-1     β-2         β-3      β-4       α-1
Secondary Structural Type         ==>     =====>tttt  =====>tt=====>   ~~~~~~~
Sugar-Binding Interaction         #                   *  *    *        *## #****
Residue Number                    1       11          21       31
Shiga/Shiga Like Toxin-1          tpDCvtGKvE ytKYNdDDTF TVKvgdkElf TnRWNLvsLL
Shiga Like Toxin-2                _aDCakGKiE fsKYNeDDTF TVKvdgkEyw TsRWNLqpLL
Shiga Like Toxin-2c               _aDCakGKiE fsKYNnDDTF TVKadgkEyw TsRWNLqpLL
Shiga like Toxin-2e               _aDCakGKiE fsKYNeDDTF TVKvsgrEyw TnRWNLqpLL


Secondary Structural Element      α-1     β-5                   β-6
Secondary Structural Type         ~~~~~~tt=====>   gttt t   ====>
Sugar-Binding Interaction                          #*#    *  #  *
Residue Number                    41      51          61
Shiga/Shiga Like Toxin-1          lSAQiTGMTV TIktnaCHnG gGFseViFr
Shiga Like Toxin-2                qSAQlTGMTV TIksstCEsG sGFaeVqFnn d
Shiga Like Toxin-2c               qSAQlTGMTV TIksstCEsG sGFaeVqFnn d
Shiga like Toxin-2e               qSAQlTGMTV TIisntCEsG sGFaqVkFn
```

Figure 1.8: Sequences of Shiga toxin and Shiga-like toxin B-subunits. Residues

conserved in all sequences are capitalized. Secondary structure: β-strands are indicated

with ==> symbols, the α–helix is indicated with ~~~, β-turns (when not overlapping other

structures) are indicated with t, the gamma turn with g. Sugar binding residues (for SLT-

1): residues forming hydrogen bonds are indicated with *, those forming only non-polar

contacts are indicated with #.

and Shiga-like toxin-1 or Verotoxin-1 (SLT-1, or VT-1) form one group: they have identical B-subunits, only 1 different amino acid in the A subunit, and complete immune cross-reactivity with each other. Shiga-like toxin-2 or Verotoxin-2 (SLT-2 or VT-2) and its variants SLT-2c and SLT-2e, form another immuno-cross-reactive group of toxins that have nearly 90% sequence identity in their subunits.

1.3.4 Target specificity of B-pentamers

With the exception of SLT-2e, the B-pentamers of all SLTs bind to the cell surface glycosphingolipid, globotriaosylceramide (Gb3) (Figure 1.9 a) (Jacewicz et al., 1986; Lindberg et al., 1987; Lingwood et al., 1987). SLT-2e binds preferentially to the related glycosphingolipid globotetraosylceramide (Gb4) (Figure 1.9 b) (DeGrandis et al., 1989). Both Gb3 and Gb4 are common cell surface markers, and are found on a number of cell types (Boyd et al., 1993). Gb3 (also called CD77) forms the P^k antigen of the P blood type system, while Gb4 forms the P antigen (Lingwood, 1993). Gb3 is expressed in cell lines, including HeLa and Vero cells, that are susceptible to SLT-1 (Lingwood, 1987). It is also found in tissues known to be affected by hemolytic E. coli disease, such as kidney endothelial cells (Boyd & Lingwood, 1989). Some correlations have been determined between levels of Gb3 or Gb4 in tissues and the tissues' susceptibility to SLT-1 or SLT-IIe respectively , although other factors, such as blood flow (Boyd et al., 1993) and possibly internal toxin processing (Sandvig & van Deurs, 1996) also play a role.

1.3.5 Roles of SLTs in Disease

1.3.5.1 A subunit mechanism of action

The A subunit bears the toxic activity of the AB_5 toxins. In the Shiga toxins, the A subunit is a ricin-like N-glycosidase which can cleave Adenine 4324 of the 28S rRNA in
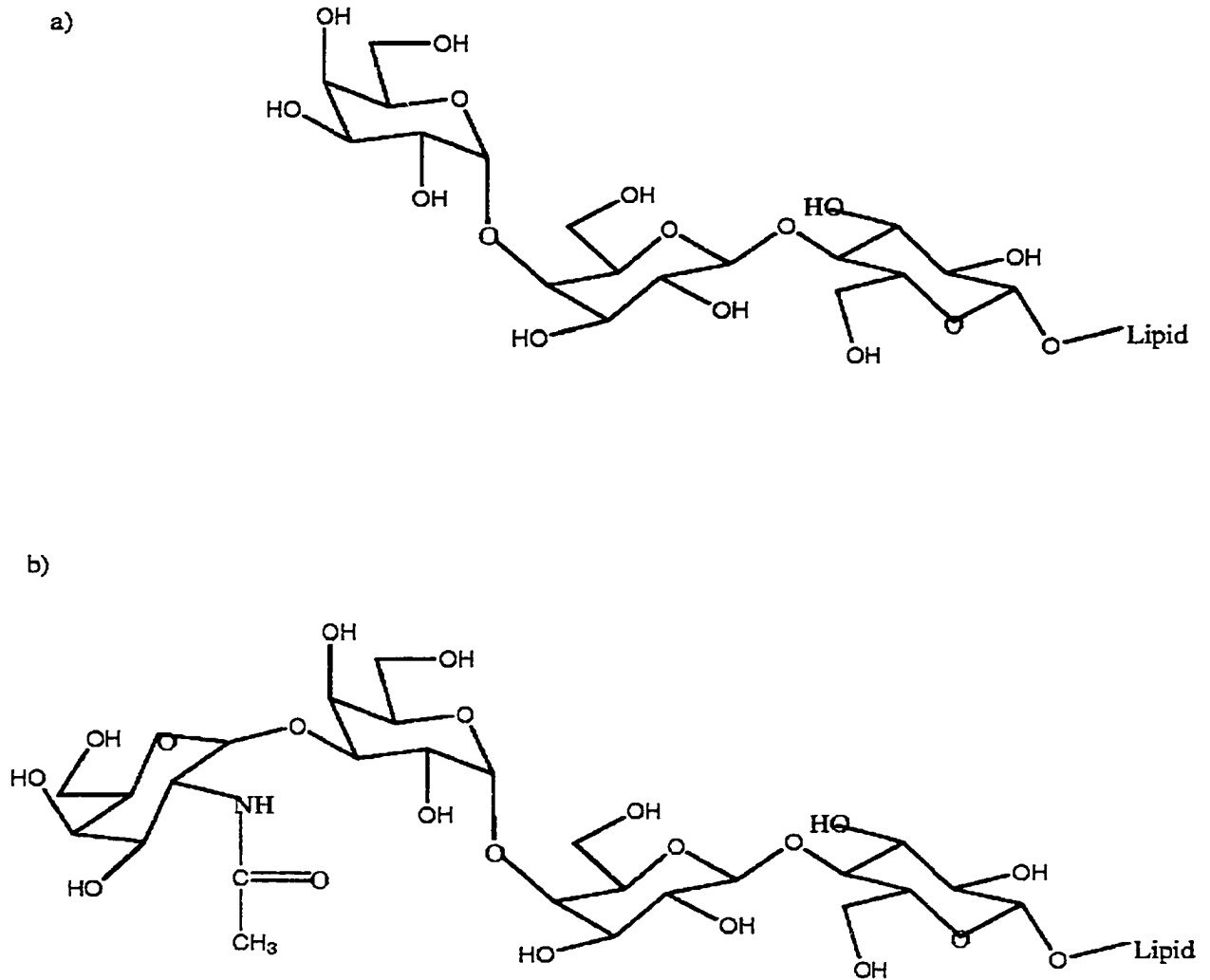
Figure 1.9: Structures of Gb$_3$ and Gb$_4$ glycolipids. (a): Gb$_3$ (b): Gb$_4$.

the 60S ribosome subunit (Endo *et al.*, 1988; Saxena *et al.*, 1989). This halts protein synthesis, and is ultimately fatal to the cell. The A subunit must be released from the B-pentamer, and the C-terminal portion of the molecule, the A_2 fragment, must be cleaved before the catalytic A_1 fragment becomes active (Fraser *et al.*, 1994; Garred *et al.*, 1995a; Garred *et al.*, 1995b; Olsnes *et al.*, 1981; Reisbig *et al.*, 1981). A disulphide linking the A_1 and A_2 fragments must also be reduced for A_1 activity (Garred *et al.*, 1997; Olsnes *et al.*, 1981; Reisbig *et al.*, 1981). The cleaving of the A subunit and the reduction of the disulphide bond linking the fragment are often assumed to be the mechanism releasing the A subunit from the B-pentamer; however this has not been directly demonstrated. It is generally assumed that the A subunit is released in the endoplasmic reticulum, although this too has not been proven.

The B pentamer is the main determinant of the toxin's effects, as it controls the specificity of the cell types affected. SLT-1, SLT-2, and SLT-2c, the Gb_3 binding toxins, all cause similar symptoms, while SLT-2e, the Gb_4 binding toxin, causes a considerably different disease (Boyd *et al.*, 1993; DeGrandis *et al.*, 1989). Mutations of SLT-2e that switch its affinity to Gb_3 cause it to have effects much like the other SLTs (Boyd *et al.*, 1993).

1.3.5.2   Hemorrhagic colitis

Shigella dysenteriae and enterohemorrhagic strains of *E. coli* reside in the intestine, and are adapted to survival in that environment. The diseases they cause might be attributed to an exaggeration of that adaptation. Enterohemorrhagic *E. coli* in naïve hosts can cause a bloody diarrhea (hemorrhagic colitis) with possible complications involving kidney damage (hemolytic uremic syndrome) or damage to other tissues (Cleary, 1992;

Cohen, 1991). The disease is generally spread as a form of food poisoning, often called

'hamburger disease', involving non-sterile cattle products or poorly cleaned vegetable

products that may have been exposed to cattle manure (Cohen, 1991; Hashimoto *et al.*,

1999; Tarr, 1995). Enterohemorrhagic *E. coli* strains such as O157:H7 are known to

have several mechanisms facilitating their survival (Cohen, 1991; Tarr, 1995; Tesh &

O'Brien, 1992) that could be the cause of disease, thus the role of the SLTs in *E. coli*

hemorrhagic colitis is not clear. As intestinal cells do produce Gb_3 (Kotani *et al.*, 1994),

it is conceivable that SLT-1 and SLT-2 assist the bacterium in establishing colonization

sites and producing lesions. It has been shown that the toxin is transported through the

epithelial cells and released into the blood stream (Acheson *et al.*, 1996), possibly

affecting intestinal endothelial cells and causing the hemorrhage (Jacewicz *et al.*, 1999).

This utilization of toxin transport into the bloodstream may underlie the most common

serious complication of hemorrhagic colitis, hemolytic uremic syndrome (HUS).

1.3.5.3   Hemolytic uremic syndrome (HUS)

In a small but significant number of hemorrhagic colitis cases, the disease is

complicated by kidney damage and possibly kidney failure (Cleary, 1992; Cohen, 1991).

Neurological damage has also been reported (Cleary, 1992; Cohen, 1991; Tarr, 1995),

and a significant number of fatalities occur, mostly among children or the elderly (Cohen,

1991; Hofmann, 1993; Tarr, 1995). These complications appear to be due to the presence

of SLTs (Hofmann, 1993). The utility to the bacterium of these effects is unclear.

Possibly it is merely a side effect of the mechanism of delivery to intestinal endothelial

cells. Gb_3 is also found as a surface marker on some immune cells, including B cells

(Mangeney *et al.*, 1991). There is some evidence that SLTs may harm those cells,

suppressing the production of IgG antibodies and facilitating bacterial survival

(Lingwood, 1996).

1.3.5.4   A treatment for HUS: Synsorb

As HUS is caused by the bacterial toxin itself, standard antibiotic treatments are

ineffective (Ostroff *et al.*, 1989; Proulx *et al.*, 1992; Ryan *et al.*, 1986). They may even

make the disease worse, by speeding the release of toxin from the periplasm of dead

bacteria (Walterspiel *et al.*, 1992). A treatment based on the receptor binding properties

of the B-pentamer has been developed (Armstrong *et al.*, 1991; Armstrong *et al.*, 1995).

Trisaccharide analogues of Gb_3 have been attached covalently to a biologically inert resin

to produce a material called "Synsorb", which is fed to HUS patients. The toxin is

predicted to bind to the resin-bound trisaccharide, sequestering it in the intestinal lumen

and causing it to be excreted eventually. Preliminary trials suggest that Synsorb has

some effect, particularly in preventing the most severe complications of HUS

(Armstrong, 1998). Work is underway to develop more effective Gb_3 analogues for the

sequestering of toxin. Structural information on the nature of Gb_3 binding by the B

pentamer has been of considerable value in this process (Kitov *et al.*, in press).

1.3.5.5 SLT-1 as a cancer therapy

A potential medical use of SLT-1 as a cancer-fighting agent has recently been

proposed. It has been shown that Gb_3 expression and presentation is increased on the

surface of some cancer cells, and that these cells are susceptible to SLT-1 (Arab *et al.*,

1998; Arab *et al.*, 1997; Farkas-Himsley *et al.*, 1995; LaCasse *et al.*, 1996; Lingwood *et*

al., 1998). Tests are now underway on whether bone marrow samples from sufferers of

multiple myeloma can be purged of cancerous cells by treatment with SLT-1 before

transplantation back into the original host (LaCasse *et al.*, 1999). While this use of SLT-1 requires no structural knowledge, the general use of the toxin as a selective cell-killing tool would probably benefit from the ability to rationally design modifications to it.

1.3.6 Previous Structural Work

1.3.6.1 The B-pentamer structure

The structure of Shiga toxin B-pentamer was originally solved in 1992 (Figure 1.8)(Stein *et al.*, 1992). The structure was observed to be similar to that of the heat-labile enterotoxin from *E. coli*, at that time the only other B-pentamer structure known (Sixma *et al.*, 1991; Sixma *et al.*, 1993). In the B-pentamer structure, the oligomer is distorted from perfect 5-fold symmetry by a small translation between adjacent monomers parallel to the pentamer axis. The cumulative effect of the translations is a significant break between two adjacent monomers at one point in the ring. This distortion was likened to the shape of a lockwasher, for which it has been named (Stein *et al.*, 1992).

1.3.6.2 The Shiga holotoxin structure

The structure of the Shiga holotoxin was determined in 1994 (Fraser *et al.*, 1994). This structure revealed that the A subunit sat on one face of the pentamer, with the C-terminus of the A_2 fragment inserted into the pore in the middle of the B-pentamer. Around 2000 $Å^2$ of surface area was buried in the interface between the A and B subunits, with approximately half of that being in the pore region. The A subunit was shown to be similar in structure to the catalytic domain of ricin. There was no sign of a lockwasher distortion in the B-pentamer of this structure, which the authors believed to indicate that the distortion was a crystal artifact of the B-pentamer structure.

1.3.6.3 Site 1 and the F30A mutant

While neither the B-pentamer nor the holotoxin structures had glycoside bound, the B-pentamer was inspected for potential binding sites. A deep groove formed at the interface between subunits contained a large patch of residues invariant among SLT-1, SLT-2, and SLT-2e. This site (Site 1) was proposed to be a sugar binding site (Stein *et al.*, 1992). In order to test this hypothesis a mutant of SLT-1 was developed, in which a phenylalanine central to the binding site (F30) was mutated to an alanine (Clark *et al.*, 1996). The F30A mutation was shown to have severely impaired carbohydrate binding and to have cytotoxicity reduced by a factor of 10^5.

1.3.6.4 Structures of SLT-1 with sugars bound

Subsequently, a structure of SLT-1 cocrystallized with Gb$_3$ was solved (Ling *et al.*, 1998). No trace of the lockwasher distortion was observed, further confirming that it was an artifact of crystallization. The more surprising result was that not one, but three sugar binding sites per monomer were observed (Figure 1.10). Not only was sugar binding observed at Site 1, but a site on the outer face of the pentamer was observed (Site 2), as well as one involving a surface tryptophan residue on the face of the pentamer opposite to the A subunit (Site 3). Subsequent structures of an SLT-2e mutant, and of several mutants of SLT-1 have confirmed the presence of the three sites (Ling, 1999). Binding studies of mutants designed to inactivate individual binding sites suggest that all sites play a role in cytotoxicity, with site 2 perhaps being the single most important (Bast *et al.*, 1999). Site 2 is also structurally equivalent to the glycolipid binding sites seen in heat-labile enterotoxin and cholera toxin (Merritt *et al.*, 1994; Sixma *et al.*, 1992).
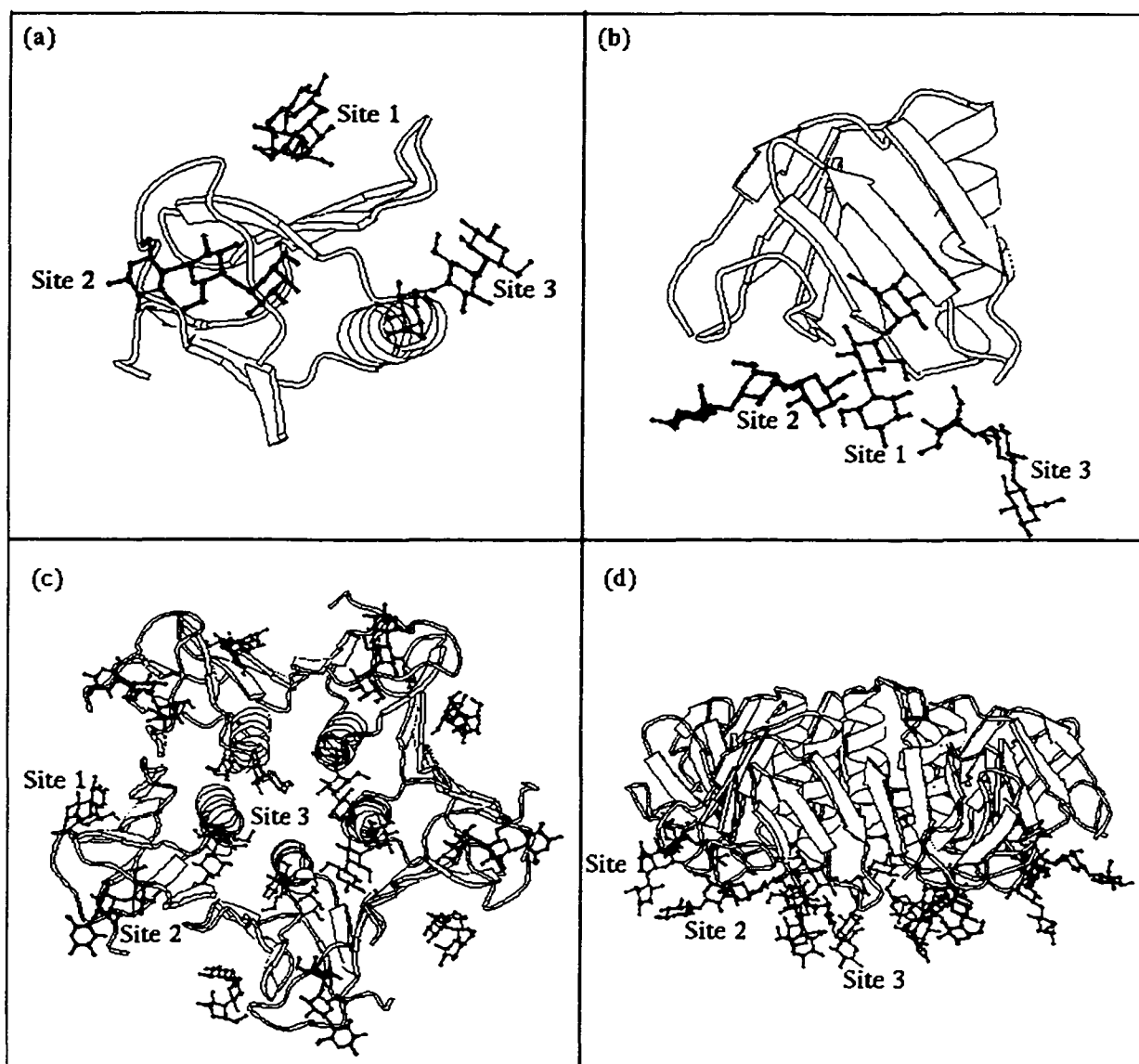
Figure 1.10: Sugar binding sites of SLT-1. From the crystal structure of Ling *et al.*, 1998. The binding sites are shown in two orientations 90° apart in (a) and (b). Sugars at Sites 1, 2, and 3 are shown in red, blue, and magenta respectively. The complete pentamer is shown in 2 orientations 90° apart in (c) and (d). This figure was made using Molscript (Kraulis, 1991).

1.3.7 Rationale for the Present Work.

While considerable work has been done on investigating the sugar binding sites of

SLT-1, the original SLT-1 structure had not been fully refined and the structure of the

F30A mutant had not been determined. Several questions about the B-pentamer crystal

structures have never been answered. The forces producing the lockwasher distortion,

unique to this crystal form, have never been explained. Crystal morphology was greatly

improved by the addition of zinc chloride to the crystallization buffer, but its effect has

never been discussed. The sugar binding sites can also be discussed in the light of later

discoveries. The present work intends to address these concerns.

References

Abrahamsson, T., Nerme, V., Stromqvist, M., Akerblom, B., Legnehed, A., Pettersson, K. & Westin Eriksson, A. (1996). Anti-thrombotic effect of a PAI-1 inhibitor in rats given endotoxin. *Thrombosis & Haemostasis* **75**, 118-26.

Acheson, D. W., Moore, R., De Breucker, S., Lincicome, L., Jacewicz, M., Skutelsky, E. & Keusch, G. T. (1996). Translocation of Shiga toxin across polarized intestinal cells in tissue culture. *Infection & Immunity* **64**, 3294-300.

Aertgeerts, K., De Bondt, H. L., De Ranter, C. & Declerck, P. J. (1994). A model of the reactive form of plasminogen activator inhibitor-1. *Journal of Structural Biology* **113**, 239-45.

Aertgeerts, K., De Bondt, H. L., De Ranter, C. & Declerck, P. J. (1995a). Crystallization and X-ray diffraction data of the cleaved form of plasminogen activator inhibitor-1. *Proteins* **23**, 118-21.

Aertgeerts, K., De Bondt, H. L., De Ranter, C. J. & Declerck, P. J. (1995b). Mechanisms contributing to the conformational and functional flexibility of plasminogen activator inhibitor-1. *Nature Structural Biology* **2**, 891-7.

Alessi, M. C., Juhan-Vague, I., Kooistra, T., Declerck, P. J. & Collen, D. (1988). Insulin stimulates the synthesis of plasminogen activator inhibitor 1 by the human hepatocellular cell line Hep G2. *Thrombosis & Haemostasis* **60**, 491-4.

Andreasen, P. A., Pyke, C., Riccio, A., Kristensen, P., Nielsen, L. S., Lund, L. R., Blasi, F. & Dano, K. (1987). Plasminogen activator inhibitor type 1 biosynthesis and mRNA level are increased by dexamethasone in human fibrosarcoma cells. *Molecular & Cellular Biology* **7**, 3021-5.

Andreasen, P. A., Riccio, A., Welinder, K. G., Douglas, R., Sartorio, R., Nielsen, L. S., Oppenheimer, C., Blasi, F. & Dano, K. (1986). Plasminogen activator inhibitor type-1: reactive center and amino-terminal heterogeneity determined by protein and cDNA sequencing. *FEBS Letters* **209**, 213-8.

Anfosso, F., Alessi, M. C., Nalbone, G.,Chomiki, N., Henry, M., & Juhan-Vague, I. (1995). Up-regulated expression of plasminogen activator inhibitor-1 in Hep G2 cells: interrelationship between insulin and insulin-like growth factor 1. *Thrombosis and Hemostasis* **73**, 268-74.

Arab, S., Murakami, M., Dirks, P., Boyd, B., Hubbard, S. L., Lingwood, C. A. & Rutka, J. T. (1998). Verotoxins inhibit the growth of and induce apoptosis in human astrocytoma cells. *Journal of Neuro-Oncology* **40**, 137-50.

Arab, S., Russel, E., Chapman, W. B., Rosen, B. & Lingwood, C. A. (1997). Expression of the verotoxin receptor glycolipid, globotriaosylceramide, in ovarian hyperplasias. *Oncology Research* **9**, 553-63.

Argraves, K. M., Battey, F. D., MacCalman, C. D., McCrae, K. R., Gafvels, M., Kozarsky, K. F., Chappell, D. A., Strauss, J. F., 3rd & Strickland, D. K. (1995). The very low density lipoprotein receptor mediates the cellular catabolism of lipoprotein lipase and urokinase-plasminogen activator inhibitor type I complexes. *Journal of Biological Chemistry* **270**, 26550-7.

Armstrong, G. D. (1998). Clinical Trials of Synsorb-Pk in Preventing Hemolytic-Uremic Syndrome. In *Escherichia coli O157:H7 and Other Shiga Toxin-Producing E. coli Strains* (Kaper, J. B. & O'Brien, A. D., eds.), pp. 374-84. American Society for Microbiology, Washington, D.C.

Armstrong, G. D., Fodor, E. & Vanmaele, R. (1991). Investigation of Shiga-like toxin binding to chemically synthesized oligosaccharide sequences. *Journal of Infectious Diseases* **164**, 1160-7.

Armstrong, G. D., Rowe, P. C., Goodyer, P., Orrbine, E., Klassen, T. P., Wells, G., MacKenzie, A., Lior, H., Blanchard, C. & Auclair, F. (1995). A phase I study of chemically synthesized verotoxin (Shiga-like toxin) Pk-trisaccharide receptors attached to chromosorb for preventing hemolytic-uremic syndrome. *Journal of Infectious Diseases* **171**, 1042-5.

Asplund-Carlson, A., Hamsten, A., Wiman, B. & Carlson, L. A. (1993). Relationship between plasma plasminogen activator inhibitor-1 activity and VLDL triglyceride concentration, insulin levels and insulin sensitivity: studies in randomly selected normo- and hypertriglyceridaemic men. *Diabetologia* **36**, 817-25.

Aulak, K. S., Eldering, E., Hack, C. E., Lubbers, Y. P., Harrison, R. A., Mast, A., Cicardi, M. & Davis, A. E. d. (1993). A hinge region mutation in C1-inhibitor (Ala436-->Thr) results in nonsubstrate-like behavior and in polymerization of the molecule. *Journal of Biological Chemistry* **268**, 18088-94.

Bacharach, E., Itin, A. & Keshet, E. (1998). Apposition-dependent induction of plasminogen activator inhibitor type 1 expression: a mechanism for balancing pericellular proteolysis during angiogenesis. *Blood* **92**, 939-45.

Bajou, K., Noel, A., Gerard, R. D., Masson, V., Brunner, N., Holst-Hansen, C., Skobe, M., Fusenig, N. E., Carmeliet, P., Collen, D. & Foidart, J. M. (1998). Absence of host plasminogen activator inhibitor 1 prevents cancer invasion and vascularization. *Nature Medicine* **4**, 923-8.

Bast, D. J., Banarjee, L., Clark, C., Read, R. J. & Brunton, J. L. (1999). The identification of three biologically relevant globotriaosyl ceramide receptor binding sites on the Verotoxin 1B subunit. *Molecular Microbiology* **32**, 953-60.

Bator, J. M., Cohen, R. L. & Chambers, D. A. (1998). Hydrocortisone regulates the dynamics of plasminogen activator and plasminogen activator inhibitor expression in cultured murine keratinocytes. *Experimental Cell Research* **242**, 110-9.

Baumann, U., Bode, W., Huber, R., Travis, J. & Potempa, J. (1992). Crystal structure of cleaved equine leucocyte elastase inhibitor determined at 1.95 A resolution. *Journal of Molecular Biology* **226**, 1207-18.

Baumann, U., Huber, R., Bode, W., Grosse, D., Lesjak, M. & Laurell, C. B. (1991). Crystal structure of cleaved human alpha 1-antichymotrypsin at 2.7 A resolution and its comparison with other serpins. *Journal of Molecular Biology* **218**, 595-606.

Bavenholm, P., de Faire, U., Landou, C., Efendic, S., Nilsson, J., Wiman, B. & Hamsten, A. (1998). Progression of coronary artery disease in young male post-infarction patients is linked to disturbances of carbohydrate and lipoprotein metabolism and to impaired fibrinolytic function [see comments]. *European Heart Journal* **19**, 402-10.

Bell, W. R. (1996). The Fibrinolytic System in Neoplasia. *Seminars in Thrombosis and Hemostasis* **22**, 459-78.

Bennett, W. F., Paoni, N. F., Keyt, B. A., Botstein, D., Jones, A. J., Presta, L., Wurm, F. M. & Zoller, M. J. (1991). High resolution analysis of functional determinants on human tissue-type plasminogen activator. *Journal of Biological Chemistry* **266**, 5191-201.

Bergum, P. W. & Erickson, L. A. (1988). Neutralization by plasminogen activator inhibitor-1 of mutants of tissue plasminogen activator. *Enzyme* **40**, 122-9.

Berkenpas, M. B., Lawrence, D. A. & Ginsburg, D. (1995). Molecular evolution of plasminogen activator inhibitor-1 functional stability. *EMBO Journal* **14**, 2969-77.

Biemond, B. J., Levi, M., Coronel, R., Janse, M. J., ten Cate, J. W. & Pannekoek, H. (1995). Thrombolysis and reocclusion in experimental jugular vein and coronary artery thrombosis. Effects of a plasminogen activator inhibitor type 1-neutralizing monoclonal antibody. *Circulation* **91**, 1175-81.

Björquist, P., Brohlin, M., Ehnebom, J., Ericsson, M., Kristiansen, C., Pohl, G. & Deinum, J. (1994). Plasminogen activator inhibitor type-1 interacts exclusively with the proteinase domain of tissue plasminogen activator. *Biochimica et Biophysica Acta* **1209**, 191-202.

Björquist, P., Ehnebom, J. & Deinum, J. (1999). Protein movement during complex-formation between tissue plasminogen activator and plasminogen activator inhibitor-1. *Biochimica et Biophysica Acta* **1431**, 24-9.

Björquist, P., Ehnebom, J., Inghardt, T. & Deinum, J. (1997). Epitopes on plasminogen activator inhibitor type-1 important for binding to tissue plasminogen activator. *Biochimica et Biophysica Acta* **1341**, 87-98.

Björquist, P., Ehnebom, J., Inghardt, T., Hansson, L., Lindberg, M., Linschoten, M., Stromqvist, M. & Deinum, J. (1998). Identification of the binding site for a low-molecular-weight inhibitor of plasminogen activator inhibitor type 1 by site-directed mutagenesis. *Biochemistry* **37**, 1227-34.

Boman, K., Hellsten, G., Bruce, A., Hallmans, G. & Nilsson, T. K. (1994). Endurance physical activity, diet and fibrinolysis. *Atherosclerosis* **106**, 65-74.

Boyd, B. & Lingwood, C. (1989). Verotoxin receptor glycolipid in human renal tissue. *Nephron* **51**, 207-10.

Boyd, B., Tyrrell, G., Maloney, M., Gyles, C., Brunton, J. & Lingwood, C. (1993). Alteration of the glycolipid binding specificity of the pig edema toxin from globotetraosyl to globotriaosyl ceramide alters *in vivo* tissue targetting and results in a verotoxin 1-like disease in pigs. *Journal of Experimental Medicine* **177**, 1745-53.

Brown, J. M. & Chambers, D. A. (1984). Effects of biological response modifiers on plasminogen activator activity in epidermal cell culture. *British Journal of Dermatology* **111**, 252-6.

Brown, J. M., Watanabe, K., Cohen, R. L. & Chambers, D. A. (1995). Molecular characterization of plasminogen activators in human gingival crevicular fluid. *Archives of Oral Biology* **40**, 839-45.

Bruce, D., Perry, D. J., Borg, J. Y., Carrell, R. W. & Wardell, M. R. (1994). Thromboembolic disease due to thermolabile conformational changes of antithrombin Rouen-VI (187 Asn-->Asp). *Journal of Clinical Investigation* **94**, 2265-74.

Brunton, J. L. (1990). The Shiga toxin family: molecular nature and possible role in disease. In *The Bacteria, Molecular Basis of Bacterial Pathogenesis* (Iglewski, B. & Clark, V., eds.), Vol. 11, pp. 377-98. Academic Press, New York.

Bruzdzinski, C. J., Riordan-Johnson, M., Nordby, E. C., Suter, S. M. & Gelehrter, T. D. (1990). Isolation and characterization of the rat plasminogen activator inhibitor-1 gene. *Journal of Biological Chemistry* **265**, 2078-85.

Buczko, W., Cierniewski, C., Kobylanska, A., Koziolkiewicz, M., Okruszek, A., Pawlowska, Z., Pluskota, E. & Stec, W. J. (1997). Modulation of plasminogen activator inhibitor type-1 biosynthesis in vitro and in vivo with oligo(nucleoside phosphorothioate)s and related constructs. *Pharmacology & Therapeutics* **76**, 161-75.

Carrell, R. W., Evans, D. L. & Stein, P. E. (1991). Mobile reactive centre of serpins and the control of thrombosis. *Nature* **353**, 576-8.

Carrell, R. W., Stein, P. E., Fermi, G. & Wardell, M. R. (1994). Biological implications of a 3 Å structure of dimeric antithrombin. *Structure* **2**, 257-70.

Cerinic, M. M., Generini, S., Partsch, G., Pignone, A., Dini, G., Konttinen, Y. T. & Del Rosso, M. (1998). Synoviocytes from osteoarthritis and rheumatoid arthritis produce plasminogen activators and plasminogen activator inhibitor-1 and display u-PA receptors on their surface. *Life Sciences* **63**, 441-53.

Cigolini, M., Tonoli, M., Borgato, L., Frigotto, L., Manzato, F., Zeminian, S., Cardinale, C., Camin, M., Chiaramonte, E., De Sandre, G. & Lunardi, C. (1999). Expression of plasminogen activator inhibitor-1 in human adipose tissue: a role for TNF-alpha? *Atherosclerosis* **143**, 81-90.

Clark, C., Bast, D., Sharp, A. M., St. Hilaire, P. M., Agha, R., Stein, P. E., Toone, E. J., Read, R. J. & Brunton, J. L. (1996). Phenylalanine 30 plays an important role in receptor binding of verotoxin-1. *Molecular Microbiology* **19**, 891-9.

Cleary, T. G. (1992). *Escherichia coli* that cause hemolytic uremic syndrome. *Infectious Disease Clinics of North America* **6**, 163-76.

Cohen, M. B. (1991). Hemmorrhagic colitis associated with *Escherichia coli* O157:H7. *Advances in Internal Medicine* **37**, 173-95.

Colucci, M., Paramo, J. A. & Collen, D. (1985). Generation in plasma of a fast-acting inhibitor of plasminogen activator in response to endotoxin stimulation. *Journal of Clinical Investigation* **75**, 818-24.

Crutchley, D. J. & Conanan, L. B. (1986). Endotoxin induction of an inhibitor of plasminogen activator in bovine pulmonary artery endothelial cells. *Journal of Biological Chemistry* **261**, 154-9.

Dalziel, A. W., Lipka, G., Chowdhry, B. Z., Sturtevant, J. M. & Schafer, D. E. (1984). Effects of ganglioside GM1 on the thermotropic behavior of cholera toxin B subunit. *Molecular & Cellular Biochemistry* **63**, 83-91.

Declerck, P. J., Alessi, M. C., Verstreken, M., Kruithof, E. K., Juhan-Vague, I. & Collen, D. (1988a). Measurement of plasminogen activator inhibitor 1 in biologic fluids with a murine monoclonal antibody-based enzyme-linked immunosorbent assay. *Blood* **71**, 220-5.

Declerck, P. J., De Mol, M., Alessi, M. C., Baudner, S., Paques, E. P., Preissner, K. T., Muller-Berghaus, G. & Collen, D. (1988b). Purification and characterization of a plasminogen activator inhibitor 1 binding protein from human plasma. Identification as a multimeric form of S protein (vitronectin). *Journal of Biological Chemistry* **263**, 15454-61.

Declerck, P. J., Juhan-Vague, I., Felez, J. & Wiman, B. (1994). Pathophysiology of fibrinolysis. *Journal of Internal Medicine* **236**, 425-32.

DeGrandis, S., Law, H., Brunton, J., Gyles, C. & Lingwood, C. A. (1989). Globotetraosylceramide is recognized by the pig edema disease toxin. *Journal of Biological Chemistry* **264**, 12520-5.

Deng, G., Royle, G., Seiffert, D. & Loskutoff, D. J. (1995). The PAI-1/vitronectin interaction: two cats in a bag? *Thrombosis & Haemostasis* **74**, 66-70.

Deng, G., Royle, G., Wang, S., Crain, K. & Loskutoff, D. J. (1996). Structural and functional analysis of the plasminogen activator inhibitor-1 binding motif in the somatomedin B domain of vitronectin. *Journal of Biological Chemistry* **271**, 12716-23.

Dieval, J., Nguyen, G., Gross, S., Delobel, J. & Kruithof, E. K. (1991). A lifelong bleeding disorder associated with a deficiency of plasminogen activator inhibitor type 1. *Blood* **77**, 528-32.

Duboscq, C., Quintana, I., Bassilotta, E., Bergonzelli, G. E., Porterie, P., Sassetti, B., Haedo, A. S., Wainsztein, N., Kruithof, E. K. & Kordich, L. (1997). Plasminogen: an important hemostatic parameter in septic patients. *Thrombosis & Haemostasis* **77**, 1090-5.

Edelberg, J. M., Reilly, C. F. & Pizzo, S. V. (1991). The inhibition of tissue type plasminogen activator by plasminogen activator inhibitor-1. The effects of fibrinogen, heparin, vitronectin, and lipoprotein(a). *Journal of Biological Chemistry* **266**, 7488-93.

Ehrlich, H. J., Gebbink, R. K., Keijer, J., Linders, M., Preissner, K. T. & Pannekoek, H. (1990). Alteration of serpin specificity by a protein cofactor. Vitronectin endows plasminogen activator inhibitor 1 with thrombin inhibitory properties. *Journal of Biological Chemistry* **265**, 13029-35.

Ehrlich, H. J., Gebbink, R. K., Keijer, J. & Pannekoek, H. (1992). Elucidation of structural requirements on plasminogen activator inhibitor 1 for binding to heparin. *Journal of Biological Chemistry* **267**, 11606-11.

Ehrlich, H. J., Keijer, J., Preissner, K. T., Gebbink, R. K. & Pannekoek, H. (1991). Functional interaction of plasminogen activator inhibitor type 1 (PAI-1) and heparin. *Biochemistry* **30**, 1021-8.

Eitzman, D. T., Fay, W. P., Lawrence, D. A., Francis-Chmura, A. M., Shore, J. D., Olson, S. T. & Ginsburg, D. (1995). Peptide-mediated inactivation of recombinant and platelet plasminogen activator inhibitor-1 in vitro. *Journal of Clinical Investigation* **95**, 2416-20.

Eldering, E., Verpy, E., Roem, D., Meo, T. & Tosi, M. (1995). COOH-terminal substitutions in the serpin C1 inhibitor that cause loop overinsertion and subsequent multimerization. *Journal of Biological Chemistry* **270**, 2579-87.

Elliott, P. R., Lomas, D. A., Carrell, R. W. & Abrahams, J. P. (1996). Inhibitory conformation of the reactive loop of alpha 1-antitrypsin. *Nature Structural Biology* **3**, 676-81.

Emeis, J. J. & Kooistra, T. (1986). Interleukin 1 and lipopolysaccharide induce an inhibitor of tissue-type plasminogen activator in vivo and in cultured endothelial cells. *Journal of Experimental Medicine* **163**, 1260-6.

Endo, Y., Tsurugi, K., Yutsudo, T., Takeda, Y., Ogasawara, T. & Igarashi, K. (1988). Site of action of a Vero toxin (VT2) from Escherichia coli O157:H7 and of Shiga toxin on eukaryotic ribosomes. RNA N-glycosidase activity of the toxins. *European Journal of Biochemistry* **171**, 45-50.

Engh, R. A., Huber, R., Bode, W. & Schulze, A. J. (1995). Divining the serpin inhibition mechanism: a suicide substrate 'spring'? *Trends In Biotechnology* **13**, 503-10.

Erickson, L. A., Ginsberg, M. H. & Loskutoff, D. J. (1984). Detection and partial characterization of an inhibitor of plasminogen activator in human platelets. *Journal of Clinical Investigation* **74**, 1465-72.

Erickson, L. A., Hekman, C. M. & Loskutoff, D. J. (1986). Denaturant-induced stimulation of the beta-migrating plasminogen activator inhibitor in endothelial cells and serum. *Blood* **68**, 1298-305.

Erickson, L. A., Schleef, R. R., Ny, T. & Loskutoff, D. J. (1985). The fibrinolytic system of the vascular wall. *Clinics in Haematology* **14**, 513-30.

Eriksson, P., Nilsson, L., Karpe, F. & Hamsten, A. (1998). Very-low-density lipoprotein response element in the promoter region of the human plasminogen activator inhibitor-1 gene implicated in the impaired fibrinolysis of hypertriglyceridemia. *Arteriosclerosis, Thrombosis & Vascular Biology* **18**, 20-6.

Estelles, A., Gilabert, J., Aznar, J., Loskutoff, D. J. & Schleef, R. R. (1989). Changes in the plasma levels of type 1 and type 2 plasminogen activator inhibitors in normal pregnancy and in patients with severe preeclampsia. *Blood* **74**, 1332-8.

Estelles, A., Gilabert, J., Grancha, S., Yamamoto, K., Thinnes, T., Espana, F., Aznar, J. & Loskutoff, D. J. (1998). Abnormal expression of type 1 plasminogen activator

inhibitor and tissue factor in severe preeclampsia. *Thrombosis & Haemostasis* **79**, 500-8.

Fa, M., Karolin, J., Aleshkov, S., Strandberg, L., Johansson, L. B. & Ny, T. (1995). Time-resolved polarized fluorescence spectroscopy studies of plasminogen activator inhibitor type 1: conformational changes of the reactive center upon interactions with target proteases, vitronectin and heparin. *Biochemistry* **34**, 13833-40.

Farkas-Himsley, H., Hill, R., Rosen, B., Arab, S. & Lingwood, C. A. (1995). The bacterial colicin active against tumor cells in vitro and in vivo is verotoxin 1. *Proceedings of the National Academy of Sciences of the United States of America* **92**, 6996-7000.

Fattal, P. G., Schneider, D. J., Sobel, B. E., & Billadello, J. J. (1992). Post-transcriptional regulation of expression of plasminogen activator inhibitor-1 by insulin and insulin like growth factor-1. *Journal of Biological Chemistry*, **267**, 12412-5.

Fay, W. P., Parker, A. C., Condrey, L. R. & Shapiro, A. D. (1997). Human plasminogen activator inhibitor-1 (PAI-1) deficiency: characterization of a large kindred with a null mutation in the PAI-1 gene. *Blood* **90**, 204-8.

Fay, W. P., Shapiro, A. D., Shih, J. L., Schleef, R. R. & Ginsburg, D. (1992). Brief report: complete deficiency of plasminogen-activator inhibitor type 1 due to a frame-shift mutation. *New England Journal of Medicine* **327**, 1729-33.

Fishman, P. H., Pacuszka, T., Hom, B. & Moss, J. (1980). Modification of ganglioside GM1. Effect of lipid moiety on choleragen action. *Journal of Biological Chemistry* **255**, 7657-64.

Foekens, J. A., Schmitt, M., van Putten, W. L., Peters, H. A., Kramer, M. D., Janicke, F. & Klijn, J. G. (1994). Plasminogen activator inhibitor-1 and prognosis in primary breast cancer. *Journal of Clinical Oncology* **12**, 1648-58.

Fraser, M. E., Chernaia, M. M., Kozlov, Y. V. & James, M. N. G. (1994). Crystal structure of the holotoxin from *Shigella dysenteriae* at 2.5 Å resolution. *Nature Structural Biology* **1**, 59-64.

Friederich, P. W., Levi, M., Biemond, B. J., Charlton, P., Templeton, D., van Zonneveld, A. J., Bevan, P., Pannekoek, H. & ten Cate, J. W. (1997). Novel low-molecular-weight inhibitor of PAI-1 (XR5118) promotes endogenous fibrinolysis and reduces postthrombolysis thrombus growth in rabbits. *Circulation* **96**, 916-21.

Fujii, S., Lucore, C. L., Hopkins, W. E., Billadello, J. J. & Sobel, B. E. (1989). Potential attenuation of fibrinolysis by growth factors released from platelets and their pharmacologic implications. *American Journal of Cardiology* **63**, 1505-11.

Gallicchio, M., Hufnagl, P., Wojta, J. & Tipping, P. (1996). IFN-gamma inhibits thrombin- and endotoxin-induced plasminogen activator inhibitor type 1 in human endothelial cells. *Journal of Immunology* **157**, 2610-7.

Ganesh, S., Sier, C. F., Griffioen, G., Vloedgraven, H. J., de Boer, A., Welvaart, K., van de Velde, C. J., van Krieken, J. H., Verheijen, J. H., Lamers, C. B. & et al. (1994). Prognostic relevance of plasminogen activators and their inhibitors in colorectal cancer. *Cancer Research* **54**, 4065-71.

Ganesh, S., Sier, C. F., Heerding, M. M., van Krieken, J. H., Griffioen, G., Welvaart, K., van de Velde, C. J., Verheijen, J. H., Lamers, C. B. & Verspaget, H. W. (1996).

Prognostic value of the plasminogen activation system in patients with gastric carcinoma. *Cancer* **77**, 1035-43.

Ganesh, S., Sier, C. F., Heerding, M. M., van Krieken, J. H., Griffioen, G., Welvaart, K., van de Velde, C. J., Verheijen, J. H., Lamers, C. B. & Verspaget, H. W. (1997). Contribution of plasminogen activators and their inhibitors to the survival prognosis of patients with Dukes' stage B and C colorectal cancer. *British Journal of Cancer* **75**, 1793-801.

Garred, Ø., Dubinina, E., Holm, P. K., Olsnes, S., van Deurs, B., Kozlov, J. V. & Sandvig, K. (1995a). Role of processing and intracellular transport for optimal toxicity of Shiga toxin and toxin mutants. *Experimental Cell Research* **218**, 39-49.

Garred, Ø., Dubinina, E., Polesskaya, A., Olsnes, S., Kozlov, J. & Sandvig, K. (1997). Role of the disulfide bond in Shiga toxin A-chain for toxin entry into cells. *Journal of Biological Chemistry* **272**, 11414-9.

Garred, Ø., van Deurs, B. & Sandvig, K. (1995b). Furin-induced cleavage and activation of Shiga toxin. *Journal of Biological Chemistry* **270**, 10817-21.

Gelehrter, T. D. & Sznycer-Laszuk, R. (1986). Thrombin induction of plasminogen activator-inhibitor in cultured human endothelial cells. *Journal of Clinical Investigation* **77**, 165-9.

Georg, B., Helseth, E., Lund, L. R., Skandsen, T., Riccio, A., Dano, K., Unsgaard, G. & Andreasen, P. A. (1989). Tumor necrosis factor-alpha regulates mRNA for urokinase-type plasminogen activator and type-1 plasminogen activator inhibitor in human neoplastic cell lines. *Molecular & Cellular Endocrinology* **61**, 87-96.

Gettins, P., Patston, P. A. & Schapira, M. (1993). The role of conformational change in serpin structure and function. *Bioessays* **15**, 461-7.

Gill, D. M. (1978). Seven Toxic Peptides that Cross Cell Membranes. In *Bacterial Toxins and Cell Membranes* (Jeljaszewica, J. & Wadstrom, T., eds.), pp. 291-332. Academic Press, New York.

Ginsburg, D., Zeheb, R., Yang, A. Y., Rafferty, U. M., Andreasen, P. A., Nielsen, L., Dano, K., Lebo, R. V. & Gelehrter, T. D. (1986). cDna cloning of human plasminogen activator-inhibitor from endothelial cells. *Journal of Clinical Investigation* **78**, 1673-80.

Gleeson, N. C., Gonsalves, R. & Bonnar, J. (1993). Plasminogen activator inhibitors in endometrial adenocarcinoma. *Cancer* **72**, 1670-2.

Goldberg, G. I., Frisch, S. M., He, C., Wilhelm, S. M., Reich, R. & Collier, I. E. (1990). Secreted proteases. Regulation of their activity and their possible role in metastasis. *Annals of the New York Academy of Sciences* **580**, 375-84.

Grant, G. A., Goldberg, G. I., Wilhelm, S. M., He, C. & Eisen, A. Z. (1992). Activation of extracellular matrix metalloproteases by proteases and organomercurials. *Matrix Supplement* **1**, 217-23.

Grenett, H. E., Benza, R. L., Fless, G. M., Li, X. N., Davis, G. C. & Booyse, F. M. (1998). Genotype-specific transcriptional regulation of PAI-1 gene by insulin, hypertriglyceridemic VLDL, and Lp(a) in transfected, cultured human endothelial cells. *Arteriosclerosis, Thrombosis & Vascular Biology* **18**, 1803-9.

Hackel, C., Czerniak, B., Ayala, A. G., Radig, K. & Roessner, A. (1997). Expression of plasminogen activators and plasminogen activator inhibitor 1 in dedifferentiated chondrosarcoma. *Cancer* **79**, 53-8.

Hamsten, A., Wiman, B., de Faire, U. & Blomback, M. (1985). Increased plasma levels of a rapid inhibitor of tissue plasminogen activator in young survivors of myocardial infarction. *New England Journal of Medicine* **313**, 1557-63.

Hanss, M. & Collen, D. (1987). Secretion of tissue-type plasminogen activator and plasminogen activator inhibitor by cultured human endothelial cells: modulation by thrombin, endotoxin, and histamine. *Journal of Laboratory & Clinical Medicine* **109**, 97-104.

Harrop, S. J., Jankova, L., Coles, M., Jardine, D., Whittaker, J. S., Gould, A. R., Meister, A., King, G. C., Mabbutt, B. C. & Curmi, P. M. (1999). The crystal structure of plasminogen activator inhibitor 2 at 2.0 Å resolution: implications for serpin function. *Structure* **7**, 43-54.

Hashimoto, H., Mizukoshi, K., Nishi, M., Kawakita, T., Hasui, S., Kato, Y., Ueno, Y., Takeya, R., Okuda, N. & Takeda, T. (1999). Epidemic of gastrointestinal tract infection including hemorrhagic colitis attributable to Shiga toxin 1-producing *Escherichia coli* O118:H2 at a junior high school in Japan. *Pediatrics* **103**, E2.

Hazes, B., Read, R.J. (1997). Accumulating evidence suggests that several AB-toxins subvert the endoplasmic reticulum-associated protein degradation pathway to enter target cells. *Biochemistry* **36**, pp.11051-4.

Heerze, L. D., Chong, P. C. & Armstrong, G. D. (1992). Investigation of the lectin-like binding domains in pertussis toxin using synthetic peptide sequences. Identification

of a sialic acid binding site in the S2 subunit of the toxin. *Journal of Biological Chemistry* **267**, 25810-5.Hekman, C. M. & Loskutoff, D. J. (1985). Endothelial cells produce a latent inhibitor of plasminogen activators that can be activated by denaturants. *Journal of Biological Chemistry* **260**, 11581-7.

Hekman, C. M. & Loskutoff, D. J. (1988). Bovine plasminogen activator inhibitor 1: specificity determinations and comparison of the active, latent, and guanidine-activated forms. *Biochemistry* **27**, 2911-8.

Henry, M., Chomiki, N., Scarabin, P. Y., Alessi, M. C., Peiretti, F., Arveiler, D., Ferrieres, J., Evans, A., Amouyel, P., Poirier, O., Cambien, F. & Juhan-Vague, I. (1997). Five frequent polymorphisms of the PAI-1 gene: lack of association between genotypes, PAI activity, and triglyceride levels in a healthy population. *Arteriosclerosis, Thrombosis & Vascular Biology* **17**, 851-8.

Hofmann, R., Lehmer, A., Buresch, M., Hartung, R. & Ulm, K. (1996a). Clinical relevance of urokinase plasminogen activator, its receptor, and its inhibitor in patients with renal cell carcinoma. *Cancer* **78**, 487-92.

Hofmann, R., Lehmer, A., Hartung, R., Robrecht, C., Buresch, M. & Grothe, F. (1996b). Prognostic value of urokinase plasminogen activator and plasminogen activator inhibitor-1 in renal cell cancer. *Journal of Urology* **155**, 858-62.

Hofmann, S. L. (1993). Southwestern Internal Medicine Conference: Shiga-like toxins in hemolytic-uremic syndrome and thrombotic thrombocytopenic purpura. *American Journal of the Medical Sciences* **306**, 398-406.

Hopkins, W. E., Westerhausen, D. R., Fujii, S., Billadello, J. J. & Sobel, B. E. (1991). Mediators of induction of augmented expression of plasminogen activator inhibitor type-1 in Hep G2 cells by platelets. *Thrombosis & Haemostasis* **66**, 239-45.

Horrevoets, A. J., Tans, G., Smilde, A. E., van Zonneveld, A. J. & Pannekoek, H. (1993). Thrombin-variable region 1 (VR1). Evidence for the dominant contribution of VR1 of serine proteases to their interaction with plasminogen activator inhibitor 1. *Journal of Biological Chemistry* **268**, 779-82.

Huber, R. & Carrell, R. W. (1989). Implications of the three-dimensional structure of alpha 1-antitrypsin for structure and function of serpins. *Biochemistry* **28**, 8951-66.

Huntington, J. A., Olson, S. T., Fan, B. & Gettins, P. G. (1996). Mechanism of heparin activation of antithrombin. Evidence for reactive center loop preinsertion with expulsion upon heparin binding. *Biochemistry* **35**, 8495-503.

Jacewicz, M., Clausen, H., Nudelman, E., Donohue-Rolfe, A. & Keusch, G. T. (1986). Pathogenesis of shigella diarrhea. XI. Isolation of a shigella toxin-binding glycolipid from rabbit jejunum and HeLa cells and its identification as globotriaosylceramide. *Journal of Experimental Medicine* **163**, 1391-404.

Jacewicz, M. S., Acheson, D. W., Binion, D. G., West, G. A., Lincicome, L. L., Fiocchi, C. & Keusch, G. T. (1999). Responses of human intestinal microvascular endothelial cells to Shiga toxins 1 and 2 and pathogenesis of hemorrhagic colitis. *Infection & Immunity* **67**, 1439-44.

Janciauskiene, S., Eriksson, S. & Wright, H. T. (1996). A specific structural interaction of Alzheimer's peptide A beta 1-42 with alpha 1-antichymotrypsin. *Nature Structural Biology* **3**, 668-71.

Janicke, F., Schmitt, M. & Graeff, H. (1991). Clinical relevance of the urokinase-type and tissue-type plasminogen activators and of their type 1 inhibitor in breast cancer. *Seminars in Thrombosis & Hemostasis* **17**, 303-12.

Janicke, F., Schmitt, M., Pache, L., Ulm, K., Harbeck, N., Hofler, H. & Graeff, H. (1993). Urokinase (uPA) and its inhibitor PAI-1 are strong and independent prognostic factors in node-negative breast cancer. *Breast Cancer Research & Treatment* **24**, 195-208.

Jin, L., Abrahams, J. P., Skinner, R., Petitou, M., Pike, R. N. & Carrell, R. W. (1997). The anticoagulant activation of antithrombin by heparin. *Proceedings of the National Academy of Sciences of the United States of America* **94**, 14683-8.

Juhan-Vague, I. (1996). Haemostatic parameters and vascular risk. *Atherosclerosis* **124**, S49-55.

Juhan-Vague, I. & Alessi, M. C. (1993). Plasminogen activator inhibitor 1 and atherothrombosis. *Thrombosis & Haemostasis* **70**, 138-43.

Juhan-Vague, I. & Alessi, M. C. (1997). PAI-1, obesity, insulin resistance and risk of cardiovascular events. *Thrombosis & Haemostasis* **78**, 656-60.

Juhan-Vague, I., Alessi, M. C., Raccah, D., Aillaud, M. F., Billerey, M., Ansaldi, J., Philip-Joet, C. & Vague, P. (1992). Daytime fluctuations of plasminogen activator inhibitor 1 (PAI-1) in populations with high PAI-1 levels. *Thrombosis & Haemostasis* **67**, 76-82.

Kaneko, M., Mimuro, J., Matsuda, M. & Sakata, Y. (1991). The plasminogen activator inhibitor-1 binding site in the kringle-2 domain of tissue-type plasminogen activator. *Biochemical & Biophysical Research Communications* **178**, 1160-6.

Keeton, M., Ahn, C., Eguchi, Y., Burlingame, R. & Loskutoff, D. J. (1995). Expression of type 1 plasminogen activator inhibitor in renal tissue in murine lupus nephritis. *Kidney International* **47**, 148-57.

Keijer, J., Linders, M., van Zonneveld, A. J., Ehrlich, H. J., de Boer, J. P. & Pannekoek, H. (1991a). The interaction of plasminogen activator inhibitor 1 with plasminogen activators (tissue-type and urokinase-type) and fibrin: localization of interaction sites and physiologic relevance. *Blood* **78**, 401-9.

Keijer, J., Linders, M., Wegman, J. J., Ehrlich, H. J., Mertens, K. & Pannekoek, H. (1991b). On the target specificity of plasminogen activator inhibitor 1: the role of heparin, vitronectin, and the reactive site. *Blood* **78**, 1254-61.

King, C. A. & Van Heyningen, W. E. (1973). Deactivation of cholera toxin by a sialidase-resistant monosialosylganglioside. *Journal of Infectious Diseases* **127**, 639-47.

Kitov, P. I., Sadowska, J. M., Mulvey, G., Armstrong, G. D., Ling, H., Pannu, N. S., Read, R. J. & Bundle, D. R. Tailored multivalency of carbohydrate ligands with unprecedented activity in neutralizing Shiga-like toxins. *Nature* **(in press)**.

Kjoller, L., Kanse, S. M., Kirkegaard, T., Rodenburg, K. W., Ronne, E., Goodman, S. L., Preissner, K. T., Ossowski, L. & Andreasen, P. A. (1997). Plasminogen activator inhibitor-1 represses integrin- and vitronectin-mediated cell migration independently of its function as an inhibitor of plasminogen activation. *Experimental Cell Research* **232**, 420-9.

Klinger, K. W., Winqvist, R., Riccio, A., Andreasen, P. A., Sartorio, R., Nielsen, L. S., Stuart, N., Stanislovitis, P., Watkins, P., Douglas, R. & et al. (1987). Plasminogen

activator inhibitor type 1 gene is located at region q21.3-q22 of chromosome 7 and genetically linked with cystic fibrosis. *Proceedings of the National Academy of Sciences of the United States of America* **84**, 8548-52.

Kluft, C., Jie, A. F., Rijken, D. C. & Verheijen, J. H. (1988). Daytime fluctuations in blood of tissue-type plasminogen activator (t-PA) and its fast-acting inhibitor (PAI-1). *Thrombosis & Haemostasis* **59**, 329-32.

Knittel, T., Fellmer, P. & Ramadori, G. (1996). Gene expression and regulation of plasminogen activator inhibitor type I in hepatic stellate cells of rat liver. *Gastroenterology* **111**, 745-54.

Kobayashi, H., Fujishiro, S. & Terao, T. (1994). Impact of urokinase-type plasminogen activator and its inhibitor type 1 on prognosis in cervical cancer of the uterus. *Cancer Research* **54**, 6539-48.

Kotani, M., Kawashima, I., Ozawa, H., Ogura, K., Ariga, T. & Tai, T. (1994). Generation of one set of murine monoclonal antibodies specific for globo-series glycolipids: evidence for differential distribution of the glycolipids in rat small intestine. *Archives of Biochemistry & Biophysics* **310**, 89-96.

Kounnas, M. Z., Henkin, J., Argraves, W. S. & Strickland, D. K. (1993). Low density lipoprotein receptor-related protein/alpha 2-macroglobulin receptor mediates cellular uptake of pro-urokinase. *Journal of Biological Chemistry* **268**, 21862-7.

Kraulis, P. J. (1991). MOLSCRIPT: A program to produce both detailed and schematic plots of protein structures. *Journal of Applied Crystallography* **24**, 946-50.

Kounnas, M. Z., Henkin, J., Argraves, W. S. & Strickland, D. K. (1993). Low density

lipoprotein receptor-related protein/alpha 2-macroglobulin receptor mediates

cellular uptake of pro-urokinase. *Journal of Biological Chemistry* **268**, 21862-7.

Kruithof, E. K., Tran-Thang, C. & Bachmann, F. (1986a). The fast-acting inhibitor of

tissue-type plasminogen activator in plasma is also the primary plasma inhibitor of

urokinase. *Thrombosis & Haemostasis* **55**, 65-9.

Kruithof, E. K., Tran-Thang, C. & Bachmann, F. (1986b). Studies on the release of a

plasminogen activator inhibitor by human platelets. *Thrombosis & Haemostasis* **55**,

201-5.

Kruithof, E. K., Tran-Thang, C., Gudinchet, A., Hauert, J., Nicoloso, G., Genton, C.,

Welti, H. & Bachmann, F. (1987). Fibrinolysis in pregnancy: a study of

plasminogen activator inhibitors. *Blood* **69**, 460-6.

Kuhn, W., Pache, L., Schmalfeldt, B., Dettmar, P., Schmitt, M., Janicke, F. & Graeff, H.

(1994). Urokinase (uPA) and PAI-1 predict survival in advanced ovarian cancer

patients (FIGO III) after radical surgery and platinum-based chemotherapy.

Gynecologic Oncology **55**, 401-9.

Kuhn, W., Schmalfeldt, B., Reuning, U., Pache, L., Berger, U., Ulm, K., Harbeck, N.,

Spathe, K., Dettmar, P., Hofler, H., Janicke, F., Schmitt, M. & Graeff, H. (1999).

Prognostic significance of urokinase (uPA) and its inhibitor PAI-1 for survival in

advanced ovarian carcinoma stage FIGO IIIc. *British Journal of Cancer* **79**, 1746-

51.

LaCasse, E. C., Bray, M. R., Patterson, B., Lim, W.-M., Perampalam, S., Radvanyi, L.

G., Keating, A., Stewart, A. K., Buckstein, R., Sandhu, J. S., Miller, N., Banerjee,

D., Singh, D., Belch, A. R., Pilarski, L. M. & Gariepy, J. (1999). Shiga-like toxin-1 receptor on human breast cancer, lymphoma, and myeloma and absence from CD34^{+} Hematopoietic stem cells: implications for *ex vivo* tumor purging and autologous stem cell transplantation. *Blood* **94**, 2901-10.

LaCasse, E. C., Saleh, M. T., Patterson, B., Minden, M. D. & Gariepy, J. (1996). Shiga-like toxin purges human lymphoma from bone marrow of severe combined immunodeficient mice. *Blood* **88**, 1561-7.

Laiho, M., Saksela, O., Andreasen, P. A. & Keski-Oja, J. (1986). Enhanced production and extracellular deposition of the endothelial-type plasminogen activator inhibitor in cultured human lung fibroblasts by transforming growth factor-beta. *Journal of Cell Biology* **103**, 2403-10.

Laiho, M., Saksela, O. & Keski-Oja, J. (1987). Transforming growth factor-beta induction of type-1 plasminogen activator inhibitor. Pericellular deposition and sensitivity to exogenous urokinase. *Journal of Biological Chemistry* **262**, 17467-74.

Lamba, D., Bauer, M., Huber, R., Fischer, S., Rudolph, R., Kohnert, U. & Bode, W. (1996). The 2.3 Å crystal structure of the catalytic domain of recombinant two-chain human tissue-type plasminogen activator. *Journal of Molecular Biology* **258**, 117-35.

Lauffenburger, D. A. (1996). Cell motility. Making connections count. *Nature* **383**, 390-1.

Lawrence, D. A., Berkenpas, M. B., Palaniappan, S. & Ginsburg, D. (1994). Localization of vitronectin binding domain in plasminogen activator inhibitor-1. *Journal of Biological Chemistry* **269**, 15223-8.

Lawrence, D. A., Ginsburg, D., Day, D. E., Berkenpas, M. B., Verhamme, I. M., Kvassman, J. O. & Shore, J. D. (1995). Serpin-protease complexes are trapped as stable acyl-enzyme intermediates. *Journal of Biological Chemistry* **270**, 25309-12.

Lawrence, D. A., Palaniappan, S., Stefansson, S., Olson, S. T., Francis-Chmura, A. M., Shore, J. D. & Ginsburg, D. (1997). Characterization of the binding of different conformational forms of plasminogen activator inhibitor-1 to vitronectin. Implications for the regulation of pericellular proteolysis. *Journal of Biological Chemistry* **272**, 7676-80.

Lencer, W. I., de Almeida, J. B., Moe, S., Stow, J. L., Ausiello, D. A. & Madara, J. L. (1993). Entry of cholera toxin into polarized human intestinal epithelial cells. Identification of an early brefeldin A sensitive event required for A1-peptide generation. *Journal of Clinical Investigation* **92**, 2941-51.

Levi, M., Biemond, B. J., van Zonneveld, A. J., ten Cate, J. W. & Pannekoek, H. (1992). Inhibition of plasminogen activator inhibitor-1 activity results in promotion of endogenous thrombolysis and inhibition of thrombus extension in models of experimental thrombosis. *Circulation* **85**, 305-12.

Levy, N. J., Ramesh, N., Cicardi, M., Harrison, R. A. & Davis, A. E. d. (1990). Type II hereditary angioneurotic edema that may result from a single nucleotide change in the codon for alanine-436 in the C1 inhibitor gene. *Proceedings of the National Academy of Sciences of the United States of America* **87**, 265-8.

Li, X. N., Grenett, H. E., Benza, R. L., Demissie, S., Brown, S. L., Tabengwa, E. M., Gianturco, S. H., Bradley, W. A., Fless, G. M. & Booyse, F. M. (1997). Genotype-specific transcriptional regulation of PAI-1 expression by hypertriglyceridemic

VLDL and Lp(a) in cultured human endothelial cells. *Arteriosclerosis, Thrombosis & Vascular Biology* **17**, 3215-23.

Lijnen, H. R., Bachmann, F., Collen, D., Ellis, V., Pannekoek, H., Rijken, D. C. & Thorsen, S. (1994). Mechanisms of plasminogen activation. *Journal of Internal Medicine* **236**, 415-24.

Lindberg, A. A., Brown, J. E., Stromberg, N., Westling-Ryd, M., Schultz, J. E. & Karlsson, K. A. (1987). Identification of the carbohydrate receptor for Shiga toxin produced by *Shigella dysenteriae* type 1. *Journal of Biological Chemistry* **262**, 1779-85.

Ling, H. (1999). Structural Studies of the Interactions Between Shiga-Like Toxins and Their Carbohydrate Receptor. Doctoral Thesis, University of Alberta.

Ling, H., Boodhoo, A., Hazes, B., Cummings, M. D., Armstrong, G. D., Brunton, J. L. & Read, R. J. (1998). Structure of the shiga-like toxin I B-pentamer complexed with an analogue of its receptor Gb3. *Biochemistry* **37**, 1777-88.

Lingwood, C. A. (1993). Verotoxins and their glycolipid receptors. *Advances in Lipid Research* **25**, 189-211.

Lingwood, C. A. (1996). Role of verotoxin receptors in pathogenesis. *Trends in Microbiology* **4**, 147-53.

Lingwood, C. A., Khine, A. A. & Arab, S. (1998). Globotriaosyl ceramide (Gb3) expression in human tumour cells: intracellular trafficking defines a new retrograde transport pathway from the cell surface to the nucleus, which correlates with sensitivity to verotoxin. *Acta Biochimica Polonica* **45**, 351-9.

Lingwood, C. A., Law, H., Richardson, S., Petric, M., Brunton, J. L., De Grandis, S. & Karmali, M. (1987). Glycolipid binding of purified and recombinant *Escherichia coli* produced verotoxin *in vitro. Journal of Biological Chemistry* **262**, 8834-9.

Liu, Y. X., Peng, X. R., Chen, Y. J., Carrico, W. & Ny, T. (1997). Prolactin delays gonadotrophin-induced ovulation and down-regulates expression of plasminogen-activator system in ovary. *Human Reproduction* **12**, 2748-55.

Lobermann, H., Lottspeich, F., Bode, W. & Huber, R. (1982). Interaction of human alpha 1-proteinase inhibitor with chymotrypsinogen A and crystallization of a proteolytically modified alpha 1-proteinase inhibitor. *Hoppe-Seylers Zeitschrift fur Physiologische Chemie* **363**, 1377-88.

Locht, C. & Keith, J. M. (1986). Pertussis toxin gene: nucleotide sequence and genetic organization. *Science* **232**, 1258-64.

Lomas, D. A. (1996). New insights into the structural basis of alpha 1-antitrypsin deficiency. *Qjm* **89**, 807-12.

Lomas, D. A., Elliott, P. R. & Carrell, R. W. (1997). Commercial plasma alpha1-antitrypsin (Prolastin) contains a conformationally inactive, latent component. *European Respiratory Journal* **10**, 672-5.

Loskutoff, D. J., Linders, M., Keijer, J., Veerman, H., van Heerikhuizen, H. & Pannekoek, H. (1987). Structure of the human plasminogen activator inhibitor 1 gene: nonrandom distribution of introns. *Biochemistry* **26**, 3763-8.

Loskutoff, D. J., Ny, T., Sawdey, M. & Lawrence, D. (1986a). Fibrinolytic system of cultured endothelial cells: regulation by plasminogen activator inhibitor. *Journal of Cellular Biochemistry* **32**, 273-80.

Loskutoff, D. J., Roegner, K., Erickson, L. A., Schleef, R. R., Huttenlocher, A., Coleman, P. L. & Gelehrter, T. D. (1986b). The dexamethasone-induced inhibitor of plasminogen activator in hepatoma cells is antigenically-related to an inhibitor produced by bovine aortic endothelial cells. *Thrombosis & Haemostasis* **55**, 8-11.

Loskutoff, D. J., Sawdey, M., Keeton, M. & Schneiderman, J. (1993). Regulation of PAI-1 gene expression in vivo. *Thrombosis & Haemostasis* **70**, 135-7.

Loskutoff, D. J. & Schleef, R. R. (1988). Plasminogen activators and their inhibitors. *Methods in Enzymology* **163**, 293-302.

Lund, L. R., Riccio, A., Andreasen, P. A., Nielsen, L. S., Kristensen, P., Laiho, M., Saksela, O., Blasi, F. & Dano, K. (1987). Transforming growth factor-beta is a strong and fast acting positive regulator of the level of type-1 plasminogen activator inhibitor mRNA in WI-38 human lung fibroblasts. *EMBO Journal* **6**, 1281-6.

Lundgren, C. H., Brown, S. L., Nordt, T. K., Sobel, B. E. & Fujii, S. (1996). Elaboration of type-1 plasminogen activator inhibitor from adipocytes. A potential pathogenetic link between obesity and cardiovascular disease. *Circulation* **93**, 106-10.

Lupu, F., Bergonzelli, G. E., Heim, D. A., Cousin, E., Genton, C. Y., Bachmann, F. & Kruithof, E. K. (1993). Localization and production of plasminogen activator inhibitor-1 in human healthy and atherosclerotic arteries. *Arteriosclerosis & Thrombosis* **13**, 1090-100.

Madison, E. L., Goldsmith, E. J., Gerard, R. D., Gething, M. J. & Sambrook, J. F. (1989). Serpin-resistant mutants of human tissue-type plasminogen activator. *Nature* **339**, 721-4.

Madison, E. L., Goldsmith, E. J., Gerard, R. D., Gething, M. J., Sambrook, J. F. & Bassel-Duby, R. S. (1990). Amino acid residues that affect interaction of tissue-type plasminogen activator with plasminogen activator inhibitor 1. *Proceedings of the National Academy of Sciences of the United States of America* **87**, 3530-3.

Mangeney, M., Richard, Y., Coulaud, D., Tursz, T. & Wiels, J. (1991). CD77: an antigen of germinal center B cells entering apoptosis. *European Journal of Immunology* **21**, 1131-40.

Meade, T. W., Ruddock, V., Stirling, Y., Chakrabarti, R. & Miller, G. J. (1993). Fibrinolytic activity, clotting factors, and long-term incidence of ischaemic heart disease in the Northwick Park Heart Study. *Lancet* **342**, 1076-9.

Medcalf, R. L., Kruithof, E. K. & Schleuning, W. D. (1988). Plasminogen activator inhibitor 1 and 2 are tumor necrosis factor/cachectin-responsive genes. *Journal of Experimental Medicine* **168**, 751-9.

Meijer, M. V., Smilde, A., Tans, G., Nesheim, M. E., Pannekoek, H. & Horrevoets, A. J. G. (1997). The Suicide Substrate Reaction Between Plasminogen Activator Inhibitor 1 and Thrombin Is regulated by the Cofactors Vitronectin and Heparin. *Blood* **90**, 1874-1882.

Merritt, E. A. & Hol, W. G. (1995). AB5 toxins. *Current Opinion in Structural Biology* **5**, 165-71.

Merritt, E. A., Sarfaty, S., van den Akker, F., Hoir, C. L., Martial, J. A. & Hol, W. G. (1994). Crystal structure of cholera toxin B-pentamer bound to receptor GM1 pentasaccharide. *Protein Science* **3**, 166-75.

Mimuro, J., Schleef, R. R. & Loskutoff, D. J. (1987). Extracellular matrix of cultured

bovine aortic endothelial cells contains functionally active type 1 plasminogen

activator inhibitor. *Blood* **70**, 721-8.

Misiura, K., Wojcik, M., Krakowiak, A., Koziolkiewicz, M., Pawlowska, Z., Pluskota,

E., Cierniewski, C. S. & Stec, W. J. (1998). Synthesis, biochemical and biological

studies on oligonucleotides bearing a lipophilic dimethoxytrityl group. *Acta

Biochimica Polonica* **45**, 27-32.

Moestrup, S. K., Nielsen, S., Andreasen, P., Jorgensen, K. E., Nykjaer, A., Roigaard, H.,

Gliemann, J. & Christensen, E. I. (1993). Epithelial glycoprotein-330 mediates

endocytosis of plasminogen activator-plasminogen activator inhibitor type-1

complexes. *Journal of Biological Chemistry* **268**, 16564-70.

Montesano, R., Roth, J., Robert, A. & Orci, L. (1982). Non-coated membrane

invaginations are involved in binding and internalization of cholera and tetanus

toxins. *Nature* **296**, 651-3.

Morange, P. E., Alessi, M. C., Verdier, M., Casanova, D., Magalon, G. & Juhan-Vague,

I. (1999a). PAI-1 produced ex vivo by human adipose tissue is relevant to PAI-1

blood level. *Arteriosclerosis, Thrombosis & Vascular Biology* **19**, 1361-5.

Morange, P. E., Aubert, J., Peiretti, F., Lijnen, H. R., Vague, P., Verdier, M., Negrel, R.,

Juhan-Vague, I. & Alessi, M. C. (1999b). Glucocorticoids and insulin promote

plasminogen activator inhibitor 1 production by human adipose tissue. *Diabetes* **48**,

890-5.

Moscatelli, D. & Rifkin, D. B. (1988). Membrane and matrix localization of proteinases: a common theme in tumor cell invasion and angiogenesis. *Biochimica et Biophysica Acta* **948**, 67-85.

Moss, J. & Vaughan, M. (1988). ADP-ribosylation of guanyl nucleotide-binding regulatory proteins by bacterial toxins. *Advances in Enzymology & Related Areas of Molecular Biology* **61**, 303-79.

Mottonen, J., Strand, A., Symersky, J., Sweet, R. M., Danley, D. E., Geoghegan, K. F., Gerard, R. D. & Goldsmith, E. J. (1992). Structural basis of latency in plasminogen activator inhibitor-1. *Nature* **355**, 270-3.

Mourey, L., Samama, J. P., Delarue, M., Petitou, M., Choay, J. & Moras, D. (1993). Crystal structure of cleaved bovine antithrombin III at 3.2 Å resolution. *Journal of Molecular Biology* **232**, 223-41.

Murzin, A. G. (1992). Familiar strangers. *Nature* **360**, 635.

Murzin, A. G. (1993). OB(oligonucleotide/oligosaccharide binding)-fold: common structural and functional solution for non-homologous sequences. *EMBO Journal* **12**, 861-7.

Naski, M. C., Lawrence, D. A., Mosher, D. F., Podor, T. J. & Ginsburg, D. (1993). Kinetics of inactivation of alpha-thrombin by plasminogen activator inhibitor-1. Comparison of the effects of native and urea-treated forms of vitronectin. *Journal of Biological Chemistry* **268**, 12367-72.

Nekarda, H., Schmitt, M., Ulm, K., Wenninger, A., Vogelsang, H., Becker, K., Roder, J. D., Fink, U. & Siewert, J. R. (1994). Prognostic impact of urokinase-type

plasminogen activator and its inhibitor PAI-1 in completely resected gastric cancer. *Cancer Research* **54**, 2900-7.

Nicosia, A., Perugini, M., Franzini, C., Casagli, M. C., Borri, M. G., Antoni, G., Almoni, M., Neri, P., Ratti, G. & Rappuoli, R. (1986). Cloning and sequencing of the pertussis toxin genes: operon structure and gene duplication. *Proceedings of the National Academy of Sciences of the United States of America* **83**, 4631-5.

Nielsen, L. S., Andreasen, P. A., Grondahl-Hansen, J., Skriver, L. & Dano, K. (1986). Plasminogen activators catalyse conversion of inhibitor from fibrosarcoma cells to an inactive form with a lower apparent molecular mass. *FEBS Letters* **196**, 269-73.

Nilsson, L., Gafvels, M., Musakka, L., Ensler, K., Strickland, D. K., Angelin, B., Hamsten, A. & Eriksson, P. (1999). VLDL activation of plasminogen activator inhibitor-1 (PAI-1) expression: involvement of the VLDL receptor. *Journal of Lipid Research* **40**, 913-9.

Nilsson, T. K. & Johnson, O. (1987). The extrinsic fibrinolytic system in survivors of myocardial infarction. *Thrombosis Research* **48**, 621-30.

Ny, T., Sawdey, M., Lawrence, D., Millan, J. L. & Loskutoff, D. J. (1986). Cloning and sequence of a cDNA coding for the human beta-migrating endothelial-cell-type plasminogen activator inhibitor. *Proceedings of the National Academy of Sciences of the United States of America* **83**, 6776-80.

Nykjaer, A., Petersen, C. M., Moller, B., Jensen, P. H., Moestrup, S. K., Holtet, T. L., Etzerodt, M., Thogersen, H. C., Munch, M., Andreasen, P. A. & et al. (1992). Purified alpha 2-macroglobulin receptor/LDL receptor-related protein binds urokinase.plasminogen activator inhibitor type-1 complex. Evidence that the alpha

2-macroglobulin receptor mediates cellular degradation of urokinase receptor-bound complexes. *Journal of Biological Chemistry* **267**, 14543-6.

Ogata, M., Chaudhary, V. K., Pastan, I. & FitzGerald, D. J. (1990). Processing of Pseudomonas exotoxin by a cellular protease results in the generation of a 37,000-Da toxin fragment that is translocated to the cytosol. *Journal of Biological Chemistry* **265**, 20678-85.

Ohlsson, M., Peng, X. R., Liu, Y. X., Jia, X. C., Hsueh, A. J. & Ny, T. (1991). Hormone regulation of tissue-type plasminogen activator gene expression and plasminogen activator-mediated proteolysis. *Seminars in Thrombosis & Hemostasis* **17**, 286-90.

Olsnes, S., Reisbig, R. & Eiklid, K. (1981). Subunit structure of Shigella cytotoxin. *Journal of Biological Chemistry* **256**, 8732-8.

Olson, S. T., Bock, P. E., Kvassman, J., Shore, J. D., Lawrence, D. A., Ginsburg, D. & Bjork, I. (1995a). Role of the catalytic serine in the interactions of serine proteinases with protein inhibitors of the serpin family. Contribution of a covalent interaction to the binding energy of serpin-proteinase complexes. *Journal of Biological Chemistry* **270**, 30007-17.

Olson, S. T., Stephens, A. W., Hirs, C. H., Bock, P. E. & Bjork, I. (1995b). Kinetic characterization of the proteinase binding defect in a reactive site variant of the serpin, antithrombin. Role of the P1' residue in transition-state stabilization of antithrombin-proteinase complex formation. *Journal of Biological Chemistry* **270**, 9717-24.

Ostroff, S. M., Kobayashi, J. M. & Lewis, J. H. (1989). Infections with *Escherichia coli* O157:H7 in Washington State. The first year of statewide disease surveillance. *Jama* **262**, 355-9.

Pannekoek, H., Veerman, H., Lambers, H., Diergaarde, P., Verweij, C. L., van Zonneveld, A. J. & van Mourik, J. A. (1986). Endothelial plasminogen activator inhibitor (PAI): a new member of the Serpin gene family. *EMBO Journal* **5**, 2539-44.

Patston, P. A., Gettins, P. G. & Schapira, M. (1994). The mechanism by which serpins inhibit thrombin and other serine proteinases. *Annals of the New York Academy of Sciences* **714**, 13-20.

Pawlowska, Z., Pluskota, E., Chabielska, E., Buczko, W., Okruszek, A., Stec, W. J. & Cierniewski, C. S. (1998). Phosphorothioate oligodeoxyribonucleotides antisense to PAI-1 mRNA increase fibrinolysis and modify experimental thrombosis in rats. *Thrombosis & Haemostasis* **79**, 348-53.

Pedersen, H., Brunner, N., Francis, D., Osterlind, K., Ronne, E., Hansen, H. H., Dano, K. & Grondahl-Hansen, J. (1994a). Prognostic impact of urokinase, urokinase receptor, and type 1 plasminogen activator inhibitor in squamous and large cell lung cancer tissue. *Cancer Research* **54**, 4671-5.

Pedersen, H., Grondahl-Hansen, J., Francis, D., Osterlind, K., Hansen, H. H., Dano, K. & Brunner, N. (1994b). Urokinase and plasminogen activator inhibitor type 1 in pulmonary adenocarcinoma. *Cancer Research* **54**, 120-3.

Philippe, J., Offner, F., Declerck, P. J., Leroux-Roels, G., Vogelaers, D., Baele, G. & Collen, D. (1991). Fibrinolysis and coagulation in patients with infectious disease and sepsis. *Thrombosis & Haemostasis* **65**, 291-5.

Podor, T. J., Joshua, P., Butcher, M., Seiffert, D., Loskutoff, D. & Gauldie, J. (1992). Accumulation of type 1 plasminogen activator inhibitor and vitronectin at sites of cellular necrosis and inflammation. *Annals of the New York Academy of Sciences* **667**, 173-7.

Pralong, G., Calandra, T., Glauser, M. P., Schellekens, J., Verhoef, J., Bachmann, F. & Kruithof, E. K. (1989). Plasminogen activator inhibitor 1: a new prognostic marker in septic shock. *Thrombosis & Haemostasis* **61**, 459-62.

Preissner, K. T., May, A. E., Wohn, K. D., Germer, M. & Kanse, S. M. (1997). Molecular crosstalk between adhesion receptors and proteolytic cascades in vascular remodelling. *Thrombosis & Haemostasis* **78**, 88-95.

Proulx, F., Turgeon, J. P., Delage, G., Lafleur, L. & Chicoine, L. (1992). Randomized, controlled trial of antibiotic therapy for *Escherichia coli* O157:H7 enteritis. *Journal of Pediatrics* **121**, 299-303.

Reisbig, R., Olsnes, S. & Eiklid, K. (1981). The cytotoxic activity of Shigella toxin. Evidence for catalytic inactivation of the 60 S ribosomal subunit. *Journal of Biological Chemistry* **256**, 8739-44.

Rifkin, D. B. (1978). Plasminogen activator synthesis by cultured human embryonic lung cells: characterization of the suppressive effect of corticosteroids. *Journal of Cellular Physiology* **97**, 421-8.

Rifkin, D. B. & Crowe, R. M. (1980). Studies on the control of plasminogen activator production by cultured human embryonic lung cells: requirements for inhibition by corticosteroids. *Journal of Cellular Physiology* **105**, 417-22.

Ryan, C. A., Tauxe, R. V., Hosek, G. W., Wells, J. G., Stoesz, P. A., McFadden, H. W., Jr., Smith, P. W., Wright, G. F. & Blake, P. A. (1986). *Escherichia coli* O157:H7 diarrhea in a nursing home: clinical, epidemiological, and pathological findings. *Journal of Infectious Diseases* **154**, 631-8.

Saksela, O., Moscatelli, D. & Rifkin, D. B. (1987). The opposing effects of basic fibroblast growth factor and transforming growth factor beta on the regulation of plasminogen activator activity in capillary endothelial cells. *Journal of Cell Biology* **105**, 957-63.

Samad, F. & Loskutoff, D. J. (1997). The fat mouse: a powerful genetic model to study elevated plasminogen activator inhibitor 1 in obesity/NIDDM. *Thrombosis & Haemostasis* **78**, 652-5.

Sandvig, K., Dubinina, E., Garred, Ø., Prydz, K., Kozlov, J. V., Hansen, S. H. & Van Deurs, B. (1993). Entry of Shiga toxin into cells. *Zentralblatt fur Bakteriologie* **278**, 296-305.

Sandvig, K., Garred, Ø., Prydz, K., Kozlov, J. V., Hansen, S. H. & van Deurs, B. (1992). Retrograde transport of endocytosed Shiga toxin to the endoplasmic reticulum. *Nature* **358**, 510-2.

Sandvig, K., Olsnes, S., Brown, J. E., Petersen, O. W. & van Deurs, B. (1989). Endocytosis from coated pits of Shiga toxin: a glycolipid-binding protein from *Shigella dysenteriae* 1. *Journal of Cell Biology* **108**, 1331-43.

Sandvig, K., Prydz, K., Ryd, M. & van Deurs, B. (1991). Endocytosis and intracellular transport of the glycolipid-binding ligand Shiga toxin in polarized MDCK cells. *Journal of Cell Biology* **113**, 553-62.

Sandvig, K. & van Deurs, B. (1996). Endocytosis, intracellular transport, and cytotoxic action of Shiga toxin and ricin. *Physiological Reviews* **76**, 949-66.

Saukkonen, K., Burnette, W. N., Mar, V. L., Masure, H. R. & Tuomanen, E. I. (1992). Pertussis toxin has eukaryotic-like carbohydrate recognition domains. *Proceedings of the National Academy of Sciences of the United States of America* **89**, 118-22.

Sawdey, M., Ny, T. & Loskutoff, D. J. (1986). Messenger RNA for plasminogen activator inhibitor. *Thrombosis Research* **41**, 151-60.

Sawdey, M. S. & Loskutoff, D. J. (1991). Regulation of murine type 1 plasminogen activator inhibitor gene expression in vivo. Tissue specificity and induction by lipopolysaccharide, tumor necrosis factor-alpha, and transforming growth factor-beta. *Journal of Clinical Investigation* **88**, 1346-53.

Saxena, S. K., O'Brien, A. D. & Ackerman, E. J. (1989). Shiga toxin, Shiga-like toxin II variant, and ricin are all single-site RNA N-glycosidases of 28 S RNA when microinjected into *Xenopus* oocytes. *Journal of Biological Chemistry* **264**, 596-601.

Schleef, R. R., Bevilacqua, M. P., Sawdey, M., Gimbrone, M. A., Jr. & Loskutoff, D. J. (1988). Cytokine activation of vascular endothelium. Effects on tissue-type plasminogen activator and type 1 plasminogen activator inhibitor. *Journal of Biological Chemistry* **263**, 5797-803.

Schleef, R. R. & Loskutoff, D. J. (1988). Fibrinolytic system of vascular endothelial cells. Role of plasminogen activator inhibitors. *Haemostasis* **18**, 328-41.

Schmitt, M., Harbeck, N., Thomssen, C., Wilhelm, O., Magdolen, V., Reuning, U., Ulm, K., Hofler, H., Janicke, F. & Graeff, H. (1997). Clinical impact of the plasminogen activation system in tumor invasion and metastasis: prognostic relevance and target for therapy. *Thrombosis & Haemostasis* **78**, 285-96.

Schreuder, H. A., de Boer, B., Dijkema, R., Mulders, J., Theunissen, H. J., Grootenhuis, P. D. & Hol, W. G. (1994). The intact and cleaved human antithrombin III complex as a model for serpin-proteinase interactions. *Nature Structural Biology* **1**, 48-54.

Schulman, S. & Wiman, B. (1996). The significance of hypofibrinolysis for the risk of recurrence of venous thromboembolism. Duration of Anticoagulation (DURAC) Trial Study Group. *Thrombosis & Haemostasis* **75**, 607-11.

Scully, M. F. (1991). Plasminogen activator-dependent pericellular proteolysis. *British Journal of Haematology* **79**, 537-43.

Seiffert, D., Mimuro, J., Schleef, R. R. & Loskutoff, D. J. (1990). Interactions between type 1 plasminogen activator inhibitor, extracellular matrix and vitronectin. *Cell Differentiation & Development* **32**, 287-92.

Sharp, A. M., Stein, P. E., Pannu, N. S., Carrell, R. W., Berkenpas, M. B., Ginsburg, D., Lawrence, D. A. & Read, R. J. (1999). The active conformation of plasminogen activator inhibitor 1, a target for drugs to control fibrinolysis and cell adhesion. *Structure* **7**, 111-8.

Shen, G. X. (1998). Vascular cell-derived fibrinolytic regulators and atherothrombotic vascular disorders. *Bioorganic & Medicinal Chemistry Letters* **1**, 399-408.

Shen, X., Minoura, H., Yoshida, T. & Toyoda, N. (1997). Changes in ovarian expression of tissue-type plasminogen activator and plasminogen activator inhibitor type-1 messenger ribonucleic acids during ovulation in rat. *Endocrine Journal* **44**, 341-8.

Sixma, T. K., Pronk, S. E., Kalk, K. H., van Zanten, B. A., Berghuis, A. M. & Hol, W. G. (1992). Lactose binding to heat-labile enterotoxin revealed by X-ray crystallography. *Nature* **355**, 561-4.

Sixma, T. K., Pronk, S. E., Kalk, K. H., Wartna, E. S., van Zanten, B. A., Witholt, B. & Hol, W. G. (1991). Crystal structure of a cholera toxin-related heat-labile enterotoxin from *E. coli*. *Nature* **351**, 371-7.

Sixma, T. K., Stein, P. E., Hol, W. G. & Read, R. J. (1993). Comparison of the B-pentamers of heat-labile enterotoxin and verotoxin-1: two structures with remarkable similarity and dissimilarity. *Biochemistry* **32**, 191-8.

Slivka, S. R. & Loskutoff, D. J. (1991). Platelets stimulate endothelial cells to synthesize type 1 plasminogen activator inhibitor. Evaluation of the role of transforming growth factor beta. *Blood* **77**, 1013-9.

Spangler, B. D. (1992). Structure and function of cholera toxin and the related *Escherichia coli* heat-labile enterotoxin. *Microbiological Reviews* **56**, 622-47.

Spraggon, G., Phillips, C., Nowak, U. K., Ponting, C. P., Saunders, D., Dobson, C. M., Stuart, D. I. & Jones, E. Y. (1995). The crystal structure of the catalytic domain of human urokinase-type plasminogen activator. *Structure* **3**, 681-91.

Sprengers, E. D. & Kluft, C. (1987). Plasminogen activator inhibitors. *Blood* **69**, 381-7.

Sprengers, E. D., Princen, H. M., Kooistra, T. & van Hinsbergh, V. W. (1985). Inhibition of plasminogen activators by conditioned medium of human hepatocytes and hepatoma cell line Hep G2. *Journal of Laboratory & Clinical Medicine* **105**, 751-8.

Stec, W. J., Cierniewski, C. S., Okruszek, A., Kobylanska, A., Pawlowska, Z., Koziolkiewicz, M., Pluskota, E., Maciaszek, A., Rebowska, B. & Stasiak, M. (1997). Stereodependent inhibition of plasminogen activator inhibitor type 1 by phosphorothioate oligonucleotides: proof of sequence specificity in cell culture and in vivo rat experiments. *Antisense & Nucleic Acid Drug Development* **7**, 567-73.

Stefansson, S. & Lawrence, D. A. (1996). The serpin PAI-1 inhibits cell migration by blocking integrin alpha V beta 3 binding to vitronectin. *Nature* **383**, 441-3.

Stefansson, S., Haudenschild, C. C. & Lawrence, D. A. (1998a). Beyond Fibrinolysis: The role of Plasminogen Activator Inhibitor-1 and Vitronectin in Vascular Wound Healing. *Trends in Cardiovascular Medicine* **8**, 175-180.

Stefansson, S., Muhammad, S., Cheng, X. F., Battey, F. D., Strickland, D. K. & Lawrence, D. A. (1998b). Plasminogen activator inhibitor-1 contains a cryptic high affinity binding site for the low density lipoprotein receptor-related protein. *Journal of Biological Chemistry* **273**, 6358-66.

Stein, P. & Chothia, C. (1991). Serpin tertiary structure transformation. *Journal of Molecular Biology* **221**, 615-21.

Stein, P. E., Boodhoo, A., Tyrrell, G. J., Brunton, J. L. & Read, R. J. (1992). Crystal structure of the cell-binding B oligomer of verotoxin-1 from *E. coli*. *Nature* **355**, 748-50.

Stiko-Rahm, A., Wiman, B., Hamsten, A. & Nilsson, J. (1990). Secretion of plasminogen activator inhibitor-1 from cultured human umbilical vein endothelial cells is induced by very low density lipoprotein. *Arteriosclerosis* **10**, 1067-73.

Strandberg, L., Lawrence, D. & Ny, T. (1988). The organization of the human-plasminogen-activator-inhibitor-1 gene. Implications on the evolution of the serine-protease inhibitor family. *European Journal of Biochemistry* **176**, 609-16.

Stratikos, E. & Gettins, P. G. (1997). Major proteinase movement upon stable serpin-proteinase complex formation. *Proceedings of the National Academy of Sciences of the United States of America* **94**, 453-8.

Stratikos, E. & Gettins, P. G. (1999). Formation of the covalent serpin-proteinase complex involves translocation of the proteinase by more than 70 A and full insertion of the reactive center loop into beta-sheet A. *Proceedings of the National Academy of Sciences of the United States of America* **96**, 4808-13.

Stringer, H. A. & Pannekoek, H. (1995). The significance of fibrin binding by plasminogen activator inhibitor 1 for the mechanism of tissue-type plasminogen activator-mediated fibrinolysis. *Journal of Biological Chemistry* **270**, 11205-8.

Stromqvist, M., Karlsson, K. E., Björquist, P., Andersson, J. O., Bystrom, M., Hansson, L., Johansson, T. & Deinum, J. (1996). Characterisation of the complex of plasminogen activator inhibitor type 1 with tissue-type plasminogen activator by mass spectrometry and size-exclusion chromatography. *Biochimica et Biophysica Acta* **1295**, 103-9.

Tang, W. H., Friess, H., di Mola, F. F., Schilling, M., Maurer, C., Graber, H. U., Dervenis, C., Zimmermann, A. & Buchler, M. W. (1998). Activation of the serine proteinase system in chronic kidney rejection. *Transplantation* **65**, 1628-34.

Tarr, P. I. (1995). Escherichia coli O157:H7: clinical, diagnostic, and epidemiological aspects of human infection. *Clinical Infectious Diseases* **20**, 1-8.

Tesh, V. L. & O'Brien, A. D. (1992). Adherence and colonization mechanisms of enteropathogenic and enterohemorrhagic *Escherichia coli*. *Microbial Pathogenesis* **12**, 245-54.

Tucker, H. M., Mottonen, J., Goldsmith, E. J. & Gerard, R. D. (1995). Engineering of plasminogen activator inhibitor-1 to reduce the rate of latency transition. *Nature Structural Biology* **2**, 442-5.

Uno, S., Nakamura, M., Ohomagari, Y., Matsuyama, S., Seki, T. & Ariga, T. (1998). Regulation of tissue-type plasminogen activator (tPA) and type-1 plasminogen activator inhibitor (PAI-1) gene expression in rat hepatocytes in primary culture. *Journal of Biochemistry* **123**, 806-12.

Urano, T., Serizawa, K., Takada, Y., Ny, T. & Takada, A. (1994). Heparin and heparan sulfate enhancement of the inhibitory activity of plasminogen activator inhibitor type 1 toward urokinase type plasminogen activator. *Biochimica et Biophysica Acta* **1201**, 217-22.

van Boeckel, C. A., Grootenhuis, P. D. & Visser, A. (1994). A mechanism for heparin-induced potentiation of antithrombin III [letter]. *Nature Structural Biology* **1**, 423-5.

Van Hinsberg, V. W., Sprengers, E. D. & Kooistra, T. (1987). Effect of thrombin on the production of plasminogen activators and PA inhibitor-1 by human foreskin microvascular endothelial cells. *Thrombosis & Haemostasis* **57**, 148-53.

van Hinsbergh, V. W., Kooistra, T., Scheffer, M. A., Hajo van Bockel, J. & van Muijen, G. N. (1990a). Characterization and fibrinolytic properties of human omental tissue mesothelial cells. Comparison with endothelial cells. *Blood* **75**, 1490-7.

van Hinsbergh, V. W., Kooistra, T., van den Berg, E. A., Princen, H. M., Fiers, W. & Emeis, J. J. (1988). Tumor necrosis factor increases the production of plasminogen activator inhibitor in human endothelial cells in vitro and in rats in vivo. *Blood* **72**, 1467-73.

van Hinsbergh, V. W., van den Berg, E. A., Fiers, W. & Dooijewaard, G. (1990b). Tumor necrosis factor induces the production of urokinase-type plasminogen activator by human endothelial cells. *Blood* **75**, 1991-8.

van Zonneveld, A. J., Curriden, S. A. & Loskutoff, D. J. (1988). Type 1 plasminogen activator inhibitor gene: functional analysis and glucocorticoid regulation of its promoter. *Proceedings of the National Academy of Sciences of the United States of America* **85**, 5525-9.

van Zonneveld, A. J., van den Berg, B. M., van Meijer, M. & Pannekoek, H. (1995). Identification of functional interaction sites on proteins using bacteriophage-displayed random epitope libraries. *Gene* **167**, 49-52.

van't Wout, J., Burnette, W. N., Mar, V. L., Rozdzinski, E., Wright, S. D. & Tuomanen, E. I. (1992). Role of carbohydrate recognition domains of pertussis toxin in

adherence of *Bordetella pertussis* to human macrophages. *Infection & Immunity* **60**, 3303-8.

Verpy, E., Couture-Tosi, E., Eldering, E., Lopez-Trascasa, M., Spath, P., Meo, T. & Tosi, M. (1995). Crucial residues in the carboxy-terminal end of C1 inhibitor revealed by pathogenic mutants impaired in secretion or function. *Journal of Clinical Investigation* **95**, 350-9.

Verspaget, H. W., Sier, C. F., Ganesh, S., Griffioen, G. & Lamers, C. B. (1995). Prognostic value of plasminogen activators and their inhibitors in colorectal cancer. *European Journal of Cancer* **31A**, 1105-9.

Wagner, O. F., de Vries, C., Hohmann, C., Veerman, H. & Pannekoek, H. (1989). Interaction between plasminogen activator inhibitor type 1 (PAI-1) bound to fibrin and either tissue-type plasminogen activator (t-PA) or urokinase-type plasminogen activator (u-PA). Binding of t-PA/PAI-1 complexes to fibrin mediated by both the finger and the kringle-2 domain of t-PA. *Journal of Clinical Investigation* **84**, 647-55.

Waley, S. G. (1980). Kinetics of suicide substrates. *Biochemical Journal* **185**, 771-3.

Waley, S. G. (1985). Kinetics of suicide substrates. Practical procedures for determining parameters. *Biochemical Journal* **227**, 843-9.

Wallberg-Jonsson, S., Dahlen, G. H., Nilsson, T. K., Ranby, M. & Rantapaa-Dahlqvist, S. (1993). Tissue plasminogen activator, plasminogen activator inhibitor-1 and von Willebrand factor in rheumatoid arthritis. *Clinical Rheumatology* **12**, 318-24.

Walterspiel, J. N., Ashkenazi, S., Morrow, A. L. & Cleary, T. G. (1992). Effect of

subinhibitory concentrations of antibiotics on extracellular Shiga-like toxin I.

Infection **20**, 25-9.

Whisstock, J., Skinner, R., & Lesk, A. M. (1998). An atlas of serpin conformations.

Trends in Biochemical Sciences **23**, 63-67.

Wilczynska, M., Fa, M., Karolin, J., Ohlsson, P. I., Johansson, L. B. & Ny, T. (1997).

Structural insights into serpin-protease complexes reveal the inhibitory mechanism

of serpins. *Nature Structural Biology* **4**, 354-7.

Wilhelm, O. G., Jaskunas, S. R., Vlahos, C. J. & Bang, N. U. (1990). Functional

properties of the recombinant kringle-2 domain of tissue plasminogen activator

produced in Escherichia coli. *Journal of Biological Chemistry* **265**, 14606-11.

Wiman, B. (1995). Plasminogen activator inhibitor 1 (PAI-1) in plasma: its role in

thrombotic disease. *Thrombosis & Haemostasis* **74**, 71-6.

Wiman, B., Csemiczky, G., Marsk, L. & Robbe, H. (1984). The fast inhibitor of tissue

plasminogen activator in plasma during pregnancy. *Thrombosis & Haemostasis* **52**,

124-6.

Wright, H. T. (1996). The structural puzzle of how serpin serine proteinase inhibitors

work. *Bioessays* **18**, 453-64.

Wright, H. T. & Scarsdale, J. N. (1995). Structural basis for serpin inhibitor activity.

Proteins **22**, 210-25.

Xue, Y., Björquist, P., Inghardt, T., Linschoten, M., Musil, D., Sjolin, L. & Deinum, J.

(1998). Interfering with the inhibitory mechanism of serpins: crystal structure of a

complex formed between cleaved plasminogen activator inhibitor type 1 and a reactive-centre loop peptide. *Structure* **6**, 627-36.

Yamamoto, K. & Loskutoff, D. J. (1997). The kidneys of mice with autoimmune disease acquire a hypofibrinolytic/procoagulant state that correlates with the development of glomerulonephritis and tissue microthrombosis. *American Journal of Pathology* **151**, 725-34.

Yamamoto, K., Loskutoff, D. J. & Saito, H. (1998). Renal expression of fibrinolytic genes and tissue factor in a murine model of renal disease as a function of age. *Seminars in Thrombosis & Hemostasis* **24**, 261-8.

Yamamoto, K. & Saito, H. (1998). A pathological role of increased expression of plasminogen activator inhibitor-1 in human or animal disorders. *International Journal of Hematology* **68**, 371-85.

Ye, S., Green, F. R., Scarabin, P. Y., Nicaud, V., Bara, L., Dawson, S. J., Humphries, S. E., Evans, A., Luc, G., Cambou, J. P. & et al. (1995). The 4G/5G genetic polymorphism in the promoter of the plasminogen activator inhibitor-1 (PAI-1) gene is associated with differences in plasma PAI-1 activity but not with risk of myocardial infarction in the ECTIM study. Etude CasTemoins de I'nfarctus du Mycocarde. *Thrombosis & Haemostasis* **74**, 837-41.

Zalewski, A., Shi, Y., Nardone, D., Bravette, B., Weinstock, P., Fischman, D., Wilson, P., Goldberg, S., Levin, D. C. & Bjornsson, T. D. (1991). Evidence for reduced fibrinolytic activity in unstable angina at rest. Clinical, biochemical, and angiographic correlates. *Circulation* **83**, 1685-91.

Zeillinger, R., Eder, S., Schneeberger, C., Ullrich, R., Speiser, P. & Swoboda, H. (1996).

Cathepsin D and PAI-1 expression in human head and neck cancer. *Anticancer*

Research **16**, 449-53.

2.0 Structure of Plasminogen Activator Inhibitor-1 at 3.0 Å*

2.1 Introduction

PAI-1, a member of the serpin family of serine proteinase inhibitors, is the main

physiological inhibitor of tissue plasminogen activator (tPA) and urokinase plasminogen

activator (uPA). These serine proteinases convert plasminogen, an inactive zymogen, to

the active enzyme plasmin, which degrades fibrin clots. Epidemiological studies have

shown that elevated circulating levels of PAI-1 are associated with coronary heart disease

and possibly atherosclerosis (Wiman, 1995). These findings have led to considerable

interest in the development of drugs that specifically inhibit PAI-1. Such drugs may have

a wider clinical application as the fibrinolytic system is also involved in ovulation, wound

healing, angiogenesis, tissue remodeling and neoplasia (Bell, 1996).

Serpins bind to their target enzymes through a highly mobile peptide loop

containing the reactive center or scissile bond (denoted P1-P1') (Schechter & Berger,

1967). The active form of a serpin is apparently a metastable folding intermediate.

Following attack of the reactive center by a target enzyme, a conformational change

occurs and the serpin-proteinase complex is trapped, probably at the acylenzyme step

(Lawrence et al., 1995; Wilczynska et al., 1995). The complex dissociates very slowly,

yielding an irreversibly inactivated cleaved serpin. The cleaved form has undergone a

---

dramatic conformational change in which the amino terminus of the cleaved reactive center loop has been inserted into the major β-sheet (sheet A), forming a new β-strand (Loebermann *et al.*, 1984). A similar loop insertion is believed to occur in the formation of the inhibited complex (Lawrence *et al.*, 1995). PAI-1 is a prototype among serpins for its ability to convert spontaneously, without cleavage, to an inactive conformation similar to the cleaved form; there is complete insertion of the intact reactive center loop in sheet A, together with release of the first strand of sheet C (Mottonen *et al.*, 1992). This form is termed "latent" since activity of the inhibitor can be restored by denaturation and renaturation. Other serpins can fold into a latent conformation (Carrell *et al.*, 1991) under mild thermal stress (Lomas *et al.*, 1995), and there is now evidence that latency plays a role in the senescence and pathology of antithrombin (Beauchamp & Carrell, 1998). In PAI-1, the spontaneous transition to latency may ensure a sufficient turnover to allow a rapid physiological response to changing circumstances. In the circulation, most PAI-1 will exist in a tight complex with the adhesive glycoprotein, vitronectin. In such a complex *in vitro*, the lifetime of active PAI-1 is doubled from about two hours to four hours at 37 ° C (Declerck *et al.*, 1988).

Here, we describe the structure of a recombinant mutant of PAI-1 that is more stable in its active form than wild-type PAI-1 (Berkenpas *et al.*, 1995). Attempts to crystallize active wild-type PAI-1 have so far been unsuccessful. The structures of latent PAI-1 (Mottonen *et al.*, 1992) and two forms of cleaved PAI-1, by itself (Aertgeerts *et al.*, 1995) and with a reactive center loop peptide bound (Xue *et al.*, 1998), are already known. The addition of our structure of active PAI-1 will make it possible to analyze the

full extent of the conformational transitions in PAI-1 without relying on homology

modeling.

2.2 Results and Discussion

2.2.1 Comparison with other active serpins

Since the first determination of a serpin structure, that of cleaved α_1-antitrypsin

(Loebermann *et al.*, 1984), many crystal structures have been determined of serpins in

various conformations. Intact, active serpins have been the most difficult to crystallize

but structures are now available for intact forms of α_1-antichymotrypsin (Wei *et al.*,

1994), antithrombin (Carrell *et al.*, 1994; Schreuder *et al.*, 1994), and α_1-antitrypsin

(Elliott *et al.*, 1996). In its general features (Figure 1.6 a), as expected, active PAI-1

resembles other active serpins.

An unusual flexibility of the reactive center loop is suggested by the markedly

different conformations of this segment in the structures of active serpins. In PAI-1, the

reactive loop also shows evidence of mobility, and its conformation in the crystal appears

to be significantly influenced by packing contacts. In two out of four independent PAI-1

molecules in the crystal (molecules B and D, discussed below), there are no packing

contacts around the loop, and it is disordered. However, in the other two molecules the

C-terminal portion of the loop is tethered by crystal packing contacts and is probably

induced to adopt an extended conformation. The four molecules have been restrained to

be almost identical (r.m.s. deviations on all atoms of less than 0.3Å), with only a few

residues at the N termini and in the reactive center loops being allowed to differ

significantly. As the A and C molecules are nearly identical (r.m.s deviation of 0.15Å on

all atoms), have the lowest overall temperature factors and have complete reactive center

loops, the A molecule will be used in the discussion. The reactive center loop of PAI-1

could not be docked to a proteinase without altering the conformation seen in the present

crystal, indicating that it must be flexible. The only active serpin that has crystallized in a

conformation that could dock to a proteinase is α_1-antitrypsin (Elliott *et al.*, 1996). As

seen in other active serpins, the reactive center loop of PAI-1 appears poised to enter a

gap between strands 3A and 5A.

2.2.2 A new mode of serpin polymerization

The four PAI-1 molecules in the P1 unit cell display pseudo-C2 symmetry. The

two unique molecules in the pseudo-C2 cell (molecules A and B) form an improper

dimer, which is related to a second dimer (molecules C and D) by a 2_1 screw axis. The

interaction between this pair of dimers is mediated primarily by an intimate contact

between the A and C molecules, in which the reactive center loop of one molecule adds a

β-strand to the edge of the A-sheet of the other molecule. Repeated application of the

screw symmetry generates an infinite chain of A and C molecules, shown in Figure 2.1.

This region is clearly visible in the electron density (Figure 2.2).

This infinite chain of molecules may be relevant to the formation of pathological

polymers of serpin molecules (Stein & Carrell, 1995), as found in the liver disease

associated with the Z variant of α_1-antitrypsin (Lomas *et al.*, 1992). However, the mode

of polymerization differs from those proposed earlier, involving the insertion of the

reactive center loop of one molecule into another molecule as an edge strand of sheet C

or the central strand of sheet A (Stein & Carrell, 1995). The interaction in the stable

Figure 2.1: Infinite chain of PAI-1 molecules in the crystal lattice. Molecules A (red) and

C (two copies in blue) are related by a pseudo-crystallographic 2_1 screw axis. The

reactive center loop of one molecule forms a new strand "7A" at the edge of the A sheet

of the other molecule. The β-strands involved in the interaction are highlighted as broad

arrows. The figure was prepared with the program Molscript (Kraulis, 1991).
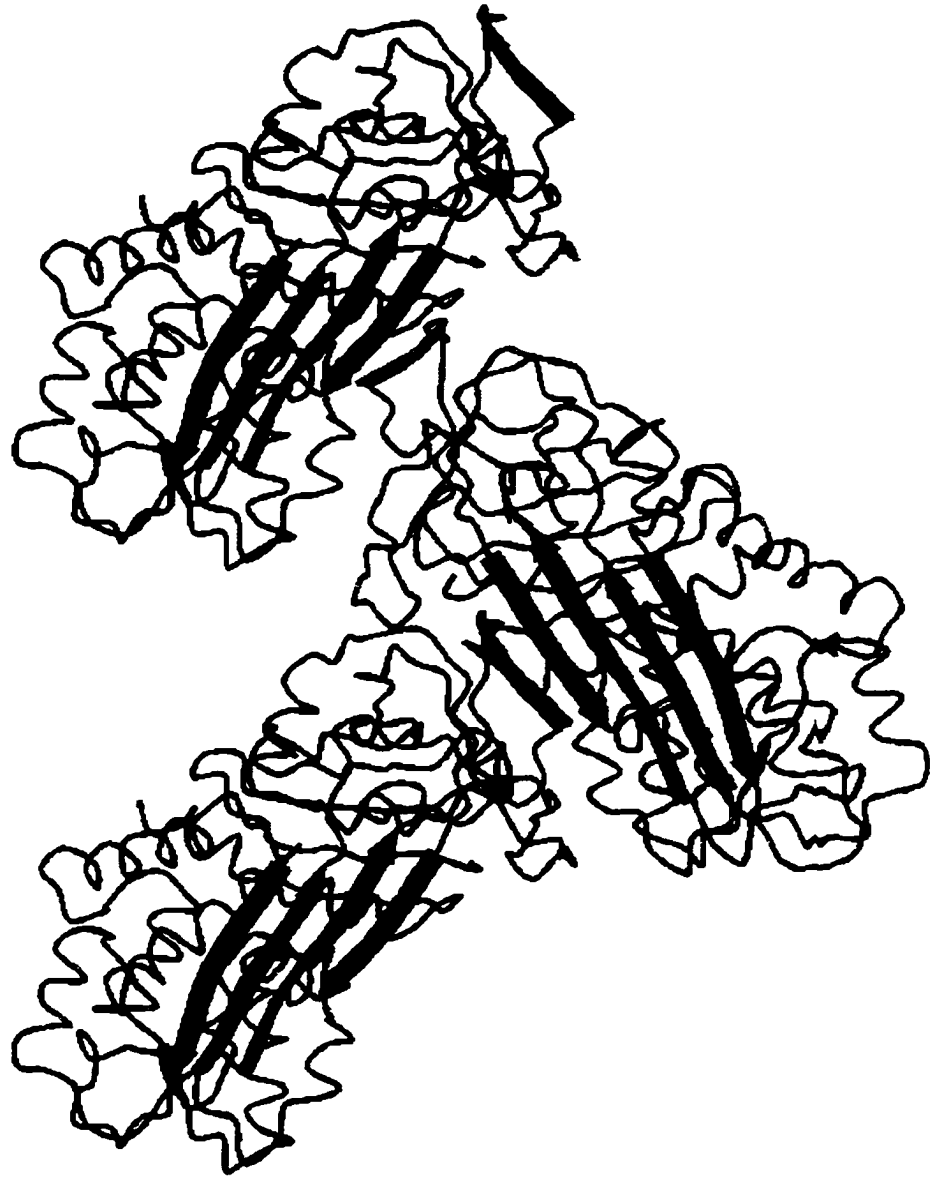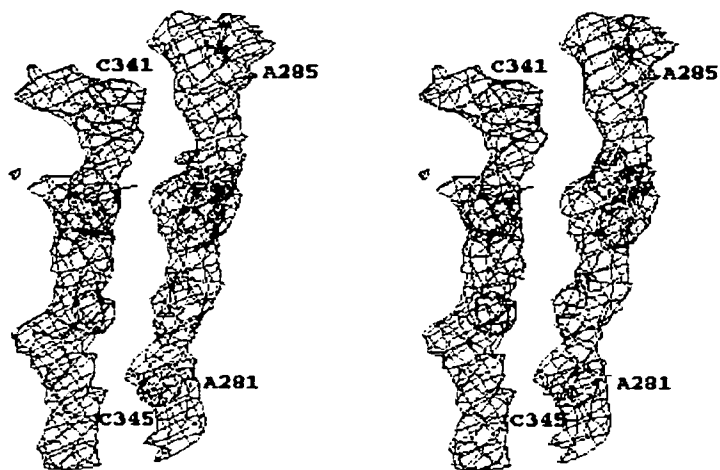
Figure 2.2 Reactive centre loop electron density. Because of the interaction, density for the reactive center loop is reasonably clear in the A and C molecules. Electron density, after averaging, is shown for the interaction between strand 6A of molecule A (residues Glu A281 - Val A284, yellow) and the reactive center loop of molecule C (Val C341 - Ala C345, red). For clarity, only electron density contours within 2.5Å of an atom in the figure are shown. The figure was prepared with the program XtalView (McRee, 1999).

mutant of PAI-1 is reversible, as the crystals can be dissolved to give active PAI-1 (data

not shown), but in other serpins such polymers could be more stable. Furthermore, the

interaction illustrates the propensity of the reactive center loop to enter into a β-sheet,

which is central to the serpin mechanism of inhibition.

2.2.3 Factors influencing the latency transition

Although PAI-1 is unusual in the speed of its transition to latency, the relevant

structural differences from other serpins are likely to be very subtle. Other inhibitory

serpins appear to exist in a metastable state, but with a larger barrier to latency so that one

must wait much longer or subject them to harsher conditions. Nonetheless, an increase of

only 4 or 5 kcal/mole in the activation energy barrier to latency would make PAI-1 stable

for months under physiological conditions. The quadruple mutant has a half life of 145h

at 37° C (Berkenpas *et al.*, 1995), so it is sufficiently stable at room temperature to

crystallize in the active form. This amounts, however, to an increase of less than

3kcal/mole in the energy of the transition state to latency.

As one would expect, all four mutations (see Figure 2.3) are in parts of the serpin

molecule where movement is known to occur during the transition from active to latent

forms. Only one mutation removes a difference between the sequence of PAI-1 and the

majority of inhibitory serpins. M354I is in strand 1C, which forms the distal hinge of the

reactive center loop and also has to be unraveled in the latency transition. The reverse

mutation to methionine at the equivalent residue (V366M) in C1-inhibitor results in

polymerization and other evidence of reactive loop insertion (Eldering *et al.*, 1995). In

Figure 2.3: Mutations that increase stability in the quadruple mutant. Overview of the structure showing the location of the four mutations, with the side chains highlighted in red. The figure was prepared with the program Molscript (Kraulis, 1991).

PAI-1, a methionine may have evolved at this position to give a conformationally labile molecule compatible with its function, whereas in C1-inhibitor, which has a higher concentration and longer half life in plasma, the same mutation has adverse consequences (Carrell & Stein, 1996).

The other three mutations are close to one another, clustered around the site where the A-sheet opens to accept the reactive center loop (Carrell & Stein, 1996). Interestingly, non-additive effects on stability were found when various single, double and triple combinations of the four mutations were evaluated (Berkenpas *et al.*, 1995). The stabilizing effects of either N150H or Q319L are only fully achieved when combined with K154T; on its own, N150H is actually slightly destabilizing. The prediction that this reflected complex structural interactions is now borne out by the structure. The loop connecting helix F with strand 3A (which includes residues 150 and 154) contains a turn of 3_{10} helix, unlike any other serpin of known structure including latent and cleaved PAI-1. This conformation is only possible in the presence of K154T, as the new threonine side chain is buried and hydrogen bonded (Figure 2.4). The other two mutations presumably also favor the 3_{10} conformation, either through burial of hydrophobic surface (Q319L) or through avoidance of steric conflict (N150H). The new conformation of the loop allows hydrogen bonds to be formed between the mainchain nitrogens of residues 151 and 152 to the sidechain of Glu 283 in strand 6A. These hydrogen bonds would have to be broken in the process of inserting the reactive center loop as a new strand between strands 3A and 5A and, together with increased rigidity of the 3_{10} helix, may account for a large part of the increased barrier to latency.
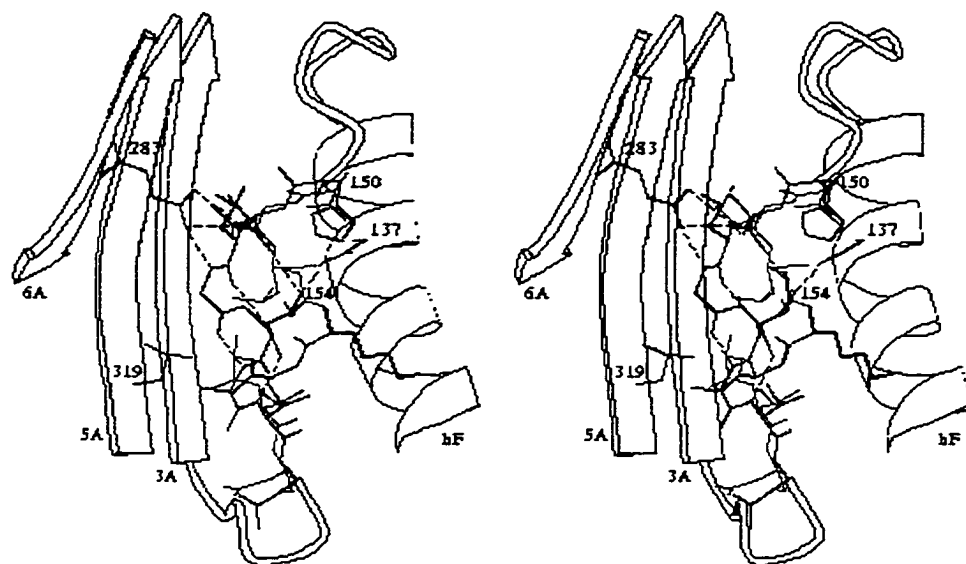
Figure 2.4: Structural change induced by mutations. Close-up view of the three mutations associated with the change in conformation to a 3_{10} helix in the loop connecting helix F to strand 3A. The active form of the stable PAI-1 mutant is shown in black, while the residues for this loop from latent PAI-1 (Mottonen *et al.*, 1992) are shown in red. The latent structure has been overlaid by superimposing residues 128-150, and residues 158-162. In other serpins latency or cleavage has no significant effect on the conformation of this loop. The figure was prepared with the program Molscript (Kraulis, 1991).

When the structure of latent PAI-1 was determined, it was found that the loop from His185 to Pro200 (strands 3C to 4C, termed the "gate") was poorly ordered (Mottonen *et al.*, 1992). It was suggested that lack of order in this loop made it easier for the C-terminal portion of the reactive center loop to move to its final position in the latent form (Tucker *et al.*, 1995). This argument is intuitively attractive, and the gate may move more readily in PAI-1 than in other serpins. However, our structure does not provide experimental support, as the gate region is well ordered. It was also suggested that an unusual position for the C-terminus caused the gate to be displaced (Tucker *et al.*, 1995), but this must be a consequence of the latency transition, as the C-terminus of active PAI-1 occupies the position seen in other serpins.

2.2.4 Vitronectin binding

The adhesive glycoprotein vitronectin binds to the active form of PAI-1, stabilizing it and altering its specificity. This interaction is specific for active PAI-1, as the affinity of vitronectin for latent, cleaved, proteinase-bound, and other forms of PAI-1 with the reactive center loop inserted into sheet A is reduced by a factor of 100 or more (Lawrence *et al.*, 1997). The change in affinity may provide a mechanism for the release of inactive PAI-1 from the extracellular matrix, followed by clearance through uptake by the LDL receptor-related protein, LRP (Stefansson *et al.*, 1998).

Recent results suggest that the binding of PAI-1 to vitronectin competes with interactions mediating cell adhesion events. Active PAI-1 has been found to compete with α_V-integrins (Stefansson & Lawrence, 1996) and the uPA receptor (Deng *et al.*,

1996) for binding to vitronectin. These results provide an explanation for the association of high levels of PAI-1 with increased risk of tumor metastasis (Deng *et al.*, 1996) and also suggest a means by which coagulation and tissue remodeling could be coordinately regulated during wound healing (Preissner *et al.*, 1997). Deficient PAI-1 expression in knockout mice has recently been shown to prevent tumor invasion and vascularization (Bajou *et al.*, 1998), supporting the proposed role of PAI-1 in metastasis.

Selection for random mutations of PAI-1 that reduce vitronectin binding, but not activity, has identified a patch of five residues near the strand 1 edge of the A sheet (Lawrence *et al.*, 1994). The insertion of the reactive center loop has been presumed to alter this surface, inhibiting binding. Indeed, comparison of the active and latent structures (Figure 2.5) reveals extensive rearrangements of the secondary structural elements in this region. Further structural studies will be required to determine the exact nature of the binding surface.

2.2.5 Binding of drugs modulating PAI-1 activity

Björquist and coworkers (Björquist *et al.*, 1998) present evidence that small molecule PAI-1 inhibitors can bind in the vicinity of Arg 76, Arg 115 and Arg 118. The site corresponds essentially with a pocket proposed as a good target for compounds inhibiting the polymerization of α_1-antitrypsin (Elliott *et al.*, 1998). This site can be seen in Fig. 2.3, above and behind helix E, and between the A sheet and helix D. The same region has been implicated in the binding of heparin (Stein & Carrell, 1995) and LRP (Stefansson *et al.*, 1998), suggesting that it is a general site for serpins to bind ligands that influence, or are influenced by, the conformational transitions.
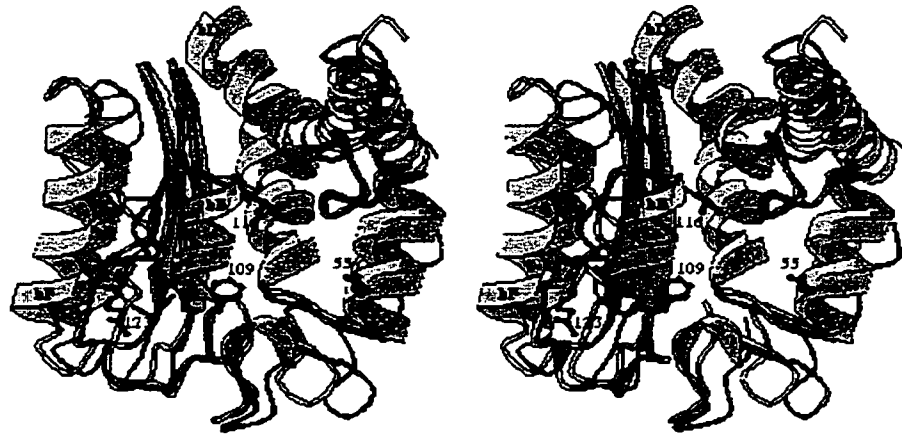
Figure 2.5: Conformational changes in the region of the vitronectin binding site that are caused by the latency transition. Latent PAI-1 (Mottonen *et al.*, 1992), shown in blue, has been overlaid on active PAI-1 (pink) by superimposing the large rigid fragment defined by Stein & Chothia (1991). Ball-and-stick models indicate the locations of mutations that affect vitronectin binding without affecting inhibitory activity (Lawrence *et al.* 1994). Helix E and strand 1A have also been shown to be important in vitronectin binding (see text for discussion). The figure was prepared with the program Molscript (Kraulis, 1991).

Our results show the profound structural changes that occur in this region on loop insertion (Figure 2.5). Conformational changes are seen in this region in other serpins and were thus expected to occur in PAI-1 as well (Björquist *et al.*, 1998). Drugs could modulate PAI-1 activity by preventing, or accelerating, the latency transition, or by slowing or eliminating loop insertion on cleavage, thus converting PAI-1 into a substrate. Because all such drugs would bind, at least initially, to the active form of PAI-1, our structure provides an ideal starting point for structure-based drug design.

2.3 Biological implications

Plasminogen activator inhibitor-1 (PAI-1), a serine proteinase inhibitor from the serpin family, is being found to play a key role in a growing number of medically-relevant pathways. Structural knowledge is essential for a detailed understanding of these processes, because PAI-1 and other serpins are exceptional in the degree to which conformational changes are required for function. Most serpins exist in a metastable state, and their mechanism of proteinase inhibition exploits the energy released when the cleaved serpin refolds into its lowest energy state. The different conformations can be distinguished by receptors, with further consequences for function.

PAI-1 is the physiological inhibitor of the fibrinolysis pathway, which in turn limits the coagulation pathway and hence prevents thrombosis. In keeping with this, the diurnal rhythm in levels of PAI-1 may account for the early morning occurrence of the majority of thromboses, and the rebound in levels after fibrinolytic treatment could contribute to the development of coronary restenosis, the scarring process which often follows balloon angioplasty of blocked arteries. PAI-1 is therefore a promising drug target for the

treatment of coronary heart disease. Useful drugs should bind to the active conformation of PAI-1, described here, but not necessarily to the latent or cleaved conformations determined in previous crystal structures.

Intriguingly, PAI-1 is now being identified as a key player in the interactions between coagulation and the cell adhesion pathways involved in tissue remodeling and metastasis. Active PAI-1 (but not its latent or cleaved forms) binds tightly to the adhesive glycoprotein vitronectin in the extracellular matrix. This binding localizes active PAI-1 at the site of its action in the fibrinolytic pathway, and also doubles its half life. However, it is now apparent that, as a vitronectin ligand, active PAI-1 competes with α_V-integrins and the uPA receptor. This potential to modulate cell adhesion to the tissue matrix opens further possibilities of rational drug design.

2.4 Materials and methods

2.4.1 Expression and purification

Mutant protein was expressed and purified as before (Berkenpas et al., 1995), or was obtained from Molecular Innovations. Purified protein was concentrated to 5 mg/ml in 10 mM cacodylate pH 6.8, 0.25 M NaCl, 1 mM EDTA.

2.4.2 Crystallization

Crystallization conditions were identified using the Crystal Screen™ sparse matrix crystallization screening kit (Hampton Research, Laguna Hills, California). Crystals were produced by the hanging drop method, mixing a drop of the protein sample with a

well sample of 27-32% saturated ammonium sulfate, 0.25 M NaCl, and 10 mM

cacodylate pH 6.8 at room temperature. Crystals formed with a few days of

equilibration, and continued to grow for approximately a week.

2.4.3 Data Collection

Data were collected from a single crystal on a Siemens multiwire area detector

mounted on a Siemens rotating anode. Crystals were cryoprotected by transfer to 25%

glycerol solutions and were cooled to 111K with an Oxford Cryostream. The data were

reduced using Xengen 2.0 (Howard *et al.*, 1987) and programs from the Biomol package

(University of Groningen). As two of the measured cell axes were close to 90°, the

program PLATON (Speck, 1990) was used to perform LePage and Delauney reduction

(Zimmerman & Burzlaff, 1985, Burzlaff & Zimmermann, 1985) analyses of the data. No

higher order symmetry could be detected.

2.4.4 Molecular Replacement

Self- and cross-rotation functions were computed with AMoRe (Navaza, 1994).

Self-rotation functions indicated two-fold symmetry parallel to the **a** axis. Cross rotation

functions, computed using latent PAI-1 (Mottonen *et al.*, 1992) as a search model,

showed four peaks. The AMoRe translation function was used to find solutions for this

set of orientations, consistent with one improper dimer (A+B) related to another (C+D)

by a 2-fold screw operation. (Molecule A is related to B by a 64° rotation and a 27Å

screw translation.) Rigid body refinement was conducted with X-PLOR (Brünger, 1993)

using data from 10 to 5 Å resolution and allowing residues 90-175 (strands 1A, 2A and

3A and associated loops and helices) to move as a rigid fragment relative to the rest of

the molecule. This allowed strand 3A to move into the position beside strand 5A that

was previously occupied by strand 4A (the reactive center loop).

2.4.5 Refinement

Refinement was carried out initially with X-PLOR and later with CNS (Brünger et

al., 1998), using the maximum likelihood refinement target MLI (MLF2 in ref. (Pannu &

Read, 1996)) and a correction for bulk solvent (Jiang & Brünger, 1994). Rounds of

refinement were alternated with rebuilding in O (Jones et al., 1991), inspecting the model

in electron density maps that had been averaged and solvent-flattened with the DEMON

package (Vellieux et al., 1995). Strict non-crystallographic symmetry (NCS) was

maintained until it became obvious that the reactive center loops in molecules A and C

differed from those in B and D, after which strong NCS restraints were imposed.

Thermal motion parameters (B values) were refined only for groups of main-chain and

side-chain atoms. The final model includes residues 7 to 379 in molecules A and C, and

residues 7 to 332 (P15) and 348 (P2') to 379 in molecules B and D. Statistics for the final

model are summarized in Table 2.1.

Table 2.1. Structure and refinement statistics

Space group	P1
Unit cell dimensions	a = 65.5 Å, b = 74.9 Å, c = 103.7 Å
	$\alpha = 91.0°$, $\beta = 93.3°$, $\gamma = 115.9°$
Resolution limits	24.0 - 2.99Å
Total observations	42,559
Unique reflections	25,369
Completeness (3.12Å- 2.99Å shell)	71.2 % (19.7 %)
R_{merge}[1] (3.16Å - 2.99Å shell)	0.102 (0.336)
Protein atoms	11,658
R-factor (R_{free}[2])	0.247 (0.292)
RMS deviations from ideal geometry	
Bond Lengths	0.009 Å
Bond Angles	1.51°
Dihedral Angles	22.6°
Improper Angles	0.70°

[1]$R_{merge} = \Sigma(|F_j| - <|F|>)/\Sigma|F_j|$

[2]Computed using 2576 reflections selected in thin shells of resolution.

References

Aertgeerts, K., De Bondt, H. L., De Ranter, C. J. & Declerck, P. J. (1995). Mechanisms contributing to the conformational and functional flexibility of plasminogen activator inhibitor-1. *Nature Structural Biology* **2**, 891-7.

Bajou, K., Noel, A., Gerard, R. D., Masson, V., Brunner, N., Holst-Hansen, C., Skobe, M., Fusenig, N. E., Carmeliet, P., Collen, D. & Foidart, J. M. (1998). Absence of host plasminogen activator inhibitor 1 prevents cancer invasion and vascularization. *Nature Medicine* **4**, 923-8.

Beauchamp, N. K. & Carrell, R. W. (1998). Antithrombins wibble and wobble (T85M/K): archetypal conformational diseases with in vivo latent-transition, thrombosis, and heparin activation. *Blood* **92**, 2696-706.

Bell, W. R. (1996). The Fibrinolytic System in Neoplasia. *Seminars in Thrombosis and Hemostasis* **22**, 459-78.

Berkenpas, M. B., Lawrence, D. A. & Ginsburg, D. (1995). Molecular evolution of plasminogen activator inhibitor-1 functional stability. *EMBO Journal* **14**, 2969-77.

Björquist, P., Ehnebom, J., Inghardt, T., Hansson, L., Lindberg, M., Linschoten, M., Stromqvist, M. & Deinum, J. (1998). Identification of the binding site for a low-molecular-weight inhibitor of plasminogen activator inhibitor type 1 by site-directed mutagenesis. *Biochemistry* **37**, 1227-34.

Brünger, A. T. (1993). *X-PLOR Version 3.1: A System for X-ray Crystallography and NMR*, Yale University Press, New Haven, CT, USA.

Brünger, A. T., Adams, P. D., Clore, G. M., DeLano, W. L., Gros, P., Grosse-Kunstleve, R. W., Jiang, J. S., Kuszewski, J., Nilges, M., Pannu, N. S., Read, R. J., Rice, L. M.,

Simonson, T. & Warren, G. L. (1998). Crystallography & NMR system: A new software suite for macromolecular structure determination. *Acta Crystallographica* **D54**, 905-21.

Burzlaff, H. & Zimmermann, H. (1985). On the metrical properties of lattices. *Zeitschrift für Kristallographie* 170, 247-62.

Carrell, R. W., Evans, D. L. & Stein, P. E. (1991). Mobile reactive centre of serpins and the control of thrombosis. *Nature* **353**, 576-8.

Carrell, R. W. & Stein, P. E. (1996). The biostructural pathology of the serpins: critical function of sheet opening mechanism. *Biological Chemistry Hoppe-Seyler* **377**, 1-17.

Carrell, R. W., Stein, P. E., Fermi, G. & Wardell, M. R. (1994). Biological implications of a 3 Å structure of dimeric antithrombin. *Structure* **2**, 257-70.

Declerck, P. J., De Mol, M., Alessi, M. C., Baudner, S., Paques, E. P., Preissner, K. T., Muller-Berghaus, G. & Collen, D. (1988). Purification and characterization of a plasminogen activator inhibitor 1 binding protein from human plasma. Identification as a multimeric form of S protein (vitronectin). *Journal of Biological Chemistry* **263**, 15454-61.

Deng, G., Curriden, S. A., Wang, S., Rosenberg, S. & Loskutoff, D. J. (1996). Is plasminogen activator inhibitor-1 the molecular switch that governs urokinase receptor-mediated cell adhesion and release? *Journal of Cell Biology* **134**, 1563-71.

Eldering, E., Verpy, E., Roem, D., Meo, T. & Tosi, M. (1995). COOH-terminal substitutions in the serpin C1 inhibitor that cause loop overinsertion and subsequent multimerization. *Journal of Biological Chemistry* **270**, 2579-87.

Elliott, P. R., Abrahams, J. P. & Lomas, D. A. (1998). Wild-type alpha 1-antitrypsin is in the canonical inhibitory conformation. *Journal of Molecular Biology* **275**, 419-25.

Elliott, P. R., Lomas, D. A., Carrell, R. W. & Abrahams, J. P. (1996). Inhibitory conformation of the reactive loop of alpha 1-antitrypsin. *Nature Structural Biology* **3**, 676-81.

Howard, A. J., Gilliland, G. L., Finzel, B. C., Poulos, T. L., Ohlendorf, D. H. & R., S. F. (1987). The use of an imaging proportional counter in macromolecular crystallography. *Journal of Applied Crystallography* **20**, 383-7.

Jiang, J. S. & Brünger, A. T. (1994). Protein hydration observed by X-ray diffraction. Solvation properties of penicillopepsin and neuraminidase crystal structures. *Journal of Molecular Biology* **243**, 100-15.

Jones, T. A., Zou, J. Y., Cowan, S. W. & Kjeldgaard, M. (1991). Improved methods for building protein models in electron density maps and the location of errors in these models. *Acta Crystallographica* **A47**, 110-9.

Kraulis, P. J. (1991). MOLSCRIPT: A program to produce both detailed and schematic plots of protein structures. *Journal of Applied Crystallography* **24**, 946-50.

Lawrence, D. A., Berkenpas, M. B., Palaniappan, S. & Ginsburg, D. (1994). Localization of vitronectin binding domain in plasminogen activator inhibitor-1. *Journal of Biological Chemistry* **269**, 15223-8.

Lawrence, D. A., Ginsburg, D., Day, D. E., Berkenpas, M. B., Verhamme, I. M., Kvassman, J. O. & Shore, J. D. (1995). Serpin-protease complexes are trapped as stable acyl-enzyme intermediates. *Journal of Biological Chemistry* **270**, 25309-12.

Lawrence, D. A., Palaniappan, S., Stefansson, S., Olson, S. T., Francis-Chmura, A. M., Shore, J. D. & Ginsburg, D. (1997). Characterization of the binding of different conformational forms of plasminogen activator inhibitor-1 to vitronectin. Implications for the regulation of pericellular proteolysis. *Journal of Biological Chemistry* **272**, 7676-80.

Loebermann, H., Tokuoka, R., Deisenhofer, J. & Huber, R. (1984). Human alpha 1-proteinase inhibitor. Crystal structure analysis of two crystal modifications, molecular model and preliminary analysis of the implications for function. *Journal of Molecular Biology* **177**, 531-57.

Lomas, D. A., Elliott, P. R., Chang, W. S., Wardell, M. R. & Carrell, R. W. (1995). Preparation and characterization of latent alpha 1-antitrypsin. *Journal of Biological Chemistry* **270**, 5282-8.

Lomas, D. A., Evans, D. L., Finch, J. T. & Carrell, R. W. (1992). The mechanism of Z alpha 1-antitrypsin accumulation in the liver. *Nature* **357**, 605-7.

McRee, D. E. (1999). XtalView/Xfit - A versatile program for manipulating atomic coordinates and electron density. *Journal of Structural Biology* **125**, 156-65.

Mottonen, J., Strand, A., Symersky, J., Sweet, R. M., Danley, D. E., Geoghegan, K. F., Gerard, R. D. & Goldsmith, E. J. (1992). Structural basis of latency in plasminogen activator inhibitor-1. *Nature* **355**, 270-3.

Navaza, J. (1994). AMoRe: an automated package for molecular replacement. *Acta Crystallographica* **A50**, 157-63.

Pannu, N. S. & Read, R. J. (1996). Improved structure refinement through maximum likelihood. *Acta Crystallographica* **A52**, 659-668.

Preissner, K. T., May, A. E., Wohn, K. D., Germer, M. & Kanse, S. M. (1997). Molecular crosstalk between adhesion receptors and proteolytic cascades in vascular remodelling. *Thrombosis & Haemostasis* **78**, 88-95.

Schechter, I., & Berger, A. (1967). On the size of the active site in proteases. I. Papain. *Biochemical & Biophysical Research Communications* **27**, 157-62.

Schreuder, H. A., de Boer, B., Dijkema, R., Mulders, J., Theunissen, H. J., Grootenhuis, P. D. & Hol, W. G. (1994). The intact and cleaved human antithrombin III complex as a model for serpin-proteinase interactions. *Nature Structural Biology* **1**, 48-54.

Speck, A. L. (1990) PLATON, an integrated tool for the analysis of the results of a single crystal structure determination. Acta Crystallographica **A46**, C-34.

Stefansson, S. & Lawrence, D. A. (1996). The serpin PAI-1 inhibits cell migration by blocking integrin alpha V beta 3 binding to vitronectin. *Nature* **383**, 441-3.

Stefansson, S., Muhammad, S., Cheng, X. F., Battey, F. D., Strickland, D. K. & Lawrence, D. A. (1998). Plasminogen activator inhibitor-1 contains a cryptic high affinity binding site for the low density lipoprotein receptor-related protein. *Journal of Biological Chemistry* **273**, 6358-66.

Stein, P. E. & Carrell, R. W. (1995). What do dysfunctional serpins tell us about molecular mobility and disease? *Nature Structural Biology* **2**, 96-113.

Tucker, H. M., Mottonen, J., Goldsmith, E. J. & Gerard, R. D. (1995). Engineering of plasminogen activator inhibitor-1 to reduce the rate of latency transition. *Nature Structural Biology* **2**, 442-5.

Vellieux, F. M. D. A. P., Hunt, J. F., Roy, S. & Read, R. J. (1995). DEMON/ANGEL: a suite of programs to carry out density modification. *Journal of Applied Crystallography* **28**, 347-351.

Wei, A., Rubin, H., Cooperman, B. S. & Christianson, D. W. (1994). Crystal structure of an uncleaved serpin reveals the conformation of an inhibitory reactive loop. *Nature Structural Biology* **1**, 251-8.

Wilczynska, M., Fa, M., Ohlsson, P. I. & Ny, T. (1995). The inhibition mechanism of serpins. Evidence that the mobile reactive center loop is cleaved in the native protease-inhibitor complex. *Journal of Biological Chemistry* **270**, 29652-5.

Wiman, B. (1995). Plasminogen activator inhibitor 1 (PAI-1) in plasma: its role in thrombotic disease. *Thrombosis & Haemostasis* **74**, 71-6.

Xue, Y., Björquist, P., Inghardt, T., Linschoten, M., Musil, D., Sjolin, L. & Deinum, J. (1998). Interfering with the inhibitory mechanism of serpins: crystal structure of a complex formed between cleaved plasminogen activator inhibitor type 1 and a reactive-centre loop peptide. *Structure* **6**, 627-36.

Zimmermann, H. & Burzlaff, H. (1985). DELOS – A computer program for the determination of a unique conventional cell. *Zeitschrift für Kristallographie* 170, 241-6.

3.0 The Structure of Active Plasminogen Activator Inhibitor-1

at 2.2 Å Resolution

3.1 Introduction.

Plasminogen Activator Inhibitor-1 (PAI-1) is a primary biological regulator of the

plasmin system of serine proteinases (see Figure 1.1). Plasmin is a serine proteinase that

acts to cleave the protein fibrin in blood clots, as well as cleaving many extracellular

matrix proteins, such as fibronectin and laminin. Plasmin is activated from its zymogen,

plasminogen, by the serine proteinase plasminogen activator (PA). There are two

principal forms of plasminogen activator: tissue plasminogen activator (tPA), the main

form found in plasma, and urokinase plasminogen activator (uPA), found in the

pericellular space of certain cell types. tPA is primarily involved in initiating the

dissolution of fibrin clots in the blood, while uPA controls various tissue remodelling

processes in which plasmin is involved. Both tPA and uPA are regulated by a group of

plasminogen activator inhibitors (PAI's), of which PAI-1 is a primary member (Lijnen *et*

al., 1994; Sprengers & Kluft, 1987).

PAI-1 is a member of the serpin family of serine proteinase inhibitors. This is a

family of large, single domain proteins (~400 amino acids) that inhibit their targets by a

remarkable mechanism (see Figures 1.5, 1.4). The proteins initially fold into a

metastable form, with the proteinase target sequence (the 'reactive centre') exposed on

the surface in a (possibly flexible) loop (Stein *et al.*, 1991; Stein *et al.*, 1990) (see Figure

1.4 a). This reactive centre loop lies above a central five-stranded β-sheet (the A sheet) which has a prominent gap between two of the central strands. The metastable form is known variously as the active, reactive, stressed, or five-stranded form. Serpins inhibit their target enzymes by a suicide-inhibitor mechanism (Wright, 1996; Wright & Scarsdale, 1995). They covalently bind the target, form an extremely stable complex (half-lives are generally measured in days), and when released are inactive as inhibitors. The post-release form is cleaved at the reactive centre, and is considerably more thermally stable than the active form. Crystal structures of cleaved serpins reveal that the N-terminal fragment of the cleaved reactive site loop has twisted at the end closest to the A sheet (the proximal hinge) and has been inserted into the gap in the middle of the sheet, forming a broader and better connected sheet (Loebermann *et al.*, 1984) (Figure 1.4 b). This more stable six-stranded form is known as the cleaved or relaxed form.

PAI-1 is noted for its near unique ability to be transformed into a latent form under physiological conditions. Latent PAI-1 is a stable 6-stranded structure with the uncleaved reactive centre loop inserted into sheet A (Mottonen *et al.*, 1992) (Figure 1.6 c). Active PAI-1 has a half-life of about 2 hours, and the latency transition serves as one of the protein's regulation mechanisms, as the latent molecule is inactive. Active PAI-1 has binding sites for several other molecules, including vitronectin (Declerck *et al.*, 1988), heparin (Ehrlich *et al.*, 1991), and fibrin (Wagner *et al.*, 1989) (Table 1.2). In particular, the interactions with vitronectin have attracted considerable interest (Figure 1.2). Active PAI-1 is stabilized by binding vitronectin (Declerck *et al.*, 1988), and in turn blocks vitronectin's RGD site, a sequence that mediates vitronectin's interactions with αv integrins (Kjoller *et al.*, 1997; Seiffert & Smith, 1997; Stefansson & Lawrence, 1996).

The interaction with vitronectin is disrupted by strand insertion following cleavage or latency so that structural transitions allow PAI-1 to serve as a molecular switch, promoting or inhibiting specific interactions depending on its state (Lawrence *et al.*, 1997). Thus several activities, such as smooth muscle cell migration using vitronectin-integrin interactions, are inhibited temporarily by active PAI-1 (Stefansson & Lawrence, 1996).

PAI-1 is of considerable medical interest. Its role in plasma clot dissolution is of direct relevance to the treatment of myocardial infarctions and strokes. Chronically elevated levels of PAI-1 are associated with atherosclerosis (Bavenholm *et al.*, 1998), myocardial infarctions (Declerck *et al.*, 1994; Juhan-Vague, 1996; Wiman, 1995), eclampsia and preeclampsia (Estelles *et al.*, 1989; Estelles *et al.*, 1998; Wiman *et al.*, 1984), and bacterial sepsis (Philippe *et al.*, 1991; Yamamoto & Loskutoff, 1996). Elevated levels of PAI-1 and tPA have also been associated with insulin resistance syndrome and other forms of obesity, and may be connected to the elevated risk of cardiovascular diseases in obese individuals (Juhan-Vague & Alessi, 1997; Samad & Loskutoff, 1997). Myocardial infarction rates have been shown to be higher in the morning, when PAI-1 concentrations are at their peak (de Bono, 1994). The role of PAI-1 in regulating uPA and vitronectin in the extracellular matrix makes it an important factor in various tissue repair and remodelling processes, such as vascular wound healing (including restenosis after balloon angioplasty) (Preissner *et al.*, 1997; Stefansson *et al.*, 1998), lupus and autoimmune kidney disease (Keeton *et al.*, 1995; Yamamoto *et al.*, 1998), angiogenesis (Moscatelli & Rifkin, 1988), chronic kidney transplant rejection (Tang *et al.*, 1998), the metastasis of certain cancers (Gandolfo *et al.*, 1996; Look &

Foekens, 1999; Pappot *et al.*, 1995; Stephens *et al.*, 1998), ovulation (Ohlsson *et al.*,

1991), and inflammation (Podor *et al.*, 1992; Seiffert *et al.*, 1990).

Because of its medical significance, PAI-1 is considered to be an important target

for drug design. In particular, inhibitors of its activity are likely to be useful drugs in the

treatment of cardiovascular diseases, as removing the inhibition of tPA ought to favor the

dissolution of blood clots. Anti-PAI-1 antibodies have been shown to have this effect in

laboratory animals (Levi *et al.*, 1992)(Abrahamsson *et al.*, 1996; Biemond *et al.*, 1995).

Tumor metastasis is also associated with excess PAI-1 activity. Inhibitory peptides

known to insert in the A sheet have been proposed as lead compounds for drug

development (Xue *et al.*, 1998). Alternatively, two small molecule compounds have been

reported in the literature as possible PAI-1 inhibitors (Figure 3.1). Astra-Hässle has

reported the development of the compound AR-H029953XX (ARH0), with a K_i of 25

μM and an IC_{50} value of 12 μM, from a known fibrinolysis enhancer, anthranilic acid, via

the intermediate compound flufenamic acid (Björquist *et al.*, 1998). Antibody binding

studies suggest that this compound binds to PAI-1 around residues 128 to 145 (helix F),

while mutational studies point to the involvement of residues Arg 76 and Arg 118. A

region near the fibrin and vitronectin binding sites is thus indicated as the inhibitor

binding site. The mechanism by which ARH0 inhibits the activity of PAI-1 is unclear.

Björquist *et al.* (1998) state that ARH0 does not turn PAI-1 into a proteinase substrate, as

occurs with the peptide inhibitors, but those authors do not propose an alternative theory.

The other small molecule inhibitor, XR5118, (XR51), with an IC_{50} of 3.5 μmol/L, has

been developed by Xenova from a *Streptomyces* diketopiperazine

a)

b)
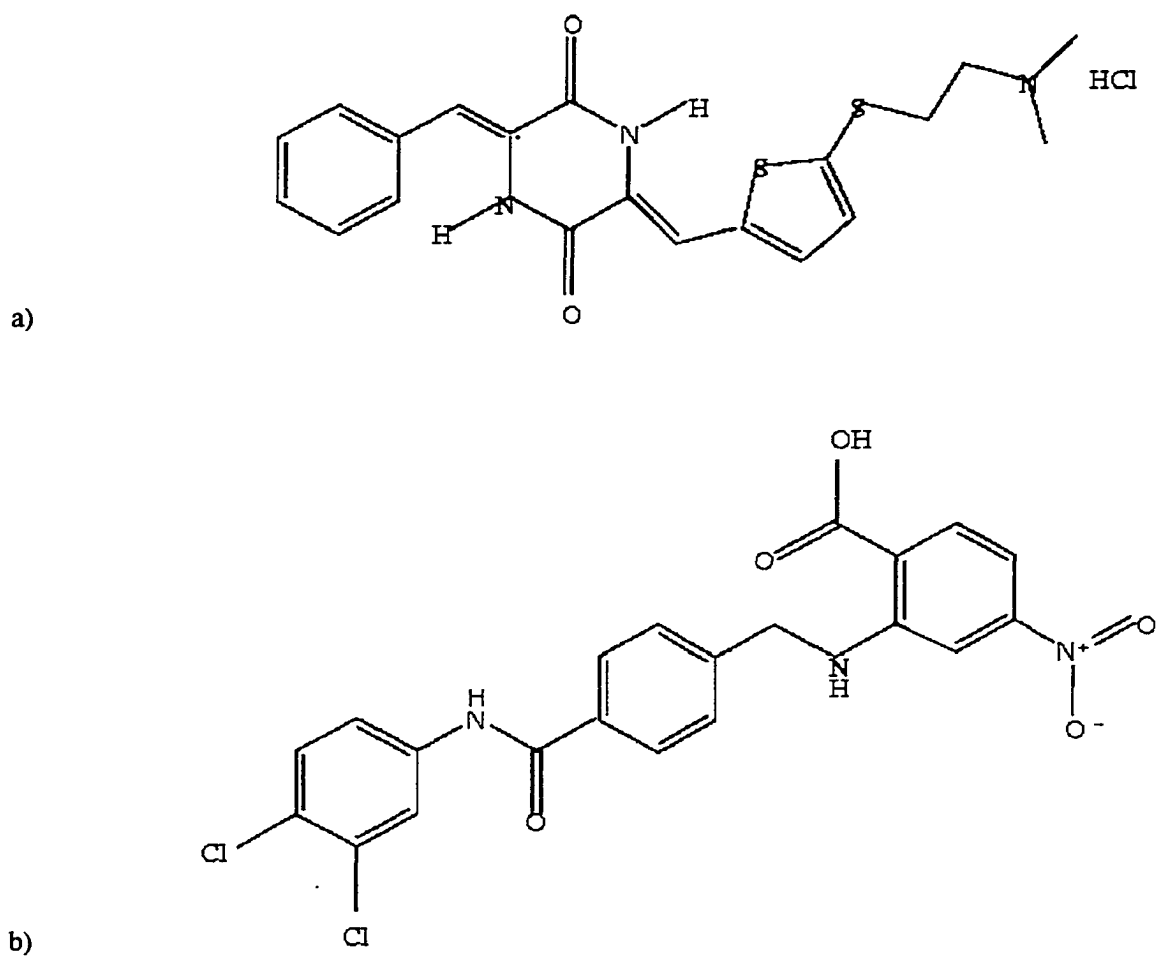
Figure 3.1: Small molecule inhibitors of PAI-1 activity. a) XR5118 (XR51). From

Freiderich *et al.* (1997) b) AR-H029953XX (ARH0). From Björquist *et al.* (1998)

product (Barnes *et al.*, 1996; Friederich *et al.*, 1997). It has been shown to disrupt antibody binding in the same location as ARH0, but its binding location has not been further defined. No work has been reported on its mechanism of action, but it has been shown to attenuate thrombus growth *in vivo*.

Considerable structural work has been done on PAI-1 (Table 1.1; Figure 1.6). It was the first serpin to be solved in the latent form (Mottonen *et al.*, 1992). Subsequently, a mutant that behaves as a substrate, not an inhibitor (A335P) was solved in the cleaved form (Aertgeerts *et al.*, 1995). Recently, a similar mutant (A335E) has been crystallized with two inhibitory pentapeptides inserted in the A sheet (Xue *et al.*, 1998). The active form was long considered to be uncrystallizable, due to its rapid conversion to the latent form. Investigation of the latency transition via random mutagenesis (Berkenpas *et al.*, 1995) led to the discovery of a quadruple mutant, clone 14-1B (N150H, K154T, Q319L, M354I) with the half-life of the active form increased from 2.0 hours at 37° C to 145.4 hours (Figure 1.3). This mutant proved to be sufficiently stable for crystallization at room temperature, and a crystal structure at 3.0 Å resolution was determined (Sharp *et al.*, 1999). This structure was adequate to explain the effects of the stabilizing mutations, to study changes at the vitronectin binding site, to demonstrate a possible mechanism for serpin polymerization, to demonstrate the flexibility of the reactive site loop, and to comment on some theories of the latency mechanism. However, its low resolution hindered making definite conclusions about many points.

In the present study, synchrotron radiation has been used to extend the resolution of the active form structure to 2.2 Å. This allows the examination of the structure to be done in greater detail with greater confidence. Significant differences have emerged

between different monomers in the asymmetric unit, and superior comparisons can be made with other forms of PAI-1. In addition, molecular docking experiments have been conducted with the small-molecule inhibitors, ARH0 and XR51, in order to explore possible modes of binding.

3.2 Methods

3.2.1 Data Collection and Reduction

Crystallization was carried out as reported previously (Sharp *et al.*, 1999). A data set was collected on BL-12B at the National Synchrotron Light Source in Brookhaven, New York, on a single crystal frozen in 25% glycerol as described previously (Sharp *et al.*, 1999). Data collection statistics are summarized in Table 3.1. Data were reduced and integrated using Denzo and Scalepack (Otwinowski & Minor, 1997). Weak diffraction could be detected to 1.95 Å in some directions, but diffraction was highly anisotropic. Test refinements in CNS (Brünger *et al.*, 1998) indicated that the R-factor and free R of the data to 2.5 Å could be improved by including the data up to 2.2 Å. This was therefore used as the limit of the useful data. Reflections considered by the Outliar program (Read, 1999) to have a statistically unlikely intensity were eliminated. A test data set for cross-validation of the refinement was selected consisting of 3410 reflections in 11 thin shells. As with the low-resolution data set, the program PLATON (Speck, 1990) was used to perform LePage and Delauney reduction (Zimmerman & Burzlaff, 1985, Burzlaff & Zimmermann, 1985) analyses of the data. No higher order symmetry could be detected.

Table 3.1: Summary of Crystallographic Data

Space Group	P1
Unit Cell Dimensions:	
a, b, c (Å)	65.25, 74.77, 103.30
α, β, γ (°)	90.90, 93.41, 115.89
Resolution Limits	67.2-2.2 Å
Total Number of Observations	285171
Number of Unique Reflections	84608
Number of Test Set Reflections	3410
Completeness of Data:	
Overall (%)	94.8
2.28-2.20 Å (%)	80.9
R_{merge}* :	
overall	0.165
2.28-2.20 Å	0.850
Number of Non-hydrogen Protein Atoms	11668
Number of Solvent Atoms (waters)	695
Mean B** of protein atoms	27.70 Å²
Mean B** of solvent atoms	31.51 Å²
R-factor†	0.228
R_{free}‡	0.27
RMS Deviations From Ideal Geometry:	
Bond Lengths (Å)	0.008
Bond Angles (°)	1.5
Dihedral Angles (°)	23.0
Improper Angles (°)	0.80

* $R_{merge} = \Sigma_{(i)} (|I_i - <I_i>|/\Sigma(I_i))$ where I_i = an individual observation and $<I_i>$ is the averaged observation for a given Miller index.

** $B=8\pi^2<u^2>$ where u is the amplitude of atomic vibration in any particular direction for a given atom.

† R-factor = $\Sigma_{(i)} (||F_{obs(h_i)}|-k|F_{c(h_i)}||/ \Sigma_{(i)}|F_{obs(h_i)}|)$ where h_i = an individual Miller index in the working set, F_{obs} = observed reflection, F_c = calculated reflection, k = scaling factor.

‡ R_{free} is calculated using the same equations as R-factor, but h_i = an individual Miller index in the test set.

3.2.2 Structure Refinement

Seven rounds of model inspection, rebuilding, refinement, and density modification were carried out. The structure was inspected and rebuilt using the XtalView package (McRee, 1999). Refinement was undertaken with CNS (Brünger *et al.*, 1998), using the mli (maximum-likelihood intensity-based) target (Pannu & Read, 1996), and bulk solvent corrections (Jiang & Brünger, 1994). Solvent-flattened and averaged maps were prepared using the DEMON/ANGEL program package (Vellieux *et al.*, 1995). As with the low resolution structure, the model was originally 4-fold restrained during refinement and the map 4-fold averaged during density modification, except where electron density or packing constraints had shown this to be unjustified. At the N-termini and the reactive site loops, where deviations could be seen between molecules A/C and B/D, only two-fold averaging and restraints were applied. (As discussed below, the two pairs of molecules are related by pseudo-crystallographic symmetry.) As refinement progressed, it became obvious that other segments were deviating from the imposed 4-fold symmetry, and these were also treated as being only two-fold symmetrical. By the final round of refinement the two-fold averaged segments included residues 4-11, 104-110, 130, 150, 159, 213-221, 240-270, and 330-352. There were also found to be sufficient differences between A/C and B/D in general that it was salutary to the refinement to weaken the four-fold restraints. Two-fold restraints were added to the weakly four-fold restrained regions, to maintain the overall level of NCS restraint. Relaxing the four fold symmetry produced improvements in the R-factor, as well as somewhat smaller improvements in the R_{free}. The final restraint weights (Table 3.2) were chosen to leave the difference between the R-factor and R_{free} to be less than 0.05. Individual temperature factors were refined for

Table 3.2: NCS restraint weights in the final round of refinement.

Units are in kcal/mole(Å)^2

Segment	4-fold restraint weight	2-fold restraint weight
4 to 11	0	300
12 to 103	50	250
104 to 110	0	300
111 to 129	50	250
130	0	300
131 to 149	50	250
150	0	300
151 to 158	50	250
159	0	300
160 to 212	50	250
213 to 221	0	300
222 to 239	50	250
240 to 270	0	300
271 to 311	50	250
312	0	300
313 to 329	50	250
330 to 333 (A/C) 330 to 332 (B/D)	0	300
340 to 352	0	300
353 to 379	50	250

all atoms, with the standard CNS restraints between bonded atoms. Solvent atoms were added with the CNS and XtalView water picking functions (Kleywegt & Brünger, 1996; McRee, 1999). Visual inspection ensured that all waters were well defined in the electron density and made hydrogen bonds (< 3.0 Å) to polar groups.

3.2.3 Docking

The DockVision package (Hart *et al.*, 1997; Hart & Read, 1992) was used to dock the small-molecule inhibitor ligands ARH0 and XR51 to PAI-1. This program package uses a Monte-Carlo algorithm to search for energetically favorable interactions between a rigid target and a flexible ligand. The energies are assessed against a pair-wise energy function that accounts for electrostatic and van der Waals interactions. An internal energy function for the ligand, including van der Waals and torsional terms, can also be included. No explicit solvent effects are included in the energy function. While docking results have been obtained that correspond well to known structures, the calculated energies do not correspond to experimentally determined binding affinities.

Docking was performed against both the A and B molecules, as preliminary results suggested that differences in their structures might have significant effects on the calculated energies. The Xue *et al.* (1998) structure of peptide-inhibited PAI-1 was used as a negative control, as the compounds do not bind to 6-stranded conformations. Models of the inhibitor ligands XR51 and ARH0 were built and minimized with the Molecular Simulations Corporation programs InsightII and Discover (Biosym, 1993a; Biosym, 1993b) (Figure 3.2). DockVision topology files were generated, and edited to allow rotation around bonds that seemed likely to be flexible based on analyses of similar moieties in the Cambridge Structural Database (Allen & Kennard, 1993). In XR51 these
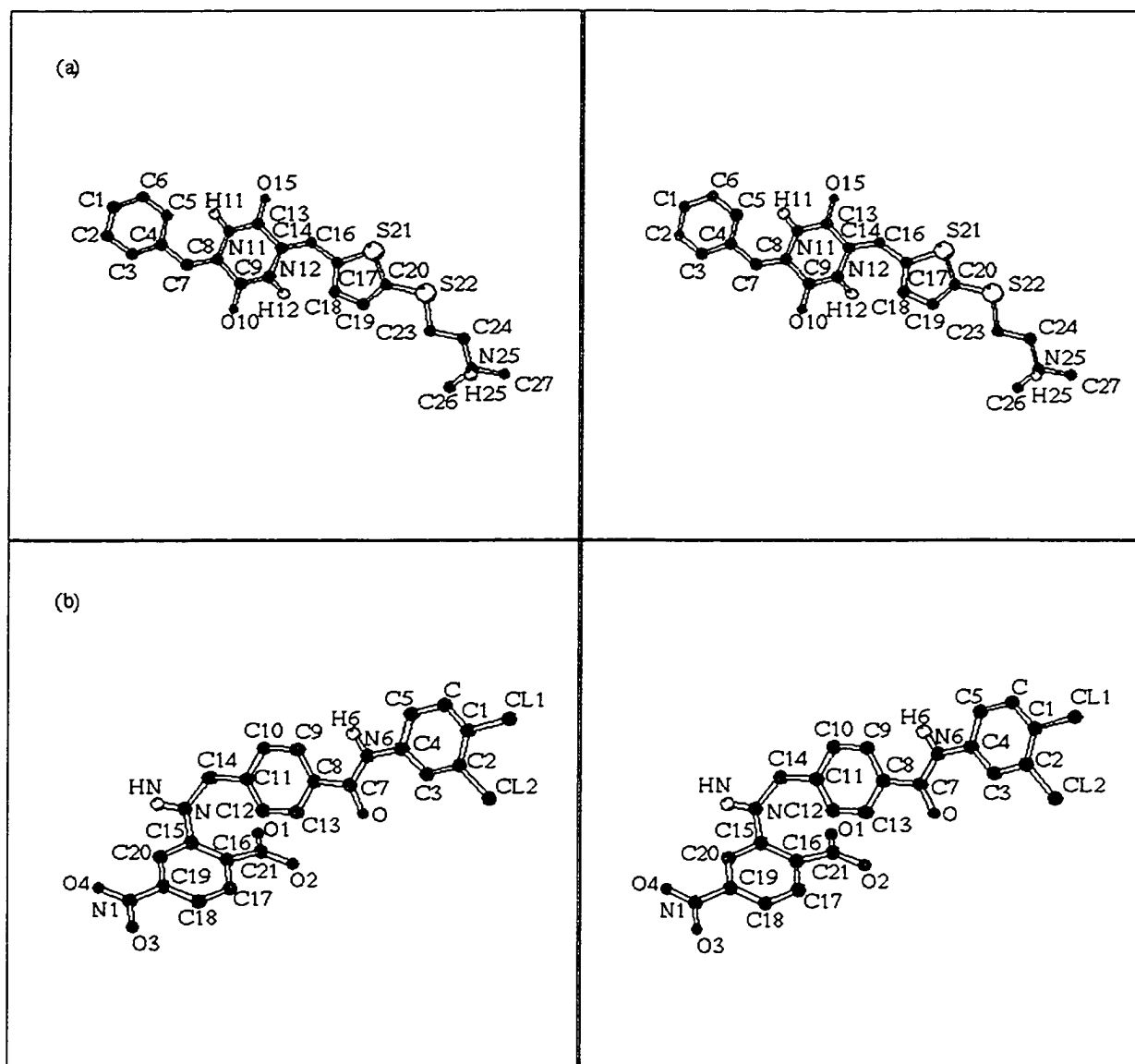
Figure 3.2: Models of Inhibitors. Model of XR51 at top and of ARH0 at bottom. The atom labelling scheme is indicated. Models were built using InsightII (Biosym, 1993b) and minimized in Discover (Biosym, 1993a). Prepared using Molscript (Kraulis, 1991).

were the bonds C4–C7, C16–C17, C20–S22, S22–C23, C23–C24, and C24–N25, while

in ARH0 these were the bonds C4–N6, C7–C8, C11–C14, and C14–N. One hundred

random conformers of each molecule were generated for flexible docking trials. Polar

hydrogens were added to the protein molecules with the DockVision program Hydroman,

then optimized using the program Network (Bass *et al.*, 1992).

Preliminary tests with the centre of each ligand constrained to be within 20 Å of

Arg 118 Cα, one of the residues believed to influence the ARH0 binding site, indicated

that a deep pocket between residues Ser 119 and Tyr 79 gave the lowest energy refined

dockings for both ligands. Therefore, in the definitive docking runs, a constraint sphere

of 10 Å radius centered on the midpoint between Ser 119 Oγ and Tyr 79 Cγ was used.

Trials were done with and without the conformational energy of the ligand being

included in the energy calculation. Five thousand trials were done in each run, with a

fraction of the lowest energy outputs being saved and run through the cluster algorithm to

eliminate near duplicates that deviate from each other by less than 2 Å rms. The lowest

energy representatives of the 10 lowest energy clusters were refined and visually

inspected.

3.3 Results

3.3.1   Final Structure

The final structure consists of residues 4 to 333 and 340 to 379 in molecules A and

C, and residues 4 to 332 and 348 to 379 in molecules B and D. 695 water molecules are

also included. The final R-factor is 0.228, with a free-R of 0.278. The PROCHECK

(Laskowski *et al.*, 1993) Ramachandran plot shows no non-glycine residues in forbidden

regions and only one (Ala B 96) on the edge of the generously allowed regions (Figure 3.3). The PROCHECK main chain and side chain parameters are all either better than or inside the preferred limits. The PROVE Z-score average and RMS are also within the preferred limits, indicating that the atomic packing densities are reasonable (Pontius *et al.*, 1996). The WHATIF package of verification programs detects no global difficulties with the structure (Vriend, 1990). The main-chain electron density is clear and unambiguous (Figure 3.4) for most of the structure, with the only problem regions being in the sequences at the molecular N-termini, at the ends of the uncompleted reactive centre loops and in the centre of turn thI1s5A (residues 310 to 315, see Figure 1.3). The relatively poor quality of the density in these regions is reflected in their high temperature factors. The N-termini and the ends of the reactive site loops were built as far as sterically reasonable residues could be placed in the electron density (Figure 3.4b). While some electron density can be seen for the missing residues in these regions, they could not be built with reasonable geometry or did not retain reasonable geometry during refinement. There is electron density for the 310 to 315 region (turn thI1s5A), but it remained ambiguous during the refinement process, and the backbone conformations of its residues frequently took sterically unlikely conformations. The final structure of this turn is sterically reasonable, with a fair fit to the electron density, and is stable during refinement, but it cannot be considered to be an unambiguous model of this region of the molecule.

Figure 3.3: Ramachandran Plot for final PAI-1 model. Adapted from PROCHECK

(Laskowski *et al.*, 1993).

Ramachandran Plot

Plot statistics

Residues in most favoured regions [A,B,L]	1152	89.2%
Residues in additional allowed regions [a,b,l,p]	139	10.8%
Residues in generously allowed regions [~a,~b,~l,~p]	1	0.1%
Residues in disallowed regions	0	0.0%
	---	---
Number of non-glycine and non-proline residues	1292	100.0%
Number of end-residues (excl. Gly and Pro)	6	
Number of glycine residues (shown as triangles)	80	
Number of proline residues	84	

Total number of residues	1462	

Based on an analysis of 118 structures of resolution of at least 2.0 Angstroms
and R-factor no greater than 20%, a good quality model would be expected
to have over 90% in the most favoured regions.

Figure 3.4: Samples of Electron Density: a) The Gate loop b) the N-terminus of the

Reactive Centre loop. Figures show electron density ≤ 1.6 Å from atoms at the 1σ level.

Prepared using BobScript (Esnouf,1997).
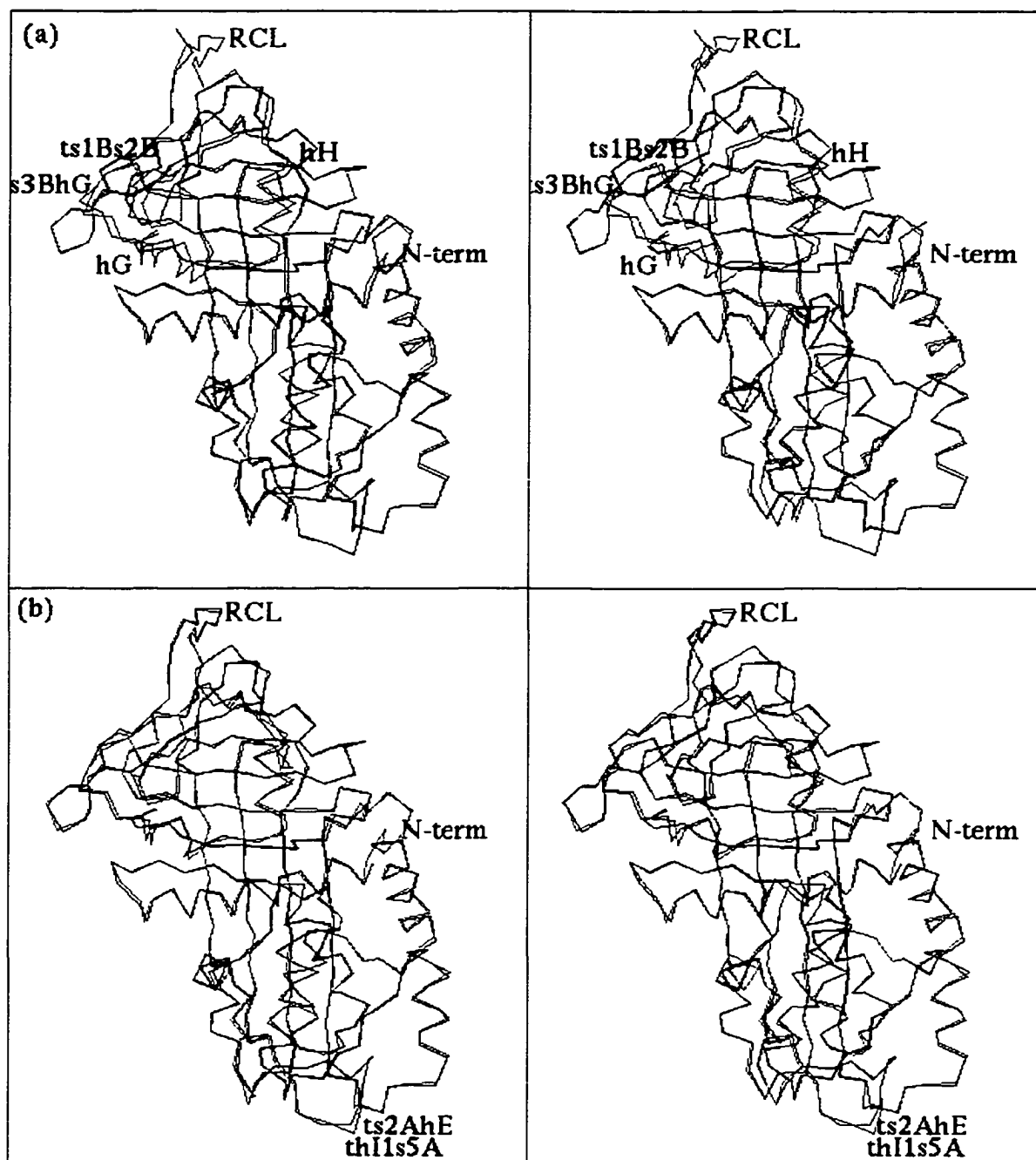
Figure 3.5: Cα traces of the new (2.2 Å) PAI-1 structure a) the new molecule A (red)

versus the new molecule B (blue); b) the new molecule A (red) versus the old (3.0 Å)

molecule A (blue). This figure was produced using Molscript (Kraulis, 1991).

3.3.2   Differences between the low and high resolution structures

The high resolution structure differs from the previous low resolution structure in five ways (Figure 3.5 b):

1)   The protein has been solvated with 695 waters.

2)   Three residues have been added onto the N-termini of all the molecules.

3)   The apparent density for residues 334 to 339 in molecules A and C seen in the low resolution structure was not clear in the high-resolution structure, and these residues were deleted. In addition, the ends of the reactive site loops in both A/C and B/D differ slightly between the two models. The latter will be discussed in section 3.3.5.

4)   As noted in the Methods section, several regions in the high-resolution model needed to be released from the 4-fold restraints imposed on the low-resolution model. The effects of this will be discussed in section 3.3.3.

5)   Residues 101 to 103 (turn ts2AhE) and 310 to 315 (turn thI1s5A) differ between the low and high resolution structures in the same way in all 4 molecules. These will be discussed in section 3.3.4, along with other regions that vary among different forms of PAI-1.

3.3.3 Differences between the A/C and B/D molecules

In the low resolution structure of PAI-1 it was concluded that, outside of the reactive site loop and the N-terminus, the four molecules in the asymmetric unit were essentially identical (Sharp *et al.*, 1999). Higher resolution allows us to define regions of significant conformational differences among the molecules. Molecules A and B, and C

and D form two pairs of improper dimers that are related to each other by a two fold screw operation that superimposes molecules A and C and molecules B and D. This gives the unit cell a pseudo-C2 symmetry. The core residues of all four molecules are the same, and the pseudo-symmetry-related pairs of molecules are still essentially identical, with none of the Cα positions deviating by more than 1 Å between A and C or B and D (Figure 3.6). There are only four areas where there are differences in Cα positions greater than 1 Å between the A/C and the B/D molecules : the N-terminus (residues 4 to 5), turn ts1Bs2B (215 to 220), turn ts3BhG and helices G and H (240 to 265), and the visible portion of the reactive site loop (348 to 349). The changes in these regions are summarized in Table 3.3 and can be seen in Figure 3.5 a. All of these differences are associated with regions where the two pairs of molecules make different crystal packing contacts (summarized in Table 3.3), and they suggest significant flexibility for these surface regions in solution. The regions from residues 215 to 220 and 240 to 265 form part of the 'gate' region, into which strand 1C inserts in the latency transition (Figure 3.7). The possible significance of this is discussed in section 3.3.6. The changes in this region involve the reorganization of several bulky hydrophobic residues.

As noted in the low-resolution structure, the reactive site loops (residues 330 to 349) have different conformations in the A/C and B/D molecules. In the A and C molecules the loop has extensive contacts with the 2-fold symmetry related molecule, including an antiparallel β-sheet interaction from residues 340 to 347. Residues 334 to 339 are invisible and presumably highly flexible. In the B and D molecules the reactive site loop has no crystal contacts; it is poorly ordered and residues 333 to 347 are

Figure 3.6: Cα distance plot for the active molecules. Distances (y-axis) are in Angstroms, sequence (x-axis) is for the mature protein. The molecules were superimposed using all mainchain atoms and the program Suppos.

10.0

9.0

8.0

7.0

6.0

5.0

4.0

3.0

2.0

1.0

0.0

1
41
81
121
161
201
241
281
321
361

——— A vs. B

·········· A vs. C
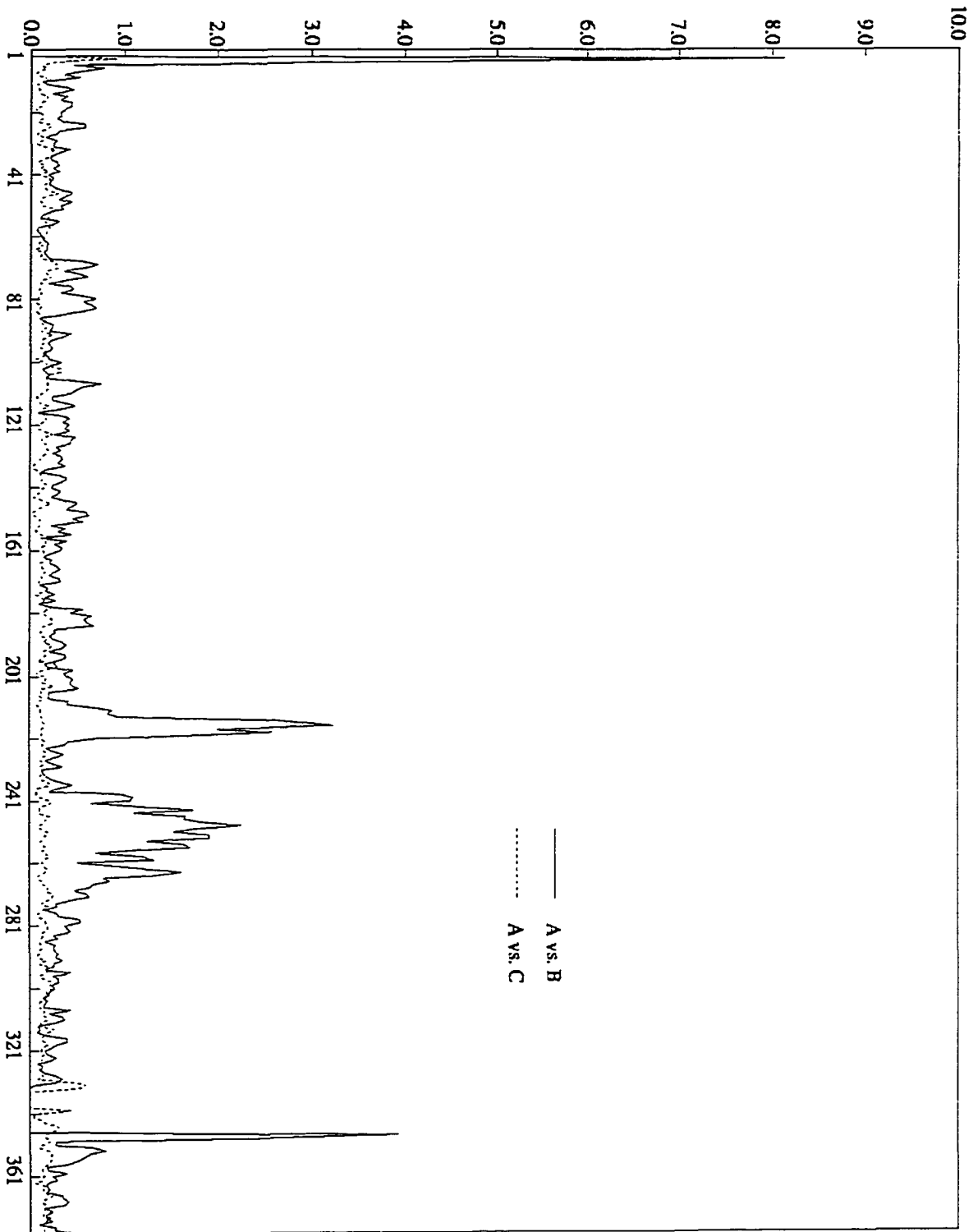
Table 3.3 Regions of active molecule B and molecule A that differ by > 1.0 Å.

Based on superpositions using the program Suppos from the Groningen Biomol

package. Regions that are not observed in the reactive site loop are indicated with

brackets.

Region	Residues	Notes
N-terminal	4-5	Different hydrogen bonds in a labile region
s1B and ts1Bs2B	215-220	Surface loop, strongly influenced by crystal contacts in A, some contacts also present in B, related to changes in the 240-274 region.
ts3BhG, hG, hH, thHs2C, s2C	240-241, 243-257, 259-260, 263-265	Affected by crystal contacts in A. (Includes Aertgeert's loop 2 (Aertgeerts *et al.*, 1995))
Reactive Centre Loop	(333-347) 348-349	Apparently disordered in B molecule, influenced by crystal contacts in A.
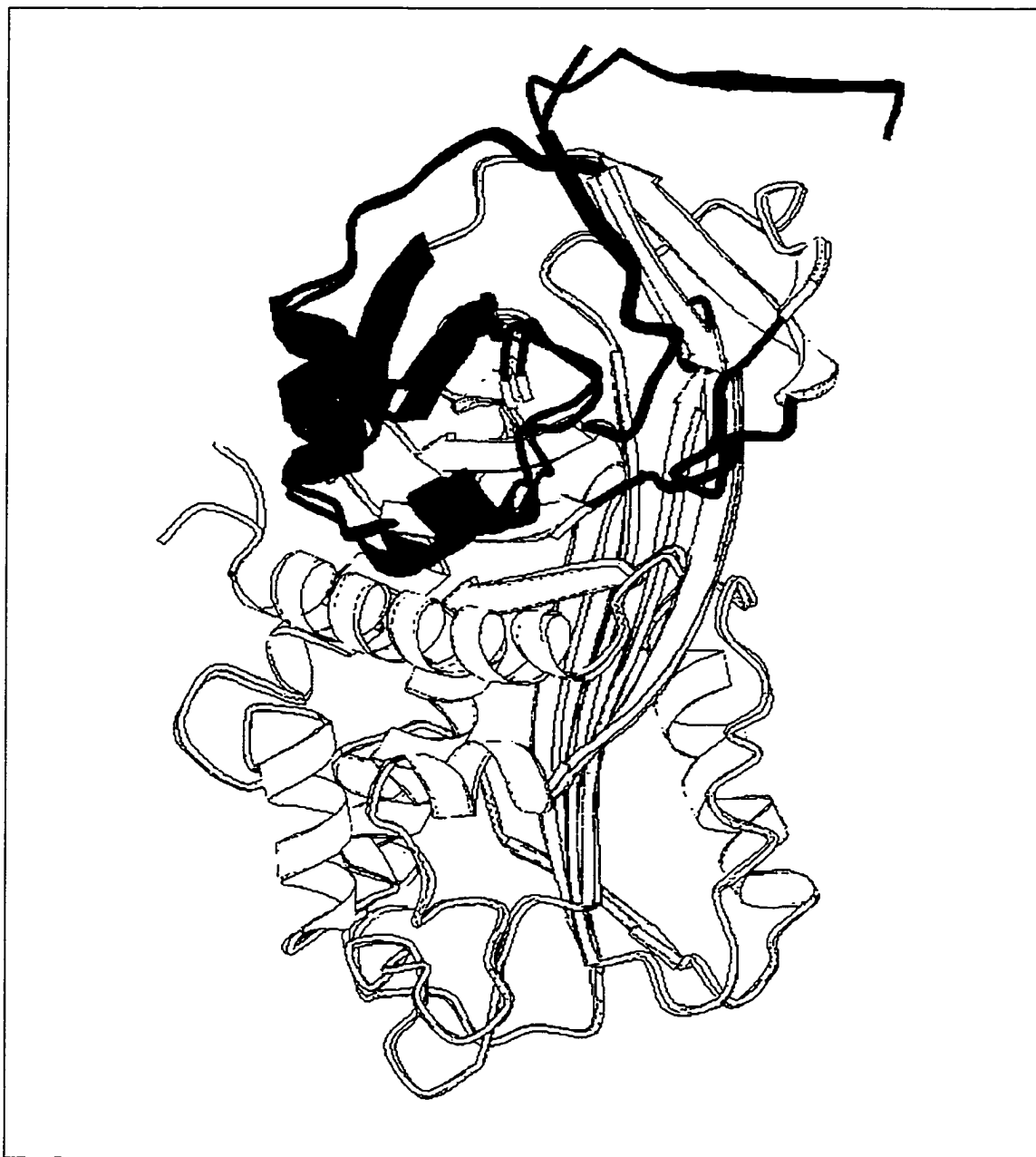
Figure 3.7: Differences between molecules A/B and C/D in the region of ts1Bs2B, ts3BhG, hG, and hH. The molecules are shown as two schematic mainchain traces, with the A sheet shown in yellow, the RCL in red, the gate loop in blue, and the C-terminus in magenta. The variable segments are coloured green in molecule A, and cyan in molecule B. This figure was produced using the Molscript program (Kraulis, 1991).

invisible. This indicates that the reactive site loop is highly flexible in the active form of the molecule.

3.3.4 Differences between the Active and the Latent, Cleaved, and Peptide-Inhibited Structures

Structures of PAI-1 are now available for the active, latent (Mottonen *et al.*, 1992), and cleaved states (Aertgeerts *et al.*, 1995), and for the cleaved state with inhibitor peptides bound (Xue *et al.*, 1998). Several large structural changes are evident during loop insertion, similar to those inferred from other serpin structures. These occur in the reactive site loop (residues 331 to 356), and the regions described by Stein and Chothia as fragment 2 (90 to 100 and 123 to 175) and the flexible joints (63 to 89) (101 to 122) (Stein & Chothia, 1991). In general the changes from the active molecule conformation are similar for the various 6-stranded forms (Table 3.4). The r.m.s.d. values of fragment 1 and fragment 2 are similar in all molecules, as are the rotations and translations of fragment 2 with respect to fragment 1. Several other areas in fragment 1 also show differences greater than 1Å. The changes in these regions are summarized in Table 3.5, and are shown in Figure 3.8.

Some of these differences are due to the crystal contacts of the molecules, including most of the differences in the N-terminus, in helix C, and in the surface segments 211 to 220, and 241 to 270. The N-terminus has been seen only in structures where it is stabilized by crystal contacts; it is possibly disordered in solution. The variability in conformation of segments 211 to 220 and 241 to 270 supports the impression, received from comparing the A and B active molecules, that this area is somewhat labile. In general, the 6-stranded structures are in conformations intermediate between those seen

Table 3.4 R.M.S.D. for fragments 1 and 2, rotation of fragment 2, and

translation of fragment 2 for the 6 stranded forms of PAI-1 versus active

PAI-1 molecule A.

Molecular form	R.M.S.D. of 944 fragment 1 (Å) mainchain atoms from the active form	R.M.S.D. of 268 fragment 2 (Å) mainchain atoms from the active form	Difference of orientation (°) of fragment 2 with respect to fragment 1 from the active form	Translation along rotation axis (Å) of fragment 2 with respect to fragment 1 from the active form
latent	1.81	1.84	4.12	-2.11
cleaved	1.10	1.74	4.81	-1.75
inhibited	1.14	1.69	5.66	-1.60

Table 3.5: Regions of the 6-stranded forms of PAI-1 that differ from active molecule A by > 1.0 Å. Based on superpositions of fragment 1 using the Biomol program Suppos. Regions that are not observed in the reactive site loop are indicated with brackets.

Region	Cleaved PAI–1	Latent PAI–1	Peptide-inhibited PAI-1	Notes
N-terminal	4-7	4-7	4-5	Different crystal contacts in a labile region
thAs6B	29	22, 24-30		Interaction of turn with RCL in latent molecule
hC	47,56			Crystal contacts in cleaved structure
Flexible joint	69-89	69-89	69-89	Hinging region between fragments
Fragment 1	90-100	90-1 00	90-100	Region that is displaced when RCL inserts
Flexible joint	101-122	101–103, 107–108, 110–122	101-122	Hinging region between fragments
Fragment 2	123-146 149-173	123–146 149–174	123-143, 150-174	Region that is displaced when RCL inserts
Gate loop	181-183, 185-186, 192	181–183, 187–198, 204–205	195	Surface loop, changed particularly by latency transition
s1B and ts1Bs2B	215-220	215–220, 229	215-220	Surface loop, influenced by crystal contacts in A, influenced by changes in gate area via the 240-274 region.
ts2Bs3B	229-230, 232	231–233	229-232	Influenced by shift of helix D (flexible joint)
ts3BhG, hG, hH, thHs2C, s2C	243-260, 263-265, 270-271	242–249, 252–257, 259–260, 263–266, 270–274	241, 243-260, 262-266, 268-272	Affected by crystal contacts in A, also by changes in the gate region (includes loop 2)
s6A	281-282, 300-302	277, 281–282, 285–289, 292, 300–301	284-286, 292	Insertion of RCL causes larger shift at C-terminus of this strand than at N-terminus
thI₁s5A, s5A	311-312, 314, 319, 326-327	311–313, 317–322	310-312, 314, 318-321	Insertion of RCL, also structure poorly defined in active molecules
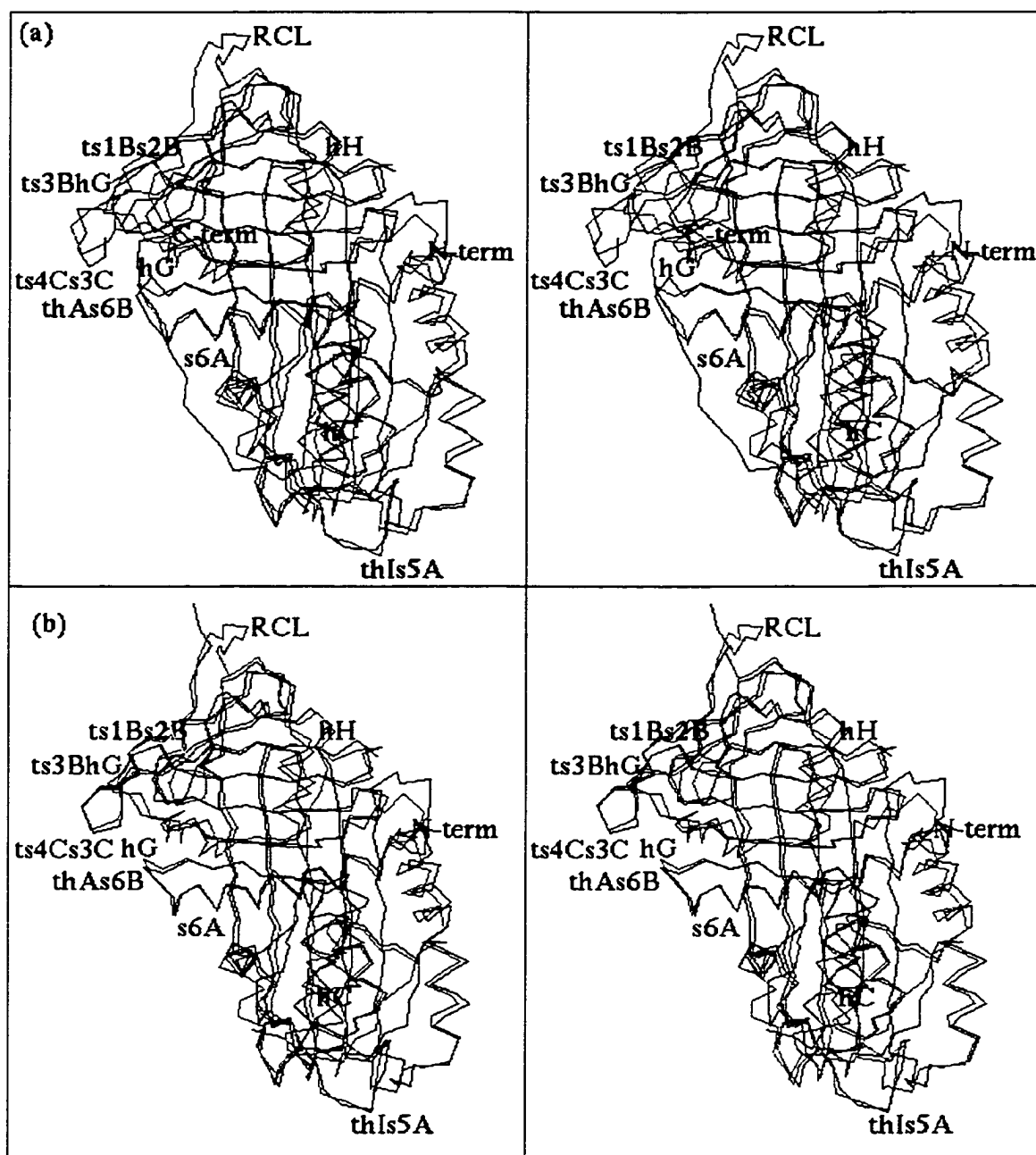
Figure 3.8: Differences between active PAI-1 and other forms. a) Cα traces of latent PAI-1 (blue) and active molecule A (red); b) Cα traces of the cleaved PAI-1 (blue) and active molecule A (red). Regions with significant differences are labeled. This figure was produced using the Molscript program (Kraulis, 1991).

in the active A and B molecules, with a tendency to be more like active molecule B. As in the comparison of the A and B active molecules, several bulky sidechains, including Phe 213, His 219, Tyr 220, Tyr 221, and Tyr 241, have varying conformations, adding to the impression of lability.

Other differences are accommodations of the displacement of the RCL, fragment 2, and the flexible joint regions (Table 3.5). The slightly larger changes seen for residues 277 to 301 and 310 to 322 in comparing fragment 1, are due to the larger degree of opening at the end of the A sheet furthest from the reactive centre and reflect a subtle change in the orientation of the strands of the A sheet. Several regions of structural difference seem to accommodate the change in position of helix D (one of the flexible joints between the fragments) upon RCL insertion. Some of the differences at the N-terminus, as well as the changes in residues 231 to 233 and 365 to 366 may be directly or indirectly influenced by the position of the D helix.

Several segments in the latent structure have unique conformations influenced by the unusual conformation of the RCL in that structure. Residues 27 to 30 are shifted by contact with the RCL, while the conformations of the gate loop, residues 181 to 198, and the C-terminus (residues 377 to 379) seem to be influenced by the latent conformation of the RCL. The conformation of the gate loop in the published latent structure is unique to that form. However, it has been described as 'disordered' (Tucker *et al.*, 1995), so the conformation may not be entirely reliable. The C-terminal residues are also displaced, to occupy a region vacated by the RCL.

While the r.m.s.d. of main chain atoms for fragment 2 is somewhat higher than for fragment 1, this is somewhat misleading. The greater degree of opening in the A sheet of

the active molecule at the end furthest from the start of RCL insertion causes changes in the relative position of the A strands that have a larger effect than they do in fragment 1. There is also a large change in conformation for residues 150 to 157 which, as is explained in Chapter 2, is probably due to mutations in that region rather than to RCL insertion.

3.3.5 Comparison of the reactive site loops in active serpins

As noted for the low resolution structure, the conformation of the reactive site loop in active PAI-1 is different from the conformations observed in other active serpin structures (Figure 3.9). In molecule A, the loop passes over helix F_1, rather than over turn ts3AhF$_1$ as occurs in most serpin molecules. This is probably due largely to crystal packing. The proximal end of the loop in molecule B is virtually identical to that in molecule A, forming a sharply kinked (but not pre-inserted) conformation similar to that seen in active antitrypsin (Elliott et al., 1996). The distal end of the loop in B differs from A in residues 348 (the first discernable residue) to 351, with residues 349 to 351 making intramolecular contacts. This suggests that in the absence of crystal contacts the loop has a different conformation or, since the loop is clearly disordered in molecule B, a different set of conformations. A disordered reactive site loop has also been observed in at least one other serpin structure lacking packing constraints in that area of the molecule (Harrop et al., 1999). The orientation of residues 348 to 351 at the distal end of the loop in molecule B suggests that its loop extends further out from the molecule. Since the density for this fragment of the reactive centre loop is still closer to the position of the
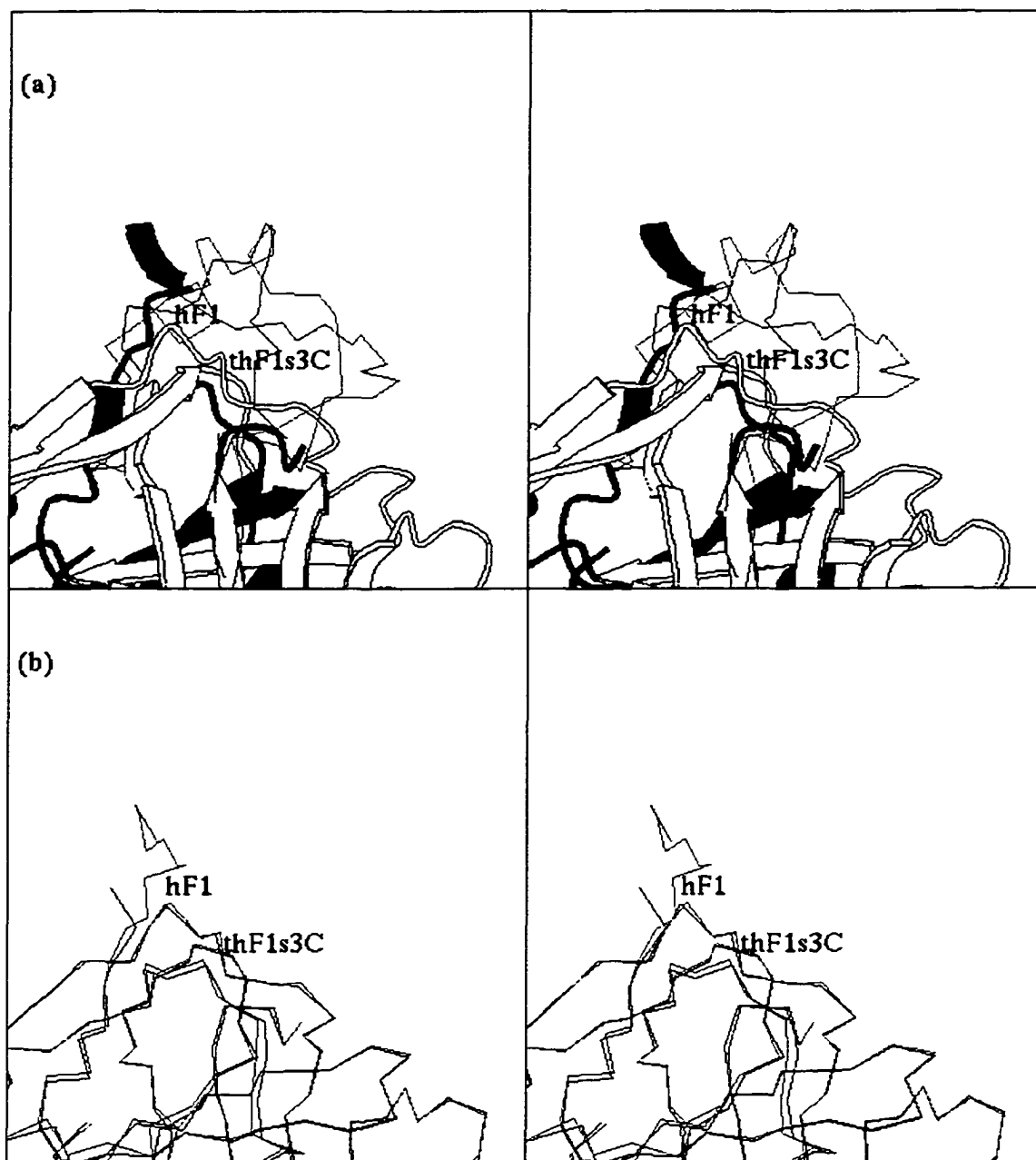
Figure 3.9: The Reactive Centre loop in active PAI-1 and other active serpin molecules.

a) Active PAI-1 molecule A is shown in ribbon form, while α_1-antitrypsin (green), anti-

chymotrypsin (purple), and antithrombin (blue) are shown as $C\alpha$ traces. b) A $C\alpha$ trace of

the active molecule A (red), and molecule B (blue). This figure was produced using the

Molscript program (Kraulis, 1991).

fragment in molecule A than that seen in antithrombin, antitrypsin, antichymotrypsin, or ovalbumin, it may also tend to lie over helix F_1.

3.3.6 The mechanism of the latency transition

The surface loop from residues 170 to 193, called the gate loop (Mottonen *et al.*, 1992) or loop 1 (Aertgeerts *et al.*, 1995), has been proposed to be involved in control of the latency transition. In the latent structure (Mottonen *et al.*, 1992), loop 1 was poorly defined and was considered in a later analysis by the authors to be disordered (Mottonen *et al.*, 1992; Tucker *et al.*, 1995) (Figures 3.10, 3.11). This disorder was proposed to facilitate the migration of the intact reactive site loop for insertion by removing a structural barrier found in other serpins. The disorder was attributed to an unique conformation of the C-terminus, which filled a pocket formed by residues Pro 276, Phe 278, Leu 280, Phe 358 and Pro 379. In other serpin structures this pocket binds residues 203 to 213, stabilizing the neighboring loop 1. The loss of this binding was therefore assumed to disorder loop 1 (Tucker *et al.*, 1995).

Coordinates for loop 1 were presented in the structure of cleaved PAI-1, which showed it somewhat displaced from the apparent position in the latent structure (Aertgeerts *et al.*, 1995). While these residues had poor stereochemistry and their positions were not clearly reliable, the apparent displacement of loop 1 narrowed the gap between loop 1 and residues 242 to 246 ('loop 2') through which the reactive site must pass in the latency transition (Aertgeerts *et al.*, 1995). It was suggested that electrostatic repulsion between charged residues in loop 1 (Arg 186, Arg 187, His 190, and Lys 191) and in the C-
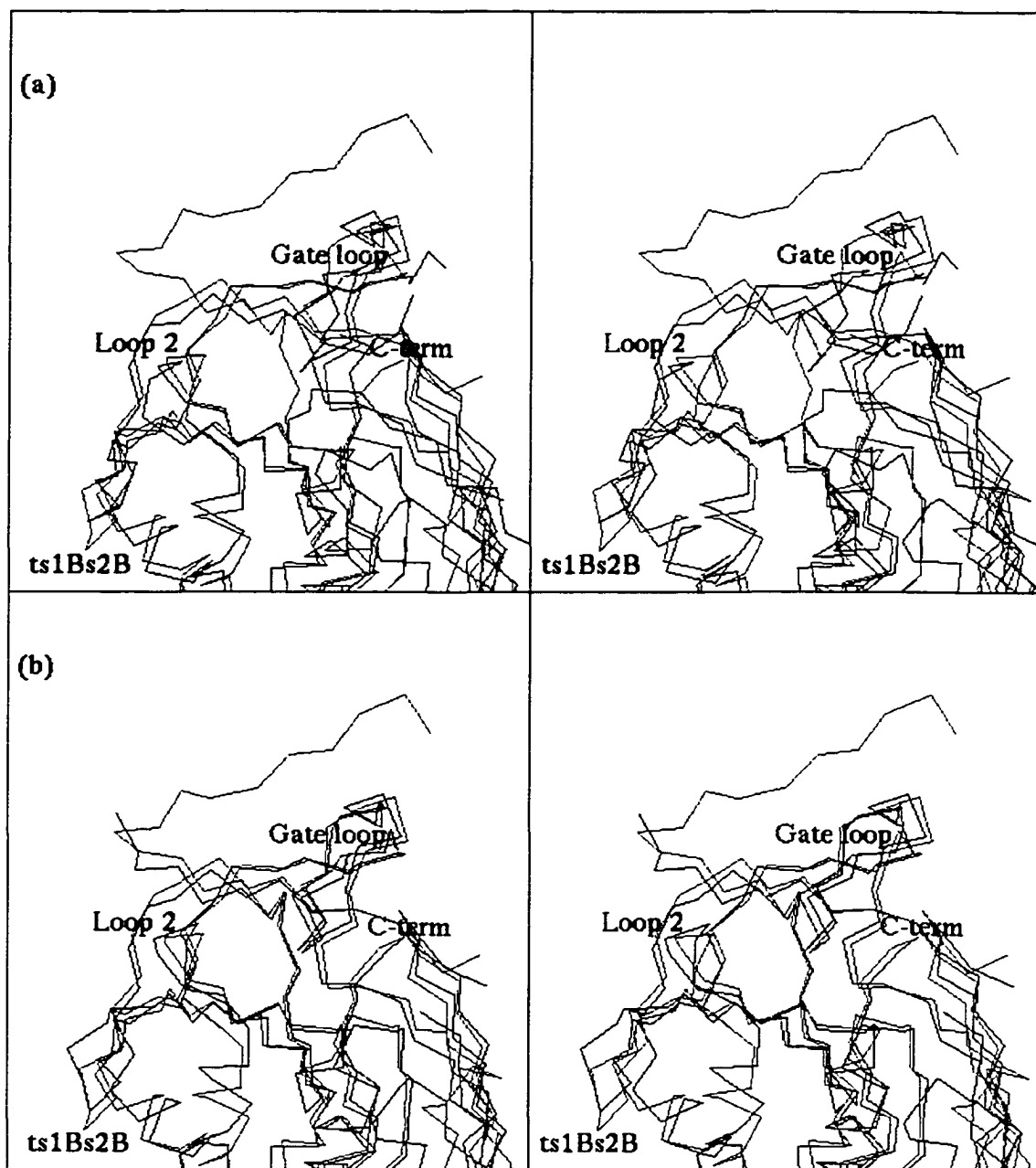
Figure 3.10: The Gate region. Superposition of the PAI-I structures. a) Cα traces are shown of the active molecule A (red) and the latent molecule (blue); b) Cα traces are shown of the active molecule A (red) and the cleaved molecule (blue). This figure was produced using the Molscript program (Kraulis, 1991).
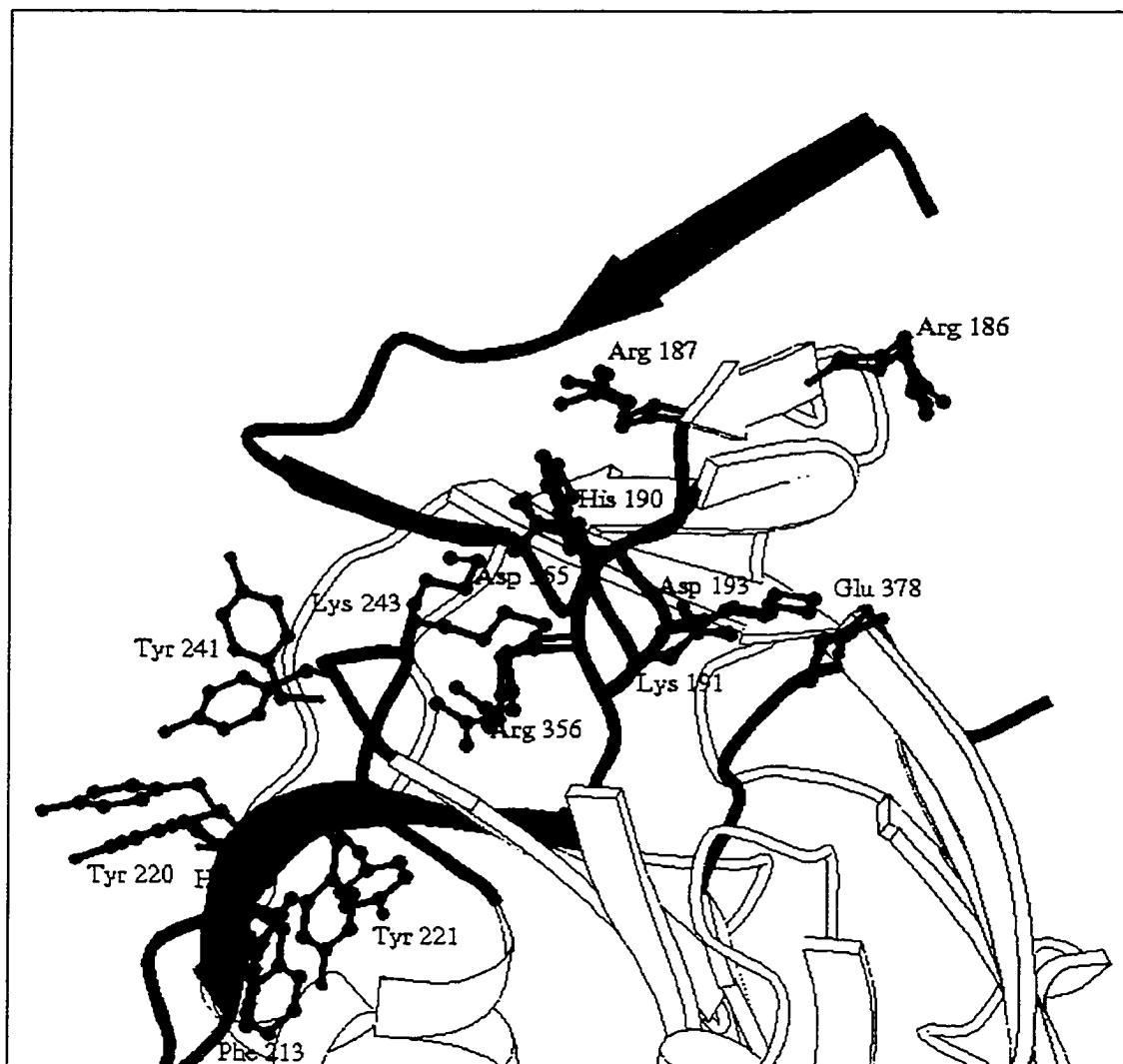
Figure 3.11: The Gate region. The Active molecule, showing the sidechains of residues involved in electrostatic interactions in the gate, or bulky residues in loop 2 or ts1Bs2B that change conformation. The A sheet is coloured yellow, the reactive centre loop is shown in red, the C-terminus in magenta, the "gate loop" or "loop 1" in blue, and "loop 2" in green. Residue orientations in molecule A are shown in red, those in molecule B are shown in blue. This figure was produced using the Molscript program (Kraulis, 1991).

terminal end of the reactive site loop (Asp 355 and Arg 356) might facilitate the latency transition, as loop 1 in PAI-1 has more charged residues than in other serpins (Aertgeerts *et al.*, 1995). Relatively large temperature factors at the end of loop 1 were also observed, which might indicate flexibility. The C-terminus of the cleaved PAI-1 molecule was in the normal position for a serpin. The coordinates deposited at the PDB, however, indicate that the model of this region has been rebuilt considerably subsequent to the original publication, altering the residue conformations on which this conclusion is based. The new coordinates are essentially identical to those reported for the peptide-inhibited cleaved structure (Xue *et al.*, 1998).

At low resolution, all of loop 1 could be clearly observed in the fourfold averaged density of our active quadruple mutant structure (Sharp *et al.*, 1999). The similarity of the conformation in molecules forming different crystal contacts suggested that the contacts were not biasing the structure, although they might be reducing the temperature factors. Relatively high temperature factors were observed for some residues between 181 and 185, especially in the B and D molecules. The C-terminus of the active PAI-1 molecule was seen to be in the ordinary location for a serpin. These facts cast doubt on the role of disorder in these regions as a causative factor in the latency transition, although they do indicate that structural rearrangements probably play a role in the mechanism.

Our high resolution structure confirms most of our previous observations. The positions of the loop 1 residues in all the active molecules are similar, with the largest Cα deviation being 0.83 Å between Ser 182 in molecules A and D. In A and C there are extensive intermolecular interactions involving residues 183 to 187 and additional minor

interactions involving residues 188 and 198. In B and D the only crystal contacts of loop

1 involve residues 181, 182 and 192. The differing contacts do not seem to influence the

conformation of loop 1. The largest variations are seen in residues 193 to 196, which

make few external contacts but which still have clear electron density. In general, there

is no more disorder indicated in this region than in any other surface loop in active PAI-1.

There is therefore no reason to assume from the model of active PAI-1 that this is an

intrinsically disordered loop, as is required by the theory of Tucker *et al.* (1995). In fact,

evidence for loop flexibility playing a role in the latency transition is stronger for loop 2

(residues 242 to 246) of Aertgeerts *et al.* (1995), which lies on the protein surface beside

loop 1. As noted earlier (section 3.3.3), loop 2 is part of a surface that is significantly

different in conformation between the A/C and B/D molecules. If this indicates that this

region is flexible, movement of loop 2 may facilitate the latency transition, in which the

reactive site loop must pass between loops 1 and 2. The degree of positional variation

seen in the solved PAI-1 structures is greater than that seen in similar comparisons of

other serpin molecules, although a certain amount of variability in the C-terminus of the

H helix is not uncommon (Figure 3.12). The conformational differences in several bulky

residues in the area, including Phe 213, His 219, Tyr 220, Tyr 221 and Tyr 241, both in

active and inserted forms of the molecule, contribute to the impression that the region is

labile. As bulky hydrophobic residues are uncommon in serpins at those positions,

except at 213, they may be contributing to the disorder of the region in some fashion,

possibly by favoring several alternative packings. Mutations of Tyr 221 to His or Ser

have been shown to decrease the rate of the latency transition, and to increase the stability

of the protein at pH 6.5 (Sui & Wiman, 1998).

The conformation of loop 1 observed in active PAI-1 is closest among serpins to that seen in active antithrombin, with a r.m.s.d. among the Cα atoms of the loop (residues 170-193 in PAI-1) of 1.50 Å (Figure 3.12), in a whole molecule superposition. In other serpin structures (ovalbumin, antitrypsin, antithrombin, and antichymotrypsin), loop 1 is closer to loop 2, narrowing the gap through which the distal region of the reactive centre loop must pass. Antithrombin is the only other serpin known to undergo the latency transition to a significant degree under non-extreme conditions. The wider gap found in PAI-1 and antithrombin may be allowing the reactive centre loop to pass between loop 1 and 2 more easily, thereby facilitating the latency transition.

The rearrangement of the C-terminus of the molecule is unique to PAI-1, not being seen in the latent form of antithrombin. PAI-1 has a short, though not uniquely short, sequence at the C-terminus, ending at Pro 379, whereas most serpins have more residues following. If this reduces the degree to which the C-terminus is anchored, it may facilitate the latency transition by making the gate region more labile.

With regards to Aertgeerts et al.'s (1995) electrostatic theory, it must first be noted that the positions of the charged residues in the active structure are somewhat different from those in the cleaved structure on which they based their prediction. Moreover, the coordinates deposited in the PDB for cleaved PAI-1 are considerably changed in the gate region, making them very similar to the active structure and the peptide-inhibited structure. Many of the residues forming part of Aertgeerts et al.'s region of positive charge in fact form interactions that should balance the charge somewhat (Figure 3.11). Hence Lys 191 forms clear salt bridges with Glu 378 and Asp193, whereas His 190 forms a salt bridge with Asp 355, which also interacts with Lys 243 in loop 2. Only Arg 186
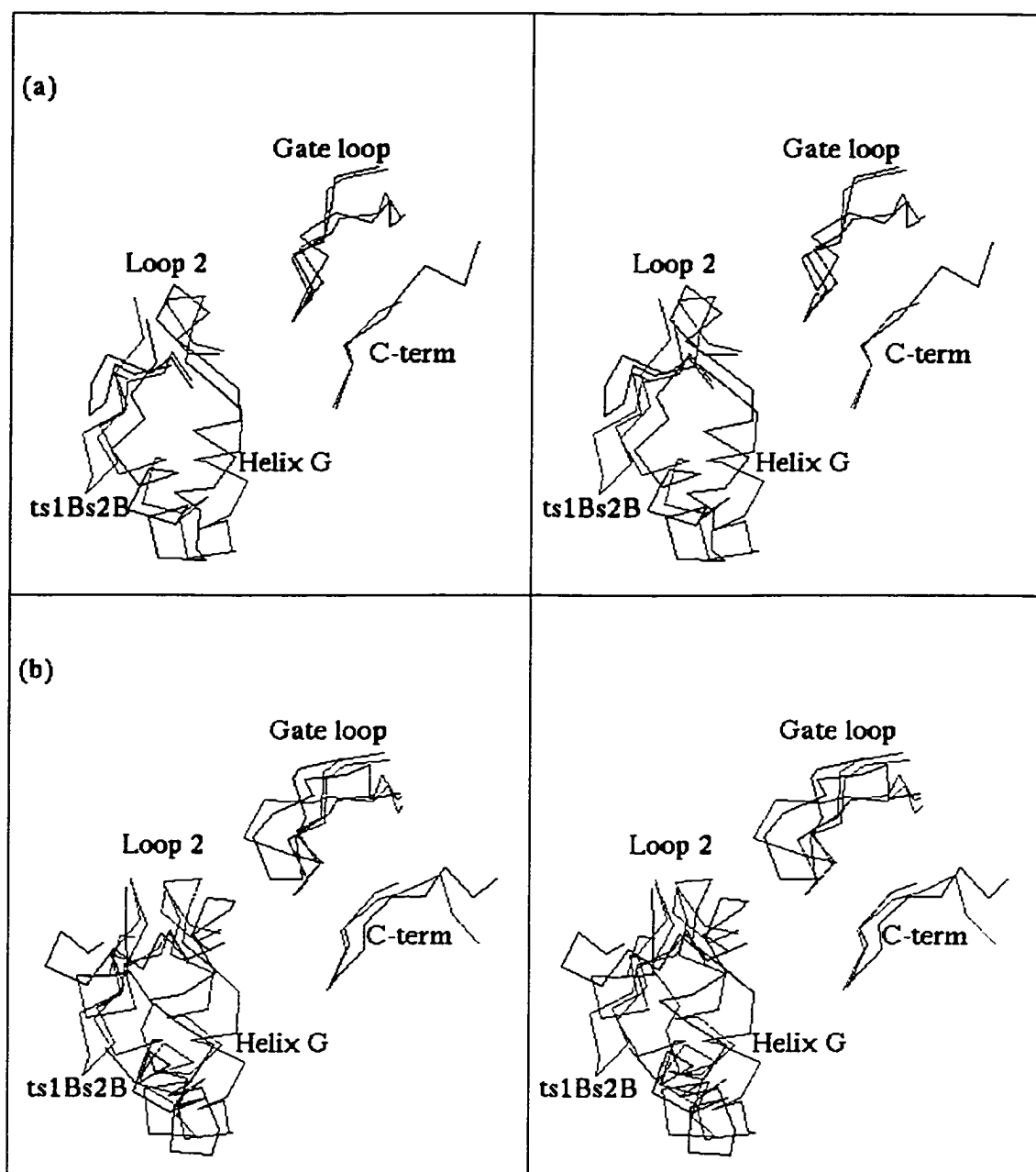
Figure 3.12: The Gate region. Superposition of the Structures of several active serpins in the gate region. Cα traces are shown of relevant regions of the active molecule A (red) (residues 186-200 (the gate loop), 211-223 (ts1Bs2B), 239-269 (loop 2), and 375-379 (the C-terminus)) along with a) antithrombin (blue); b) α₁-antitrypsin (green) and anti-chymotrypsin (blue). This figure was produced using the Molscript program (Kraulis, 1991).

and Arg 187, further from Arg 356, do not seem to have their charge requirements satisfied locally. Interestingly, the side chain of Arg 356 is in close proximity to that of Lys 243. This may cause some local instability, and contribute to the shift of loop 2. Detailed conclusions are difficult to draw, as the differences in loop 2 between molecules A and B modify the positions of these atoms somewhat.

Wright has proposed that an intramolecular deamidation at the Asn 172–Gly 173 sequence, unique to PAI-1 among the serpins, might facilitate spreading of the A sheet (Wright, 1996). Our crystal structure shows nothing unusual about these residues. While one deamidation product, an Asp–Gly sequence, would be isosteric with Asn–Gly and therefore indistinguishable by X-ray crystallography, the other possible products, a D or L isoaspartate group followed by a Gly, or the intermediate Asp-succinimidyl-Gly form, would be expected to be obvious in the electron density map. As the crystals were grown over several days at room temperature, if this rearrangement occurred to a significant extent, it should be noticeable in the electron density. The deamidation reaction is generally known to occur with a half-life measured in days, while the latency transition occurs with a half-life measured in hours. In addition, the crystal structure provides no obvious mechanism for catalyzing the deamidation reaction at a faster rate than would occur normally. Our structure cannot be said to lend support to the deamidation theory.

Based on residue correlation values, Harrop *et al.* (1999) proposed that the presence of buried Arg 271 and solvent exposed Leu 272 in strand 2C might destabilize that strand. This could destabilize the C sheet, and reduce the degree to which strand 1C is anchored in the structure, facilitating the latency transition. While this is a noteworthy suggestion, the high-resolution structure indicates some caveats. While the side chain of

Leu 272 is exposed to solvent, the head group of Arg 271 is not buried, and in fact forms

a hydrogen bond with solvent atoms in molecules A/C. Harrop *et al.* (1999) suggest that

Arg 271 might be stabilized by a salt bridge with Glu 350. Such a salt bridge is observed

in the B/D molecules, but not in the A/C molecules, where they face away from each

other. Comparing the electron density in all the molecules suggests there is significant

variation in the area, typical of surface residues. Nevertheless, the effect of the mutation

R271C is to increase the half life of the latency transition from 2 hours to 5.4 hours

(Berkenpas *et al.*, 1995), supporting Harrop *et al.*'s theory.

Finally, if the positions observed for the RCL in the active PAI-1 structure are

biologically significant, the average position would be considerably closer to the gate

region than in most other serpin structures. This could serve to facilitate the latency

transition, as only a 4 or 5 kcal decrease in activation energy from that found in normal

serpins is required to increase the latency transition to the rate observed in PAI-1.

3.3.7 Mutation Sites

In the low-resolution structure of active PAI-1, the sites of the 4 mutations that

retarded the latency transition were analyzed to explain their effects. While only general

conclusions about decreased lability could be drawn at the M354I site, the N150H,

K154T, and Q319L mutations resulted in a rearrangement of the thFs3A turn from a

series of bends in the latent, cleaved, and peptide inhibited forms into a 3_{10} helix in the

active form. The rearrangement appears to make this segment (overlying the A sheet of

the protein) more rigid, and facilitates the formation of hydrogen bonds to the main body

of the protein. The overall effect of the mutations could be to reduce the rate of the latency transformation by hindering loop insertion (Sharp *et al.*, 1999).

In general the high resolution structure confirms these ideas. The only major change in the structure at high-resolution is to be seen at His 150, where crystal packing leaves the side chain in different conformations in the B/D and A/C molecules (Figure 3.13 a). The conformation in molecule B is more likely to occur in the absence of crystal contacts, as an intramolecular hydrogen bond is formed between the His 150 sidechain and Ser 149 Oγ. The extra bond may serve to make the segment more rigid. The hydrogen bonds previously reported between Glu 283 and residues 152 and 153 in the segment are clearly present.

Ile 354 occupies roughly the same space that Met 354 does in the peptide-inhibited structure. The M354I mutation may influence the packing of the nearby Ile 237, whose conformation is different between the active and the peptide-inhibited structures (Figure 3.13 b). The effect of a rearrangement of Ile 237, which lies in strand 3B, is not obvious, but Berkenpas *et al.* (1995) found several latency-retarding mutations in strand 3B.

3.3.8   Docking Results

Computational docking of ligands remains a challenging problem, but good progress is being made. In the CASP2 challenge, the DockVision package used in this work performed well in blind tests on problems of similar difficulty to those of docking XR51 and ARH0 to PAI-1; a docking close to the correct answer was among the top few choices for five of six test cases (Hart *et al.*, 1997). For both XR51 and ARH0, the lowest energy dockings (with or without the conformational energies of the ligands included) yielded structures of sufficient similarity that generalizations about the apparent
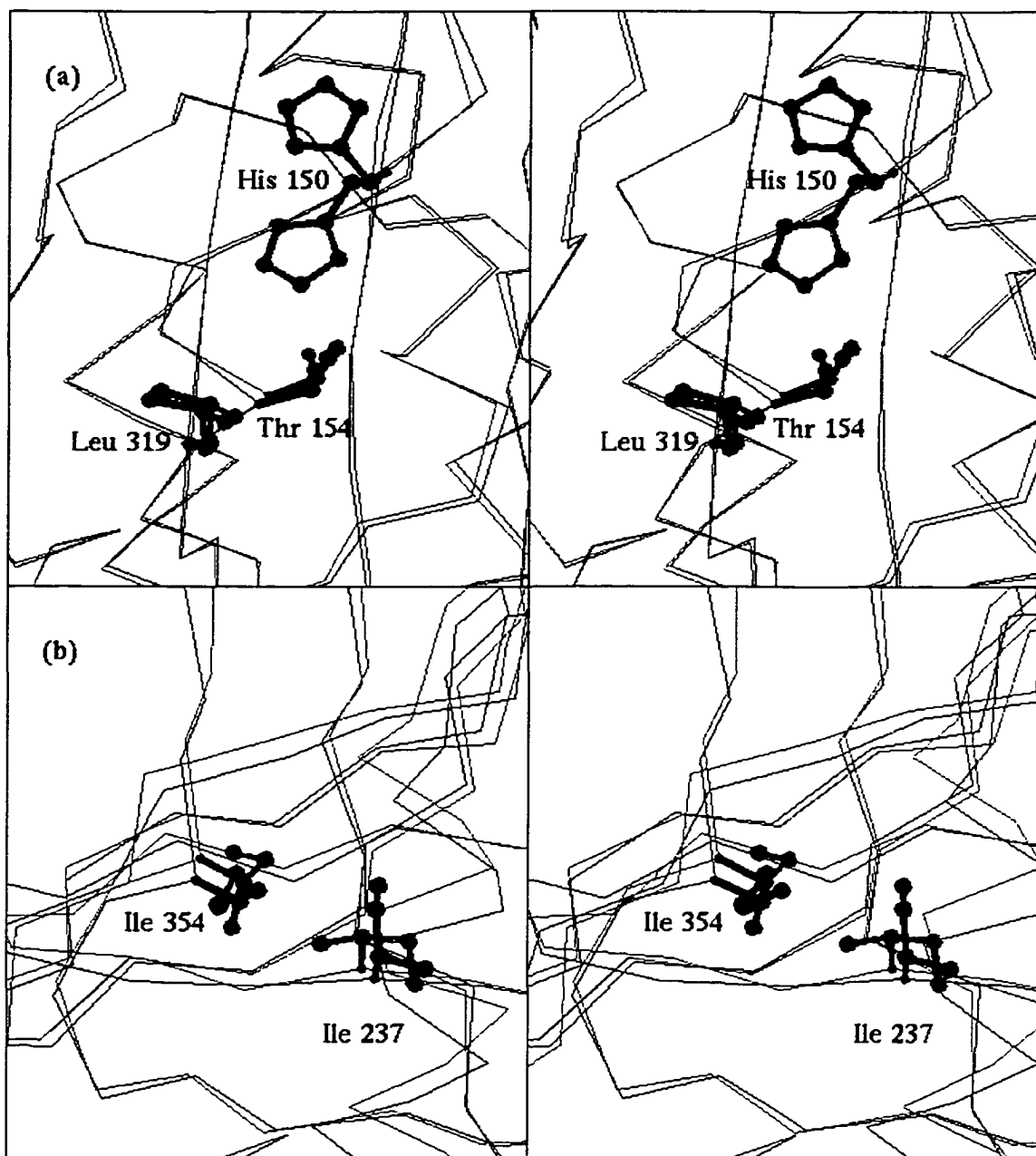
Figure 3.13: The mutated residues. a) The cluster of mutated sidechains is shown with

Cα traces of molecule A (red) and molecule B (blue). b) The residue 354 site from

molecule A (red) is shown with the same region in the peptide inhibited structure (blue).

This figure was produced using the Molscript program (Kraulis, 1991).

nature of inhibitor binding can be made. The docking results are summarized in Tables 3.6 and 3.7. The ligands dock in similar fashion against both the A and the B molecules, although the lowest energy dockings were found to occur with the B molecule. This may be due to a slight difference in the tilt of the side chain ring of Tyr 79 and a different conformation of the side chain of Met 45; both these residues contribute to the side surfaces of the inhibitor binding pocket. (Note that the docking program does not allow for flexibility in the protein target.) Significantly higher energies were found for docking against the peptide-inhibited form of PAI-1, with the best energy being −19.66 kcal/mole for XR51 and −1.81 kcal/mole for ARH0. Even the lowest energy dockings of the inhibitors against the peptide-inhibited form had not inserted into the binding pocket to any significant degree. The region occupied by the inhibitors in dockings against the active forms of PAI-1 is filled in the peptide-inhibited form by a changed conformation of residues 93 to 96, and a change of the side chain rotamer of Tyr 79. These changes narrow the pocket considerably (Figure 3.14).

The lowest energy structures of XR51 docked against the A and B molecules all have similar conformations, with the central diketopiperazine ring stacked against the side chains of Tyr 79 and Met 45 (Figure 3.15). All have similar (but not identical) conformations for the phenyl group, which inserts further into the pocket and packs against Leu 75. The thiophene ring, the alkyl chain, and the tertiary amine group are more variable in conformation, resting outside the tightest regions of the pocket and packing between the side chains on the protein surface. These results are consistent with the development history of XR51; the diketopiperazine and phenyl rings have been conserved from the original *Streptomyces* natural product, but the thiophene ring and the

Table 3.6: Docking results for XR51. The dockings with best energies (both with and without conformational energies of the ligands). Clear hydrogen bonds (good geometry and donor-acceptor distances < 3.5 Å) are listed. For the sake of comparison, energies computed including conformational energy are shown for the best dockings obtained without a conformational energy term.

Protein Molecule	Docking output identification code	Docking energy with conformational energy (kcal/mol)	Docking energy without conformational energy (kcal/mol)	Hydrogen bonds	Notes
B	Bce1	-19.66		Asp 95 N - O15	
B	Bce2	-19.13		none	
B	Bce3	-16.17		none	
A	Ace1	-16.13		Asp 95 N - O15 N25 - Arg 118 O	
A	Ace2	-14.90		N25 - Arg 118 O	Lies in side pocket
A	Ace3	-13.65		Asp 95 N - O15	
B	Bnce1	-0.77	-50.66	N25 - Arg 118 O	
B	Bnce2	-5.77	-48.95	Asp 95 N - O15	
A	Ance1	-12.86	-48.88	Asp 95 N - O15 N25 - Thr 142 O	
B	Bnce3	-7.30	-47.54	Asp 95 N - O15	
A	Ance2	-5.58	-47.32	Asp 95 N - O15	
A	Ance3	-1.33	-47.01	Asp 95 N - O10	central ring flipped

Table 3.7: Docking results for ARH0. The dockings with best energies (both with and without conformational energies of the ligands). Clear hydrogen bonds (good geometry and donor-acceptor distances < 3.5 Å) are listed. For the sake of comparison, energies computed including conformational energy are shown for the best dockings obtained without a conformational energy term.

Protein Molecule	Docking output identification code	Docking energy with conformational energy (kcal/mole)	Docking energy without conformational energy (kcal/mole)	Hydrogen bonds	Notes
B	Bce1	-0.77		His 143 Nε2 - O Thr 93 Oγ1 – O2	
B	Bce2	-0.66		N6 - Arg 118 O Thr 93 Oγ1 – O2	
A	Ace1	-0.29		His 143 Nε2 - O Asp 95 N - O1	
A	Ace2	0.48		N6 - Arg 118 O	
B	Bce3	2.20		N - Phe 117 O Ser 41 Oγ - O3	Alternate orientation
B	Bce4	3.33		Asp 95 N - O1	
B	Bnce1	-1.81	-54.22	Asp 95 N - O1 N6 - Arg 118 O	
B	Bnce2	-1.56	-54.12	Asp 95 N - O1 His 143 Nε2 - O	
B	Bnce3	2.51	-52.49	Asp 95 N - O1 His 143 Nε2 - O	
A	Ance1	3.79	-52.46	Asp 95 N - O1 His 143 Nε2 - O	
A	Ance2	0.63	-51.88	Asp 95 N - O1 His 143 Nε2 - O Tyr 37 OH - O2	
A	Ance3	2.17	-51.65	Asp 95 N – O2 N –Phe 117 O	Alternate orientation

(a)   (b)
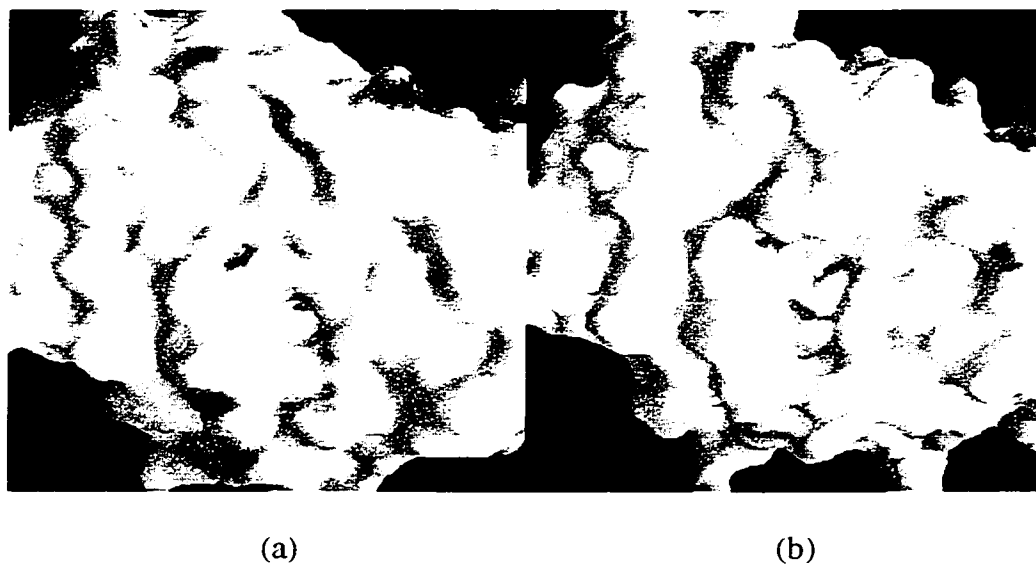
Figure 3.14: The putative inhibitor binding surface. Molecular surfaces are shown for the protein with electrostatic potential displayed. Regions of positive charge are in blue, and regions of negative charge are in red. a) The face in peptide-inhibited PAI-1; b) the face in active molecule B. Figure produced using GRASP (Nicholls *et al.*, 1991).

tail have been changed considerably (Charlton *et al.*, 1996),(Friederich *et al.*, 1997). In the lowest energy structure, one of the ketone oxygens (O15) forms a hydrogen bond with Asp 95 N, while the hydroxyl group of Tyr 79 interacts with the thiophene sulphur. Minor rearrangements of the protein would also optimize potential hydrogen bonds between the diketopiperazine nitrogen (N11) on the inhibitor and Asp 95 OD1, and between the ternary amine nitrogen (N25) and Thr 142 O. As the order of magnitude improvement in IC_{50} values between XR51 and the original lead compound appears to be due to improvement in the thiophene ring and tail, it is unfortunate that their effect is not more clearly indicated by the dockings. In the course of drug development the thiophene ring had replaced a more hydrophobic phenyl group. This could improve the energetics of the interaction of the ring with the amphiphilic environment near the protein surface.

A few significant conformational deviations are observed among docked structures of relatively low energy. These include a structure with the diketopiperazine ring flipped but unchanged in position, and one with the diketopiperazine ring between the edge of the Tyr 79 side chain and the Arg 118 main chain. In both of these forms, the region occupied by the phenyl group is the same, whereas in the form with the alternate ring site the thiophene and acyl groups shift considerably. In the 40 low-energy dockings inspected, one comparatively high energy structure has just the alkyl tail of the inhibitor in the pocket. The tertiary amine barely reaches the region occupied by the phenyl ring in other dockings, making this a relatively shallow docking.

Figure 3.15: XR51 docked on molecule B. a) Docking Bce1. Carbon atoms are shown in grey, nitrogen atoms in blue, oxygen atoms in red, sulpher atoms in yellow, and polar hydrogen atoms on the inhibitor are in white. The protein is shown as a ribbon diagram with sidechains mentioned in the text shown in ball and stick with white bonds and labeled. The inhibitor is shown in ball and stick form with yellow bonds. b) The 6 lowest energy dockings of XR51. These are: Bce1 (red), Bce2 (blue), Bce3 (purple), Ace1 (green), Ace2 (cyan), Ace3 (yellow). This figure was produced using the Molscript program (Kraulis, 1991).
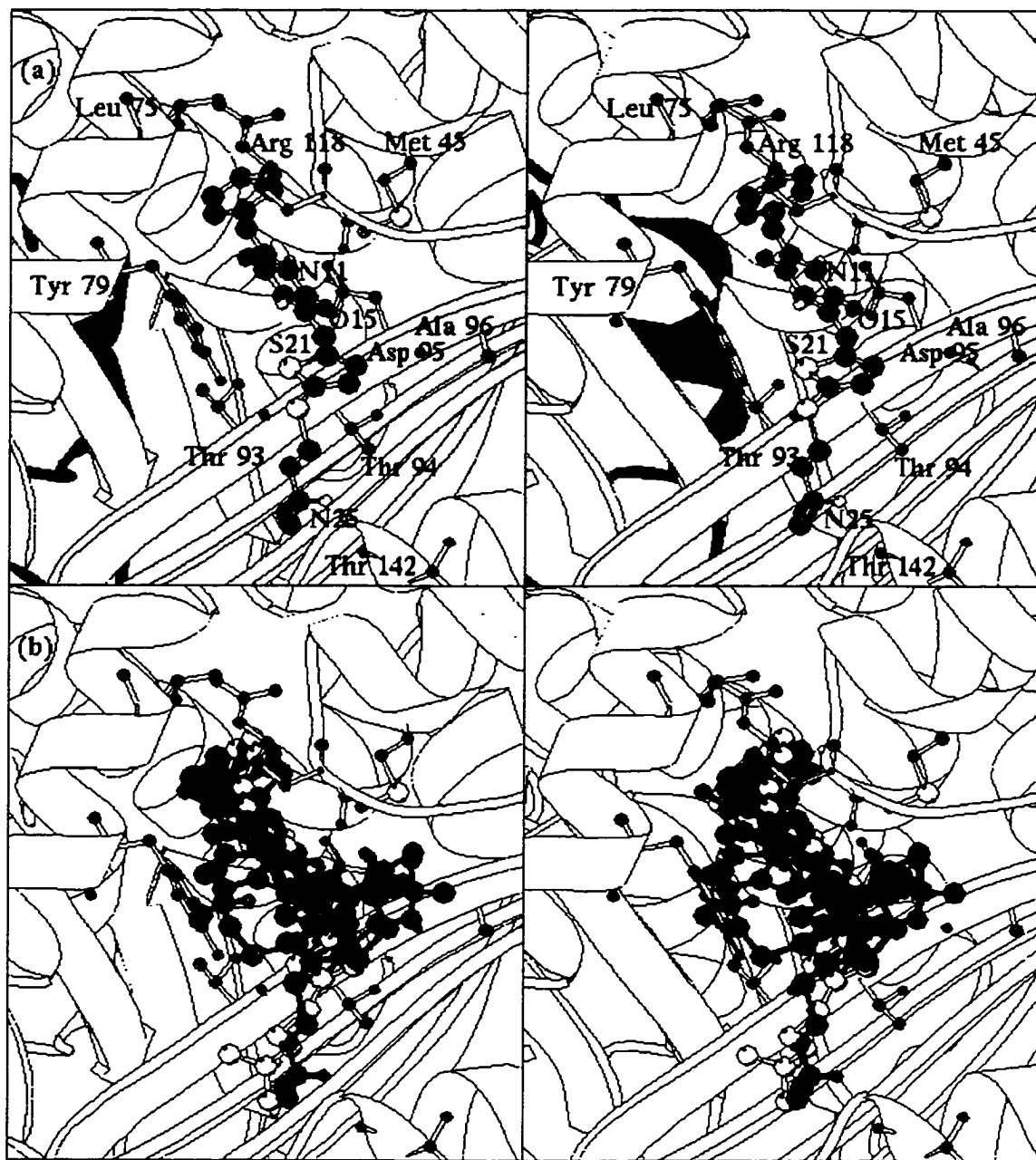
The lowest energy dockings of ARH0 all occur with the carboxyl and nitro derivatized ring occupying the space midway between the diketopiperazine and phenyl rings in XR51 (Figure 3.16). This is consistent with the development of ARH0 from anthranilic acid (2-aminobenzoic acid) via flufenamic acid, as this ring is a slightly more heavily derivatized form of anthranilic acid (Björquist *et al.*, 1998). The carboxyl group of ARH0, found in the original anthranilic acid, forms reasonably good hydrogen bonds with Asp 95 N and Thr 93 Oγ1. The nitro group, absent from the lead compounds, does not form any hydrogen bonds with good geometry but does occupy a hydrophilic pocket. The other two rings in the compound are more variably positioned. In the lowest energy docking, a hydrogen bond forms between the ligand's peptide nitrogen (N6) and Arg 118 O. In other low energy conformations, N6 forms bonds with Tyr 79 Oη or O, or the ligand peptide carbonyl forms a bond to His 143 Nϵ2.

The other significant deviation among the lowest energy dockings of ARH0 is the orientation of the carboxyl and nitro derivatized ring. In some of the low energy dockings the ring occupies the same location but has a slightly different orientation. The carboxyl oxygens interact with Asp 95 N and Ser 119 Oγ, and the amine nitrogen (N) interacts with Phe 117 O. In this form, the ring is not inserted as deeply in the pocket and the carboxyl group is more exposed.

Björquist *et al.* (1998) report testing several variants of ARH0 with different groups in place of the acid moiety, including nitro, tetrazole, and amidino groups. While the tetrazole group had similar inhibitory activities to the carboxyl, the nitro or amidino groups decreased the effectiveness of the compound by two orders of magnitude. It is difficult to reconcile these effects with the lowest energy docking that we observed.

Figure 3.16: ARH0 docked on molecule B. a) Docking Bnce1. Carbon atoms are shown in grey, nitrogen atoms in blue, oxygen atoms in red, sulpher atoms in yellow, chlorine atoms in green, and polar hydrogen atoms on the inhibitor are in white. The protein is shown as a ribbon diagram with sidechains mentioned in the text shown in ball and stick with white bonds and labeled. The inhibitor is shown in ball and stick form with yellow bonds. b) The 6 lowest energy dockings of ARH0. These are: Bnce1 (red), Bnce2 (blue), Bce1 (purple), Bce2 (green), Ace1 (cyan), Ace2 (yellow). This figure was produced using the Molscript program (Kraulis, 1991)
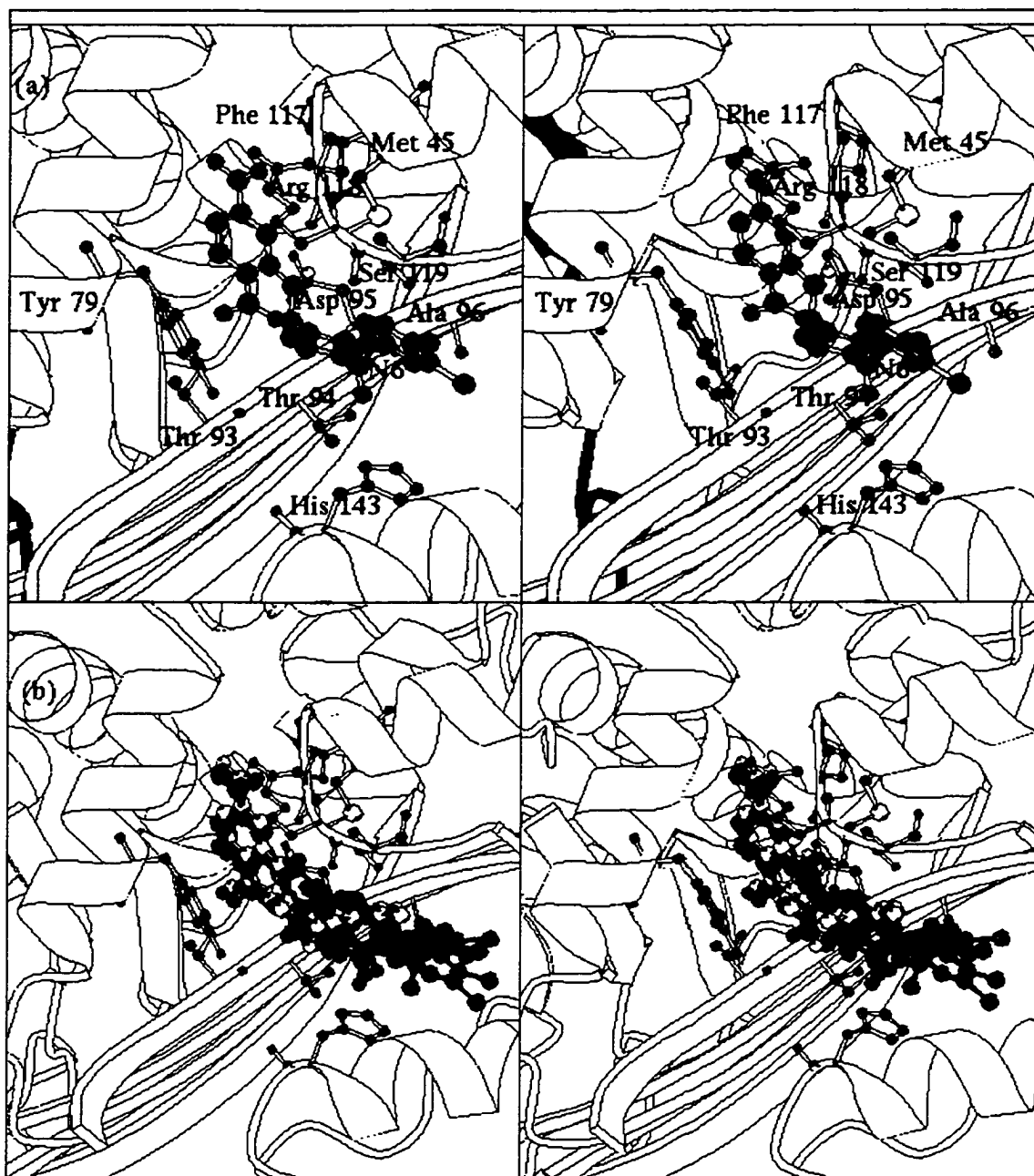
Positively charged groups at the carboxyl site could be accommodated by the side chain of Asp 95. The nitro and amidino groups are sufficiently small that they would not be expected to disrupt the interactions formed by the carboxyl group in the lowest energy docking, and the hydrogen bond donor/acceptors should be able to accept the amidino group with no more than proton shifts. The bulky tetrazole group would be harder to accommodate, except perhaps in the alternative low-energy docking.

In the dockings of energies low enough to merit inspection, there were several with the ortho-dichlorinated phenyl ring inserted into the pocket. This ring is inserted deeper in the hole than the carboxyl and nitro derivatized ring, but not as deeply as the phenyl group on XR51. No consistent location was observed for the carboxyl and nitro derivatized ring in these dockings. Several different orientations are observed for the dichlorinated ring, suggesting that it does not pack very tightly in the binding pocket. These forms would, however, be able to accommodate changes to the carboxyl and nitro derivatized ring, such as a tetrazole.

It is not as easy to assign a most-favoured docking in the case of ARH0 as it is with XR51. The lowest energy docking, with the carboxyl and nitro derivatized ring in the pocket, has the advantage of placing the original lead compound in well-defined contact with the protein, but makes it hard to explain the effects of changing the carboxyl group. The dockings with the dichlorinated ring in the pocket do have higher energies, but the DockVision energy calculation does not account for solvation effects, which might make placing the highly derivatized ring outside the protein more favourable. Placing the charged groups outside the pocket is consistent with the abolition of binding by mutating arginine groups around the pocket to glutamates, as noted by Björquist *et al.* (1998).

However, the results they obtained substituting the carboxylate with groups of varying charge do not indicate a clear salt bridge interaction. While it is difficult to make a firm conclusion from docking studies alone, the possible binding conformations seen in these docking studies could be assessed by mutating residues predicted to be involved in binding, such as Asp 95.

The docking experiments do demonstrate the feasibility of small molecules binding in this area of PAI-1, and suggest ways in which such molecules could be improved. In general, the portion of the inhibitors that appears to be interacting in a reproducible way with the binding pocket consists of two planar six-membered rings connected by a bridge of one or two atoms. In both XR51 and ARH0 the third ring interacts with the surface side chains at the top of the pocket, but it does not seem to be well anchored in a specific conformation. As the pocket is fairly broad and not especially hydrophobic, at least one ring should be the core of a number of groups capable of forming hydrogen bonds and contacts with the groups lining the sides of the pocket. The dockings of XR51 suggest that there is room for motion perpendicular to the plane of the diketopiperazine ring as well as parallel to it. Therefore groups that gave the molecule some width along that dimension might improve the binding as well. As the inner regions of the pocket have a slight negative charge, positively charged or electron accepting groups might also be good derivatives to try.

The mechanism by which ARH0 inhibits the activity of PAI-1 is unclear. As the binding site is on the edge of the A sheet, retarding the RCL insertion into the A sheet would appear to be an obvious mechanism. Blocking insertion into the A sheet, by mutations or by inserting peptides mimicking the reactive site loop, has been shown to

turn serpins into substrates for their target enzymes (Chang *et al.*, 1996). As inhibitors

cannot be docked in the narrower pocket found in six-stranded forms of PAI-1, inhibitors

bound to the active form could retard insertion and turn PAI-1 into a substrate. However,

Björquist *et al.* (1998) report that ARH0 does not turn PAI-1 into a substrate. While the

data demonstrating this are not shown, these results would discredit the most obvious

explanation.

The region to which the inhibitors are believed to bind has been reported to be a

binding site for tPA on the basis of antibody experiments (Keijer *et al.*, 1991). ARH0

might therefore inhibit the formation of the Michaelis complex with tPA (Keijer *et al.*,

1991). More recent papers have suggested that this interaction occurs in the inhibited

covalent serpin-protease complex (Björquist *et al.*, 1997; Wilczynska *et al.*, 1997). In

that case, a disruption of the interaction would probably turn PAI-1 into a substrate

(Björquist *et al.*, 1997). However, these results have been challenged by new

flourescence and antibody binding data questioning the presence of a serpin-proteinase

interaction in this region in the covalent inhibited complex (Björquist *et al.*, 1999;

Stratikos & Gettins, 1999). It therefore remains possible that the inhibitors do prevent the

formation of the Michaelis complex. As the deep pocket is a major feature in this face, it

is reasonable for it to play a role in protein-protein specificity. The filling of the pocket

with an inhibitor molecule could then disrupt an important interaction. Moieties of the

inhibitor projecting from the pocket would also tend to disrupt the interaction, which

could explain why the inhibitor molecules have a third ring and/or tail that does not fit

into the pocket.

Another possible mode of interaction derives fro•m the observation that the structure

of active antithrombin has a reactive site loop that is pɪre-inserted (Carrell *et al.*, 1994).

This means that a few residues have been inserted intoɔ the A sheet in the active form

(Carrell *et al.*, 1994). This was initially proposed to beɛ involved in activating the

molecule, by starting insertion into sheet A and restricɪting the conformational flexibility

of the reactive centre loop (Bjork *et al.*, 1993; Bode & Huber, 1991; Carrell *et al.*, 1994;

Schreuder *et al.*, 1994). This is known as the pre-equiɪllibrium conformational change

model (Bjork *et al.*, 1992). However, the relevance of⁻pre-inserted forms of serpins has

been challenged by the discovery of serpin structures ₅such as that of active human α1-

antitrypsin (Elliott *et al.*, 1998; Elliott *et al.*, 1996) andɪ serpin 1K from *Manduca sexta*

(Li *et al.*, 1999), with RCLs that are already in classicaɪl serine proteinase substrate

conformations without pre-insertion. Furthermore, su⅛sequent work strongly suggests

that pre-insertion serves to inactivate antithrombin (Cɪnang *et al.*, 1996), and that the

activation of antithrombin by heparin is due to structurɪal rearrangements that lead to the

expulsion of the pre-inserted segment (Huntington *et aɪl.*, 1996; Jin *et al.*, 1997; van

Boeckel *et al.*, 1994).

As the PAI-1 structure (solved in the absence of ɪheparin) shows no evidence of pre-

insertion, the relevance of pre-insertion to PAI-1's owɪn activation by heparin is unclear.

The activation of PAI-1 by vitronectin or by heparin haɪs been suggested by fluorescence

studies to involve structural rearrangements, in particuↄlar changes that increase the

motion of the reactive centre (Fa *et al.*, 1995; Urano eɪt *al.*, 1994). As pre-insertion would

be expected to decrease the lability of the loop somewɪhat, these results might indicate the

expulsion of a pre-inserted loop as in antithrombin. If⁻PAI-1 did form a pre-inserted

complex to a significant extent in solution, that might explain both the activation by heparin and the inhibition by factors that could hinder opening and closing of the A sheet. If a pre-inserted PAI-1 was unable to form a Michaelis complex with PA, than ARH0 could inhibit the molecule without turning it into a substrate by 'freezing' the molecule in a pre-inserted state. However there are important problems with this theory. Firstly, there is no evidence for pre-insertion in the active structure, or for any obvious quaternary restraint from the crystal packing that would prevent pre-insertion. Secondly, the best kinetics evidence available (Meijer *et al.*, 1997), suggests that heparin activates PAI-1 via a template mechanism, that is, it brings PAI-1 and tPA into close proximity and facilitates their binding. The consensus is therefore that there is no need for a structural rearrangement as in antithrombin.

Alternatively, if pre-insertion were required for PAI-1 to form a reactive site loop conformation that could be cleaved by PA, an inhibitor frustrating the opening of the A sheet might prevent the serpin from forming a complex with its target enzyme. While this runs against the paradigm provided by antithrombin, pre-insertion might serve to increase the degree of order in PAI-1's reactive centre loop, which may be disordered in comparison to other serpins. The two serpin structures that have reactive centres in the classic serine proteinase substrate conformation, α_1-antitrypsin, and *Manduca sexta* serpin 1K are not pre-inserted (Elliott *et al.*, 1998; Elliott *et al.*, 1996; Li *et al.*, 1999). However, the differences between these two structures indicates that serpins can take more than one reactive centre loop conformation that could serve as bait for a serine proteinase. In this case, the structure presented in this paper would not be the actual active form, but a similar conformation stabilized by the crystal structure. Declerck has

suggested the existence of an extra 'substrate' form of PAI-1 (Declerck *et al.*, 1992), however, since the 'inhibitor stabilized' form considered here is not a substrate, this is probably not the form seen here.

Further work would be required to test either the 'inhibitor induced' or the 'inhibitor stabilized' pre-insertion theories, as they require several unsubstantiated postulates. While these theories offer a way to retain the attractive idea that the inhibitors perform their function by preventing rearrangements of the A sheet, the lack of evidence for pre-insertion in PAI-1 is an obvious stumbling block.

Thus, if the results of Björquist *et al.* (1998) are considered to disprove the attractive theory that the inhibitors turn PAI-1 into a substrate, the theory that they disrupt an interaction necessary to form the PA/PAI-1 Michaelis complex would appear to be the most likely. Theories involving either the stabilization of an inhibitory pre-inserted complex, or the disruption of a catalytically necessary pre-inserted complex, while having some attractive features, must be considered to be less likely.

The dockings do not resolve the mechanism by which the inhibitors work. The fact that the inhibitors do not fit into the pocket in peptide-inhibited PAI-1 accords with the evidence that ARH0 does not bind to 6-stranded forms of PAI-1. The presence of the inhibitor molecules in the pocket would be expected to hinder the rearrangements on this face of the molecule, so mechanisms involving an inhibition of the opening of sheet A would be supported by these dockings. Alternatively, if the pocket were required for the binding of tPA or an activating molecule to PAI-1, the inhibitors could be expected to disrupt the interaction.

3.4 Conclusions

The high-resolution structure of PAI-1 at 2.2 Å allows us to refine many of the conclusions drawn from the low resolution structure. Changes in the structure at high resolution make little difference to the conclusions about the effects of the mutations, the conformation of the reactive centre loop, or the significance of the reactive centre loop polymerization, but other features are observed that do allow more specific proposals to be made about the mechanism of latency and about the binding of inhibitors.

The most dramatic revelation from the high resolution structure is the difference between the A/C pair and B/D pair molecules in the back side of the gate (turn ts1Bs2B and turn ts3BhG and helices G and H). This probably indicates a considerable degree of flexibility in an entire face of the PAI-1 molecule, which is apparently not paralleled in any other serpin. The flexibility may facilitate the latency transition, as these residues form one side of the 'gate' through which the reactive centre loop must pass in forming latent PAI-1. The variation in this region must certainly be considered when comparing different forms of PAI-1.

By contrast, the relatively minor change seen in the 'gate loop' (residues 181 to 190) has implications for other theories explaining the latency transition, as does the standard conformation that we observe for the C-terminus. Both of these suggest that the disordered gate loop and the unusually positioned (or possibly completely disordered) C-terminus observed in latent PAI-1 are products of the latency transformation, not pre-existing conditions as proposed by Tucker *et al.* (1995). As the structures of cleaved and peptide-inhibited PAI-1 have conformations for these regions similar to the active PAI-1,

the differences observed in the latent form should be viewed as being due to the latency

transition, and not a result of PAI-1 strand insertion in general.

With regard to latency, our high resolution structure supports (with a few

qualifications) Harrop *et al.*'s (1999) theory about the destabilization of the C sheet, but

not the C-terminus and disordered gate loop theory of Tucker *et al.* (1995), the

electrostatic theory of Aertgeerts *et al.* (1995), and the deamidation theory of Wright *et*

al. (1996). Nevertheless, many of the observations and parts of the theories of Tucker *et*

al. (1995) and Aertgeerts *et al.* (1995) remain significant and intriguing, and should be

reassessed in view of the new information supplied by the active structure. Two

completely new possibilities for a mechanism of latency are supplied by the high

resolution structure. One is the potential role of the mobility of residues 215 to 220 and

240 to 265 in facilitating motion through the gate. The other is the possibility that the

reactive centre loop tends to be closer to the gate loop in PAI-1 than in most serpins, thus

encouraging insertion.

Our docking of inhibitor molecules confirms that the deep pocket between sheet A,

helix D, and helix E is a probable binding site for inhibitors. Likely binding

conformations can be identified for both ligands. For XR51, the docking with the phenyl

ring inserted deepest in the pocket and the diketopiperazine ring interacting with Tyr79

seems the most probable. In the case of ARH0, the most probable conformation is not as

clear. The dockings with the carboxyl, nitro derivatized phenyl ring inserted in the

pocket are the best energetically, but those with the dichlorinated phenyl ring inserted are

in better accord with experiments on the effects of substituting the carboxyl group with

other moieties. The docking models could be tested by mutating specific residues in

PAI-1, in particular Tyr 79, or by altering the derivatization of the inhibitors. Useful information and specific ideas for the improvement of the inhibitors can also be drawn from the models.

In general, although the resolution of the structure can only be described as 2.2 Å in the most optimistic sense, by the use of 4 fold averaging and NCS restraints a structure of similar quality to that of the peptide inhibited PAI-1 has been achieved. Combined with the deposition of a cleaved structure of high quality, and the availability of a structure of PAI-1 in the latent conformation, a set of PAI-1 models as complete as is available for any serpin has now been assembled. Hopefully, this will be of assistance in determining the mechanism of PAI-1's functions, and in designing drugs and other treatments for conditions involving the activity of PAI-1.

References

Abrahamsson, T., Nerme, V., Stromqvist, M., Akerblom, B., Legnehed, A., Pettersson, K. & Westin Eriksson, A. (1996). Anti-thrombotic effect of a PAI-1 inhibitor in rats given endotoxin. *Thrombosis & Haemostasis* 75, 118-26.

Adams, P. D., Pannu, N. S., Read, R. J. & Brünger, A. T. (1997). Cross-validated maximum likelihood enhances crystallographic simulated annealing refinement. *Proceedings of the National Academy of Sciences of the United States of America* **94**, 5018-23.

Aertgeerts, K., De Bondt, H. L., De Ranter, C. J. & Declerck, P. J. (1995). Mechanisms contributing to the conformational and functional flexibility of plasminogen activator inhibitor-1. *Nature Structural Biology* 2, 891-7.

Allen, F. H. & Kennard, O. (1993). 3D search and research using the Cambridge structural database. *Chemical Design Automation News* 8, 31-7.

Barnes, C. S., Faint, R. W., Dwyer, M. C., Critchley, D. J. P., Templeton, D., Folkes, A. J., Charlton, P. A. & Bevan, P. (1996). *British Journal of Pharmacology* 118, Suppl. 97P.

Bass, M. B., Hopkins, D. F., Jaquysh, W. A. & Ornstein, R. L. (1992). A method for determining the positions of polar hydrogens added to a protein structure that maximizes protein hydrogen bonding. *Proteins* 12, 266-77.

Bavenholm, P., de Faire, U., Landou, C., Efendic, S., Nilsson, J., Wiman, B. & Hamsten, A. (1998). Progression of coronary artery disease in young male post-infarction

patients is linked to disturbances of carbohydrate and lipoprotein metabolism and to impaired fibrinolytic function. *European Heart Journal* **19**, 402-10.

Berkenpas, M. B., Lawrence, D. A. & Ginsburg, D. (1995). Molecular evolution of plasminogen activator inhibitor-1 functional stability. *EMBO Journal* **14**, 2969-77.

Biemond, B. J., Levi, M., Coronel, R., Janse, M. J., ten Cate, J. W. & Pannekoek, H. (1995). Thrombolysis and reocclusion in experimental jugular vein and coronary artery thrombosis. Effects of a plasminogen activator inhibitor type 1-neutralizing monoclonal antibody. *Circulation* **91**, 1175-81.

Biosym. (1993a). *Discover User Guide, version 3.1.0*, Biosym Technologies, San Diego.

Biosym. (1993b). *Insight II User Guide, version 2.3.0.*, Biosym Technologies, San Diego.

Bjork, I., Nordling, K., Larsson, I. & Olson, S. T. (1992). Kinetic characterization of the substrate reaction between a complex of antithrombin with a synthetic reactive-bond loop tetradecapeptide and four target proteinases of the inhibitor. *Journal of Biological Chemistry* **267**, 19047-50.

Bjork, I., Nordling, K. & Olson, S. T. (1993). Immunologic evidence for insertion of the reactive-bond loop of antithrombin into the A beta-sheet of the inhibitor during trapping of target proteinases. *Biochemistry* **32**, 6501-5.

Björquist, P., Ehnebom, J. & Deinum, J. (1999). Protein movement during complex-formation between tissue plasminogen activator and plasminogen activator inhibitor-1. *Biochimica et Biophysica Acta* **1431**, 24-9.

Björquist, P., Ehnebom, J., Inghardt, T. & Deinum, J. (1997). Epitopes on plasminogen activator inhibitor type-1 important for binding to tissue plasminogen activator. *Biochimica et Biophysica Acta* **1341**, 87-98.

Björquist, P., Ehnebom, J., Inghardt, T., Hansson, L., Lindberg, M., Linschoten, M., Stromqvist, M. & Deinum, J. (1998). Identification of the binding site for a low-molecular-weight inhibitor of plasminogen activator inhibitor type 1 by site-directed mutagenesis. *Biochemistry* **37**, 1227-34.

Bode, W. & Huber, R. (1991). Ligand binding: proteinase-protein inhibitor interactions. *Current Opinion in Structural Biology* **1**, 45-52.

Brünger, A. T. (1992). The Free *R* Value: a Novel Statistical Quantity for Assessing the Accuracy of Crystal Structures. *Nature* **355**, 472-474.

Brünger, A. T., Adams, P. D., Clore, G. M., DeLano, W. L., Gros, P., Grosse-Kunstleve, R. W., Jiang, J. S., Kuszewski, J., Nilges, M., Pannu, N. S., Read, R. J., Rice, L. M., Simonson, T. & Warren, G. L. (1998). Crystallography & NMR system: A new software suite for macromolecular structure determination. *Acta Crystallographica* **D54**, 905-21.

Brünger, A. T., Krukowski, A. & Erickson, J. W. (1990). Slow-cooling protocols for crystallographic refinement by simulated annealing. *Acta Crystallographica* **A46**, 585-93.

Brünger, A. T., Kuriyan, J. & Karplus, M. (1987). Crystallographic *R* factor Refinement by Molecular Dynamics. *Science* **235**, 458-460.

Burzlaff, H. & Zimmermann, H. (1985). On the metrical properties of lattices. *Zeitschrift für Kristallographie* **170**, 247-62.

Carrell, R. W., Stein, P. E., Fermi, G. & Wardell, M. R. (1994). Biological implications of a 3 Å structure of dimeric antithrombin. *Structure* **2**, 257-70.

Chang, W. S., Wardell, M. R., Lomas, D. A. & Carrell, R. W. (1996). Probing serpin reactive-loop conformations by proteolytic cleavage. *Biochemical Journal* **314**, 647-53.

Charlton, P. A., Faint, R. W., Bent, F., Bryans, J., Chicarelli-Robinson, I., Mackie, I., Machin, S. & Bevan, P. (1996). Evaluation of a low molecular weight modulator of human plasminogen activator inhibitor-1 activity. *Thrombosis & Haemostasis* **75**, 808-15.

de Bono, D. (1994). Significance of raised plasma concentrations of tissue-type plasminogen activator and plasminogen activator inhibitor in patients at risk from ischaemic heart disease. *British Heart Journal* **71**, 504-7.

Declerck, P. J., De Mol, M., Alessi, M. C., Baudner, S., Paques, E. P., Preissner, K. T., Muller-Berghaus, G. & Collen, D. (1988). Purification and characterization of a plasminogen activator inhibitor 1 binding protein from human plasma. Identification as a multimeric form of S protein (vitronectin). *Journal of Biological Chemistry* **263**, 15454-61.

Declerck, P. J., De Mol, M., Vaughan, D. E. & Collen, D. (1992). Identification of a conformationally distinct form of plasminogen activator inhibitor-1, acting as a noninhibitory substrate for tissue-type plasminogen activator. *Journal of Biological Chemistry* **267**, 11693-6.

Declerck, P. J., Juhan-Vague, I., Felez, J. & Wiman, B. (1994). Pathophysiology of fibrinolysis. *Journal of Internal Medicine* **236**, 425-32.

Ehrlich, H. J., Keijer, J., Preissner, K. T., Gebbink, R. K. & Pannekoek, H. (1991). Functional interaction of plasminogen activator inhibitor type 1 (PAI-1) and heparin. *Biochemistry* **30**, 1021-8.

Elliott, P. R., Abrahams, J. P. & Lomas, D. A. (1998). Wild-type alpha 1-antitrypsin is in the canonical inhibitory conformation. *Journal of Molecular Biology* **275**, 419-25.

Elliott, P. R., Stein, P. E., Bilton, D., Carrell, R. W. & Lomas, D. A. (1996). Structural explanation for the deficiency of S alpha 1-antitrypsin. *Nature Structural Biology* **3**, 910-1.

Esnouf, R. M. (1997). An extensively modified version of Molscript that includes greatly enhanced coloring capabilities. *Journal of Molecular Graphics* **15**, 133-8.

Estelles, A., Gilabert, J., Aznar, J., Loskutoff, D. J. & Schleef, R. R. (1989). Changes in the plasma levels of type 1 and type 2 plasminogen activator inhibitors in normal pregnancy and in patients with severe preeclampsia. *Blood* **74**, 1332-8.

Estelles, A., Gilabert, J., Grancha, S., Yamamoto, K., Thinnes, T., Espana, F., Aznar, J. & Loskutoff, D. J. (1998). Abnormal expression of type 1 plasminogen activator inhibitor and tissue factor in severe preeclampsia. *Thrombosis & Haemostasis* **79**, 500-8.

Fa, M., Karolin, J., Aleshkov, S., Strandberg, L., Johansson, L. B. & Ny, T. (1995). Time-resolved polarized fluorescence spectroscopy studies of plasminogen activator inhibitor type 1: conformational changes of the reactive center upon interactions with target proteases, vitronectin and heparin. *Biochemistry* **34**, 13833-40.

Friederich, P. W., Levi, M., Biemond, B. J., Charlton, P., Templeton, D., van Zonneveld, A. J., Bevan, P., Pannekoek, H. & ten Cate, J. W. (1997). Novel low-molecular-weight inhibitor of PAI-1 (XR5118) promotes endogenous fibrinolysis and reduces postthrombolysis thrombus growth in rabbits. *Circulation* **96**, 916-21.

Gandolfo, G. M., Conti, L. & Vercillo, M. (1996). Fibrinolysis components as prognostic markers in breast cancer and colorectal carcinoma. *Anticancer Research* **16**, 2155-9.

Harrop, S. J., Jankova, L., Coles, M., Jardine, D., Whittaker, J. S., Gould, A. R., Meister, A., King, G. C., Mabbutt, B. C. & Curmi, P. M. (1999). The crystal structure of plasminogen activator inhibitor 2 at 2.0 Å resolution: implications for serpin function. *Structure* **7**, 43-54.

Hart, T. N., Ness, S. R. & Read, R. J. (1997). Critical evaluation of the research docking program for the CASP2 challenge. *Proteins* **Suppl**, 205-9.

Hart, T. N. & Read, R. J. (1992). A multiple-start Monte Carlo docking method. *Proteins* **13**, 206-22.

Huntington, J. A., Olson, S. T., Fan, B. & Gettins, P. G. (1996). Mechanism of heparin activation of antithrombin. Evidence for reactive center loop preinsertion with expulsion upon heparin binding. *Biochemistry* **35**, 8495-503.

Jiang, J. S. & Brünger, A. T. (1994). Protein hydration observed by X-ray diffraction. Solvation properties of penicillopepsin and neuraminidase crystal structures. *Journal of Molecular Biology* **243**, 100-15.

Jin, L., Abrahams, J. P., Skinner, R., Petitou, M., Pike, R. N. & Carrell, R. W. (1997). The anticoagulant activation of antithrombin by heparin. *Proceedings of the National Academy of Sciences of the United States of America* **94**, 14683-8.

Juhan-Vague, I. (1996). Haemostatic parameters and vascular risk. *Atherosclerosis* **124**, S49-55.

Juhan-Vague, I. & Alessi, M. C. (1997). PAI-1, obesity, insulin resistance and risk of cardiovascular events. *Thrombosis & Haemostasis* **78**, 656-60.

Keeton, M., Ahn, C., Eguchi, Y., Burlingame, R. & Loskutoff, D. J. (1995). Expression of type 1 plasminogen activator inhibitor in renal tissue in murine lupus nephritis. *Kidney International* **47**, 148-57.

Keijer, J., Linders, M., van Zonneveld, A. J., Ehrlich, H. J., de Boer, J. P. & Pannekoek, H. (1991). The interaction of plasminogen activator inhibitor 1 with plasminogen activators (tissue-type and urokinase-type) and fibrin: localization of interaction sites and physiologic relevance. *Blood* **78**, 401-9.

Kjoller, L., Kanse, S. M., Kirkegaard, T., Rodenburg, K. W., Ronne, E., Goodman, S. L., Preissner, K. T., Ossowski, L. & Andreasen, P. A. (1997). Plasminogen activator inhibitor-1 represses integrin- and vitronectin-mediated cell migration independently of its function as an inhibitor of plasminogen activation. *Experimental Cell Research* **232**, 420-9.

Kleywegt, G. J. & Brünger, A. T. (1996). Checking your imagination: applications of the free R value. *Structure* **4**, 897-904.

Kraulis, P. J. (1991). MOLSCRIPT: A program to produce both detailed and schematic plots of protein structures. *Journal of Applied Crystallography* **24**, 946-50.

Laskowski, R. A., MacArthur, M. W., Moss, D. S. & Thornton, J. M. (1993). PROCHECK: a program to check the stereochemical quality of protein structures. *Journal of Applied Crystallography* **26**, 283-91.

Lawrence, D. A., Palaniappan, S., Stefansson, S., Olson, S. T., Francis-Chmura, A. M., Shore, J. D. & Ginsburg, D. (1997). Characterization of the binding of different conformational forms of plasminogen activator inhibitor-1 to vitronectin. Implications for the regulation of pericellular proteolysis. *Journal of Biological Chemistry* **272**, 7676-80.

Levi, M., Biemond, B. J., van Zonneveld, A. J., ten Cate, J. W. & Pannekoek, H. (1992). Inhibition of plasminogen activator inhibitor-1 activity results in promotion of endogenous thrombolysis and inhibition of thrombus extension in models of experimental thrombosis. *Circulation* **85**, 305-12.

Li, J., Wang, Z., Canagarajah, B., Jiang, H., Kanost, M. & Goldsmith, E. J. (1999). The structure of active serpin 1K from Manduca sexta. *Structure* **7**, 103-9.

Lijnen, H. R., Bachmann, F., Collen, D., Ellis, V., Pannekoek, H., Rijken, D. C. & Thorsen, S. (1994). Mechanisms of plasminogen activation. *Journal of Internal Medicine* **236**, 415-24.

Loebermann, H., Tokuoka, R., Deisenhofer, J. & Huber, R. (1984). Human alpha 1-proteinase inhibitor. Crystal structure analysis of two crystal modifications, molecular model and preliminary analysis of the implications for function. *Journal of Molecular Biology* **177**, 531-57.

Look, M. P. & Foekens, J. A. (1999). Clinical relevance of the urokinase plasminogen activator system in breast cancer. *Apmis* **107**, 150-9.

McRee, D. E. (1999). XtalView/Xfit - A versatile program for manipulating atomic coordinates and electron density. *Journal of Structural Biology* **125**, 156-65.

Meijer, M. v., Smilde, A., Tans, G., Nesheim, M. E., Pannekoek, H. & Horrevoets, A. J. G. (1997). The Suicide Substrate Reaction Between Plasminogen Activator Inhibitor 1 and Thrombin is regulated by the Cofactors Vitronectin and Heparin. *Blood* **90**, 1874-1882.

Moscatelli, D. & Rifkin, D. B. (1988). Membrane and matrix localization of proteinases: a common theme in tumor cell invasion and angiogenesis. *Biochimica et Biophysica Acta* **948**, 67-85.

Mottonen, J., Strand, A., Symersky, J., Sweet, R. M., Danley, D. E., Geoghegan, K. F., Gerard, R. D. & Goldsmith, E. J. (1992). Structural basis of latency in plasminogen activator inhibitor-1. *Nature* **355**, 270-3.

Nicholls, A., Sharp, K. A. & Honig, B. (1991). Protein folding and association: insights from the interfacial and thermodynamic properties of hydrocarbons. *Proteins* **11**, 281-96.

Nykjaer, A., Petersen, C. M., Moller, B., Jensen, P. H., Moestrup, S. K., Holtet, T. L., Etzerodt, M., Thogersen, H. C., Munch, M., & Andreasen, P. A.(1992). Purified alpha 2-macroglobulin receptor/LDL receptor-related protein binds urokinase.plasminogen activator inhibitor type-1 complex. Evidence that the alpha 2-macroglobulin receptor mediates cellular degradation of urokinase receptor-bound complexes. *Journal of Biological Chemistry* **267**, 14543-6.

Ohlsson, M., Peng, X. R., Liu, Y. X., Jia, X. C., Hsueh, A. J. & Ny, T. (1991). Hormone regulation of tissue-type plasminogen activator gene expression and plasminogen activator-mediated proteolysis. *Seminars in Thrombosis & Hemostasis* **17**, 286-90.

Otwinowski, Z. & Minor, W. (1997). Processing of X-Ray Diffraction Data Collected in Oscillation Mode. *Methods in enzymology* **276**, 307-326.

Pannu, N. S. & Read, R. J. (1996). Improved structure refinement through maximum likelihood. *Acta Crystallographica* **A52**, 659-668.

Pappot, H., Gardsvoll, H., Romer, J., Pedersen, A. N., Grondahl-Hansen, J., Pyke, C. & Brunner, N. (1995). Plasminogen activator inhibitor type 1 in cancer: therapeutic and prognostic implications. *Biological Chemistry Hoppe-Seyler* **376**, 259-67.

Philippe, J., Offner, F., Declerck, P. J., Leroux-Roels, G., Vogelaers, D., Baele, G. & Collen, D. (1991). Fibrinolysis and coagulation in patients with infectious disease and sepsis. *Thrombosis & Haemostasis* **65**, 291-5.

Podor, T. J., Joshua, P., Butcher, M., Seiffert, D., Loskutoff, D. & Gauldie, J. (1992). Accumulation of type 1 plasminogen activator inhibitor and vitronectin at sites of cellular necrosis and inflammation. *Annals of the New York Academy of Sciences* **667**, 173-7.

Pontius, J., Richelle, J. & Wodak, S. J. (1996). Deviations from standard atomic volumes as a quality measure for protein crystal structures. *Journal of Molecular Biology* **264**, 121-36.

Preissner, K. T., May, A. E., Wohn, K. D., Germer, M. & Kanse, S. M. (1997). Molecular crosstalk between adhesion receptors and proteolytic cascades in vascular remodelling. *Thrombosis & Haemostasis* **78**, 88-95.

Read, R. J. (1999). Detecting outliers in non-redundant diffraction data. *Acta Crystallographica* **D55**, 1759-1764.

Read, R. J. (1986). Improved Fourier coefficients for maps using phases from partial structures with errors. *Acta Crystallographica* **A42**, 140-9.

Rice, L. M. & Brünger, A. T. (1994). Torsion angle dynamics: reduced variable conformational sampling enhances crystallographic structure refinement. *Proteins* **19**, 277-90.

Samad, F. & Loskutoff, D. J. (1997). The fat mouse: a powerful genetic model to study elevated plasminogen activator inhibitor 1 in obesity/NIDDM. *Thrombosis & Haemostasis* **78**, 652-5.

Schreuder, H. A., de Boer, B., Dijkema, R., Mulders, J., Theunissen, H. J., Grootenhuis, P. D. & Hol, W. G. (1994). The intact and cleaved human antithrombin III complex as a model for serpin-proteinase interactions. *Nature Structural Biology* **1**, 48-54.

Seiffert, D., Mimuro, J., Schleef, R. R. & Loskutoff, D. J. (1990). Interactions between type 1 plasminogen activator inhibitor, extracellular matrix and vitronectin. *Cell Differentiation & Development* **32**, 287-92.

Seiffert, D. & Smith, J. W. (1997). The cell adhesion domain in plasma vitronectin is cryptic. *Journal of Biological Chemistry* **272**, 13705-10.

Sharp, A. M., Stein, P. E., Pannu, N. S., Carrell, R. W., Berkenpas, M. B., Ginsburg, D., Lawrence, D. A. & Read, R. J. (1999). The active conformation of plasminogen activator inhibitor 1, a target for drugs to control fibrinolysis and cell adhesion. *Structure* **7**, 111-8.

Speck, A. L. (1990) PLATON, an integrated tool for the analysis of the results of a single crystal structure determination. *Acta Crystallographica* **A46**, C-34.

Sprengers, E. D. & Kluft, C. (1987). Plasminogen activator inhibitors. *Blood* **69**, 381-7.

Stefansson, S., Haudenschild, C. C. & Lawrence, D. A. (1998). Beyond Fibrinolysis: The role of Plasminogen Activator Inhibitor-1 and Vitronectin in Vascular Wound Healing. *Trends in Cardiovascular Medicine* **8**, 175-180.

Stefansson, S. & Lawrence, D. A. (1996). The serpin PAI-1 inhibits cell migration by blocking integrin alpha V beta 3 binding to vitronectin. *Nature* **383**, 441-3.

Stein, P. & Chothia, C. (1991). Serpin tertiary structure transformation. *Journal of Molecular Biology* **221**, 615-21.

Stein, P. E., Leslie, A. G., Finch, J. T. & Carrell, R. W. (1991). Crystal structure of uncleaved ovalbumin at 1.95 Å resolution. *Journal of Molecular Biology* **221**, 941-59.

Stein, P. E., Leslie, A. G., Finch, J. T., Turnell, W. G., McLaughlin, P. J. & Carrell, R. W. (1990). Crystal structure of ovalbumin as a model for the reactive centre of serpins. *Nature* **347**, 99-102.

Stephens, R. W., Brunner, N., Janicke, F. & Schmitt, M. (1998). The urokinase plasminogen activator system as a target for prognostic studies in breast cancer. *Breast Cancer Research & Treatment* **52**, 99-111.

Stratikos, E. & Gettins, P. G. (1999). Formation of the covalent serpin-proteinase complex involves translocation of the proteinase by more than 70 A and full insertion of the reactive center loop into beta-sheet A. *Proceedings of the National Academy of Sciences of the United States of America* **96**, 4808-13.

Sui, G. C. & Wiman, B. (1998). Stability of plasminogen activator inhibitor-1: role of tyrosine 221. *FEBS Letters* **423**, 319-23.

Tang, W. H., Friess, H., di Mola, F. F., Schilling, M., Maurer, C., Graber, H. U., Dervenis, C., Zimmermann, A. & Buchler, M. W. (1998). Activation of the serine proteinase system in chronic kidney rejection. *Transplantation* **65**, 1628-34.

Tucker, H. M., Mottonen, J., Goldsmith, E. J. & Gerard, R. D. (1995). Engineering of plasminogen activator inhibitor-1 to reduce the rate of latency transition. *Nature Structural Biology* **2**, 442-5.

Urano, T., Serizawa, K., Takada, Y., Ny, T. & Takada, A. (1994). Heparin and heparan sulfate enhancement of the inhibitory activity of plasminogen activator inhibitor type 1 toward urokinase type plasminogen activator. *Biochimica et Biophysica Acta* **1201**, 217-22.

van Boeckel, C. A., Grootenhuis, P. D. & Visser, A. (1994). A mechanism for heparin-induced potentiation of antithrombin III. *Nature Structural Biology* **1**, 423-5.

Vellieux, F. M. D. A. P., Hunt, J. F., Roy, S. & Read, R. J. (1995). DEMON/ANGEL: a suite of programs to carry out density modification. *Journal of applied crystallography* **28**, 347-351.

Vriend, G. (1990). WHAT IF: a molecular modeling and drug design program. *Journal of Molecular Graphics* **8**, 52-6.

Wagner, O. F., de Vries, C., Hohmann, C., Veerman, H. & Pannekoek, H. (1989). Interaction between plasminogen activator inhibitor type 1 (PAI-1) bound to fibrin and either tissue-type plasminogen activator (t-PA) or urokinase-type plasminogen activator (u-PA). Binding of t-PA/PAI-1 complexes to fibrin mediated by both the finger and the kringle-2 domain of t-PA. *Journal of Clinical Investigation* **84**, 647-55.

Wilczynska, M., Fa, M., Karolin, J., Ohlsson, P. I., Johansson, L. B. & Ny, T. (1997). Structural insights into serpin-protease complexes reveal the inhibitory mechanism of serpins. *Nature Structural Biology* **4**, 354-7.

Wiman, B. (1995). Plasminogen activator inhibitor 1 (PAI-1) in plasma: its role in thrombotic disease. *Thrombosis & Haemostasis* **74**, 71-6.

Wiman, B., Csemiczky, G., Marsk, L. & Robbe, H. (1984). The fast inhibitor of tissue plasminogen activator in plasma during pregnancy. *Thrombosis & Haemostasis* **52**, 124-6.

Wright, H. T. (1996). The structural puzzle of how serpin serine proteinase inhibitors work. *Bioessays* **18**, 453-64.

Wright, H. T. & Scarsdale, J. N. (1995). Structural basis for serpin inhibitor activity. *Proteins* **22**, 210-25.

Xue, Y., Björquist, P., Inghardt, T., Linschoten, M., Musil, D., Sjolin, L. & Deinum, J. (1998). Interfering with the inhibitory mechanism of serpins: crystal structure of a complex formed between cleaved plasminogen activator inhibitor type 1 and a reactive-centre loop peptide. *Structure* **6**, 627-36.

Yamamoto, K. & Loskutoff, D. J. (1996). Fibrin deposition in tissues from endotoxin-treated mice correlates with decreases in the expression of urokinase-type but not tissue-type plasminogen activator. *Journal of Clinical Investigation* **97**, 2440-51.

Yamamoto, K., Loskutoff, D. J. & Saito, H. (1998). Renal expression of fibrinolytic genes and tissue factor in a murine model of renal disease as a function of age. *Seminars in Thrombosis & Hemostasis* **24**, 261-8.

Zimmermann, H. & Burzlaff, H. (1985). DELOS – A computer program for the

determination of a unique conventional cell. *Zeitschrift für Kristallographie* 170,

241-6.

4.0 Refinement of the Native Structures of Wild-Type and F30A Mutant Shiga-Like Toxin-1.*

4.1 Introduction

Enterohemorrhagic strains of *Escherichia coli,* such as O157:H7, produce Shiga-like toxins (SLTs, also called verotoxins) that are believed to play a role in the pathogenesis of hemorrhagic colitis, and to be the main cause of hemolytic uremic syndrome (HUS). These conditions constitute the 'hamburger disease' form of food poisoning, which causes discomfort, serious kidney damage, and occasionally death, particularly in children and seniors (Reviewed in Karmali, 1989).

There are two types of SLT found in enterohemorrhagic *E. coli* strains: SLT-1 and SLT-2. These show considerable sequence identity to each other and, as their name suggests, to the Shiga toxin of *Shigella dysenteriae*, to which SLT-1 is virtually identical (Karmali, 1989) (Figure 1.8). All these toxins, like the enterotoxin of *Vibrio cholerae*, the heat-labile enterotoxin of enteropathogenic *E. coli*, and the toxin of *Bordetella pertussis*, are AB$_5$ toxins. A toxic A subunit is attached to a pentamer of cell surface receptor-binding B subunits responsible for cell entry (Brunton, 1990; Brunton, 1994; Burnette, 1994; Moss & Vaughan, 1988; O'Brien & Holmes, 1987; Spangler, 1992). The nature of the A subunit varies among the members of the AB$_5$ family. In Shiga toxin and the SLTs, it is a ricin-like N-glycosidase that cleaves an adenine from the 60S ribosomal particle, fatally halting cellular protein synthesis (Endo *et al.*, 1988; Saxena *et al.*, 1989).

---

* Portions of this chapter has been published. Clark *et al.*, Molecular Microbiology, 19:891-899.

The B-pentamer serves as a lectin, binding cell surface glycolipids and facilitating toxin entry into the cell by endocytosis and retrograde transport (Donohue-Rolfe *et al.*, 1984; Olsnes *et al.*, 1981). Shiga toxin, SLT-1, SLT-2, and the variant strain SLT-2c all bind the glycolipid globotriaosylceramide (Gb$_3$) (Jacewicz *et al.*, 1986; Lindberg *et al.*, 1987; Lingwood *et al.*, 1987; Waddell *et al.*, 1990), which targets the toxin to a variety of cells, including endothelial cells, enteric cells, kidney cells, and some immune system and neural cells (Boyd *et al.*, 1993; Cohen *et al.*, 1990; Richardson *et al.*, 1992; Zoja *et al.*, 1992). Variant SLT-2e preferentially binds the related glycolipid globotetraosylceramide, Gb$_4$, modifying the target cell specificity with stronger binding to gastrointestinal cells and different classes of neural cells, and resulting in a symptomatically different edema disease of pigs (Boyd *et al.*, 1993; DeGrandis *et al.*, 1989; Samuel *et al.*, 1990).

Antibiotic treatments of HUS have been shown to be ineffective, probably due to the enhanced release of SLT from the periplasm of dead bacteria (Neill, 1998). A technique that focuses on inhibiting cell entry by the B-pentamer has shown some promise in preliminary trials (Armstrong *et al.*, 1995). Patients are fed Synsorb, a chromatographic resin to which the trisaccharide moiety of Gb$_3$ has been attached covalently, in order to competitively bind toxin in the intestine before it has an opportunity to cause cellular damage. Work is underway to provide glycoside derivatives with greater toxin binding affinity (Kitov, in press). These efforts have been aided considerably by a series of crystal structures of the B-pentamer, including some with glycosides bound (Ling, 1999; Ling *et al.*, 1998; Stein *et al.*, 1992).

The structure of the B-pentamer of SLT-1 was published in 1992 (Stein *et al.*, 1992). This revealed a structure similar to that of the previously solved heat-labile enterotoxin, suggesting that they were related proteins despite a lack of sequence identity (Sixma *et al.*, 1991; Sixma *et al.*, 1993). The pentamer is arranged around a central pore lined by α-helices (Figure 1.7). The outer surface of the protein is formed by antiparallel 6-stranded β-sheets, for which 3 strands are contributed by 1 monomer, and the remaining strands by its neighbor.

The quaternary structure of the B-pentamer of SLT-1 was seen to differ from that of heat-labile enterotoxin in that the SLT-1 B-pentamer lacked perfect 5-fold symmetry (Stein *et al.*, 1992). Instead, a translational motion along the rotational axis imparts a screw rotation that disrupts the interface between two monomers (Figure 4.1). The distortion from a proper rotation was similar to that seen in a lockwasher, in comparison to a normal washer. The distortion was thus referred to as the lockwasher distortion. This was suspected to be an artifact of crystallization, a suspicion that was supported by the structure of the Shiga holotoxin, where the B-pentamer had proper 5-fold symmetry (Fraser *et al.*, 1994). Zinc ions bound to the B-pentamer were also thought to be artifacts that served to mediate crystal contacts (Stein *et al.*, 1992).

The Shiga holotoxin structure revealed that the central pore of the B-pentamer is occupied by the C-terminal helix of the A monomer (Fraser *et al.*, 1994). This interaction forms about half of the 2000 Å^2 of buried surface area between the A and B parts of the holotoxin. The outer sides and the face of the B-pentamer opposite the A subunit are not covered by this interaction, which correlated with a proposal that the carbohydrate binding site was in this region.
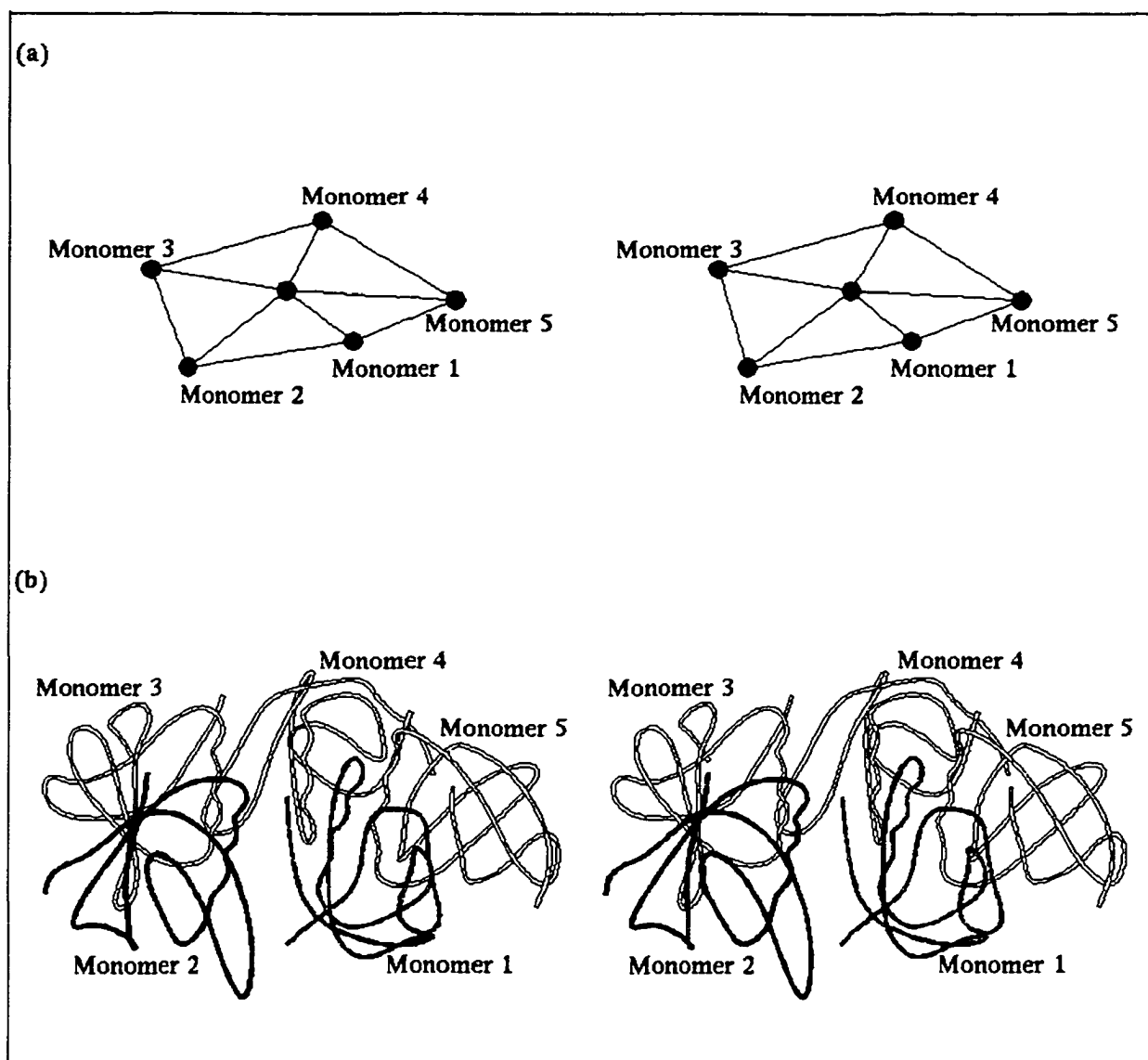
Figure 4.1: The lockwasher distortion. Based on Stein *et al.*, 1992. Part (a) shows a schematic view of the distortion. The monomers are represented by spheres located at their centres of mass, while the centre of mass of the pentamer is represented by the central blue dot. A Cα trace of the pentamer in the same orientation is shown in (b) with monomers 1 and 2 shown in red and blue respectively. This figure was made using Molscript (Kraulis, 1991).

Investigation of the B-pentamer structure had revealed a patch of conserved amino acid residues in a deep groove at the monomer-monomer interfaces (Stein *et al.*, 1992). This was proposed as a Gb3 binding site (later referred to as Site 1) (Figure 1.10). A prominent hydrophobic group in the middle of this region, Phe 30, was mutated to an alanine, in order to test the role of this site in receptor binding (Clark *et al.*, 1996). This mutation reduces the glycoside binding ability of the toxin dramatically and the cytotoxicity of the holotoxin by a factor of 10^5.

Cocrystallization of the B-pentamer with a Gb3 analogue was later undertaken, and revealed some surprising results (Ling *et al.*, 1998). While sugar binding was observed at Site 1, binding could also be observed at two other sites on each monomer: in the middle of the bulging outer face of each monomer (Site 2), and at the site of the solvent-exposed Trp 34 residues circling the pore on the face opposite to the A subunit (Site 3)(Figure 1.10). Subsequent work on mutant forms of SLT-1 and SLT-2e have confirmed the existence of the three distinct binding sites (Ling, 1999). While Phe 30 makes a tangential contact with Site 2, it does not contact Site 3 at all. A double mutant form of Phe 30 and Trp 34 retains sugar binding at Site 2. As Site 2 is more consistently occupied in the various crystal forms, the relative importance of the binding sites, and the significance of the F30A mutation, remain unclear.

In the present work, the structures of the native wild-type and F30A mutant B-pentamers are refined completely. This allows detailed investigation of several points about the structures. The nature of the lockwasher distortion and the forces causing it are discussed, the effect of zinc ions on the crystal morphology is explained, the unliganded

conformation of the sugar binding sites is described and the effect of the F30A mutation on Site 1 is considered.

4.2 Methods

4.2.1 Diffraction Data

Both wild-type and F30A mutant verotoxin B subunits were supplied by Dr. J. L. Brunton (University of Toronto), and were prepared as previously reported (Ramotar *et al.*, 1990). Both were crystallized under similar conditions using the hanging drop method (Boodhoo *et al.*, 1991). Crystals could be obtained using protein solutions of 5 to 8 mg/ml and a well solution of either 10 to 12 % PEG 8000 with 50 mM MOPS, pH 6.8 to 7.0 or 1.6 to 1.8 M Na/K phosphate, pH 6.8 to 7.0. The addition of 1.5 mM zinc chloride improved the morphology of the wild-type crystals from thin plates to thicker prisms (Stein *et al.*, 1992) but had no effect on the crystals of the mutant protein (Clark *et al.*, 1996).

Data collection methods and statistics have previously been reported for the wild-type structure (Stein *et al.*, 1992) and for the F30A mutant (Clark *et al.*, 1996), and are summarized in Table 4.1. The wild-type data set was collected with a San Diego-style multiwire counter area detector with a Rigaku rotating anode source. The mutant data set was collected using the screenless Weissenberg camera (Sakabe, 1991) at the Photon Factory in Tsukuba, Japan. For this data set, data from thirty-four imaging plates in two different crystal orientations were indexed with a unit cell that was virtually isomorphous with that of the wild-type data set.

Table 4.1 Data Collection Statistics for Native and F30A Mutant Verotoxin B

Subunits.

	Native	**Mutant**
Space group	$P2_12_12_1$	$P2_12_12_1$
Unit cell dimensions:		
a, b, c (Å)	59.6, 102.4, 56.1	59.8, 102.5, 56.0
α, β, γ (°)	90.00, 90.00, 90.00	90.00, 90.00, 90.00
Resolution limits (Å)	24.7-2.2	51.7-2.0
Total number of observations	84,281	94,920
Number of unique reflections	17,298	23,368
Number of test set reflections	757	1030
Completeness of data:		
Overall (%)	95.9	97.5
Highest resolution shell (%)	87.5 (2.34-2.20 Å)	94.3 (2.13-2.00 Å)
R_{merge}*:	0.054	0.07

* $R_{merge} = \Sigma_{(i)} (|I_i - <I_i>|/\Sigma(I_i))$ where I_i = an individual observation and $<I_i>$ is the averaged observation for a given Miller index.

4.2.2 Model refinement

The preliminary wild-type structure (Stein *et al.*, 1992) was used as the starting model for further refinement of the wild-type and mutant structures. For the wild-type, the complete model structure, with all waters and zinc atoms was used; for the mutant, the phenyl ring was deleted from residue 30 and the waters, but not the zinc atoms, were removed. The structures were then subjected to alternating rounds of refinement and structure adjustment. XPLOR (Brünger *et al.*, 1987) was used to carry out energy minimization and B-factor refinement, applying weak restraints on non-crystallographic symmetry (NCS). The program O (Jones *et al.*, 1991) was employed for structure adjustment. Fo-Fc and 2Fo-Fc maps were calculated with the Groningen Biomol program package, with SIGMAA model bias corrections (Read, 1986). Data from the program PROCHECK (Laskowski *et al.*, 1993) were used to indicate structural regions requiring adjustment. After two rounds of refinement and adjustment, further techniques were employed in an attempt to resolve uncertain details. Structures with Trp 34 sidechains deleted from all monomers were refined with XPLOR to determine if a clear orientation for this poorly resolved residue could be obtained, with negative results. Various refinement alternatives were tested at this point, with TNT (Tronrud, 1992) without NCS restraints having the best effect. TNT refinement took the mutant structure from an R-factor of 0.228 to 0.198 and the wild-type from a R-factor of 0.222 to 0.194. It was found necessary to restrain the zinc-oxygen and zinc-nitrogen distances to values determined from a search of the CSD database (Allen & Kennard, 1993). Final refinement led to values of 0.192 for the R-factors of both structures.

Initial refinements were carried out before the use of cross-validation (Brünger, 1992) had become established practice. In order to test the validity of the low level of NCS restraint used in the refinement, and to provide an R_{free} value, the models output from TNT were subjected to further refinement with the program CNS (Brünger *et al.*, 1998). A test data set was selected, using the same reflections in both data sets, and the structures were refined with constant temperature molecular dynamics runs (Brünger *et al.*, 1990) to reduce overfitting in the free set. In the course of these dynamics runs, both the R-factor and the R_{free} rose. In the case of the mutant structures the R-factor increased from 0.185 to 0.250, while the R_{free} increased from 0.187 to 0.277. In the case of the wild-type, the R-factor increased from 0.171 to 0.232, while the R_{free} increased from 0.172 to 0.257. A series of minimization runs testing different NCS restraints was carried out. Judging from the R-factors and from the differences between the R and R_{free}, it appeared to be best not to apply restraints to residues affected by the lockwasher distortion or by crystal contacts, while a low level of restraint was best for the remaining residues. A simulated annealing run was then used to give the models used for the final data statistics. The close correspondence maintained between the R and R_{free} supports the merits of the weighting scheme.

4.3 Results and Discussion

4.3.1 Preliminary difference Fourier analysis.

The mutant data were initially compared to the native data by difference Fourier analysis, using F_{nat}-F_{mut} amplitudes to 2.2 Å. The five strongest positive peaks in the map were found at the sites of the Phe 30 side chains and are due to the loss of the side

chains in the mutant protein (Figure 4.2). Small negative peaks in their vicinity appear to indicate small motions in neighboring side chains. Stronger negative peaks were at the sites of the crystallographic zinc atoms, indicating higher occupancies in the mutant. There were no major peaks away from the mutation and zinc sites, indicating that there were no other significant changes between the native and mutant structures. Thus the mutation of the phenyl ring appears to cause minor rearrangements at the mutation sites and no rearrangements in the overall secondary or tertiary structures.

4.3.2 Overall quality of structure

The refinement statistics for the final models of the wild type and mutant proteins are summarized in Table 4.2. The structures of the wild type and mutant proteins are similar overall to the original model, although several minor errors in side chain location have been corrected. The water structure has been considerably revised, with several of the original waters deleted and many new ones added. Several of the residues have atoms that remain poorly resolved in the final structure; they are summarized in Table 4.3. In general, these represent disordered side chains. The final structures have been analyzed by several validation programs, including PROCHECK (Laskowski *et al.*, 1993), PROVE (Pontius *et al.*, 1996), and the WHATIF package (Vriend, 1990), and no global problems have been determined. The ϕ and ψ angles of all non-glycine residues in the structures are in allowed regions of the Ramachandran plot-(Figures 4.3 and 4.4). Typical electron density for the final structures is shown in Figure 4.5.

As noted in the original structure paper, the toxin does not display perfect 5-fold symmetry, but instead has a small screw distortion. Four of the 5 pairs of adjacent
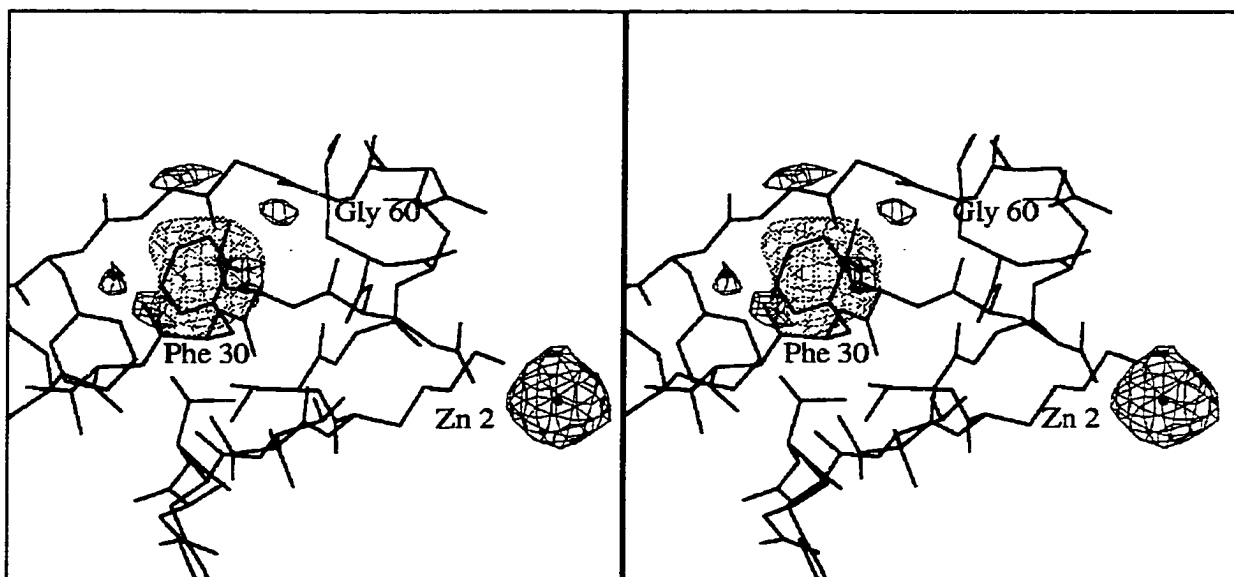
Figure 4.2: Fnat-Fmut difference map of VT1B and Phe-30-Ala mutant showing residue

30 of monomer 4 and Zn 2. Positive electron density is indicated with light grey lines

and negative electron density with black lines. The strongest positive and negative in the

structure are shown in this figure. Electron density is contoured at four times the root

mean density. This figure was made with BobScript (Esnouf, 1997).

Table 4.2: Data Refinement Statistics for Native and F30A Mutant Verotoxin B Subunits.

	Native	Mutant
Monomers/asymmetric unit	5 (1 pentamer)	5 (1 pentamer)
Number of non-hydrogen protein atoms	2700	2670
Number of ion atoms (Zn^{++})	2	2
Number of solvent atoms (waters)	135	121
Mean B^{**} of protein atoms (Å^2)	25.39	25.69
Mean B^{**} of solvent atoms (Å^2)	43.87	39.32
R-factor[†]	0.209	0.218
R_{free}[‡]	0.212	0.219
RMS deviations from ideal geometry:		
Bond lengths (Å)	0.007	0.007
Bond angles (°)	1.2	1.3
Dihedral angles (°)	24.0	24.2
Improper angles (°)	0.67	0.68

[**] $B=8\pi^2<u^2>$ where u is the amplitude of atomic vibration in any given direction for a given atom.

[†] R-factor $= \Sigma_{(i)} (\|F_{obs(h_i)}\|-k\|F_{c(h_i)}\|/ \Sigma_{(i)}\|F_{obs(h_i)}\|)$ where h_i = an individual Miller index in the working set, F_{obs} = observed reflection, F_c = calculated reflection, k = scaling factor.

[‡] R_{free} is calculated using the same equations as R-factor, but h_i = an individual Miller index in the test set.

Table 4.3: Residues with poor fit to electron density[*].

Residue	Mutant Subunits	Wild-Type Subunits
Lysine 8	4	1, 4
Glutamate 10	5	5
Lysine 13	1, 5	1, 5
Aspartate 16	2	2
Aspartate 18		2
Valine 24	5	
Aspartate 26	3	
Lysine 27	5	
Glutamate 28	5	3
Tryptophan 34	2	2
Valine 50	1	
Arginine 69	1, 3, 5	1, 3, 5

[*]Poor fit is indicated by at least one atom being out of density in a map contoured at the level of the root-mean-square density of the map.
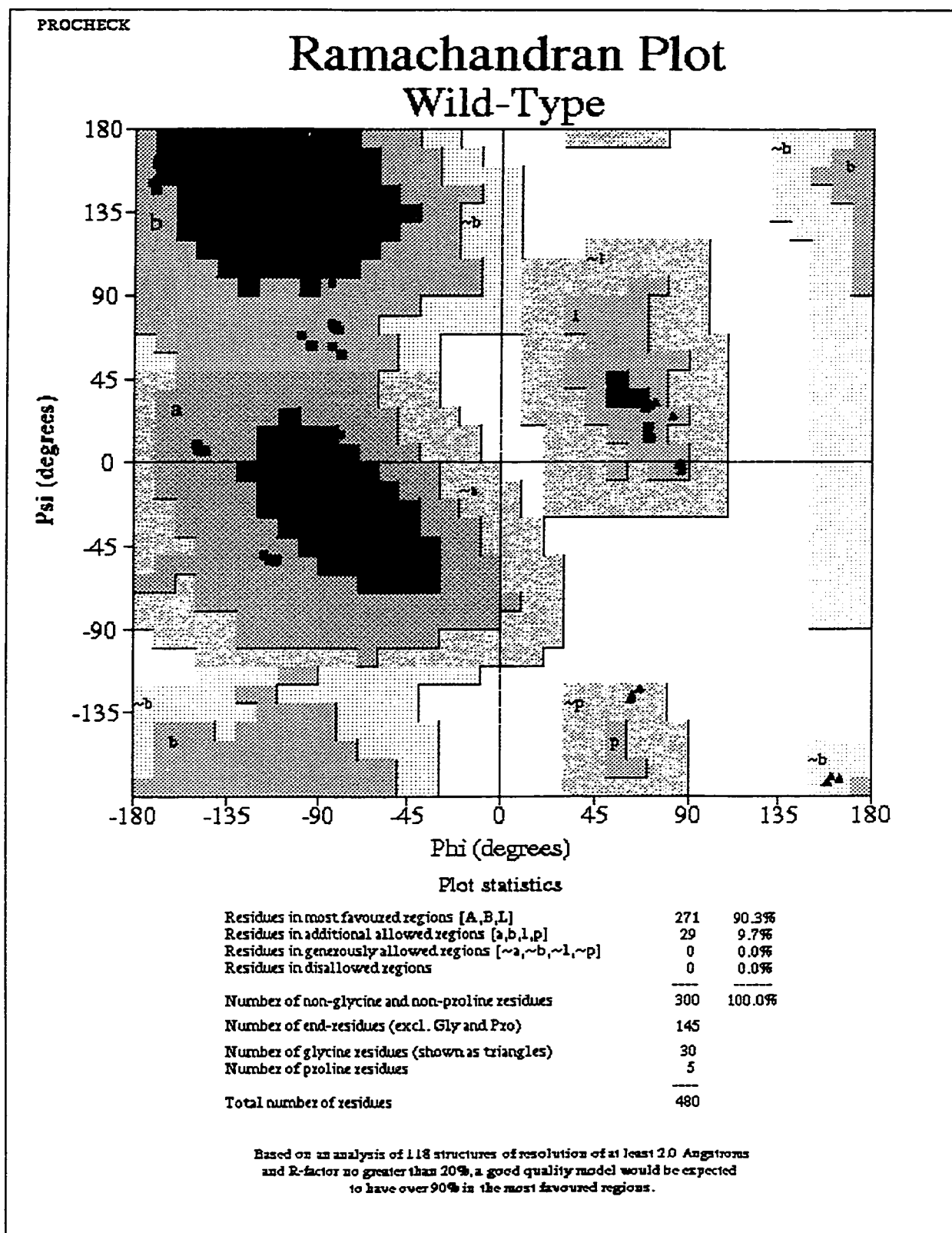
Figure 4.3: Ramachandran plot of the wild-type pentamer. Adapted from PROCHECK (Laskowski *et al.*, 1993).

PROCHECK

Ramachandran Plot
Mutant

Psi (degrees)

Phi (degrees)

Plot statistics

Residues in most favoured regions [A,B,L]	267	89.0%
Residues in additional allowed regions [a,b,l,p]	33	11.0%
Residues in generously allowed regions [~a,~b,~l,~p]	0	0.0%
Residues in disallowed regions	0	0.0%
	---	---
Number of non-glycine and non-proline residues	300	100.0%
Number of end-residues (excl. Gly and Pro)	133	
Number of glycine residues (shown as triangles)	30	
Number of proline residues	5	

Total number of residues	468	

Based on an analysis of 118 structures of resolution of at least 2.0 Angstroms
and R-factor no greater than 20%, a good quality model would be expected
to have over 90% in the most favoured regions.

Figure 4.4: Ramachandran plot of the mutant pentamer. Adapted from PROCHECK
(Laskowski *et al.*, 1993).
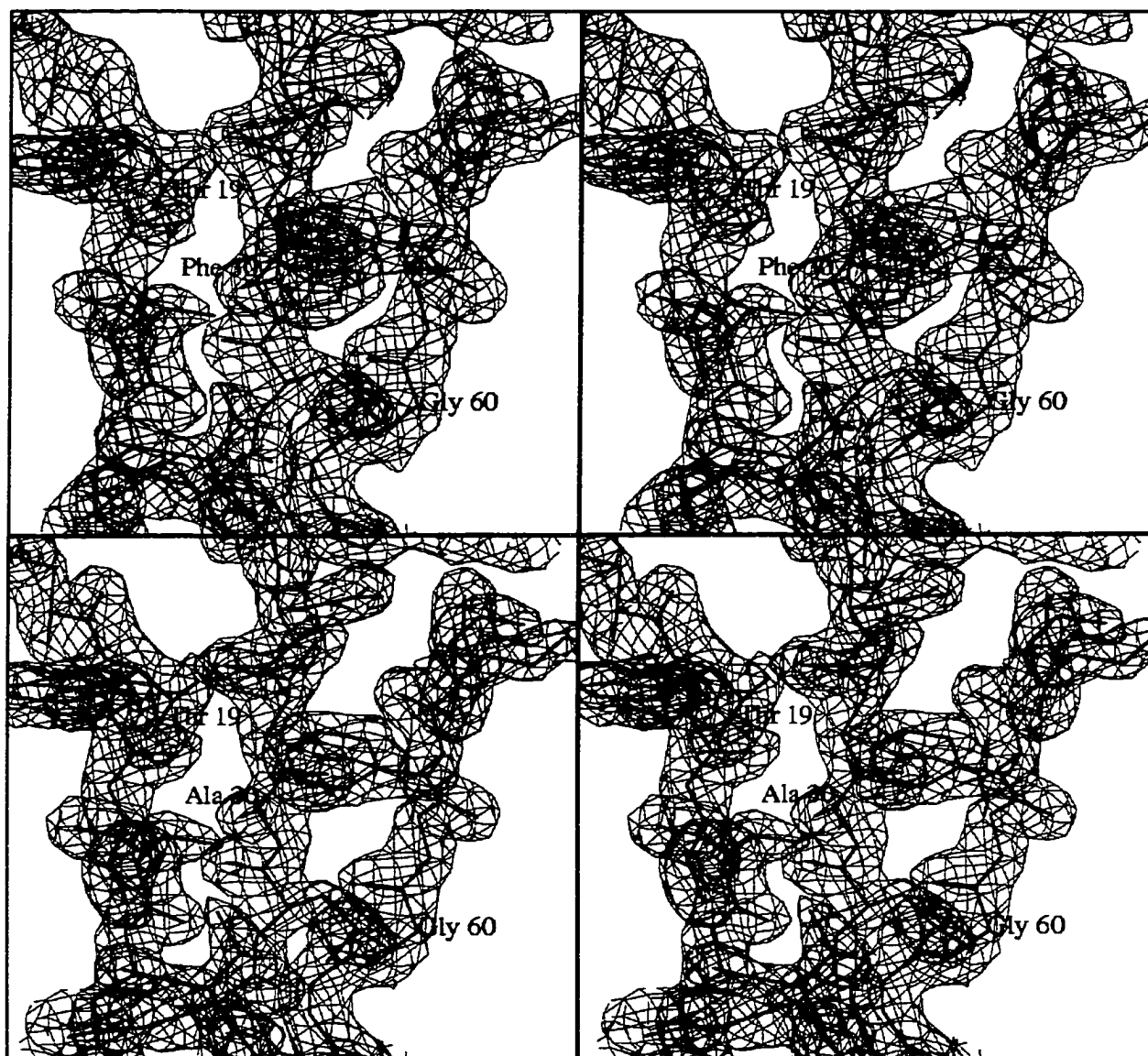
Figure 4.5: Electron density at the mutation site in (a) the wild type structure; (b) the mutant structure. Density is contoured at the 1 σ level. Figure produced using Bobscript (Esnouf, 1997).

monomers are related by a 72° rotation and a 1.3 Å translation. This leads to the monomer-monomer interface between the final pair, monomers 1 and 2, being considerably different. Distortion from perfect five-fold symmetry has not been observed to such a great extent in other toxin B-pentamer structures, including other crystal forms of Shiga-like toxin-1, and is presumably due to stresses produced by the crystal packing (discussed below).

In general, the structures of all monomers in the native and mutant structures are very similar to each other, as well as being similar to those in other SLT-1 structures. The similarity is, for the most part, only violated at the site of crystal contacts, and at the lockwasher-distorted interface between monomers 1 and 2. These changes are summarized in Table 4.4. Variations in conformation occur at other residues, but probably indicate poorly resolved or disordered residues.

4.3.3 Changes at the Mutation Site

In general, the refined structures of native wild-type and F30A mutant SLT-1 confirm the observation from difference Fourier analysis that the mutation causes little structural change apart from elimination of the phenyl ring (Figure 4.7(a)). There are few obvious changes other than at the immediate site of the mutation. Investigation of the region is complicated by the problem that the F30A mutation occurs in a sequence with a certain degree of flexibility, as can be judged by comparing r.m.s.d. values between different monomers, and by slightly elevated temperature factors in the region. It is also on the edge of two regions (26 to 28 and 34 to 36) known to be influenced by crystal contacts, while one neighboring strand (residues 13 to 19) is influenced by the lockwasher distortion in molecule 2.

Table 4.4: Residue ranges with conformations affected by crystal contacts or by the lockwasher distortion. The residues affected by the lockwasher distortion are shown in Figure 4.6.

Segment	Deviating monomer(s)	Cause
1-2	2	Crystal contact
13-19	2	Lockwasher interface
26-28	1, 4	Crystal contacts
34-35	1, 2, other monomers to a smaller degree	Crystal contacts
37-39	2	Crystal contact
41	2	Lockwasher interface
45	2	Lockwasher interface
46-47	1,3	Crystal contacts
48	1	Lockwasher interface
55	All monomers	Crystal contacts
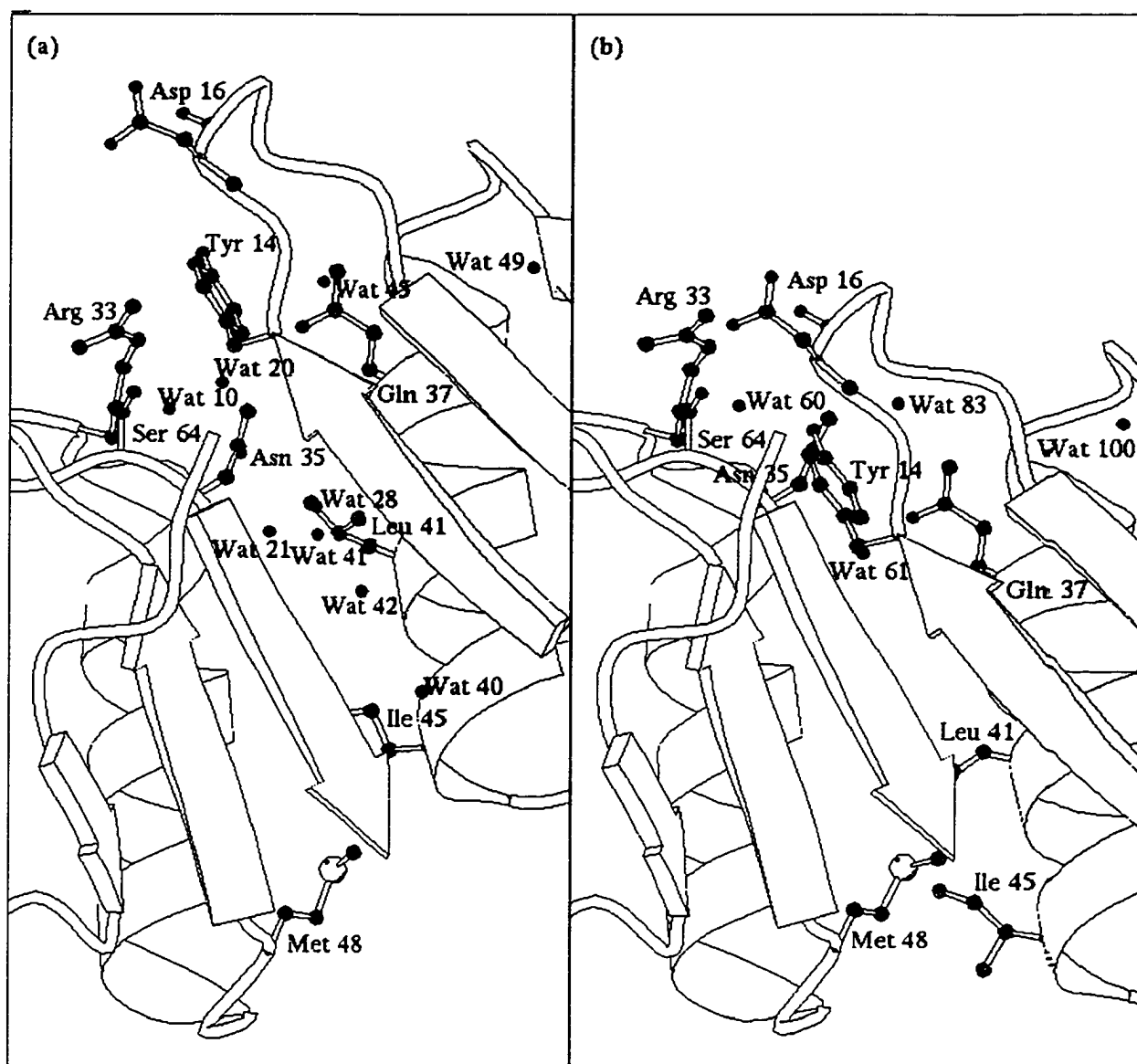
Figure 4.6: Monomer-monomer interfaces in the native structure. The lockwasher-distorted interface between monomers 1 and 2 is shown in (a), while the more typical interface between monomers 3 and 4 is shown in (b). Monomers 1 and 3 are in white, while monomers 2 and 4 are in yellow. Residues mentioned in the text are shown. The new waters found between monomers 1 and 2 are 20, 21, 40, 41, and 42 (forming hydrogen bond bridges), and 45 and 49 (no hydrogen bond bridges between monomers). Waters forming hydrogen bond bridges in normal pentamers include 83, 88, 89, and 100. This figure was made using Molscript (Kraulis, 1991).
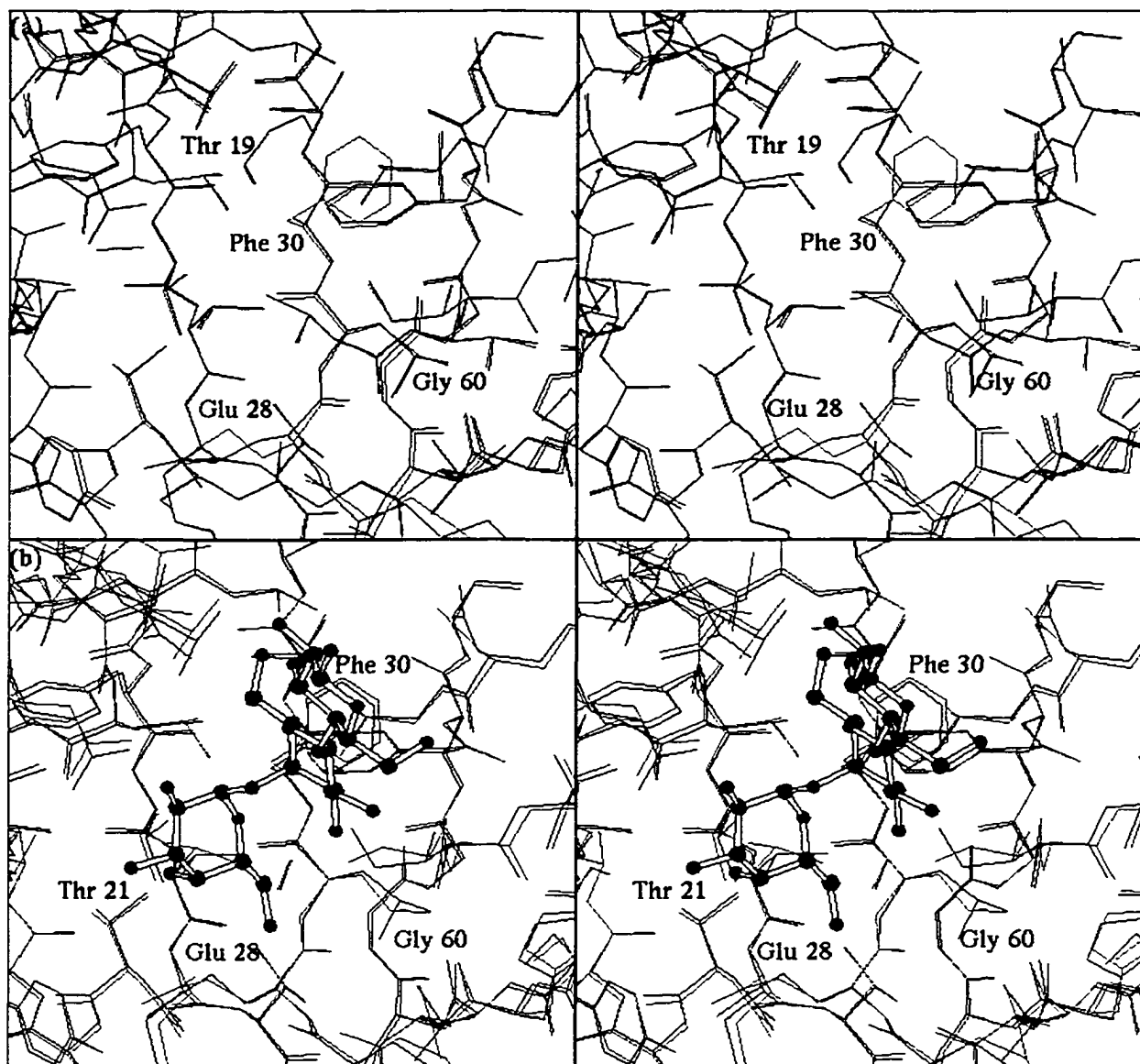
Figure 4.7: The mutation site/ sugar binding site 1. (a) Comparison of the mutation site in the wild-type and mutant structures (monomer 4). The wild-type monomer is in red, the mutant in black. Residues mentioned in the text are labeled. (b) Comparison of the native wild-type and the sugar bound structure of SLT-1 (Ling *et al.*, 1998). The native molecule is in black, the sugar-bound molecule in red, with the trisaccharide shown in ball-and-stick form. This figure was made using Molscript (Kraulis, 1991).

The most reproducible difference at the mutation site is a positive rotation of the ψ angle of residue 30 by about 8°. This tends to place the Cβ and carbonyl oxygen atoms into a greater variety of positions than those found in the wild-type structure. β-strand 4 (residues 27 to 31) tends to move away from the core of the toxin, but not in all subunits. The absence of the hydrophobic effect that solvent would exert on the phenyl ring of Phe 30 may cause these differences.

In the mutant structure, the segments neighboring the mutation site (residues 19 to 24 and 59 to 64) may shift into the region otherwise occupied by the phenyl group. The shifts, however, are not consistent among monomers and are at the borderline of significance according to Sigmaa (Read, 1986) and Luzzati (Luzzati, 1952) error estimates (around 0.2 to 0.3 Å). The clearest motion is around Gly 60, which is consistently around 0.3Å closer to residue 30 in the mutant structure. Shifts at residue 19 are also visible but are only of significant amplitude in monomer 2, where residue 19 is influenced by the lockwasher distortion.

4.3.4 The Crystallographic Zinc Atoms and Their Binding Sites.

In the refined crystal structures, two zinc ions can be seen coordinated to the N-termini of three of the pentamer subunits-(Figure 4.8). The more clearly observed ion (Zn 1) binds the N-termini of monomer 2 from one pentamer and monomer 4 from a crystallographically-related pentamer, while the less clearly observed ion (Zn 2) is coordinated by the N-terminus of monomer 3. Both ions are octahedrally coordinated. Thr 1 serves as a bidentate ligand via its amino and carbonyl groups, and the remaining vertices of the octahedron are occupied by waters (2 for Zn 1, 4 for Zn 2). Zn 2 is clearly less well defined, especially in the native structure, and has had its occupancy set to 0.5.
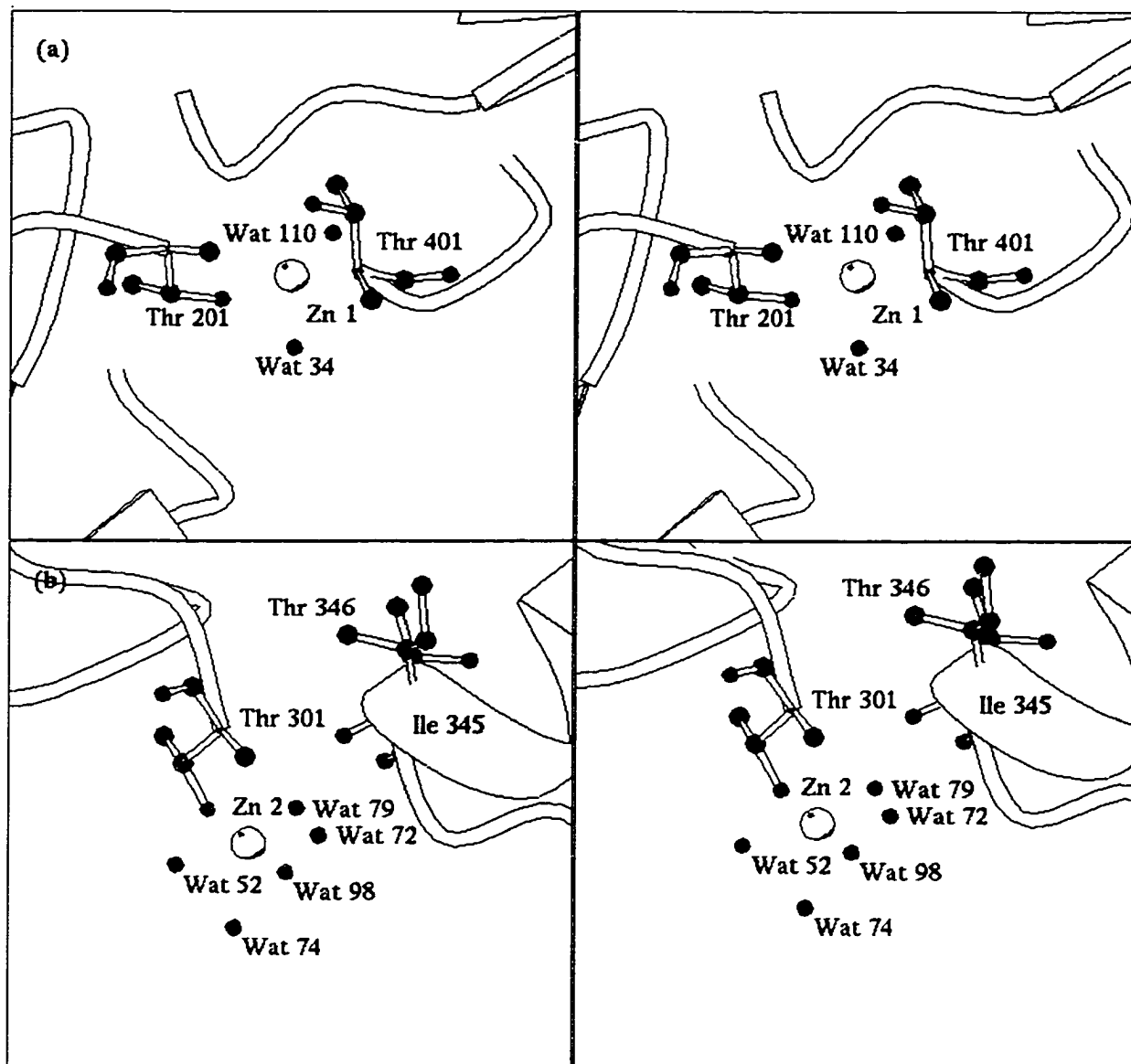
Figure 4.8: Stabilizing effect of zinc molecules on crystal contacts (I). Residue numbers are incremented by their subunit, hence residue 1 in monomer 2 is 201 etc.. (a) Zinc site 1. Monomer 2 is shown in white, the symmetry related monomer 4 in yellow. Residues and water molecules liganding the zinc are shown in ball and stick form and labelled. (b) Zinc site 2. Two symmetry related copies of monomer 3 are shown in white and yellow. The liganding atoms are shown in ball and stick form, as well as water 79, Ile 45, and Thr 46. Water 72 forms crystal contacts with the carbonyl of Ile 45 and, via water 79, with the carbonyl of Thr 46. This figure was made using Molscript (Kraulis, 1991).

The octahedral geometry of the ligands to Zn 2 is still clear in the mutant structure. The identity of Zn 1 and 2 as zinc is supported by the observation that they were replaced by cadmium when a crystal was grown in the presence of $CdCl_2$ to serve as a heavy-atom derivative (Stein & Read, unpublished). The third 'zinc' site originally reported was reinterpreted as a water, and was subsequently deleted entirely. The structure of the N-terminus of monomer 4 does not appear to be distorted from that of non-liganding monomers, however monomer 2 has a slightly different N-terminus that may be invoked by the crystal contact. Like monomer 4, monomer 3 does not have an unusual N-terminus, but a small difference between the native and mutant monomers may be due to the zinc ion, as the change moves the liganding atoms towards the ion.

The addition of zinc chloride to the crystallization buffer was observed to improve the morphology of the native, but not the mutant crystals. The crystals were improved from thin plates to more solid prisms, growing perpendicular to the (010) face. It is clear that Zn 1, bridging crystallographically-related molecules along the crystallographic b axis, could facilitate crystallization in that direction. In the crystals, there are regions of relatively few contacts at approximately $b = 0$ and $b = \frac{1}{2}$, which is where Zn 1 is located (Figure 4.9). It is not clear why the addition of zinc did not improve the morphology of the mutant crystal, as the mutation site does not appear to affect the zinc binding site. It may be unwise to generalize, as few crystallization trials were undertaken with the mutant.

4.3.5 The Lockwasher Distortion.

As noted above, the B-pentamer in the asymmetric unit of both the mutant and native structures is distorted from perfect 5-fold symmetry by the presence of a translational
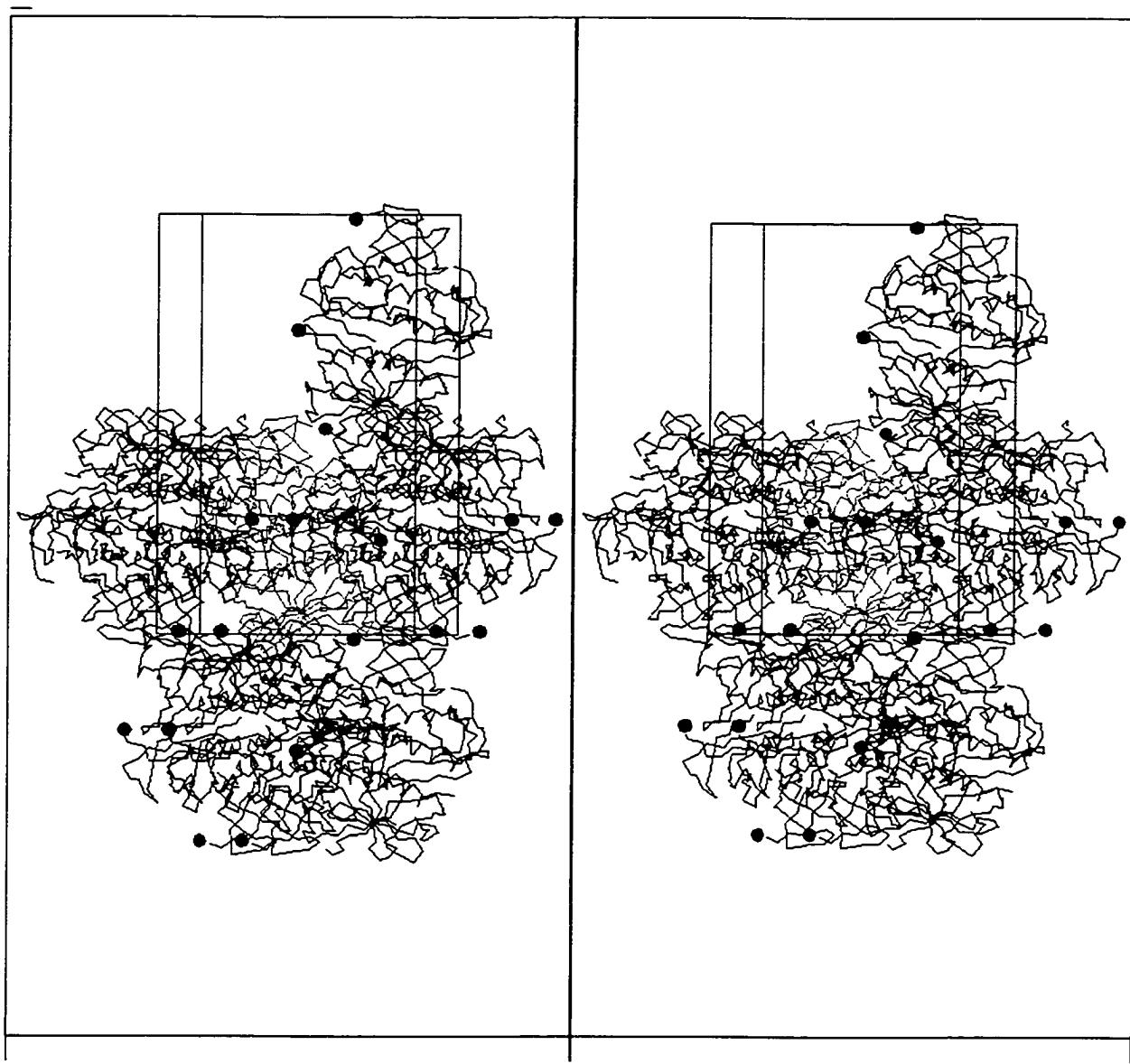
Figure 4.9: Stabilizing effect of zinc molecules on crystal contacts (II). A crystal unit cell

is shown with a central pentamer (purple) and several surrounding pentamers (black).

Zinc atoms at site 1 are shown in red, at site 2 in blue. The site 1 zinc atoms can be seen

to occupy an otherwise thin region of density near the $a=0$ and $a=0.5$ planes. This figure

was made using Molscript (Kraulis, 1991).

component. This gives the pentamer a shape reminiscent of a lockwasher, for which the distortion has been named (Stein *et al.*, 1992), and disrupts the interface between molecules 1 and 2 (Figure 4.1). A distortion of this magnitude has not been seen in other B-pentamer structures (Ling, 1999; Ling *et al.*, 1998), solved in other spacegroups with glycosides bound and/or with other mutations. It is also not observed in the structure of the holotoxin (Fraser *et al.*, 1994), or in B-pentamer structures from other toxins (Merritt *et al.*, 1994a; Sixma *et al.*, 1991; van den Akker *et al.*, 1996; Zhang *et al.*, 1995). NMR studies of the B-pentamer also do not detect the distortion (Richardson *et al.*, 1997; Shimizu *et al.*, 1998). For these reasons, the lockwasher distortion is generally considered to be an artifact of protein packing in this particular crystal form. It is still of interest, insofar as it gives some information on the stability of the monomer-monomer interfaces, and indicates at least one way the pentamer can be distorted by external forces. As the A subunit is known to be released from the B-pentamer after endocytosis in its pathway to the cytoplasm, the stability and lability of the B-pentamer are of some interest.

The average rotation between individual monomers is 72° and the translation is about 1.3Å, but there is some variation between different pairs of monomers - (Table 4.5). As might be expected, the variations are similar in the wild-type and mutant structures. The greatest discrepancy (not counted in the average) is the anomalous interface between monomers 1 and 2.

The lockwasher distortion, as might be expected, destroys most of the interface interactions found between the other monomer pairs (Figure 4.6). The interface formed between monomers 1 and 2 packs in a different fashion, compensating to some degree for

Table 4.5: Rotation and translation between neighboring monomers in the mutant and wild type SLT-1 structures.

Monomer-monomer interaction	Wild type		mutant	
	Rotation (°)	Translation (Å)	Rotation (°)	Translatio n (Å)
1 to 2	69.5	-6.1	69.8	-6.2
2 to 3	71.7	1.9	71.8	1.9
3 to 4	70.7	1.2	70.4	1.2
4 to 5	74.0	1.7	73.9	1.9
5 to 1	74.3	-1.2	74.2	1.1

the lost interactions. All of the main-chain to main-chain hydrogen bonds, formed between β-strands 2 and 6, are lost at the lockwasher interface. Hydrogen bonds involving side chains are also invariably disrupted. The latter bonds were poorly conserved however, with the exception of those between Ser 64 Oγ and Asp 16 Oδ1 and Arg 33 Nη1 and Asp 16 O. An otherwise unobserved bond is formed between Asn 35 Nδ2, and Gln 37 Oε1 at the 1-2 interface. In all, 6 well conserved and about 8 poorly conserved hydrogen bonds are lost (including some with a salt-bridge character), while one new bond is formed.

Three well conserved water-mediated hydrogen bonds, observed between all other subunits, are disrupted in the 1-2 interface, as well as 2 poorer bridges observed only between some other subunits. However, five new waters mediating hydrogen bonds between monomers 1 and 2 are present between the two subunits, offsetting the loss of the other water mediated hydrogen bonds. Two other waters between monomers 1 and 2 interact with groups that form intermonomer hydrogen bonds in other interfaces, but do not form bridging hydrogen bonds. Therefore, at most 10 protein-water-protein hydrogen bonds found at the interface of other subunits are lost, while 15 clearly defined new ones are formed, as well as three other water-protein hydrogen bonds.

The normal non-polar contacts are also disrupted in the 1-2 interface. This interface has only 930 $Å^2$ of solvent inaccessible surface area, in comparison to the 1260 $Å^2$ seen in other interfaces. The unique water binding sites cover some of the extra exposed surface, but a great deal more is exposed without forming crystallographically detectable intra-pentamer contacts. Few hydrophobic residues appear to be exposed to solvent as a result

of the distortion, while the shift of Tyr 14 allows it to remain somewhat buried in the interface.

The effects of the lockwasher distortion can be summarized as the loss of a small number of hydrogen bonds in the protein-protein interface, and the exposure of about 330 $Å^2$ of otherwise solvent inaccessible surface area. The pentamer forms 36 clear crystal contact hydrogen bonds as well as 45 clear water-mediated hydrogen bonds. As the crystal contacts also bury about 6350 $Å^2$ of otherwise exposed surface area, the distortion of the pentamer to form the crystal contacts can be seen to be desirable. Why these crystal contacts induce a lockwasher distortion remains to be discussed.

Eight pentamers form crystal contacts with the verotoxin B-pentamer. While all of these probably contribute to the stabilization of the distorted pentamer, certain interactions do seem particularly significant. A combination of screw translations along the a-axis and unit cell translations leads to a series of interactions where the bulging outer face of monomers 1 and 3 are inserted into the concave pore regions of the pentamer (Figure 4.10). These interactions provide the most extensive crystal contacts, with 1020 or 1090 $Å^2$ respectively of buried surface area. Since monomer 1 is one of the inserted monomers, and since the inserted monomers form extensive interactions with the pore-side of monomers 1 and 2, the formation of these interactions could supply the driving force to form the lockwasher distortion. Ling (1999) has observed that the lockwasher distortion is only seen in pentamers in which the wild-type residue Trp 34 has not been mutated. This observation may relate to the fact that these residues cluster around one end of the pore, and interact with the inserted molecule A in the lockwasher

crystal form (Figure 4.10). Less extensive interactions along the 2_1 screw axis parallel to b, involving monomer 2, may also contribute to stabilizing the distortion (Figure 4.11).

While the lockwasher distortion is an artifact of crystallization, it does point to an underlying weakness in the interactions stabilizing the pentamer. The junctions between pairs of monomers are the points where the pentamer ring is the narrowest, indicating the weakness of the monomer-monomer interactions. Fraser et al. (1994), have suggested that the insertion of the A tail may stabilize the pentamer somewhat; the insertion of the tail results in the burial of 2000 Å^2 of surface area. Relatively weak monomer-monomer interactions may be related to pentamer function, possibly with regard to pentamer assembly or dissociation. By analogy to the case of *Pseudomonas* exotoxin A (Ogata et al., 1990), the A subunit is believed to dissociate from the B-ring before entering the cytosol. While the cleavage of the A subunit into the enzymatic A_1 and B-pentamer binding and inhibitory A_2 domains, and the reduction of the disulphide between them, may be the mechanism of release, dissociation from the B-pentamer might also play a role. The cleaving of the A subunit into the A_1 fragment and the A_2 fragment is believed to be primarily carried out by the serine proteinase furin in the trans-golgi network (Garred et al., 1995b). However, there is evidence for the B-pentamer transfer to the endoplasmic reticulum, and for that transfer serving to target the A subunit there (Khine & Lingwood, 1994; Sandvig et al., 1992; Sandvig et al., 1994). The post-cleavage association of the subunits may be facilitated by the presence of a disulphide connecting the A_1 and A_2 fragments, but a mutation disrupting the disulphide reduces the toxicity severely only when toxin internalization is unusually prolonged
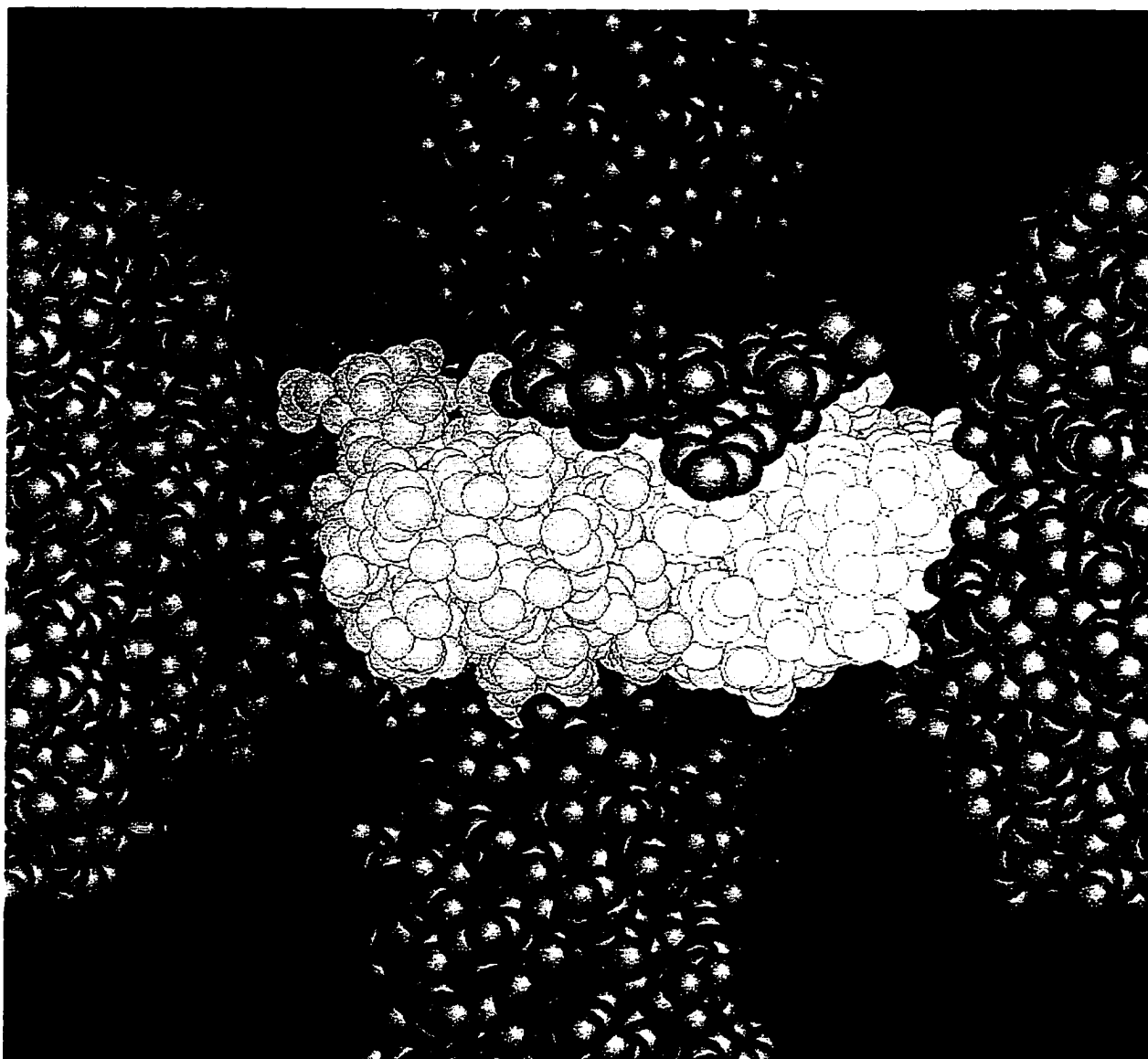
Figure 4.10: Crystal contacts mediated by 2_1 translations parallel to the a axis.

Molecules related by crystal symmetry to a central molecule are shown. The central

molecule (white) has subunits 1 and 2 coloured in red and yellow respectively.

Molecules related by the 2_1 translation (cyan) and translated by lattice vectors -1 0 0

(green) 0 0 -1 (purple-blue), and -1 0 -1 (magenta) are shown. The Trp 34 residues in all

subunits are shown in blue-grey. This figure was made using GRASP (Nicholls *et al.*,

1991).
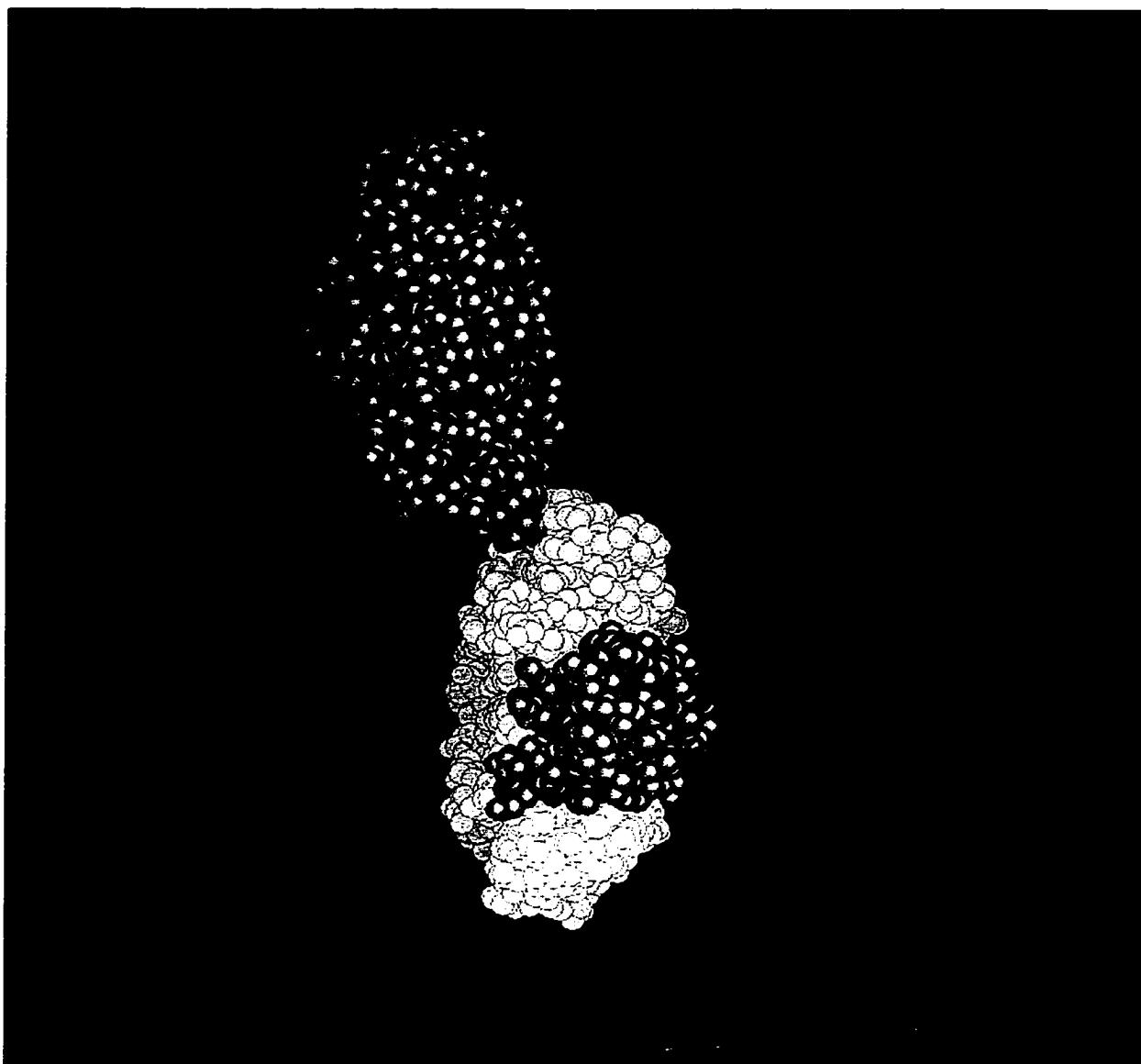
Figure 4.11: Crystal contact along the 2_1 translation parallel to the b axis. The central

molecule (white) has subunits 1 and 2 coloured in red and yellow respectively. The

molecule in green is transformed by the $Y2_1$ translation, and by the lattice vector 1 0 -1.

This figure was made using GRASP (Nicholls et al., 1991).

(Garred *et al.*, 1997). Hence non-covalent interactions may also aid in stabilizing the AB$_5$ complex after proteolytic nicking of the A subunit. The mechanisms of dissociation of the A subunit from the B pentamer would therefore be important to toxicity. For dissociation, the binding of the A and the B$_5$ moieties of the toxin would have to be reversible. If the pentamer surrounding the tail were too stable, it could retard the insertion and extraction of the tail from the AB$_5$ complex. A role for dissociation of the A and B subunits in toxin entry is supported by studies of Shiga toxin mutated to remove the furin cleavage site (Garred *et al.*, 1995a). While this mutation reduces toxicity, it does not eliminate it, with intact A subunit being cleaved by the proteinase calpain after reaching the cytosol. Therefore, the uncleaved A subunit can be released from the B subunit. An analogy can be drawn with pertussis toxin, where the A subunit does not undergo proteolytic processing. Instead, for the dissociation of the A subunit and toxicity it requires the binding of an ATP molecule to the holotoxin (Hausman *et al.*, 1990; Moss *et al.*, 1986). Crystallographic studies have shown that the ATP disrupts interactions in the pore interface, presumably destabilizing the holotoxin structure (Hazes *et al.*, 1996).

4.3.6   Sugar binding Sites

The solution of several structures of SLTs co-crystallized with glycosides has given information about the nature of the sugar binding sites that was not available when the wild-type and F30A mutant structures were first solved. These sites can now be re-investigated, and the significance of the F30A site can now be reassessed.

The F30A mutation was originally designed to test binding at Site 1. As noted above, the mutation has little or no effect on the protein structure away from residue 30

itself. Some of the residues that may be influenced by the removal of the phenyl group (residues 19 to 24, 59 to 64) are also credited with playing a role in receptor sugar binding at Site 1 (Ling, 1999; Ling *et al.*, 1998) (Figure 4.6). Thr 21 and Gly 60 in particular are known to form hydrogen bonds with the Galactose rings of Gb$_3$ (Ling *et al.*, 1998). The shift of Gly 60 is sufficiently large and consistent among monomers to justify proposing that it has a role in influencing the mutant's ability to interact with the receptor at Site 1. Glu 28 is another hydrogen bond-forming residue at Site 1, and also forms a water mediated bond (Ling, 1999; Ling *et al.*, 1998). In the refined B-pentamer structures, Glu 28 appears to be somewhat disordered and the water molecule is not visible, suggesting that it may not be present until after sugar binding. However, the loss of the phenyl ring is the most obvious influence of the mutation on Site 1 and is therefore probably the primary mediator of the effect.

Site 2 is the best-defined sugar binding site in the crystal structures where mutations have not been employed to disable it (Ling, 1999; Ling *et al.*, 1998). Several side chains are involved in sugar binding at this site (Figure 4.12 a). Phe 30 is tangentially involved in this site via a hydrophobic contact, however its deletion has been shown not to affect the sugar binding conformation significantly (Ling, 1999). Another residue with a hydrophobic contact, Gly 62, is in the region whose conformation may be slightly affected by the mutation. However, the F30A mutation probably does not affect sugar binding at Site 2 significantly.

Several residues shown to form hydrogen bonds with Gb$_3$ at binding Site 2 show signs of slight disorder in the native crystal form. The sidechain termini of residues Asp 16, Asn 32, and Arg 33 have poor electron density, or refined poorly, suggesting that in
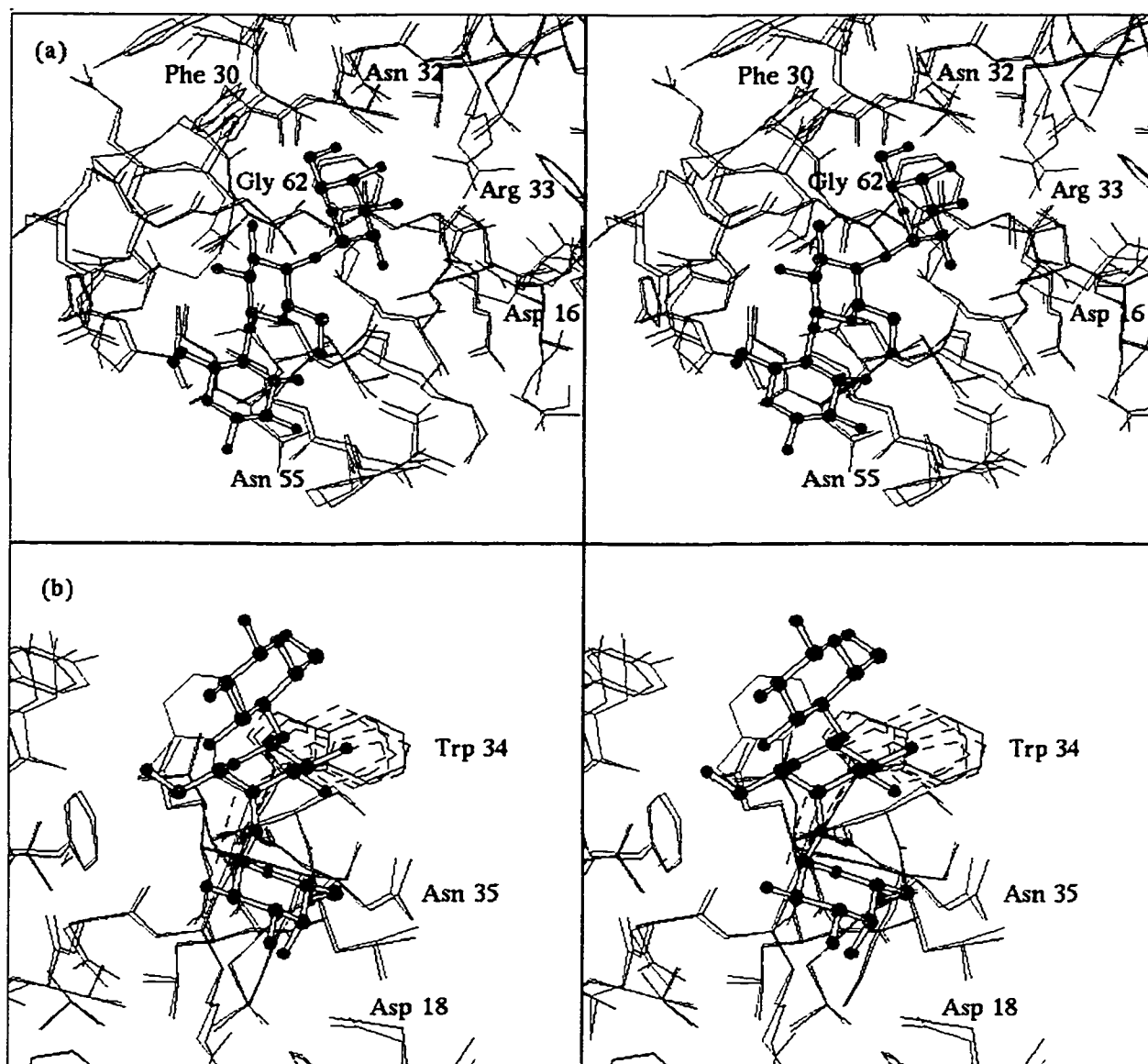
Figure 4.12: Sugar bindings sites 2 and 3. (a) Site 2. The native wild-type (monomer 4)

is in black, the Gb$_3$ complex in red. with the trisaccharide shown in ball-and-stick form.

(b) Site 3. The mutant (monomer 4) is in black, the Gb$_3$ complex in red. with the

trisaccharide shown in ball-and-stick form. The Trp 34 residues from other native

monomers are superimposed in dashed black lines. This figure was made using

Molscript (Kraulis, 1991).

the absence of the sugar they may be slightly disordered. The sidechain of Asn 55 shows different conformations in different subunits, which are stabilized by various crystal contacts.

The primary interaction at Site 3 is between the glycolipid and the residue Trp 34 (Figure4.12 b). In the refined native and mutant structures this residue is poorly resolved, and the electron density seems to suggest that the side chains of different subunits adopt different conformations depending on crystal contacts and other external influences. This agrees with the lack of order observed at this site in the Shiga holotoxin, and supports Ling *et al.*'s theory that the side chain is disordered until the saccharide is bound (Ling *et al.*, 1998). The other residues involved in sugar binding, Asp 18 and Asn 35, also appear to have slightly disordered side chains, so their binding conformation may be conferred by the interaction with the saccharide.

Some of the sites occupied by sugar oxygens in the protein-carbohydrate complex structures can be seen to be occupied by waters in the native structures. At Site 1, the location of O4 of Gal 1 is occupied by a water in at least 3 monomers from the native or mutant structures. At Site 2 the location of O6 from Gal 1 is occupied by a water in all sites except monomer 1 in the mutant structure. At Site 3 O5 of Gal 1 is occupied by a water in at least 3 monomers from the native or mutant structures. While this analysis is limited by the limited resolution of the native structures, it does indicate that some sugar binding residues have their hydrogen bonding potential fulfilled by solvent in the absence of sugar, which may have implications for the thermodynamics of binding.

The F30A mutant has been shown to have a very definite effect on Gb3 binding and on cytotoxicity (Clark *et al.*, 1996). The binding of the free trisaccharide was severely

reduced, from a K_d of approximately 2 mM to the limits of detectability. In a lipid milieu assay, the binding of Gb3 was reduced by a factor of 4 and there was a 10-fold reduction in the number of binding sites as measured by Scatchard analysis (Cantor & Schimmel, 1980). The cytotoxicity was also reduced by a factor of 10^5. These results were originally considered to indicate that the mutation had destroyed the primary binding site for Gb3, presumed to be Site 1.

The subsequent structures of SLT-1 (Ling, 1999; Ling *et al.*, 1998) have, however, tended to suggest that Site 2 is at least as important as Site 1, if not more. In the SLT-1 plus Gb3-methoxycarbonyloctyl (Pk-MCO trisaccharide) structure, the full saccharide is always seen at Site 2, but only one or two carbohydrate residues are visible in electron density at Site 1. The density at Site 2 is also superior in the structure of the GT3 mutant of SLT-2e, although the residues at the binding sites are somewhat different. The structure of the G62T mutant, which has the greatest reduction of cytotoxicity of any studied mutant, shows binding at Site 2 to be completely eliminated. Some binding is present at Site 1; 3 sites of the pentamer are blocked by crystal contacts, an unblocked site is unoccupied, and Gb3 binds at the fifth site, apparently stabilized by crystal contacts. A series of mutant structures in the same spacegroup (W34A, F30A/W34A, D17E/W34A) showed no binding at Site 1, even in subunits where the site was completely unblocked, and when the binding site was distant from the mutation sites. The fact that Site 2 usually shows full occupancy unless eliminated by mutations, while Site 1 is often blocked by crystal contacts, tends to suggest that Site 2 has better binding, as it can clearly dominate the crystallization process while Site 1 cannot. A galabiose disaccharide is only seen to bind at Site 2 (H. Ling, unpublished results). NMR studies

also support Site 2 as the primary binding site (Shimizu *et al.*, 1998). Site 2 is also the

sugar binding location observed in cholera toxin and heat-labile enterotoxin (Merritt *et*

al., 1994b; Sixma *et al.*, 1992). Nonetheless, one should bear in mind that the binding

experiments with the Shiga-like toxins have all used soluble carbohydrates. *In vivo*, the

cell-surface trisaccharides are presented by glycolipids embedded in a membrane, which

could well alter the relative affinities.

Despite the above observations on sugar binding in various crystal structures, the

F30A mutation indisputably has a strong effect on cytotoxicity and toxin-receptor

binding. It is hard to explain the data showing F30A eliminating the majority of the

binding sites on the pentamer without invoking some sort of effect at Site 2. Such an

effect might be mediated through the non-polar contacts between the Site 2 glycoside and

Phe 30, and the effects on the loop containing residues 60 to 62, which are involved at

Site 2. However, these are minor and subtle effects. In the structure of the F30A/W34A

mutant, Site 2 was fully occupied, and the nature of the sugar binding was unchanged

(Ling, 1999).

Although the F30A mutation shows only minimal alteration of Site 2, its general

effects might still be felt on the receptor binding of the pentamer as a whole. The

receptor binding constants of the individual sites on SLT-1 are around $10^3\,M^{-1}$ for Gb$_3$ in

solution, in contrast to its cell binding constant of $10^9\,M^{-1}$ (Fuchs *et al.*, 1986; St. Hilaire

et al., 1994). Cholera toxin has a cell-binding constant of $10^9\,M^{-1}$, but a much higher free

saccharide binding constant of $10^6\,M^{-1}$ (Cuatrecasas, 1973; Holmgren *et al.*, 1974;

Schafer & Thakur, 1982). It has therefore been suggested that binding at multiple sites is

necessary for high-affinity toxin binding to the cell surface (Ling *et al.*, 1998). The loss

of a set of ligand binding sites could have a severe effect on the binding of the pentamer to a lipid surface. The effects that the mutations have on the cytotoxicity make more sense if more than one site is considered to contribute to the pentamer binding (Bast *et al.*, 1999). The most severe loss of toxicity (by a factor of 10^{-7} from the wild type toxin) comes with the G62T mutation, which eliminates Site 2, and may also affect Site 1 to a lesser extent. The next most severe effects (by a factor of 10^{-6}) come with the F30A/W34A or the D17E/W34A mutations, where Sites 1 and 3 are affected, but Site 2 is left intact. Mutations which should only affect site 1 significantly, D17E or F30A, have even smaller effects (by a factor of 5×10^{-5} and 10^{-5} respectively), while W34A, affecting Site 3 (generally considered to be relatively minor) has the smallest effect (by a factor of 10^{-2}). Hence Site 1, while probably not as effective as Site 2 at binding, may contribute significantly to the overall binding. It has also been observed that SLTs bind best to mixtures of different lipid-trisaccharide combinations (Pellizzari *et al.*, 1992). This has led to the suggestion that different sites, at different distances from the presumed location of the cell binding surface, may be able to bind saccharides displayed at different distances and angles from the surface (Nyholm *et al.*, 1996). In addition, cytotoxicity could reflect the effects of F30A and the other mutations at other events in the toxin's journey into the cell, and not reflect surface glycolipid binding. The targeting of different glycolipids to different subcellular compartments has been suggested to be involved in the retrograde transport process, with longer chain fatty acids being more likely to be transported to the ER (Sandvig *et al.*, 1994). Possibly lipids binding to Site 1 favour transport to the ER.

The multiple binding sites, besides improving the binding of glycolipids, may aid the viability of the bacteria by allowing the pentamer to bind saccharides in different fashions, which would offer some protection against variations in the host's saccharide content, or against minor variations in saccharide modification. It would also allow the bacteria to have sites that are fully active, and sites that are evolving to reflect changes in the host saccharide content, in the same functional toxin.

4.4   Conclusions

The refinement of the native crystal structures of wild-type and mutant SLT-1 has facilitated the analysis of a number of issues. The crystallographic zinc sites have been described, and the mechanism by which zinc binding improved the morphology of the wild-type crystals has been related to the improvement of crystal contacts between symmetry related monomers 2 and 4 along the b axis. Similarly, the crystal contacts influencing the 'lockwasher' distortion of the molecule have been shown to be related to crystal contacts that insert monomers 1 and 3 into the pore faces of symmetry related molecules. The extensive crystal contacts allowed by those interactions apparently enable the disruption of the normal contacts found in the pentamer.

The F30A mutation has been confirmed to have little effect away from the immediate area of the mutated residue. While it is just possible that the F30A mutation influences the binding at Site 2, it seems more likely that the considerable reduction in sugar binding capacity and cytotoxicity caused by the mutation are due to the elimination of Site 1. This confirms that Site 1 is a glycoside binding site of significant importance. The native conformation of residues at the sugar binding sites are usually similar to the

sugar-bound conformation, although there is evidence that several, particularly Trp 34 at Site 3, are disordered in the absence of sugars.

In general, the refined structures tend to confirm that multiple binding sites are probably important either in cell surface sugar binding, or else in some other factor related to cytotoxicity, such as intracellular trafficking of the toxin. The labile nature of the B-pentamer, suggested by the lockwasher distortion, may also be significant either in toxin assembly, or else in the process of dissociation of the A and B subunits during intracellular trafficking.

References

Allen, F. H. & Kennard, O. (1993). 3D search and research using the Cambridge structural database. *Chemical Design Automation News* **8**, 31-7.

Armstrong, G. D., Rowe, P. C., Goodyer, P., Orrbine, E., Klassen, T. P., Wells, G., MacKenzie, A., Lior, H., Blanchard, C. & Auclair, F. (1995). A phase I study of chemically synthesized verotoxin (Shiga-like toxin) Pk-trisaccharide receptors attached to chromosorb for preventing hemolytic-uremic syndrome. *Journal of Infectious Diseases* **171**, 1042-5.

Boodhoo, A., Read, R. J. & Brunton, J. (1991). Crystallization and preliminary X-ray crystallographic analysis of verotoxin-1 B-subunit. *Journal of Molecular Biology* **221**, 729-31.

Boyd, B., Tyrrell, G., Maloney, M., Gyles, C., Brunton, J. & Lingwood, C. (1993). Alteration of the glycolipid binding specificity of the pig edema toxin from globotetraosyl to globotriaosyl ceramide alters *in vivo* tissue targetting and results in a verotoxin 1-like disease in pigs. *Journal of Experimental Medicine* **177**, 1745-53.

Brünger, A. T. (1992). The Free *R* Value: a Novel Statistical Quantity for Assessing the Accuracy of Crystal Structures. *Nature* **355**, 472-474.

Brünger, A. T., Adams, P. D., Clore, G. M., DeLano, W. L., Gros, P., Grosse-Kunstleve, R. W., Jiang, J. S., Kuszewski, J., Nilges, M., Pannu, N. S., Read, R. J., Rice, L. M., Simonson, T. & Warren, G. L. (1998). Crystallography & NMR system: A new software suite for macromolecular structure determination. *Acta Crystallographica* **D54**, 905-21.

Brünger, A. T., Krukowski, A. & Erickson, J. W. (1990). Slow-cooling protocols for crystallographic refinement by simulated annealing. *Acta Crystallographica* **A46**, 585-93.

Brünger, A. T., Kuriyan, J. & Karplus, M. (1987). Crystallographic *R* factor Refinement by Molecular Dynamics. *Science* **235**, 458-460.

Brunton, J. L. (1990). The Shiga toxin family: molecular nature and possible role in disease. In *The Bacteria, Molecular Basis of Bacterial Pathogenesis* (Iglewski, B. & Clark, V., eds.), Vol. 11, pp. 377-98. Academic Press, New York.

Brunton, J. L. (1994). Molecular biology and role in disease of the verotoxin (Shiga-like toxins) of *Escherichia coli*. In *Molecular Genetics of Bacterial Pathogenesis* (Miller, N. L., Kaper, J. B., Portnoy, D. A. & Isberg, R. R., eds.), pp. 391-404. ASM Press, Washington D. C.

Burnette, W. N. (1994). AB5 ADP-ribosylating toxins: comparative anatomy and physiology. *Structure* **2**, 151-8.

Clark, C., Bast, D., Sharp, A. M., St. Hilaire, P. M., Agha, R., Stein, P. E., Toone, E. J., Read, R. J. & Brunton, J. L. (1996). Phenylalanine 30 plays an important role in receptor binding of verotoxin-1. *Molecular Microbiology* **19**, 891-9.

Cohen, A., Madrid-Marina, V., Estrov, Z., Freedman, M. H., Lingwood, C. A. & Dosch, H. M. (1990). Expression of glycolipid receptors to Shiga-like toxin on human B lymphocytes: a mechanism for the failure of long-lived antibody response to dysenteric disease. *International Immunology* **2**, 1-8.

Cuatrecasas, P. (1973). Gangliosides and membrane receptors for cholera toxin. *Biochemistry* **12**, 3558-66.

DeGrandis, S., Law, H., Brunton, J., Gyles, C. & Lingwood, C. A. (1989). Globotetraosylceramide is recognized by the pig edema disease toxin. *Journal of Biological Chemistry* **264**, 12520-5.

Donohue-Rolfe, A., Keusch, G. T., Edson, C., Thorley-Lawson, D. & Jacewicz, M. (1984). Pathogenesis of Shigella diarrhea. IX. Simplified high yield purification of Shigella toxin and characterization of subunit composition and function by the use of subunit-specific monoclonal and polyclonal antibodies. *Journal of Experimental Medicine* **160**, 1767-81.

Endo, Y., Tsurugi, K., Yutsudo, T., Takeda, Y., Ogasawara, T. & Igarashi, K. (1988). Site of action of a Vero toxin (VT2) from Escherichia coli O157:H7 and of Shiga toxin on eukaryotic ribosomes. RNA N-glycosidase activity of the toxins. *European Journal of Biochemistry* **171**, 45-50.

Esnouf, R. M. (1997). An extensively modified version of Molscript that includes greatly enhanced coloring capabilities. *Journal of Molecular Graphics* **15**, 133-8.

Fraser, M. E., Chernaia, M. M., Kozlov, Y. V. & James, M. N. G. (1994). Crystal structure of the holotoxin from *Shigella dysenteriae* at 2.5 Å resolution. *Nature Structural Biology* **1**, 59-64.

Fuchs, G., Mobassaleh, M., Donohue-Rolfe, A., Montgomery, R. K., Grand, R. J. & Keusch, G. T. (1986). Pathogenesis of Shigella diarrhea: rabbit intestinal cell microvillus membrane binding site for Shigella toxin. *Infection & Immunity* **53**, 372-7.

Garred, Ø., Dubinina, E., Holm, P. K., Olsnes, S., van Deurs, B., Kozlov, J. V. & Sandvig, K. (1995a). Role of processing and intracellular transport for optimal toxicity of Shiga toxin and toxin mutants. *Experimental Cell Research* **218**, 39-49.

Garred, Ø., Dubinina, E., Polesskaya, A., Olsnes, S., Kozlov, J. & Sandvig, K. (1997). Role of the disulfide bond in Shiga toxin A-chain for toxin entry into cells. *Journal of Biological Chemistry* **272**, 11414-9.

Garred, Ø., van Deurs, B. & Sandvig, K. (1995b). Furin-induced cleavage and activation of Shiga toxin. *Journal of Biological Chemistry* **270**, 10817-21.

Hausman, S. Z., Manclark, C. R. & Burns, D. L. (1990). Binding of ATP by pertussis toxin and isolated toxin subunits. *Biochemistry* **29**, 6128-31.

Hazes, B., Boodhoo, A., Cockle, S. A. & Read, R. J. (1996). Crystal structure of the pertussis toxin-ATP complex: a molecular sensor. *Journal of Molecular Biology* **258**, 661-71.

Holmgren, J., Mansson, J. E. & Svennerholm, L. (1974). Tissue receptor for cholera exotoxin: structural requirements of G11 ganglioside in toxin binding and inactivation. *Medical Biology* **52**, 229-33.

Jacewicz, M., Clausen, H., Nudelman, E., Donohue-Rolfe, A. & Keusch, G. T. (1986). Pathogenesis of shigella diarrhea. XI. Isolation of a shigella toxin-binding glycolipid from rabbit jejunum and HeLa cells and its identification as globotriaosylceramide. *Journal of Experimental Medicine* **163**, 1391-404.

Jones, T. A., Zou, J. Y., Cowan, S. W. & Kjeldgaard, M. (1991). Improved methods for building protein models in electron density maps and the location of errors in these models. *Acta Crystallographica* **A47**, 110-9.

Karmali, M. A. (1989). Infection by verocytotoxin-producing *Escherichia coli*. *Clinical Microbiology Reviews* **2**, 15-38.

Khine, A. A. & Lingwood, C. A. (1994). Capping and receptor-mediated endocytosis of cell-bound verotoxin (Shiga-like toxin). 1: Chemical identification of an amino acid in the B subunit necessary for efficient receptor glycolipid binding and cellular internalization. *Journal of Cellular Physiology* **161**, 319-32.

Kitov, P. I., Sadowska, J. M., Mulvey, G., Armstrong, G. D., Ling, H., Pannu, N. S., Read, R. J. & Bundle, D. R. Tailored multivalency of carbohydrate ligands with unprecedented activity in neutralizing Shiga-like toxins. *Nature* **(in press)**.

Kraulis, P. J. (1991). MOLSCRIPT: A program to produce both detailed and schematic plots of protein structures. *Journal of Applied Crystallography* **24**, 946-50.

Laskowski, R. A., MacArthur, M. W., Moss, D. S. & Thornton, J. M. (1993). PROCHECK: a program to check the stereochemical quality of protein structures. *Journal of Applied Crystallography* **26**, 283-91.

Lindberg, A. A., Brown, J. E., Stromberg, N., Westling-Ryd, M., Schultz, J. E. & Karlsson, K. A. (1987). Identification of the carbohydrate receptor for Shiga toxin produced by *Shigella dysenteriae* type 1. *Journal of Biological Chemistry* **262**, 1779-85.

Ling, H. (1999). Structural Studies of the Interactions Between Shiga-Like Toxins and Their Carbohydrate Receptor. Doctoral Thesis, University of Alberta.

Ling, H., Boodhoo, A., Hazes, B., Cummings, M. D., Armstrong, G. D., Brunton, J. L. & Read, R. J. (1998). Structure of the shiga-like toxin I B-pentamer complexed with an analogue of its receptor Gb3. *Biochemistry* **37**, 1777-88.

Lingwood, C. A., Law, H., Richardson, S., Petric, M., Brunton, J. L., De Grandis, S. & Karmali, M. (1987). Glycolipid binding of purified and recombinant *Escherichia coli* produced verotoxin *in vitro*. *Journal of Biological Chemistry* **262**, 8834-9.

Luzzati, V. (1952). Traitement Statistique des Erreurs dans la Determination des Structures Cristallines. *Acta Crystallographica* **5**, 802-10.

Merritt, E. A., Sarfaty, S., van den Akker, F., C, L. H., Martial, J. A. & Hol, W. G. (1994a). Crystal structure of cholera toxin B-pentamer bound to receptor GM1 pentasaccharide. *Protein Science* **3**, 166-75.

Merritt, E. A., Sixma, T. K., Kalk, K. H., van Zanten, B. A. & Hol, W. G. (1994b). Galactose-binding site in *Escherichia coli* heat-labile enterotoxin (LT) and cholera toxin (CT). *Molecular Microbiology* **13**, 745-53.

Moss, J., Stanley, S. J., Watkins, P. A., Burns, D. L., Manclark, C. R., Kaslow, H. R. & Hewlett, E. L. (1986). Stimulation of the thiol-dependent ADP-ribosyltransferase and NAD glycohydrolase activities of *Bordetella pertussis* toxin by adenine nucleotides, phospholipids, and detergents. *Biochemistry* **25**, 2720-5.

Moss, J. & Vaughan, M. (1988). ADP-ribosylation of guanyl nucleotide-binding regulatory proteins by bacterial toxins. *Advances in Enzymology & Related Areas of Molecular Biology* **61**, 303-79.

Neill, M. A. (1998). Treatment of disease due to Shiga toxin-producing *Escherichia coli*: infectious disease management. In *Escherichia coli O157:H7 and other Shiga-toxin producing E. coli Strains* (Kaper, J. B. & O'Brien, A. D., eds.), pp. 357-363. ASM Press, Washington D.C.

Nicholls, A., Sharp, K. A. & Honig, B. (1991). Protein folding and association: insights from the interfacial and thermodynamic properties of hydrocarbons. *Proteins* **11**, 281-96.

Nyholm, P. G., Magnusson, G., Zheng, Z., Norel, R., Binnington-Boyd, B. & Lingwood, C. A. (1996). Two distinct binding sites for globotriaosyl ceramide on verotoxins: identification by molecular modelling and confirmation using deoxy analogues and a new glycolipid receptor for all verotoxins . *Chemistry & Biology* **3**, 263-75.

O'Brien, A. D. & Holmes, R. K. (1987). Shiga and Shiga-like toxins. *Microbiological Reviews* **51**, 206-20.

Ogata, M., Chaudhary, V. K., Pastan, I. & FitzGerald, D. J. (1990). Processing of Pseudomonas exotoxin by a cellular protease results in the generation of a 37,000-Da toxin fragment that is translocated to the cytosol. *Journal of Biological Chemistry* **265**, 20678-85.

Olsnes, S., Reisbig, R. & Eiklid, K. (1981). Subunit structure of Shigella cytotoxin. *Journal of Biological Chemistry* **256**, 8732-8.

Pellizzari, A., Pang, H. & Lingwood, C. A. (1992). Binding of verocytotoxin 1 to its receptor is influenced by differences in receptor fatty acid content. *Biochemistry* **31**, 1363-70.

Picking, W. D., McCann, J. A., Nutikka, A. & Lingwood, C. A. (1999). Localization of the binding site for modified Gb_3 on verotoxin 1 using fluorescence analysis. *Biochemistry* **38**, 7177-84.

Pontius, J., Richelle, J. & Wodak, S. J. (1996). Deviations from standard atomic volumes as a quality measure for protein crystal structures. *Journal of Molecular Biology* **264**, 121-36.

Ramotar, K., Boyd, B., Tyrrell, G., Gariepy, J., Lingwood, C. & Brunton, J. (1990). Characterization of Shiga-like toxin I B subunit purified from overproducing clones of the SLT-I B cistron. *Biochemical Journal* **272**, 805-11.

Read, R. J. (1986). Improved Fourier coefficients for maps using phases from partial structures with errors. *Acta Crystallographica* **A42**, 140-9.

Richardson, J. M., Evans, P. D., Homans, S. W. & Donohue-Rolfe, A. (1997). Solution structure of the carbohydrate-binding B-subunit homopentamer of verotoxin VT-1 from E. coli. *Nature Structural Biology* **4**, 190-3.

Richardson, S. E., Rotman, T. A., Jay, V., Smith, C. R., Becker, L. E., Petric, M., Olivieri, N. F. & Karmali, M. A. (1992). Experimental verocytotoxemia in rabbits. *Infection & Immunity* **60**, 4154-67.

Sakabe, N. (1991). X-ray diffraction data collection system for modern protein crystallography with a Weissenberg camera and an imaging plate using synchrotron radiation. *Nuclear Instruments and Methods in Physical Research* **A303**, 448-63.

Samuel, J. E., Perera, L. P., Ward, S., O'Brien, A. D., Ginsburg, V. & Krivan, H. C. (1990). Comparison of the glycolipid receptor specificities of Shiga-like toxin type II and Shiga-like toxin type II variants. *Infection & Immunity* **58**, 611-8.

Sandvig, K., Garred, Ø., Prydz, K., Kozlov, J. V., Hansen, S. H. & van Deurs, B. (1992). Retrograde transport of endocytosed Shiga toxin to the endoplasmic reticulum. *Nature* **358**, 510-2.

Sandvig, K., Ryd, M., Garred, Ø., Schweda, E., Holm, P. K. & van Deurs, B. (1994). Retrograde transport from the Golgi complex to the ER of both Shiga toxin and the nontoxic Shiga B-fragment is regulated by butyric acid and cAMP. *Journal of Cell Biology* **126**, 53-64.

Saxena, S. K., O'Brien, A. D. & Ackerman, E. J. (1989). Shiga toxin, Shiga-like toxin II variant, and ricin are all single-site RNA N-glycosidases of 28 S RNA when microinjected into Xenopus oocytes. *Journal of Biological Chemistry* **264**, 596-601.

Schafer, D. E. & Thakur, A. K. (1982). Quantitative description of the binding of GM1 oligosaccharide by cholera enterotoxin. *Cell Biophysics* **4**, 25-40.

Shimizu, H., Field, R. A., Homans, S. W. & Donohue-Rolfe, A. (1998). Solution structure of the complex between the B-subunit homopentamer of verotoxin VT-1 from *Escherichia coli* and the trisaccharide moiety of globotriaosylceramide. *Biochemistry* **37**, 11078-82.

Sixma, T. K., Pronk, S. E., Kalk, K. H., van Zanten, B. A., Berghuis, A. M. & Hol, W. G. (1992). Lactose binding to heat-labile enterotoxin revealed by X-ray crystallography. *Nature* **355**, 561-4.

Sixma, T. K., Pronk, S. E., Kalk, K. H., Wartna, E. S., van Zanten, B. A., Witholt, B. & Hol, W. G. (1991). Crystal structure of a cholera toxin-related heat-labile enterotoxin from *E. coli*. *Nature* **351**, 371-7.

Sixma, T. K., Stein, P. E., Hol, W. G. & Read, R. J. (1993). Comparison of the B-pentamers of heat-labile enterotoxin and verotoxin-1: two structures with remarkable similarity and dissimilarity. *Biochemistry* **32**, 191-8.

Spangler, B. D. (1992). Structure and function of cholera toxin and the related

Escherichia coli heat-labile enterotoxin. Microbiological Reviews 56, 622-47.

St. Hilaire, P. M., Boyd, M. K. & Toone, E. J. (1994). Interaction of the Shiga-like toxin

type 1 B-subunit with its carbohydrate receptor. Biochemistry 33, 14452-63.

Stein, P. E., Boodhoo, A., Tyrrell, G. J., Brunton, J. L. & Read, R. J. (1992). Crystal

structure of the cell-binding B oligomer of verotoxin-1 from E. coli. Nature 355,

748-50.

Tronrud, D. E. (1992). Conjugate-Direction Minimization: an Improved Method for the

Refinement of Macromolecules. Acta Crystallographica A48, 912-6.

van den Akker, F., Sarfaty, S., Twiddy, E. M., Connell, T. D., Holmes, R. K. & Hol, W.

G. (1996). Crystal structure of a new heat-labile enterotoxin, LT-IIb. Structure 4,

665-78.

Vriend, G. (1990). WHAT IF: a molecular modeling and drug design program. Journal of

Molecular Graphics 8, 52-6.

Waddell, T., Cohen, A. & Lingwood, C. A. (1990). Induction of verotoxin sensitivity in

receptor-deficient cell lines using the receptor glycolipid globotriosylceramide.

Proceedings of the National Academy of Sciences of the United States of America

87, 7898-901.

Zhang, R. G., Westbrook, M. L., Westbrook, E. M., Scott, D. L., Otwinowski, Z., Maulik,

P. R., Reed, R. A. & Shipley, G. G. (1995). The 2.4 A crystal structure of cholera

toxin B subunit pentamer: choleragenoid. Journal of Molecular Biology 251, 550-

62.

Zoja, C., Corna, D., Farina, C., Sacchi, G., Lingwood, C., Doyle, M. P., Padhye, V. V.,

Abbate, M. & Remuzzi, G. (1992). Verotoxin glycolipid receptors determine the

localization of microangiopathic process in rabbits given verotoxin-1. *Journal of*

Laboratory & Clinical Medicine **120**, 229-38.

5.0 General Conclusions

5.1 General

In the introduction to Chapter 1, it was stated that understanding the effects of the molecular environment on the structure of a protein is important for understanding the protein's function, and that this is illustrated in the cases discussed in this thesis. This is seen in observations involving the crystal contacts in the structures that have been presented, and in the interactions, or implied interactions, that the structures have with ions, small molecule inhibitors, glycolipids, and with other macromolecules.

5.2 Active PAI-1 at 3.0 Å Resolution.

The structure of PAI-1 at low resolution reveals a great deal of information about the protein, some of it via the crystal contacts that the molecules make. The different conformations of the A/C molecules and the B/D molecules in the unit cell gives information on the flexibility of the molecule.

The disorder of the reactive centre loop (RCL) in the B/D molecules suggests that, in the absence of stabilizing contacts, this loop is highly flexible and does not have a fixed conformation. A disordered loop has also been seen recently in the structure of plasminogen activator inhibitor-2 (Harrop *et al.*, 1999); it remains to be seen if this is a feature of serpins that interact with plasminogen activator, or if it is a general property of the reactive centre loop in the absence of stabilizing interactions such as crystal contacts.

By contrast, the reactive centre loop in the A/C molecules is mostly ordered, due to crystal contacts it makes with the edge of the A sheet in other molecules. This may

indicate a mechanism of serpin polymerization, a form of intermolecular interaction with important clinical considerations for several serpins (Stein & Carrell, 1995). Whether or not the interactions in the active PAI-1 structure indicate a form of polymerization with biological significance, they do confirm that the reactive centre loop tends to take an extended β-sheet-like conformation when suitable stabilizing molecular contacts are present. This has relevance not only to serpin polymerization and to the dimerization of antithrombin III (Carrell *et al.*, 1994; Schreuder *et al.*, 1994), but also to the insertion of the loop into the A sheet following RCL cleavage, or the latency transition. Possibly a preference for extended conformations is helpful in the insertion of the RCL into the reactive site of serine proteinases, as their standard binding mode has the P_4 to P_1 residues in a β-strand conformation.

In contrast to the reactive centre loop, the clear electron density of the gate loop (strands 4C and 3C, residues 170 to 193) and the similarity in its structure between the A/C and B/D molecules suggests that it is well ordered. This is in contrast to the disorder found in the latent structure (Mottonen *et al.*, 1992), although it is similar to the structures found in the cleaved and peptide-inhibited forms of PAI-1 (Aertgeerts *et al.*, 1995; Xue *et al.*, 1998). This may require some revision of the theory that disorder in this loop facilitates the latency transition (Tucker *et al.*, 1995), possibly viewing the disorder as a result of the transition, not as a pre-existing cause. The motion of the C-terminus may serve as a lock, preventing the reactive centre loop from re-threading itself through the gate region, while the increase in entropy of the gate loop may offset the loss in entropy in the reactive centre loop.

Four mutations stabilize the active form of PAI-1 (N150H, K154T, Q319L, M354I). While it has been hard to attribute a particular effect to the mutation at residue 354, the other 3 mutations seem to have a dramatic effect on the conformation of loop thFs3A (residues 150 to 158). They appear to transform it from a series of turns, seen in other forms of PAI-1, into a 3_{10} helix in the mutant. Since this loop covers the region into which the RCL must insert, the mutation may make this region more rigid and create a greater barrier to insertion.

The ability of PAI-1 to interact with certain macromolecules, particularly vitronectin, is believed to mediate some important physiological effects (Deng *et al.*, 1996). Most of these interactions are only made with one form of PAI-1, this being the active form in the case of vitronectin (Lawrence *et al.*, 1997). The interaction surface on PAI-1 differs substantially between the active and the various inserted forms of the structure. Several other macromolecules are believed to interact with this surface. Thus a beginning has been made in understanding the intermolecular interactions of PAI-1 at the molecular level.

5.3 PAI-1 at 2.2 Å Resolution.

The refinement of PAI-1 at higher resolution not only confirms most of the conclusions from the lower-resolution structure, it allows some further observations to be made. Many of these observations relate to further deviations observed between the A/C and B/D molecules that became unambiguously visible at the higher resolution.

The most obvious of these is the large change in the neighboring segments ts3Bs2B (residues 211 to 221) and helix G, ts3BhG, helix H (residues 241 to 270). The different conformations stabilized by crystal contacts suggest that these regions are able to move

significantly in the active form. As they form one side of the 'gate' through which strand 1C must pass during the latency transition, this motion may facilitate the transition. The active structure also supports the proposed theory that Arg 284 and Leu 285 are in orientations that should reduce the stability of strand 1C (Harrop *et al.*, 1999).

We have modelled the interaction of PAI-1 with two small molecule inhibitors. The high resolution crystal structure confirms the presence of a deep pocket that should form an ideal small-molecule binding site on the surface of active PAI-1. This is in the vicinity of the known binding sites of the two inhibitors according to antibody and mutational studies (Björquist *et al.*, 1998; Friederich *et al.*, 1997). Inhibitor docking trials with the program DockVision (Hart *et al.*, 1997; Hart & Read, 1992) were carried out on the face of PAI-1 containing the putative binding site. These dockings have demonstrated that the lowest energy conformations for the inhibitors are found when they are inserted into the proposed binding pocket. The refined docking results suggest that XR51 fits into the pocket with its phenyl ring inserted deepest and the diketopiperazine ring stacking against Tyr 79, which is consistent with available information. ARH0 is suggested to be inserted with the carboxyl and nitro derivatized ring deepest, which is plausible, but not perfectly consistent with all data reported for the compound (Björquist *et al.*, 1998). The dockings do support the feasibility of using this region as a drug design target, and suggest possible methods by which the inhibitors could be improved.

5.4 Refinement of wild-type and F30A mutant Shiga-like toxin structures

The refined structures of wild-type and F30A mutant Shiga-like toxin contain useful information which is obtained from the interaction of the pentamer with ions and

symmetry-related pentamers. The investigation of sites known to be involved in globotriaosylceramide binding is also illuminating.

The improvement of the crystal growth perpendicular to the (010) face by the addition of zinc chloride can be explained by the supplementation of weak contacts on the screw axis parallel to the b axis via the coordination by protein groups of Zn1.

The lockwasher distortion observed in the pentamer can be explained as being favourable for the formation of extensive crystal contacts. While essentially an artifact of crystallization, it points to an underlying weakness of the intermonomer contacts within the pentamer. This lends some credence to the idea that that interactions with the A subunit, or with sugar ligands, may stabilize the pentamer in an important fashion. The instability of the pentamer may play a role in the assembly or dissociation of the holotoxin.

The F30A mutation seems to have little effect on the B-pentamer structure away from the mutated residue. It is likely that the considerable effect that this mutation has on glycolipid binding and cytotoxicity is mediated through interactions at sugar binding Site 1, which is centred on that residue. It is just possible that the effects are also mediated through Site 2, which interacts tangentially with the mutated residue, however it is hard to see these contacts having much effect. In the structure of the double mutant F30A/W30A, no change was seen in sugar binding at Site2 (Ling, 1999). This suggests that Site 1 is an important binding site for glycolipids, although probably not as important as Site 2.

Less information can be obtained from our structure with respect to other sugar binding sites, although Ling's observation that Trp 34 is disordered in the absence of

glycolipid is confirmed (Ling, 1999). In general, the results support the idea that binding at multiple sites, and at multiple classes of sites plays an important role in the Shiga-toxin cell binding affinity and toxicity.

5.5   General Lessons

The work in this thesis underlines the importance of NCS symmetry and crystal contacts as tools in the interpretation of protein structures. NCS averaging was an essential tool in the solution of the low resolution PAI-1 structure, and was also helpful at high resolution. Correct handling of the NCS weighting proved to be an important factor in obtaining optimal structures of both PAI-1 and refined Shiga-like toxins. Comparisons of NCS related monomers gave useful information about the reliability of structural features, and yielded useful information about variations in structure, in particular variations caused by crystal contacts.

While crystal contacts are generally considered to be troublesome artifacts, in the case of PAI-1 they yielded at least two valuable insights: a new mechanism of polymerization for reactive centre loops, and evidence for significant structural variability in certain surface loops in the gate area of the molecule. In the case of Shiga-like toxin-1, it is also possible that the lockwasher distortion is an indication of a significant instability in the isolated pentamer, although the significance of this is not clear.

In general, when one solves a macromolecular structure containing multiple quasi-identical subunits, alike macroscopically but containing minor variations, one is obtaining several different macromolecular structures at once. In the cases presented in this thesis, this has supplied extra information from the structures, enriching the process of structure

solution. The potential of analyzing NCS variations in crystal structures containing

multiple subunits should always be considered.